Evgenia Ovchinnikova

Genetic analysis of symbiosome formation

Evgenia Ovchinnikova

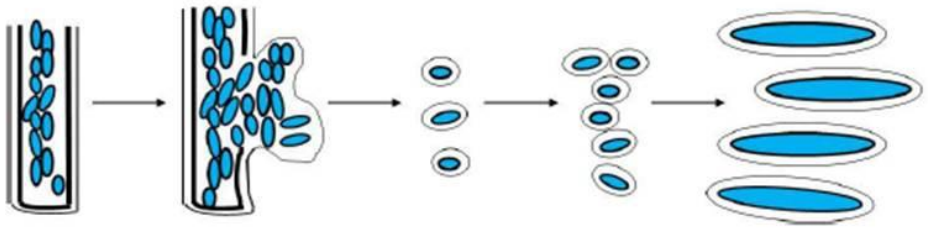

Genetic analysis of symbiosome formation

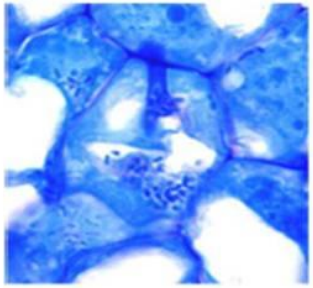

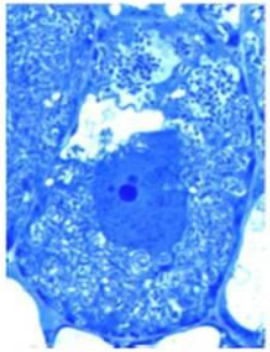

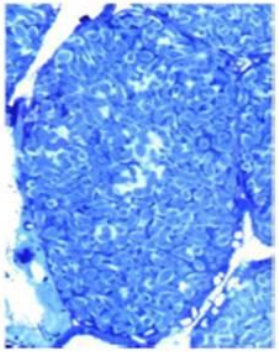

Genetic analysis of symbiosome formation

Evgenia Ovchinnikova

Thesis committee

Thesis supervisors

Prof. dr. T. Bisseling
Professor of Molecular Biology (Development Biology of Plants)
Wageningen University

Prof. dr. I.A. Tikhonovich
Professor of Genetics
All-Russia Research Institute for Agricultural Microbiology, St. Petersburg, Russia

Thesis co-supervisor

Dr. ir. E.H.M. Limpens
Assistant professor, Laboratory of Molecular Biology
Wageningen University

Other members

Prof. dr. ir. E. Jacobsen, Wageningen University
Dr. ir. P.E.J. Smit, Wageningen University
Dr. P. Mergaert, Institut des Sciences du Végétal, Centre National de la Recherche Scientifique, Gif sur Yvette, France
Dr. S. Goormachtig, Ghent University, Belgium

This research was conducted under the auspices of the Graduate School of Experimental Plant Sciences

Genetic analysis of symbiosome formation

Evgenia Ovchinnikova

Thesis

submitted in fulfilment of the requirements for the degree of doctor
at Wageningen University
by the authority of the Rector Magnificus
Prof. dr. M.J. Kropff,
in the presence of the
Thesis Committee appointed by the Academic Board
to be defended in public
on Wednesday 19 September 2012
at 1:30 p.m. in the Aula

Evgenia Ovchinnikova
Genetic analysis of symbiosome formation
147 pages

PhD thesis, Wageningen University, Wageningen, NL (2012)
With references, with summaries in Dutch and English

ISBN 978-94-6173-361-0

The research for this thesis was supported by The Netherlands Organization for Scientific Research (NWO)/Russian Federation for Basic Research (RFFI) grant for Centre of Excellence 047.018.001

Thesis content

Outline of the thesis **7**

Chapter 1 (General introduction) **9**

Chapter 2 (Synteny-based cloning of pea symbiotic genes using Medicago as intergenomic cloning vehicle) **33**

Chapter 3 (IPD3 controls the formation of nitrogen-fixing symbiosomes in pea and *Medicago* spp.) **54**

Chapter 4 (Synteny-based cloning of pea *Sym41* identifies an essential role of the LRR-receptor kinase PsSym19 in symbiosome formation and development) **77**

Chapter 5 (Towards the identification of pea Sym31, a putative sucrose transporter controlling symbiosome differentiation?) **103**

Chapter 6 (Summarizing discussion) **126**

Nederlandse samenvatting **141**

Curriculum Vitae **145**

Educational statement of EPS **147**

Outline of the thesis

Endosymbiotic interactions form a fundament of life as we know it and are characterized by the formation of new specialized membrane compartments, in which the microbes are hosted inside living plant cells (Parniske, 2000). A striking example is the symbiosis between legumes and nitrogen-fixing *Rhizobium* bacteria (rhizobia), which represents the most important source of biologically fixed nitrogen. The accommodation of rhizobia as novel nitrogen fixing organelles, called symbiosomes, inside the cells of a novel organ, the root nodule, forms the heart of this ecologically and agriculturally important symbiosis. Understanding how these organelles are made will be key to exploit this symbiosis for sustainable agriculture in the future. In this thesis, we undertook a genetic approach to identity key components that control symbiosome formation especially in the genetically well-characterized garden pea (*Pisum sativum*) system. At the start of this thesis, the most extensive and morphologically best-characterized collection of mutants impaired in symbiosome formation was, and currently still is, available in pea. However, the cloning of the corresponding genes is severely hampered by its large genome size and recalcitrance to genetic transformation. Therefore, we used the model legume *Medicago truncatula* (Medicago) as reference genome to clone pea symbiosome mutants via a synteny-based cloning approach. We focused especially on three mutants in pea, named *sym33, sym41* and *sym31*, which are affected most early in symbiosome formation: namely blocked in the release of bacteria from cell wall bound infection threads inside root nodule cells (*sym33* and *sym41*) or induction of the subsequent differentiation of the symbiosomes (*sym31*).

In Chapter 1, a general introduction is given on the process of symbiosome formation in legume root nodules. In this introduction, we focus on mechanisms by which these new nitrogen-fixing organelles are formed and address some of the recent insights, most of which were obtained after the start of this thesis, into plant components that control this process, which have been obtained from genetic studies in pea and the model legumes Medicago and *Lotus japonicus* (Lotus).

Pea is part of the Papillionoid legume subfamily and closely related to the model legume Medicago. It has been shown that there is extensive synteny between the pea and Medicago genomes, which offers an efficient strategy to clone pea gene using Medicago as intergenomic cloning vehicle. In Chapter 2, we outline this synteny-based cloning approach and the molecular tools that we created to clone the pea genes required for symbiosome formation. In addition, we describe an efficient method to obtain transgenic roots via *Agrobacterium rhizogenes* mediated root transformation in pea that facilitates the functional analysis of pea genes in root endosymbioses.

In Chapter 3, we report the cloning of the pea *Sym33* and Medicago *SYM1* genes those mutants are most strongly impaired in their ability to form symbiosomes, i.e. the release of rhizobia from the cell wall bound infection threads. Both pea *Sym33* and Medicago *SYM1*

encode the interacting protein of DMI3, IPD3. IPD3 was shown to interact with DMI3/CCaMK, a calcium- and calmodulin-dependent kinase that is an essential component of the common symbiotic signaling pathway for both rhizobial and mycorrhizal symbioses. Our data reveal a novel, key role for IPD3 in symbiosome formation and development. Further, we show that MtIPD3 is required for the expression of a nodule-specific remorin MtSYMREM1, which is required for proper infection thread growth and essential for symbiosome formation.

In Chapter 4, we report the synteny-based cloning of the pea *sym41* mutant that is also impaired in the release of the bacteria from the infection threads. We show that *Sym41* represents a weak allele of the common symbiotic signaling gene *PsSym19*/*MtDMI2*, a leucine-rich repeat domain containing receptor kinase that is essential for both rhizobial and mycorrhizal endosymbiosis. *Sym41* contains a splice-site mutation in intron 9, by which the formation of a functional transcript is reduced by ~90%. The implication of Sym19/DMI2 together with the identified role of Sym33/IPD3 in symbiosome formation (Chapter 3) strongly indicate that rhizobia have co-opted the signaling pathway from the ancient mycorrhizal symbiosis to be hosted as new organelles inside root nodule cells.

In Chapter 5, we describe the synteny-based mapping of pea *sym31*, a mutant impaired in symbiosome differentiation. By making use of the synteny with Medicago, we fine mapped the *Sym31* gene to a region of ~2.5 cM, which corresponds to a <450 kb region in Medicago. In this syntenic region, one gene *MtN3.1*, a putative sugar transporter stands out as prime candidate to control symbiosome differentiation. We describe and discuss our efforts to determine the role of this gene in symbiosome differentiation in pea and Medicago.

In Chapter 6, we summarize and discuss our current insight into symbiosome formation and its relation to the arbuscular mycorrhiza and we give a perspective on the future of cloning the pea genes required for endosymbiosis.

Chapter 1

General Introduction

Symbiosome formation in legume root nodules

Microbes are able to invade eukaryotic cells and establish a new niche where they can survive and replicate. Such endosymbioses are widespread and play important roles in evolution. In fact, the eukaryotic cell evolved from the endosymbiotic engulfment of prokaryotes resulting in the formation of organelles such as mitochondria and chloroplasts (Margulis, 1981). A striking example of the intracellular accommodation of prokaryotes in plants occurring nowadays is the mutualistic endosymbiosis between legumes and nitrogen-fixing Rhizobium bacteria (rhizobia), which is the most important source of biologically fixed nitrogen. The formation of new membrane compartments where the rhizobia are hosted as novel nitrogen-fixing organelles, called symbiosomes (Roth and Stacey, 1989), is at the heart of this endosymbiosis. In this introduction, we focus on the mechanisms by which nitrogen-fixing symbiosomes are formed and address some of the recent insights obtained by genetic studies in pea and the model legumes *Medicago truncatula* (Medicago) and *Lotus japonicus* (Lotus).

Nodule formation and infection

The establishment of a Rhizobium-legume symbiosis involves the formation of a novel organ on the root of the plant, called the root nodule. The formation of this organ starts with the dedifferentiation of root cortical cells that enter the cell cycle and are reprogrammed to form a nodule primordium. At the same time, rhizobia invade the root and developing primordium via cell wall bound infection structures, called infection threads (Brewin et al., 2004). Most commonly, such infection threads originate in root hairs that curl around attached bacteria through a continued reorientation of the growth direction of the root hair by which rhizobia become entrapped in a closed cavity and form a microcolony (Emons and Mulder, 2000; Jones et al., 2007). However, alternative infection mechanisms such as crack entry between cells can occur in certain legumes (Held et al., 2010). Inside the curl, the plant cell wall is locally degraded, the plasma membrane invaginates, and new membrane and cell wall material is deposited forming a tubular infection thread that grows to the base of the root hair. Subsequently, the bacteria are released into the apoplast at the boundary with the underlying cortical cell. There, a new trans-cellular infection thread can be initiated, and this process continues to guide bacteria to the nodule primordium cells. The path followed by the infection threads is marked by activated cortical cells forming so-called pre-infection threads, which are phragmoplast-like cytoplasmic bridges that traverse the central vacuole (Yang et al. 1994; Timmers et al., 1998). When the infection threads reach the cells of the nodule primordium, bacteria are released from the infection threads and are taken up into the cells through an

endocytosis-like process by which symbiosomes are formed. After the infection threads invade the nodule primordium, a meristem is established that continues to add cells to the developing nodule (Timmers et al., 1998). In indeterminate nodules of pea and Medicago, this meristem persists at the apex of the nodule by which an elongated nodule is formed with a highly ordered zonal organization where infection followed by symbiosome formation continuously occurs in cells that leave the meristem and enter the so-called infection zone (Fig.1; Vasse et al., 1990). In determinate nodules of Lotus the meristem is active only for a short period, and infected cells that already contain symbiosomes can divide resulting in round nodules (Brewin, 1991). Genetic studies (see Nod factor signaling) have shown that the infection process can be uncoupled from the organogenesis program in indeterminate nodules, however, both processes need to be tightly coordinated to allow a successful symbiosis (Popp and Ott, 2011). If the infection threads do not reach the primordium before a meristem is formed, they fail to infect this primordium, infection threads are arrested in the root outer cortex, and nodule development is blocked at an early stage (Timmers et al., 1998). Similarly, infection threads are blocked in the epidermis if cortical cells are not activated (Murray et al., 2007; Plet et al., 2011). In both cases, symbiosomes are never formed, and rhizobia remain locked inside infection threads. This suggests that a specific cellular program needs to be triggered to allow symbiosome formation, which involves activation of the cell cycle and possibly endoreduplication cycles (see below).

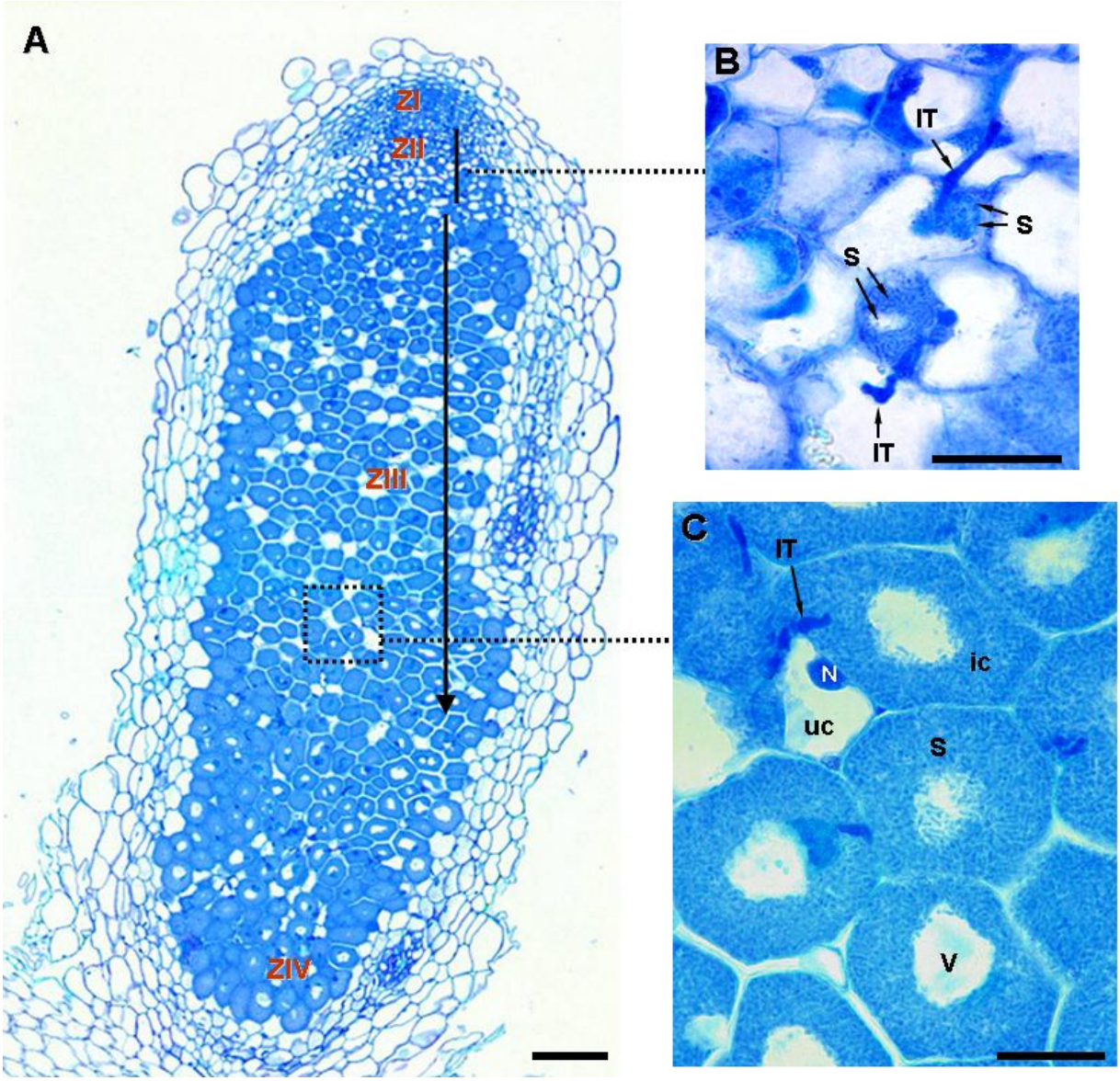

Fig.1. Structural organization of an indeterminate pea nodule. **A**, Longitudinal semithin section of the nodule: ZI–meristematic zone, ZII–infection zone, ZIII–fixation zone, ZIV–senescence zone. **B**, Close-up of the nodule cells in zone II where symbiosome formation starts; **C**, Close-up of the nodule cells in zone III containing mature symbiosomes. In all micrographs: IT–infection thread, S–symbiosomes, N–nucleus, V–vacuole, ic–infected cell, uc–uninfected cell. Bars: A–100 µm; B, C–25 µm.

Symbiosome formation and development

Symbiosome formation starts with the formation of a so-called unwalled infection droplet, a region on the infection thread where the cell wall is locally degraded and the plasma membrane invaginates (Fig.2). This allows rhizobia to come into close contact with the host plasma membrane, and subsequently the bacteria are individually pinched off into the cytoplasm by which they become surrounded by a plant-derived membrane (Fig.2), the symbiosome membrane. Next, the bacterium (now called bacteroid) and the surrounding symbiosome/peribacteroid membrane divide, and they start filling the cells. In the indeterminate nodules of pea and Medicago, bacterial and symbiosome membrane division are strictly

coupled by which symbiosome compartments contain a single bacteroid (Fig.2). Release of bacteria and symbiosome division occur in the distal end (~3-4 cell layers) of the infection zone just below the nodule meristem (Fig.1). As described by Vasse et al. (1990), the newly released rod-shaped bacteria in this zone are similar in size to free-living bacteria and are called type 1 bacteroids. The bacteroids stop dividing and start to differentiate (Fig.2) by which they become much larger, elongated or branched (Y-shaped in pea nodules) bacteroids (type 2) in the proximal part of the infection zone. Next, the type 2 bacteroids stop elongating and develop into type 3 bacteroids that almost completely fill the infected nodule cells (Fig.1C).

The differentiation processes in the infection zone correlate with endoreduplication and cell enlargement occurring in both host and bacterial cells (Cebolla et al., 1999; Mergeart, 2006). The induction of endoreduplication cycles in nodule cells of Medicago was shown controlled by the cell-cycle anaphase-promoting complex activator CCS52A (Cebolla et al., 1999; Vindarell et al., 2003). Knockdown of the *CCS52A* gene specifically in the nodule reduced cell size and ploidy levels and impaired symbiosome formation and maintenance (Vindarell et al., 2003). It is thought that the polyploidy of the infected nodule cells facilitates an increased metabolic activity required to maintain the numerous symbiosomes. Interestingly, host nuclear polyploidy appears a common theme in plant biotrophic interactions, both symbiotic and pathogenic where the microbes are hosted inside living plant cells (Wildersmuth, 2010).

When the symbiosomes reach their mature form (type 4) they are able to fix atmospheric nitrogen, which is facilitated by the micro-aerobic conditions in the infected nodules cells of the fixation zone (Fig.1) and correlates with the induction of the bacterial nitrogen fixation (*Nif*) genes (Yang et al., 1991; Soupene et al., 1995; Ott et al., 2005). Some cells originating from the meristem are never infected by the bacteria and these can be seen as relatively small uninfected cells in between the large infected cells (Fig.1). Uninfected cells are thought to play a role in metabolite transport to and from infected cells (White et al., 2007). Eventually, as the nodule ages (starting ~3-4 weeks post-inoculation), the symbiosis starts to break down, and senescence of symbiosomes (type 5 bacteroids) and host cells occurs in the so-called senescent zone (Fig.1; Vasse et al., 1990).

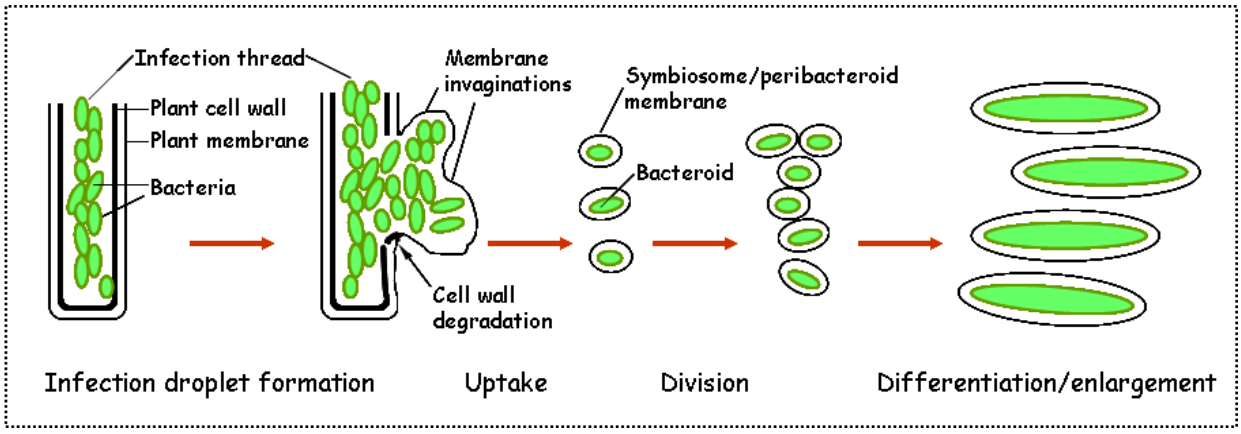

Fig.2. Schematic representation of the symbiosome formation process. Symbiosome formation starts with the formation of a so-called unwalled infection droplet, a region on the infection thread where the cell wall is locally degraded and the plasma membrane invaginates. As a result, bacteria come into close contact with the host plasma membrane. Subsequently bacteria are individually "pinched off" into the cytoplasm, by which they become surrounded by a plant-derived membrane, the symbiosome membrane. Next, the bacterium (now called bacteroid) and the surrounding symbiosome/peribacteroid membrane divide. Finally, the bacteroids stop dividing and start to differentiate, by that they become much larger and elongated and reach their mature nitrogen-fixing state.

Terminal differentiation of bacteroids

The process of symbiosome differentiation described above involves a terminal differentiation of the bacteroids as they in loose their ability to divide and reproduce when isolated from the nodules (Mergaert et al., 2006). This terminal differentiation is determined by the host plant and is not a general characteristic of symbiosomes (Mergeart et al., 2006). For example, in determinate nodules of Lotus and soybean, multiple (2-6) bacteroids can be found in a single symbiosome due to either symbiosome fusion or bacterial division. Typically, these bacteroids remain the same size as bacteria inside the infection threads, and they retain the ability to divide when isolated from the nodules. Terminal differentiation also does not depend on nodule type because several mimosoid (Mimosoideae) legumes that form indeterminate nodules do not terminally differentiate their symbiosomes (Ishihara et al., 2011; Marchetti et al., 2011; Kereszt et al., 2011). Instead, terminal differentiation of bacteroids seems to be characteristic for legumes of the so-called inverted-repeat-lacking (IRLC) clade of Papillionoideae (Wojciecowski et al., 2004; Mergeart et al., 2006). A detailed evaluation of terminal bacteroid differentiation in the legume family indicates that the non-terminal differentiated state is ancestral to the differentiated one, and the latter likely evolved several times independently in the Papilionoidea (Oono et al., 2010).

It was recently shown that the terminal differentiation of bacteroids is triggered by a family of nodule-specific cysteine-rich (NCR) peptides, which resemble defensin-like antimicrobial peptides (Van de Velde et al., 2010; Maroti et al., 2011). The NCR peptide genes are specific for the IRLC legumes and lacking in the genomes of sequenced non-IRLC legumes such as soybean and Lotus (Alunni et al., 2007). In Medicago, they represent a large gene family of

more than 450 members, most of which are expressed relatively late during nodule development specifically in infected cells although several members are expressed early in the infection zone of the nodule (Mergaert et al., 2003). The NCR peptides are targeted to the symbiosomes. Treatment of *Rhizobium* cultures with purified NCR peptides triggered responses that resemble terminal differentiation, such as cell elongation and inhibition of cell division (Van de Velde et al., 2010). Furthermore, expression of a Medicago NCR peptide in the infected cells of Lotus nodules triggered terminal differentiation of bacteroids in this non-IRLC legume. The exact targets of the NCR peptides are currently unknown, and they may differ among the individual members. These peptides appear to be processed by a nodule-specific signal peptidase complex (Wang et al., 2010; Van de Velde et al., 2010). In the Medicago mutant *defective in nitrogen fixation 1* (*dnf1*) (Mitra and Long, 2004), symbiosomes fail to differentiate, and the bacteroids morphologically resemble free-living rhizobia. It has been shown that the *DNF1* gene encodes a nodule-specific signal peptidase SPC22 subunit. Due to a mutation in the SPC22 subunit in *Mtdnf1*, the signal peptide of the NCR peptides was not cleaved off, by which the peptides got stuck in the ER and were not (or were very inefficiently) targeted to the symbiosomes. This also supports the existence of a symbiosis-specific exocytotic pathway required for the symbiosome formation (see below).

Interestingly, it was recently found that antimicrobial peptides (although different from the NCRs) in insects regulate the growth of vertically transmitted endosymbiotic bacteria by the inhibition of their cell division, induction of polyploidy, and cell size much like terminally differentiated symbiosomes (Login et al., 2011). Thus, it seems that insects and plants adopted a similar strategy to “domesticate” the bacterial symbionts (Login et al., 2011).

Symbiosome membrane identity

Symbiosome formation involves a major reorganization of the host endomembrane system and requires a massive production of membrane to make the thousands of symbiosome compartments that fill the infected cells. There is ~40x more symbiosome membrane than plasma membrane in an infected cell (Robertson and Lyttleton, 1984; Whitehead and Day 1997). It was generally believed that the uptake of rhizobia into the host cells involved an endocytosis process similar to the phagocytic uptake of bacteria in animal cells (Via et al., 1997; Knodler et al., 2002; Brumell and Grinstein, 2004; Behnia and Munro, 2005). However, a recent systematic analysis of the identity of the symbiosome membrane in the host endomembrane system of Medicago showed that symbiosome formation does not follow the default endocytotic pathway (Limpens et al., 2009). By studying the association of so-called membrane identity markers (SNARE proteins and Rab GTPase) for the different endomembrane compartments with the symbiosome membrane, it has been shown that symbiosomes never acquire the early endosomal/trans-Golgi network marker SYP4 or the late endosomal/prevacuolar marker RAB5. Instead, the symbiosome membrane acquires the plasma membrane t-SNARE SYP132 from

the start of symbiosome formation throughout its development (Catalano et al., 2005; Limpens et al., 2009). After the symbiosomes stop dividing and differentiating to their nitrogen fixing form, the vacuolar/transitory late endosomal marker Rab7 did occur on the symbiosome membrane, and it is required to control the proper development of the symbiosome (Cheon et al., 1993; Limpens et al., 2009). In contrast, vacuolar SNARE proteins did not mark the symbiosome membrane of developing and mature nitrogen fixing symbiosomes, indicating that symbiosomes are not vacuolar compartments as suggested by Mellor (1989). Only when the symbiosomes start to fuse and form lytic vacuole-like compartments during nodule senescence, vacuolar SNAREs did associate with the fusing symbiosome membranes. Therefore, symbiosomes appear to acquire a mosaic (plasma membrane (SYP132) and late endosomal (Rab7)) identity, and the delay in acquiring (lytic) vacuolar identity (e.g., vacuolar SNAREs) most likely ensures their survival and maintenance as individual units (Limpens et al., 2009). The presence of Rab7 on the symbiosome membrane may indicate that symbiosomes can intercept vacuole-targeted proteins, which could explain the reported presence of several vacuolar enzymes in the symbiosome space (Mellor, 1989; Whitehead and Day, 1997; Jones et al., 2007). These are likely transported to the vacuole via late endosomes. Setting up this special status (prone to becoming a lytic vacuole) may be an additional mechanism used by the host to keep the rhizobial symbiont under control and to retrieve invested nutrients when symbiosomes are no longer required.

The presence of the plasma membrane SNARE SYP132 from the start on the symbiosome membrane suggests an important role of the delivery of exocytotic vesicles and their associated cargo to allow the uptake of bacteria and subsequent symbiosome development. This is also supported by the fusion of ER and Golgi-derived vesicles with the infection droplet and symbiosome membranes (Robertson and Lyttleton, 1982; Roth and Stacey, 1989; Cheon et al., 1994). The NCR peptides described above may also be key cargo of such specific exocytotic pathway to allow symbiosome differentiation. Interestingly, the symbiosome-localized SYP132 is transcriptionally upregulated in infected nodule cells as well as in root cortical cells colonized by AM fungi (Limpens, *unpublished;* Hogekamp et al., 2011). This may suggest a shared exocytotic pathway for the formation of symbiosomes and arbuscules.

Symbiosomes as organelles (nutrient exchange)

A major function of the symbiosome membrane, in addition to preventing a pathogenic response, is to facilitate the efficient exchange of nutrients between the two partners (White et al., 2007; Oldroyd et al., 2011; Kereszt et al., 2011). Several observations indicate that nitrogen-fixing symbiosomes can be regarded as genuine (transient) plant organelles that provide ammonium to the plant.

Transcriptome analysis of bacteroids, especially on the terminally differentiated symbiosomes in indeterminate legumes of pea and Medicago, showed that rhizobia switch off

most housekeeping genes and many aspects of normal reproductive development. This includes many ribosomal proteins, enzymes involved in amino acid production, membrane/cell surface components, and proteins involved in RNA synthesis and/or DNA repair (Becker et al., 2004; Chang et al., 2007; Karunakaran et al., 2009; Oldroyd et al., 2011). Thus, rhizobial bacteroids become strictly dependent on the host cells to deliver key metabolites. This is supported by the identification of a number of transporter proteins in proteomics studies that are associated with the symbiosome membrane, although the exact function of many of these is unknown (White et al., 2007; Oldroyd et al., 2011). Carbon supply to the bacteroids involves the transport of photosynthates in the form of sucrose to the nodules via the phloem, which is thought to be converted into organic acids in the uninfected nodule cells and subsequently supplied to the infected cells. Although several putative sugar transporters are found at the symbiosome membrane, dicarboxylates, especially malate appear to be the main source of carbon for the symbiosomes, which is further supported by the essential role of the rhizobial dicarboxylate transport system for nitrogen fixation and symbiosome development (Lodwig and Poole, 2003; Yurgel and Kahn, 2004; White et al., 2007). However, additional carbon sources may be involved. Symbiosomes, especially in pea require a supply of branched amino acids for their early development (Lodwig et al., 2003; Prell et al., 2009, 2010). In turn, bacteroids/symbiosomes release fixed nitrogen as ammonia to the plant and at the same time switch off their-own ammonia assimilation into amino acids (Patriarca et al., 2002). In indeterminate nodules of pea and Medicago, the ammonium released by the symbiosomes is assimilated into glutamate and exported out of the nodule mainly as asparagine (Patriarca et al., 2002; White et al., 2007). In contrast, in determinate nodules of Lotus or soybean, ammonium is exported in the form of ureides (Goggin et al., 2003).

The recent cloning of two plant genes essential for nitrogen fixation further highlights the dependency of symbiosomes on the supply of metabolites and minerals by the host cell. One of these genes encodes the nodule-specific sulfate transporter SST1, which is targeted to the symbiosome membrane in Lotus nodules and controls the nitrogen-fixing ability of the symbiosomes (Krusell et al., 2005). This indicates an essential role for sulfate supply by the host, which may be required as a cofactor for a functional nitrogenase complex (Krusell et al., 2005). The second gene encodes the legume-specific homocitrate synthase FEN1; homocitrate is an essential metabolite that rhizobia need to fix nitrogen as it is a key component of the iron-molybdenum cofactor in the nitrogenase complex (Hakoyama et al., 2009). Interestingly, the gene encoding homocitrate synthase, *NifV* is lacking in the genomes of most rhizobial species fixing nitrogen exclusively inside the infected nodule cells. This lack of NifV is compensated by the plant through the expression of a specific homocitrate synthase encoded by the legume-specific *FEN1* gene. A knockout mutant of *FEN1* in Lotus forms nodules unable to fix nitrogen although these are normally infected (Hakoyama et al., 2009). This highlights the intimate interconnection between both partners and analogy to organelles such as mitochondria or

chloroplasts. Like mitochondria and chloroplasts (King 2002; Sheahan et al., 2004), symbiosomes can be distributed between two daughter cells when an infected cell divides. This has been demonstrated in white lupine nodules where connections with the cytoskeleton ensure the equal distribution of the symbiosomes over the daughter cells, especially at low symbiosome numbers (Gonzalez-Sama et al., 2004; Fedorova et al., 2005). This suggests that the mechanism/machinery that controls organelle distribution during cytokinesis also recognizes symbiosomes as genuine organelles.

Nod factor signalling

Both nodule formation and infection thread formation are set in motion by the perception of rhizobial signal molecules, the Nod factors that are produced by the bacteria in response to specific flavonoids secreted by the plant (Oldroyd and Downie, 2004). Nod factors are lipo-chitooligosaccharides that generally consist of a β-1,4-linked *N*-acetyl glucosamine backbone of 4 or 5 residues of which the non-reducing terminal residue contains an acyl chain (Truchet et al., 1991). Depending on the rhizobial species, different acyl chains and specific decorations at the reducing and non-reducing terminal residues can be present, which help determine host specificity, especially at the level of infection thread formation (Ardourel et al., 1994). Genetic approaches in Medicago, Lotus, and pea have identified key components involved in Nod factor (NF) perception and signal transduction (Fig.3).

Nod factors are perceived by the LysM-domain containing receptor kinases such as NFP/LYK3/LYK4 in Medicago, Sym10/Sym2/Sym37 in pea, and NFR5/NFR1 in Lotus (Limpens et al., 2003; Madsen et al., 2003; Radutoiu et al., 2003; Arrighi et al., 2006; Smit et al., 2007; Zhukov et al., 2008). These receptors trigger ion fluxes leading to a depolarization of the plasma membrane and Ca^{2+} oscillations in and around the nucleus (Oldroyd and Downie, 2006; Capoen et al., 2009). The activation of this Ca^{2+} spiking response also requires a plasma membrane LRR receptor kinase MtDMI2/PsSym19/LjSymRK (Ané et al., 2002; Postma et al., 1990; Schneider et al., 1999; Endre et al. 2002; Stracke et al. 2002) as well as components of a nuclear pore complex (Kanamori et al., 2006; Saito et al., 2007; Groth et al., 2010), and a putative cation channel MtDMI1/PsSym8/LjCastor and LjPollux located at the nuclear envelope (Ané et al., 2004; Edwards et al., 2007; Charpentier et al. 2008). The resulting Ca^{2+} signature is decoded by a nuclear Ca^{2+}/calmodulin-dependent kinase MtDMI3/PsSym9/LjCCaMK (Duc and Messager, 1989; Kneen et al., 1994; Lévy et al. 2004; Catoira et al., 2000; Mitra et al., 2004; Tirichine et al., 2006). The CCaMK activation subsequently triggers transcriptional changes leading to root hair curling as well as cortical cell divisions and to the phosphorylation of its interacting protein IPD3/CYCLOPS (Messinese et al., 2007; Yano et al., 2008). The NF induced gene expression requires the transcription factors NSP1, NSP2, and NIN (Schauser et al., 1999; Kalo et al., 2005; Smit et al., 2005; Heckmann et al., 2006; March et al., 2007). Gain-of-function mutations in CCaMK lead to the formation of spontaneous nodules in the absence of rhizobia,

and these are sufficient to allow nodule formation as well as rhizobial infection and even occasionally symbiosome formation when upstream components of the signalling pathway are missing (Hayashi et al., 2010; Madsen et al., 2010). This implies that the primary role of NF perception is the activation of MtDMI3/PsSym9/LjCCaMK.

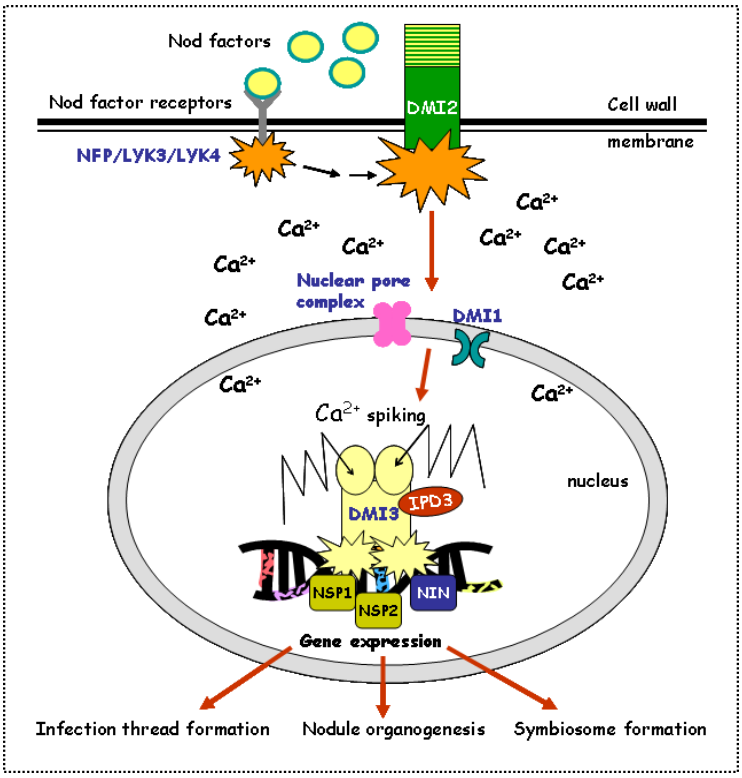

Fig.3. Nod factor perception and signal transduction. Nod factors are perceived by LysM domain containing receptor kinases MtNFP/LYK3/LYK4 (PsSym10/Sym37/Sym2, LjNFR5/NFR1). These receptors trigger ion fluxes leading to a depolarization of the plasma membrane and Ca^{2+} oscillations (Ca^{2+} spiking) in and around the nucleus via the plasma membrane-localized LRR receptor kinase MtDMI2 (PsSym19/LjSymRK) and a putative cation channel MtDMI1 (PsSym8/LjCastor and Pollux) located at the nuclear envelope. The Ca^{2+} signature is decoded by a nuclear Ca^{2+}/calmodulin-dependent kinase MtDMI3 (PsSym9/LjCCaMK) that forms a protein complex with MtIPD3 (PsSym33/LjCYCLOPS). This complex triggers transcriptional changes leading to specific symbiotic responses such as infection thread formation, nodule organogenesis, and symbiosome formation. These transcriptional changes are mediated by transcription factors NSP1/NSP2 (PsSym7) and NIN (PsSym35).

The induction of cortical cell divisions in the Rhizobium-legume symbiosis further requires the activation of the cytokinin-receptor, called CRE1 in Medicago (Gonzalez-Rizzo et al., 2006) and LHK1 in Lotus (Tirichine et al., 2007). A *LHK1* knockout mutation blocks cortical cell activation, but not infection thread formation in the root hairs (Murray et al., 2007). A gain-of-function mutation in this cytokinin receptor triggers the formation of spontaneous nodules, which depends on the transcription factors NSP1/NSP2 and NIN, but it is not sufficient to allow rhizobial infection in the absence of CCaMK/DMI3 activation (Madsen et al., 2010; Plet et al., 2011). These studies suggest that cytokinin may be generated upon activation of DMI3 in the epidermis as a mobile signal to coordinate cortical cell activation with infection thread growth to allow a successful symbiosis (Plet et al., 2011; Oldroyd et al., 2011).

Several studies indicate that the NF signalling pathway is also active in the nodule. All components are expressed especially in the infection zone of the nodule where symbiosome formation starts (Bersoult et al., 2005; Capoen et al., 2005; Limpens et al., 2005). Knockdown of *SymRK/DMI2* by RNAi or by its ectopic expression in a mutant background was shown to cause a block in the release of rhizobia from the cell wall bound infection threads while nodule formation and infection thread growth still occurred (Capoen et al., 2005; Limpens et al., 2005).

Similarly, introduction of a rice *CCaMK/DMI3* ortholog in a Medicago *dmi3* mutant resulted in a partial complementation where nodules contained infection threads, however, bacteria were not released (Godfroy et al., 2006). Furthermore, attempts to complement *nsp1* mutants with a *Nicotiana benthamiana NSP1* gene resulted in aberrant early senescent symbiosomes (Heckmann et al., 2006). These data suggested a role of NF signalling in symbiosome formation and development. The cloning and functional characterization of *IPD3* gene in pea (mutated in *sym33* (Tsyganov et al., 1998; Voroshilova et al., 2009) and Medicago (mutated in *sym1*/TE7 (Benaben et al., 1995)) and the identification of a splice-site mutation in the *DMI2* ortholog in pea *sym41* (Morzhina et al., 2000; Voroshilova et al., 2009) as reported in Chapters 2 and 3 of this thesis, now clearly demonstrate an essential role of the NF signalling pathway in symbiosome formation and development. These mutants further highlight the intimate, yet enigmatic (see also below) relationship between cell-cycle activation and symbiosome formation and development (Voroshilova et al., 2009). Our data further show that IPD3 is essential for the induction of a nodule-specific remorin (MtSYMREM1) which was shown to interact with DMI2 and the NF receptors LYK3 and NFP (Lefebvre et al., 2010). Interestingly, a knockout mutant of *MtSYMREM1* also causes a block in the release bacteria from the infection threads inside the nodule (Lefebvre et al., 2010). These data as well as the upregulation of several NF signalling components in the infection zone of the nodule suggest that a threshold level of NF signalling is required to allow the switch from infection thread growth to symbiosome formation (Kereszt et al., 2011). The induction of MtSYMREM1 in the nodule may be required to control the activity of the signalling receptors, or alternatively this lipid raft-associated protein could play a role in forming a local membrane domain that facilitates unwalled infection droplet formation/symbiosome formation (Lefebvre et al., 2010).

Interestingly, components of the Nod factor signalling pathway are also essential to allow a symbiotic association with arbuscular mycorrhizal (AM) fungi (Parniske, 2008). This ancient endosymbiosis dates back ~450 million years and occurs in >80% of current land plants. It involves the formation of a symbiotic interface containing highly branched hyphae inside cortical cells of the host root, called an arbuscule (Parniske, 2008). Therefore, rhizobia appear to have co-opted the signalling pathway to establish a symbiosis from the more ancient arbuscular mycorrhiza. The recent finding that AM fungi produce lipo-chitooligosaccharide signal molecules that are strikingly similar to the Nod factors produced by bacteria (Maillet et al., 2011) supports this. Furthermore, a recent study in the only non-legume able to establish a rhizobial symbiosis, *Parasponia* showed that a single NFP ortholog controls both arbuscule formation and fixation thread formation (Op den Camp et al., 2011). Such fixation threads are highly branched intracellular thread-like structures that form the symbiotic compartment where the rhizobia fix nitrogen, and these can be considered equivalent to the symbiosomes (Sprent, 2007). Similar fixation threads are observed in more basal legume species and are thought to represent a more primitive stage from which symbiosomes evolved (Naisbitt et al., 1992; Sprent, 2007). This

would also be in line with the observed plasma membrane identity of the symbiosome membrane (Limpens et al., 2009). Therefore, it is probable that during evolution rhizobia acquired the ability to produce Nod factors (Sullivan and Ronson, 1998) which provided them the ability to use the ancient AM machinery to establish an intracellular interface.

Genetic analysis of symbiosome formation

Forward genetic screens (as well as reverse genetic approaches) in pea, Medicago and Lotus, have identified numerous plant mutants that are able to form nodules but are impaired in their ability to fix atmospheric nitrogen, so-called Fix$^-$ mutants. These Fix$^-$ mutants can be divided into three main categories depending on their morphological characteristics (Table 1): 1) no release of bacteria from the infection threads, 2) no bacteroid/symbiosome differentiation, and 3) impaired functionality/maintenance of symbiosomes (early senescence). Since the start of this thesis, several of the corresponding genes have been identified (see also previous paragraphs) and are starting to give insight into this key step of the symbiosis as summarized in Table 1. However, many of the mutants, especially in the two model legumes Medicago and Lotus have not yet been well characterized at the morphological level.

Two recently identified mutants in Medicago suggest a complex role of different plant hormones in nodule and symbiosome development. One of these is the Medicago *latd/nip* mutant. This mutant is impaired in the formation and maintenance of lateral root and nodule meristems, infection thread growth and the release of bacteria from infection threads in the nodule primordium (Veereshlingam et al., 2004; Bright et al., 2005; Yendrek et al., 2010; Harris and Dickstein, 2010). Three mutant alleles have been identified with varying phenotypes ranging from a block of the infection thread growth in the epidermis in the strongest allele through nodules containing symbiosomes that are less effective in the weakest (Teillet et al., 2008). Interestingly, the application of abscisic acid (ABA) can rescue the lateral root defect of *latd/nip*. However, the inhibitory effect of ABA on nodule formation (Ding et al., 2008) prevented the assessment whether ABA action is required for symbiosome formation. *LATD/NIP* encodes a member of the NRT1 (PTR1) nitrate and di/tripeptide transporter family and may potentially transport ABA although its precise function is unclear (Harris and Dickstein, 2010). The correlation between a block in meristem formation and release of bacteria from the infection threads again suggests an intimate link between cell cycle control and symbiosome formation. This is further supported by the identification of the CCAAT-transcription factor HAP2 that is expressed in the nodule meristem where it controls meristem initiation or maintenance (Combier et al., 2006). Knockdown of *HAP2* resulted in small round nodules that lacked a functional meristem, and bacteria were not released from the infection threads.

Another study identified a nodule-enhanced ethylene-response factor, EFD that negatively controls nodule initiation and infection in the epidermis; however, it is required in the nodule to control symbiosome formation and differentiation (Vernie et al., 2008). EFD was shown to

induce the type-A cytokinin response regulator RR4, which is thought to function as a negative regulator of cytokinin signalling. This suggests that regulation of cytokinin signalling is important to allow the proper development of symbiosomes, which may be related to its effects on the cell cycle.

Recently identified genes required for symbiosome development in Lotus include *IGN1* and *SEN1* (Kumagai et al., 2007; Hakoyama et al., 2012). *IGN1* encodes a novel ankyrin repeat protein with a PEST sequence in the amino-terminus and transmembrane domains at the carboxy-terminus (Kumagai et al., 2007). Ankyrin repeats are generally involved in protein-protein interactions, and the PEST domain is a target for proteolytical degradation. The *ign1* mutant shows early fusion of symbiosomes and formation of lytic compartments, i.e. premature senescence. Strikingly, IGN1 protein was not detected in the symbiosome membrane although it was detected in the plasma membrane fraction of the nodule. This might suggest that IGN1 marks a different exocytotic pathway than that involved in the symbiosome formation although it was not shown in which cell type the gene is active. It could be that *IGN1* is active in non-infected cells of the nodule, and the gene controls symbiosome maintenance in an indirect manner.

SEN1 encodes a legume-specific nodulin21-like protein that is homologous to a vacuolar iron transporter and present on the symbiosome membrane (Hakoyama et al., 2012). The *sen1* mutant is impaired in symbiosome differentiation at an early stage of nodule formation and unable to fix nitrogen (Hakoyama et al., 2012). Because iron plays an essential role in many aspects of symbiosome development and it is a component of iron-molybdenum cofactor in the nitrogenase complex, SEN1 may be required to transport iron to the bacteroids.

Table 1. Identified genes required for the symbiosome formation and development

Gene name	Mutant/RNAi phenotype	Gene product	(Putative) Function	Reference
CCS52A (Mt)	Reduced cell size, decreased ploidy levels of the cells, impaired symbiosome formation and maintenance	Cell-cycle anaphase-promoting complex activator	Induces endoreduplication cycles in the nodule	Cebolla et al., 1999; Vindarell et al., 2003
NCR peptide genes *(Mt)*	–	Nodule-specific cysteine-rich peptides	Symbiosome development, terminal differentiation of bacteroids	Mergaert et al., 2003; Van de Velde et al., 2010; Maroti et al., 2011
DNF1 (Mt)	Fix$^-$, small symbiosomes, bacteroids do not differentiate and resemble free-living bacteria	Nodule-specific signal peptidase SPC22 subunit	Remove the signal peptide sequence from NCR peptides	Wang et a l., 2010
SST1 (Lj)	Fix$^-$, premature senescence of nodules	Nodule-specific sulfate transporter	Sulfate supply of bacteroids	Krusell et al., 2005
FEN1 (Lj)	Fix$^-$, symbiosome differentiation is blocked	Homocitrate synthase/	Supply of bacteroids by homocitrate,	Hakoyama et al., 2009
SymRK (Lj), DMI2 (Mt), Sym19/Sym 41 (Ps)	Fix$^-$, block in the released of rhizobia from infection threads, hypertrophied infection threads, premature senescence of symbiosomes	Leucine-rich repeat receptor kinase	Trigger Ca^{2+} oscillations, activation of Ca^{2+}/calmodulin kinase CCaMK/DMI3/Sym9	Capoen et al., 2005; Limpens et al., 2005; Morzhina et al., 2000; Voroshilova et al., 2009; Chapter 4
CYCLOPS (Lj), IPD3 (Mt), Sym33 (Ps)	Fix$^-$, block in the released of rhizobia from infection threads, blocked infection thread formation	Interacting protein of DMI3	Activity and stability of Ca^{2+}/calmodulin kinase CCaMK (DMI3/Sym9); nduction of *SYMREM1* expression	Messinese et al., 2007; Yano et al., 2008; Benaben et al., 1995; Tsyganov et al., 1998; Chapter 3; Ovchinnikova et al., 2011
SYMREM1 (Mt)	Fix$^-$, block in the released of rhizobia from infection threads	Nodule-specific symbiotic remorin	Interact with Nod factor receptors and SymRK/DMI2	Lefebvre et al., 2010
LATD/NIP (Mt)	Fix$^-$, block in the released of rhizobia from infection threads, blocked infection thread formation, symbiosomes do develop	Putative transporter of nitrate and di/tripeptide transporter family	Transport of nitrate, abscisic acid and/or other compounds	Veereshlingam et al., 2004; Bright et al., 2005; Yendrek et al., 2010; Harris and Dickstein, 2010; Teillet et al., 2008)

Table 1. (Continued)

HAP2 (Mt)	Fix$^-$, block in the released of rhizobia from infection threads	CCAAT-transcription factor	Nodule meristem initiation and maintenance	Combier et al., 2006
EFD (Mt)	Fix$^-$, block in the released of rhizobia from infection threads, hypertrophied infection threads	Nodule-enhanced ethylene-response transcription factor	induce the type-A cytokinin response regulator *RR4*	Vernie et al., 2008
IGN1 (Lj)	Fix$^-$, premature senescence of symbiosomes	Ankyrin repeat PEST protein	Protein-protein interaction, proteolytic degradation	Kumagai et al., 2007
SEN1 (Lj)	Fix$^-$, premature senescence of symbiosomes	Nodulin21-like protein	Putative iron transporter	Hakoyama et al., 2012

Concluding remarks

The intracellular accommodation of rhizobia as novel nitrogen-fixing organelles forms the heart of the Rhizobium-legume symbiosis. Until recently, genetic studies in the model legumes Medicago and Lotus mainly focused on the identification of the signalling components that control NF perception, nodule organogenesis, and rhizobial infection in the epidermis (for a recent review see Popp and Ott, 2011). In the last few years, significant progress has been made in the genetic analysis of symbiosome formation and development as described in this introduction and in the next chapters of this thesis. However, many of the identified Fix$^-$ mutants, especially in Medicago and Lotus have not been well characterized. To date, the most extensive and best-characterized set of Fix$^-$ mutants is still available in pea. However, the large genome size and recalcitrance to genetic transformation severely hamper the identification of the underlying genes. Fortunately, the extensive synteny between pea and Medicago offers an efficient strategy to clone pea genes using the Medicago genome as reference (Young et al., 2011) as applied in this thesis. Finally, genetic screens for Fix$^-$ mutants are far from being saturated. Therefore, continued genetic studies and the identification of the corresponding genes will undoubtedly shed more light on this key step in endosymbiosis in the future. Furthermore, research on basal legume species that show alternative infection and intracellular accommodation strategies will be important to understand the evolutionary constraints to host the microbes intracellularly (Sprent et al., 2007; Op den Camp et al., 2011).

REFERENCES

Alunni, B., Kevei, Z., Redondo-Nieto, M., Kondorosi, A., Mergaert, P., Kondorosi, E. (2007) Genomic organization and evolutionary insights on *GRP* and *NCR* genes, two large nodule-specific gene families in *Medicago truncatula*. *Mol. Plant-Microbe Interact.*, 9: 1138–1148.

Ané, J.M., Lévy, J., Thoquet, P., Kulikova, O., de Billy, F., Penmetsa, V., Kim, D.J., Debellé, F., Rosenberg, C., Cook, D.R. et al. (2002) Genetic and cytogenetic mapping of DMI1, DMI2, and DMI3 genes of Medicago truncatula involved in Nod factor transduction, nodulation, and mycorrhization. *Mol. Plant-Microbe Interact.,* 15(11): 1108–1118.

Ané, J.M., Kiss, G.B., Riely, B.K., Penmetsa, R.V., Oldroyd, G.E., Ayax, C., Lévy, J., Debellé, F., Baek, J.M., Kalo, P., et al. (2004) *Medicago truncatula DMI1* required for bacterial and fungal symbioses in legumes. *Science* 30: 1364–1367.

Arrighi J.F., Barre, A., Ben Amor, B., Bersoult, A., Soriano, L., Mirabella, R., Carvalho-Niebel, F., Journet, E., Ghérardi, M., Huguet, T., Geurts, R., Dénarié, J., Rougé, P., Gough, C. (2006) The *Medicago truncatula* LysM-receptor kinase gene family includes *NFP* and new nodule-expressed genes. *Plant Physiol,* 142: 265–279.

Ardourel, M., Demont, N. Debellé, F. Maillet, F. de Billy, F. Promé, J.C. Dénarié, J. and Truchet. G. (1994) *Rhizobium meliloti* lipooligosaccharide nodulation factors: Different structural requirements for bacterial entry into target root hair cells and induction of plant symbiotic developmental responses. *Plant Cell*, 6: 1357–1374.

Becker, D., Geiger, D., Dunkel, M., Roller, A., Bertl, A., Latz, A., Carpaneto, A. Dietrich, P., Roelfsema, M.G.R., Voelker, C. et al. (2004) AtTPK4, an Arabidopsis tandem-pore K+ channel, poised to control the pollen membrane voltage in a pH- and Ca^{2+}-dependent manner. *Proc. Natl Acad. Sci. USA*, 101: 15621–15626.

Bénaben, V., Duc, G., Lefebvre, V., Huguet, T. (1995) TE7, An Inefficient Symbiotic Mutant of *Medicago truncatula* Gaertn cv. Jemalong. *Plant Physiol.*, 107: 53–62.

Behnia, R. and Munro, S. (2005) Organelle identity and the signposts for membrane traffic. *Nature* 438: 597–604.

Bersoult, A., Camut, S., Perhald, A., Kereszt, A., Kiss, G.B., Cullimore, J.V. (2005) Expression of the *Medicago truncatula DMI2* gene suggests roles of the symbiotic nodulation receptor kinase in nodules and during early nodule development. *Mol. Plant-Microbe Interact***,** 18: 869–876.

Brewin, N. J. (2004). Plant cell wall remodelling in the *Rhizobium*-legume symbiosis. *Crit. Rev. Plant Sci.,* 23: 293–316.

Bright, L. J., Liang, Y., Mitchell, D. M., Harris, J. M. (2005) The *LATD* gene of *Medicago truncatula* is required for both nodule and root development. *Mol. Plant-Microbe Interact.,* 18: 521–532.

Brumell, J.H. and S. Grinstein (2004) *Salmonella* redirects phagosomal maturation. *Curr. Opin. Microbiol.,* 7: 78–84.

Capoen, W., Goormachtig, S., De Rycke, R., Schroeyers, K., and Holsters, M. (2005) SrSymRK, a plant receptor essential for symbiosome formation. *Proc. Natl. Acad. Sci. U.S.A.,* 102: 10369–10374.

Capoen, W., Den Herder, H., Sun, J., Verplancke, C., De Keyser, A., De Rycke, R., Goormachtig, S., Oldroyd, G., Holster, M. (2009) Calcium spiking patterns and the role of the calcium/calmodulin-

dependent kinase CCaMK in lateral root base nodulation of *Sesbania rostrata*. *Plant Cell,* 21(5): 1526–540.

Catalano, C. M., Lane, W. S., Sherrier, D. J. (2004) Biochemical characterization of symbiosome membrane proteins from *Medicago truncatula* root nodules. *Electrophoresis* 25: 519–531.

Catoira, R., Galera, C., de Billy, F., Penmetsa, R.V., Journet, E.P., Maillet, F., Rosenberg, C., Cook, D., Gough, C., Dénarié, J. (2000) Four genes of *Medicago truncatula* controlling components of a Nod factor transduction pathway. *Plant Cell*, 12: 1647–1666.

Cebolla, A., Vinardell, J.M., Kiss, E., Oláh, B., Roudier, F., Kondorosi, A., and Kondorosi, E. (1999) The mitotic inhibitor *ccs52* is required for endoreduplication and ploidy-dependent cell enlargement in plants. *EMBO J.,* 18: 101–109.

Chang, W.S., Franck, L.W., Cytryn, E., Jeong, S., Joshi, T., Emerich, W.D., Sadowsky, M.J., Xu, D., Stacey, G. (2007) An oligonucleotide microarray resource for transcriptional profiling of *Bradyrhizobium japonicum*. *Mo.l Plant-Microbe Interact.,* 20: 1298–1307.

Charpentier, M., Bredemeier, R., Wanner, G., Takeda, N., Schleiff, E., Parniske, M. (2008) Lotus japonicus CASTOR and POLLUX are ion channels essential for perinuclear calcium spiking in legume root endosymbiosis. *Plant Cell*, 20: 3467–3479.

Cheon, C.I., Lee, N.G., Siddique, A.B.M., Bal, A.K., Verma, D.P.S. (1993) Roles of plant homologs of Rab1p and Rab7p in the biogenesis of the peribacteriol membrane, a subcellular compartment formed *de novo* during root nodule symbiosis. *EMBO J*., 12: 4125–35.

Cheon C.I., Hong, Z., Verma, D.P.S. (1994) Nodulin-24 follows a novel pathway for integration into the peribacteroid membrane in soybean root nodules. *J. Biol. Chem.,* 269: 6598–6602.

Combier, J. P., Frugier, F., de Billy, F., Boualem, A., El-Yahyaoui, F., Moreau, S., Vernié, T., Ott, T., Gamas, P., Crespi, M., and Niebel, A. (2006) MtHAP2-1 is a key transcriptional regulator of symbiotic nodule development regulated by microRNA169 in *Medicago truncatula*. *Genes Dev.*, 20: 3084–3088.

Ding, Y., Kalo, P., Yendrek, C., Sun, J., Liang. Y., Marsh, J.F., Harris, J.M., Oldroyd, G.E.D. (2008) Abscisic acid coordinates Nod factor and cytokinin signaling during the regulation of nodulation in *Medicago truncatula*. *Plant Cell*, 20: 2681–2695.

Duc, G. and Messager, A. (1989) Mutagenesis of pea (*Pisum sativum* L.) and the isolation of mutants for nodulation and nitrogen fixation. *Plant Sci.,* 60: 207–213.

Edwards, A., Heckmann, A.B., Yousafzai, F., Duc, G., Downie, J.A. (2007) Structural implications of mutations in the pea SYM8 symbiosis gene, the DMI1 ortholog, encoding a predicted ion channel. *Mol. Plant-Microbe Interact.,* 20: 1183–1191.

Endre, G., Kereszt, A., Kevei, Z., Mihacea, S., Kaló, P., Kiss, G. (2002) A receptor kinase gene regulating symbiotic nodule development. *Nature* 417: 962–966.

Emons, A.M.C. and Mulder, B.M. (2000) How the deposition of cellulose microfibrils builds cell wall architecture. *Trends Plant Sci.,* 5: 35–40.

Fedorova, E., Redondo, F.J., Koshiba, T., de Felipe, M.R., Pueyo, J.J., Lucas, M.M. (2005) Aldehyde oxidase (AO) in the root nodules of *Lupinus albus* and *Medicago truncatula*: identification of AO in meristematic and infection zones. *Mol. Plant-Microbe Interact.,* 18: 405–413.

Godfroy, O., Debellé, F., Timmers, T., Rosenberg, C. (2006) A rice calcium- and calmodulin-dependent protein kinase restores modulation to a legume mutant. *Mol. Plant-Microbe Interact.,* 19(5): 495–501.

Goggin, D.E., Lipscombe, R., Fedorova, E., Millar, A.H., Mann, A., Atkins, C.A., Smith, P.M.C. (2003) Dual intracellular localization and targeting of aminoimidazole ribonucleotide synthetase in cowpea. *Plant Physiol.,* 131: 1033–1041.

Gonzalez-Sama, A., Lucas, M.M., de Felipe, M.R., Pueyo, J.J. (2004) An unusual infection mechanism and nodule morphogenesis in white lupin (*Lupinus albus*). *New Phytol.,* 163: 371–380.

Groth, M., Takeda, N., Perry, J. Uchida, H., Brachmann, A., Sato, S., Tabata, S., Kawaquchi, M., Wang, T.L., Parniske, M. (2010) NENA, a Lotus japonicus homolog of Sec13, is required for rhizodermal infection by arbuscular mycorrhiza fungi and rhizobia but dispensable for cortical endosymbiotic development. *Plant Cell*, 22: 2509–2526.

Hakoyama, T., Niimi, K., Watanabe, H., Tabata, R., Matsubara, J., Sato, S., Nakamura, Y., Tabata, S., Jichun, L., Matsumoto, T., et al. (2009) Host plant genome overcomes the lack of a bacterial gene for symbiotic nitrogen fixation. *Nature* 462: 514–517.

Hakoyama, T., Niimi, K., Yamamoto, T., Isobe, S., Sato, S., Nakamura, Y., Tabata, S., Kumagai, H., Umehara, Y., Brossuleit, K. et al. (2012) The Integral Membrane Protein SEN1 is Required for Symbiotic Nitrogen Fixation in *Lotus japonicus* Nodules. *Plant Cell Physiol*., 53: 225–236.

Harris J.M. and Dickstein, R. (2010) Control of root architecture and nodulation by the *LATD/NIP* transporter. *Plant Signaling & Behavior*, 5: 1386–1390.

Hayashi, T., Banba, M., Shimoda, Y., Kouchi, H., Hayashi, M., Imaizumi-Anraku, H. (2010) A dominant function of CCaMK in intracellular accommodation of bacterial and fungal endosymbionts. *Plant J.*, 63:141–154.

Heckmann, A. B., Lombardo, F., Miwa, H., Perry, J. A., Bunnewell, S., Parniske, M., Wang, T. L., Downie, J. A. (2006) *Lotus japonicus* nodulation requires two GRAS domain regulators, one of which is functionally conserved in a non-legume. *Plant Physiol.,* 142: 1739–1750.

Held, M., Hossain, M. S., Yokota, K., Bonfante, P., Stougaard, J., Szczyglowski, K. (2010) Common and not so common symbiotic entry. *Trends Plant Sci.*, 15: 540–545.

Hogekamp, C., Arndt, D., Pereira, P.A., Becker, J.D., Hohnjec, N., Küster, H. (2011) Laser microdissection unravels cell-type-specific transcription in arbuscular mycorrhizal roots, including CAAT-box transcription factor gene expression correlating with fungal contact and spread. *Plant Physiol.,* 157(4): 2023–2043.

Ishihara, H., Koriyama, H., Osawa, A., Zehirov, G., Yamaura, M., Kucho, K. I., Abe, M., Higashi, S., Kondorosi, E., Mergaert, P., Uchiumi, T. (2011) Characteristics of bacteroids in indeterminate nodules of the leguminous tree *Leucaena glauca*. *Microbes Environ.*, 26: 156–159.

Jones, K. M., Kobayashi, H., Davies, B. W., Taga, M. E., Walker, G.C. (2007) How rhizobial symbionts invade plants: The *Sinorhizobium-Medicago* model. *Nat. Rev. Microbiol.,* 5: 619–633.

Kaló, P., Gleason, C., Edwards, A., Marsh, J., Mitra, R.M., Hirsch, S., Jakab, J., Sims, S., Long, S.R., Rogers, J., et al. (2005) Nodulation signaling in legumes requires NSP2, a member of the GRAS family of transcriptional regulators. *Science* 308: 1786–1789.

Kanamori N., **Madsen, L., Radutoiu, S., Frantescu, M., Quistgaard, E., Miwa, H., Downie, A., James, E.K., Felle, H.H., Haaning, L.L. et al.** (2006) A nucleoporin is required for induction of Ca^{2+} spiking

in legume nodule development and essential for rhizobial and fungal symbiosis. *Proc. Natl. Acad. Sci. USA,* 103: 359–364.

Karunakaran, R., Haag, A. F., East, A. K., Ramachandran, V. K., Prell, J., James, E. K., Scocchi, M., Ferguson, G. P., Poole, P. S. (2010) BacA is essential for bacteroid development in nodules of galegoid, but not phaseoloid legumes. *J. Bacteriol.,* 192: 2920–2928.

Kereszt, A., Mergaert, P., Maroti, G., Kondorosi, E. (2011) Innate immunity effectors and virulence factors in symbiosis. *Cur. Opinion Microbiol.,* 14: 76–81.

King, S.M. (2002) Dyneins motor on in plants. *Traffic*, 3: 930–931.

Kneen, B.E., Weeden, N.F., LaRue, T.A. (1994) Non-nodulating mutants of *Pisum sativum* L. cv. Sparkle. *J. Hered.,* 85: 129–133.

Knodler, L. A., Celli, J., Hardt, W.-D., Vallance, B. A., Yip, C. & Finlay, B. B. (2002) *Salmonella* effectors within a single pathogenicity island are differentially expressed and translocated by separate type III secretion systems. *Mol. Microbiol.,* 43: 1089–1103.

Krusell, L., Krause, K., Ott, T., Desbrosses, G., Krämer, U., Sato, S., Nakamura, Y., Tabata, S., James, E.K., Sandal et al. (2005) The sulfate transporter SST1 is crucial for symbiotic nitrogen fixation in *Lotus japonicus* root nodules. *Plant Cell*, 17: 1625–1636.

Kumagai, H., Hakoyama, T., Umehara, Y., Sato, S., Kaneko, T., Tabata, S., Kouchi, H. (2007) A novel ankyrin-repeat membrane protein, IGN1, is required for persistence of nitrogen-fixing symbiosis in root nodules of *Lotus japonicus*. *Plant Physiol.,* 143: 1293–1305.

Lefebvre, B., Timmers, T., Mbengue, M., Moreau, S., Hervé, C., Tóth, K., Bittencourt-Silvestre, J., Klaus, D., Deslandes, L., Godiard, et al. (2010) A remorin protein interacts with symbiotic receptors and regulates bacterial infection. *Proc. Natl. Acad. Sci. USA,* 107: 2343–2348.

Lévy, J., Bres, C., Geurts, R., Chalhoub, B., Kulikova, O., Duc, G., Journet, E.P., Ané, J.M., Lauber, E., Bisseling, T., et al. (2004) A putative Ca^{2+} and calmodulin-dependent protein kinase required for bacterial and fungal symbioses. *Science* 303: 1361–1364.

Limpens, E., Ivanov, S., van Esse, W., Voets, G., Fedorova, E., Bisseling, T. (2009) Medicago N_2-fixing symbiosomes acquire the endocytic identity marker Rab7 but delay the acquisition of vacuolar identity. *Plant Cell,* 21: 2811–2828.

Limpens, E., Franken, C., Smit, P., Willemse, J., Bisseling, T., Geurts, R. (2003) LysM domain receptor kinases regulating rhizobial Nod factor-induced infection. *Science* 302: 630–633.

Limpens, E., Mirabella, R., Fedorova, E., Franken, C., Franssen, H., Bisseling, T., Geurts, R. (2005) Formation of organelle-like N_2-fixing symbiosomes in legume root nodules is controlled by *DMI2. Proc. Natl. Acad. Sci. USA,* 102: 10375–10380.

Lodwig, E. and Poole, P. (2003) Metabolism of *Rhizobium* bacteroids. *CRC Crit. Rev. Plant Sci.,* 22: 37–78.

Login, F.H., Balmand, S., Vallier, A., Vincent-Monégat, C., Vigneron, A., Weiss-Gayet, M., Rochat, D., Heddi, A. (2011) Antimicrobial Peptides Keep Insect Endosymbionts Under Control. *Science* 334(6054): 362–365.

Madsen, E.B., Madsen, L.H., Radutoiu, S., Olbryt, M., Rakwalska, M., Szczyglowski, K., Sato, S., Kaneko, T., Tabata, S., Sandal, N., et al. (2003) A receptor kinase gene of the LysM type is involved in legume perception of rhizobial signals. *Nature* 425: 637–640.

Madsen, L.H., Tirichine, L., Jurkiewicz, A., Sullivan, J.T., Heckmann, A.B., Bek, A.S., Ronson, C.W., James, E.K. Stougaard, J. (2010) The molecular network governing nodule organogenesis and infection in the model legume Lotus japonicus. *Nature Communications,* 1: 1–12.

Maillet, F., Poinsot, V., Andre, O., Puech-Pages, V., Haouy, A., Gueunier, M., Cromer, L., Giraudet, D. Formey, D., Niebel, A. et al. (2011) Fungal lipochitooligosaccharide symbiotic signals in arbuscular mycorrhiza. *Nature* 469: 58–63.

Marsh, J. F., Rakocevic, A., Mitra, R. M., Brocard, L., Sun, J., Eschstruth, A., Long, S. R., Schultze, M., Ratet, P., Oldroyd, G. E. (2007) *Medicago truncatula* NIN is essential for rhizobial-independent nodule organogenesis induced by autoactive calcium/calmodulin-dependent protein kinase. *Plant Physiol.,* 144: 324–335.

Marchetti, M., Catrice, O., Batut, J., Masson-Boivin, C. (2011) Cupriavidus taiwanensis bacteroids in *Mimosa pudica* indeterminate nodules are not terminally differentiated. *Appl. Environ. Microbiol.,* 77: 2161–2164.

Margulis L. (1981) Symbiosis in cell evolution. In: New York: W.H. Freeman, 1993, 452 p.

Maróti, G., Kereszt, A., Kondorosi, E., Mergaert, P. (2011) Natural roles of antimicrobial peptides in microbes, plants and animals. *Res. Microbiol.,* 162: 363–374.

Mellor, R.B. (1989) Bacteroids in the *Rhizobium*-legume symbiosis inhabit plant internal lytic compartment: implications for other microbial endosymbioses. *J. Exp. Bot.* 40: 831–839.

Mergeart, P., Uchiumi, T., Alunni, B., Evanno, G., Cheron, A., Catrice, O., Mausset, A.E., Barloy-Hubler, F., Galibert, F., Kondorosi, A., Kondorosi, E. (2006) Eukaryotic control on bacterial cell cycle and differentiation in the Rhizobium–legume symbiosis. *PNAS*, 103(13): 5230–5235.

Mergaert, P., Nikovics, K., Keleman, Z., Maunoury, N., Vaubert, D., Kondorosi, A., Kondorosi, E. (2003) A Novel Family in *Medicago truncatula* Consisting of More Than 300 Nodule-Specific Genes Coding for Small, Secreted Polypeptides with Conserved Cysteine Motifs. *Plant Physiol.,* 132: 161–173.

Messinese, E., Mun, J. H., Yeun, L. H., Jayaraman, D., Rougé, P., Barre, A., Lougnon, G., Schornack, S., Bono, J. J., Cook, D. R., Ané, J. M. (2007) A novel nuclear protein interacts with the symbiotic DMI3 calcium- and calmodulin-dependent protein kinase of *Medicago truncatula*. *Mol. Plant-Microbe Interact.,* 20: 912–921.

Mitra, R.M. and Long, S.R. (2004) Plant and bacterial symbiotic mutants define three transcriptionally distinct stages in the development of the *Medicago truncatula*/*Sinorhizobium meliloti* symbiosis. *Plant Physiol.,* 134: 595–604.

Morzhina, E,V., Tsyganov, V.E., Borisov, A.Y., Lebsky, V.K., Tikhonovich, I.A. (2000) Four developmental stages identified by genetic dissection of pea (*Pisum sativum* L.) root nodule morphogenesis. *Plant Science*, 155: 75–83.

Murray, J. D., Karas, B. J., Sato, S., Tabata, S., Amyot, L., Szczyglowski, K. (2007) A cytokinin perception mutant colonized by *Rhizobium* in the absence of nodule organogenesis. *Science* 315: 101–104.

Naisbitt, T., James, E.K., Sprent, J.I. (1992) The evolutionary significance of the legume genus *Chamaecrista*, as determined by nodule structure. *New Phytol.,* 122: 487–492.

Oldroyd, G. E., Murray, J. D., Poole, P. S., Downie, J. A. (2011) The rules of engagement in the legume-rhizobial symbiosis. *Annul. Rev. Genet.,* 45: 119–144.

Oldroyd, G.E.D. and Downie, J.A. (2006) Nuclear calcium changes at the core of symbiosis signalling. *Curr. Opin. Plant Biol.,* 9: 351–357.

Oldroyd, G.E. and Downie, J.A. (2004) Calcium, kinases and nodulation signalling in legumes. *Nat. Rev. Mol. Cell Biol.*, 5: 566–576.

Oono, R., Schmitt, I., Sprent, J.I., Denison, R.F. (2010) Multiple evolutionary origins of legume traits leading to extreme rhizobial differentiation. *New Phytol.,* 187: 508–520.

Op den Camp, R., Streng, A., De Mita, S., Cao, Q., Polone, E., Liu, W., Ammiraju, J.S.S., Kudrna, D., Wing, R., Untergasser, A., et al. (2011) LysM-Type Mycorrhizal Receptor Recruited for Rhizobium Symbiosis in Nonlegume *Parasponia. Science*, 331(6019): 909–912.

Ott, T., van Dongen, J.T., Gunther, C., Krusell, L., Desbrosses, G., Vigeolas, H., Bock, V., Czechowski, T., Geigenberger, P., Udvardi, M.K. (2005) Symbolic leghemoglobins are crucial for nitrogen fixation in legume root nodules but not for general plant growth and development. *Curr. Biol.,* 15: 531–535.

Parniske M. (2000) Intracellular accommodation of microbes by plants: a common developmental program for symbiosis and disease? *Curr. Opin. Plant Biol.,* 3: 320–328.

Parniske, M. (2008) Arbuscular mycorrhiza: The mother of plant root endosymbioses. *Nat. Rev. Microbiol.,* 6: 763–775.

Patriarca, E.J., Tate, R., Iaccarino, M. (2002) Key role of bacterial metabolism in *Rhizobium*-plant symbiosis. *Microbiol. Mol. Biol. Rev.,* 66: 203–222.

Plet, J., Wasson, A., Ariel, F., Le Signor, C., Baker, D., Mathesius, U., Crespi, M., Frugier, F. (2011) MtCRE1-dependent cytokinin signaling integrates bacterial and plant cues to coordinate symbiotic nodule organogenesis in *Medicago truncatula*. *Plant J.,* 65: 622–633.

Popp, C. and Ott, T. (2011) Regulation of signal transduction and bacterial infection during root nodule symbiosis. *Cur. Opin. Plant Biol.,* 14: 458–467.

Postma, J.G., Jager, D., Jacobsen, E., Feenstra, W.J. (1990) Studies on a non-fixing mutant of pea (Pisum sativum L.). 1. Phenotypical description and bacteroid activity. *Plant Science,* 68: 151–161.

Prell, J., White, J. P., Bourdes, A., Bunnewell, S., Bongaerts, R. J., Poole, P. (2009) Legumes regulate *Rhizobium* bacteroid development and persistence by the supply of branched-chain amino acids. Proc. Natl. Acad. Sci. U.S.A., 106: 12477–12482.

Prell, J., Bourdès, A., Kumar, S., Lodwig, E., Hosie, A., Kinghorn, S., White, J., Poole, P. (2010) Role of symbiotic auxotrophy in the *Rhizobium*-legume symbioses. *PLoS ONE*, 5: e13933.

Radutoiu, S., Madsen, L.H., Madsen, E.B., Felle, H.H., Umehara, Y., Gronlund, M., Sato, S., Nakamura, Y., Tabata, S., Sandal. N., et al. (2003) Plant recognition of symbiotic bacteria requires two LysM receptor-like kinases. *Nature* 425: 585–592.

Roth, L.E. and Stacey, G. (1989) Bacterium release into host cells of nitrogen-fixing soybean nodules: the symbiosome membrane comes from three sources. *Eur. J. Cell Biol.,* 49:13–23.

Robertson, J.G. and Lyttleton, P. (1984) Division of peribacteroid membranes in root nodules of white clover. *J. Cell Sci*., 69:147–157.

Robertson, J.G. and Lyttleton, P. (1982) Coated and smooth vesicles in the biogenesis of cell walls, plasma membranes, infection threads, and peribacteroid membranes in root hairs and nodules of white clover. *J. Cell Sci.,* 58: 63–78.

Saito, K., Yoshikawa, M., Yano, K., Miwa, H., Uchida, H., Asamizu, E., Sato, S., Tabata, S., Imaizumi-Anraku, H., Umehara, Y. et al. (2007) NUCLEOPORIN85 is required for calcium spiking, fungal and bacterial symbioses, and seed production in *Lotus japonicus. Plant Cell***,** 19: 610–624.

Schauser, L., Roussis, A., Stiller, J., Stougaard, J. (1999) A plant regulator controlling development of symbiotic root nodules. *Nature* 402: 191–195.

Schneider, A., Walker, S.A., Poyser, S., Sagan, M., Ellis, T.H., Downie, J.A. (1999) Genetic mapping and functional analysis of a nodulation-defective mutant (*sym19*) of pea (*Pisum sativum* L.). *Mol. Gen. Genet.,* 262: 1–11.

Sheahan, M.B., Rose, R.J., McCurdy, D.W. (2004) Organelle inheritance in plant cell division: the actin cytoskeleton is required for unbiased inheritance of chloroplasts, mitochondria and endoplasmic reticulum in dividing protoplasts. *Plant J*., 37: 379–390.

Smit, P., Limpens, E., Geurts, R., Fedorova, E., Dolgikh, E., Gough, C., Bisseling, T. (2007) Medicago LYK3, an entry receptor in rhizobial nodulation factor signalling. *Plant Physiol.,* 145: 183–191.

Smit, P., Raedts, J., Portyank,o V., Debelle, F., Gough. C., Bisseling, T., Geurts, R. (2005) NSP1 of the GRAS protein family is essential for rhizobial Nod factor–induced transcription. *Science* 308: 1789–1791.

Soupène, E., Foussard, M., Boistard, P., Truchet, G., and Batut, J. (1995) Oxygen as a key developmental regulator of *Rhizobium meliloti* N2-fixation gene expression within the alfalfa root nodule. *Proc. Natl. Acad. Sci. USA,* 92: 3759–3763.

Sprent, J.I. (2007) Evolving ideas of legume evolution and diversity: a taxonomic perspective on the occurrence of nodulation*. New Phytol.,* 174: 11–25.

Stracke, S., Kistner, C., Yoshida, S., Mulder, L., Sato, S., Kaneko, T., Tabata, S., Sandal, N., Stougaard, J., Szczyglowski, K., Parniske, M. (2002) A plant receptor-like kinase required for both bacterial and fungal symbiosis. *Nature* 417: 959–962.

Sullivan, J. T. and Ronson, C. W. (1998) Evolution of rhizobia by acquisition of a 500-kb symbiosis island that integrates into a phe-tRNA gene. *Proc. Nat. Acad. Sci. USA,* 95: 5145–5149.

Teillet, A., Garcia, J., de Billy, F., Gherardi, M., Huguet, T., Barker, D.G., de Carvalho-Niebel, F., Journet, E.P. (2008) *api*, a novel *Medicago truncatula* symbiotic mutant impaired in nodule primordium invasion. *Mol. Plant-Microbe Interact.,* 21: 535–546.

Timmers, A.C., Auriac, M.C., de Billy, F., Truchet, G. (1998) Nod factor internalization and microtubular cytoskeleton changes occur concomitantly during nodule differentiation in alfalfa. *Development* 125: 339–349.

Tirichine, L., Imaizumi-Anraku, H., Yoshida, S., Murakami, Y., Madsen, L.H., Miwa, H., Nakagawa, T., Sandal, N., Albrektsen, A. S., Kawaguchi, M. et al. (2006) Deregulation of a Ca2+/calmodulin-dependent kinase leads to spontaneous nodule development. *Nature* 441: 1153–1156.

Tirichine, L., Sandal, N., Madsen, L.H., Radutoiu, S., Albrektsen, A. S., Sato, S., Asamizu, E., Tabata, S., Stougaard, J. (2007) A gain-of-function mutation in a cytokinin receptor triggers spontaneous root nodule organogenesis. *Science* 2315: 104–107.

Truchet, G., Roche, P., Lerouge, P., Vasse, J., Camut, S., de Billy, F., Prome, J., Denarie, J. (1991) Sulphated lipo-oligosaccharide signals of *Rhizobium meliloti* elicit root nodule organogenesis in alfalfa. *Nature* 351: 670–673.

Tsyganov, V.E., Morzhina, E.V., Stefanov, S.Y., Borisov, A.Y., Lebsky, V.K., Tikhonovich, I.A. (1998) The pea (*Pisum sativum* L) genes *sym33* and *sym40* control infection thread formation and root nodule function*. Mol. Gen. Genet.,* 259: 491–503.

Tu, J.C. (1974) Relationship between the membrane envelopes of rhizobial bacteroids and the plasma membrane of the host cell as demonstrated by histochemical localization of adenyl cyclase. *J. Bacteriol.,* 119: 986–991.

Van de Velde, W., Zehirov, G., Szatmari, A., Debreczeny, M., Ishihara, H., Kevei, Z., Farkas, A., Mikulass, K., Nagy, A., Tiricz, et al. (2010) Plant peptides govern terminal differentiation of bacteria in symbiosis. *Science* 327: 1122–1126.

Vasse, J., de Billy, F., Camut, S., Truchet, G. (1990) Correlation between ultrastructural differentiation of bacteroids and nitrogen fixation in Alfalfa nodules. *J. Bacteriol.,* 172: 4295–4306.

Veereshlingam, H., Haynes, J.G., Sherrier, D.J., Penmetsa, R.V., Cook, D.R., Dickstein, R. (2004) *nip*, a symbiotic *Medicago truncatula* mutant that forms root nodules with aberrant infection threads and plant defense-like response. *Plant Physiol.,* 136: 3692–3702.

Vernié, T., Moreau, S., de Billy, F., Plet, J., Combier, J. P., Rogers, C., Oldroyd, G., Frugier, F., Niebel, A., Gamas, P. (2008) EFD is an ERF transcription factor involved in the control of nodule number and differentiation in *Medicago truncatula*. *Plant Cell,* 20: 2696–2713.

Via, L. E., Deretic, D., Ulmer, R. J., Hibler, N. S., Huber, L. A. Deretic, V. (1997) Arrest of mycobacterial phagosome maturation is caused by a block in vesicle fusion between stages controlled by rab5 and rab7. *J. Biol. Chem.,* 272: 13326–13331.

Vindarell, J.M., Fedorova, E., Cebolla, A., Kevei, Z., Horvath, G., Kelemen, Z., Tarayre, S., Roudier, F., Mergaert, P., Kondorosi, A., Kondorosi, E. (2003) Endoreduplication Mediated by the Anaphase-Promoting Complex Activator CCS52A Is Required for Symbiotic Cell Differentiation in *Medicago truncatula* Nodules. *Plant Cell,* 15(9): 2093–2105.

Voroshilova, V. A., Demchenko, K. N., Brewin, N. J., Borisov, A. Y., Tikhonovich I. A. (2009) Initiation of a legume nodule with an indeterminate meristem involves proliferating host cells that harbour infection threads. *New Phytol.,* 181: 913–923.

Wang, D., Griffitts, J., Starker, C., Fedorova, E., Limpens, E., Ivanov, S., Bisseling, T., Long S.R. (2010) A nodule-specific protein secretory pathway required for nitrogen-fixing symbiosis. *Science* 327: 1126–1129.

Wildermuth, M.C. (2010) Modulation of host nuclear ploidy: a common plant biotroph mechanism. *Cur. Opin. Plant Biol.*, 13: 1–10.

White, J., Prell, J., James, E.K., Poole, P. (2007) Nutrient Sharing between Symbionts. *Plant Physiol.,* 144: 604–614.

Whitehead, L. F. and Day, D. A. (1997) The peribacteroid membrane. *Physiol. Plant.,*100: 30–44.

Wojciechowski, M. F., Lavin, M., Sanderson, M. J. (2004) A phylogeny of legumes (*Leguminosae*) based on analysis of the plastid *matK* gene resolves many well-supported sublcades within the family. *Am. J. Bot.,* 91: 1846–1862.

Yang, W.C., de Blank, C., Meskiene, I., Hirt, H., Bakker, J., van Kammen, A., Franssen, H., Bisseling, T. (1994) *Rhizobium* Nod Factors Reactivate the Cell Cycle during Infection and Nodule Primordium Formation, but the Cycle is Only Completed in Primordium Formation. *Plant Cell*, 6: 1415–1426.

Yang, W.C., Horvath, B., Hontelez, J., van Kammen, A., Bisseling, T. (1991) *In situ* localization of *Rhizobium* RNAs in pea root nodules: *nifA* and *nifH* localization. *Mol. Plant-Microbe Interact.,* 4: 464–468.

Yano, K., Yoshida, S., Müller, J., Singh, S., Banba, M., Vickers, K., Markmann, K., White, C., Schuller, B., Sato, S., et al. (2008) CYCLOPS, a mediator of symbiotic intracellular accommodation. *Proc. Natl. Acad. Sci. USA,* 105: 20540–20545.

Yendrek, C. R., Lee, Y. C., Morris, V., Liang, Y., Pislariu, C. I., Burkart, G., Meckfessel, M. H., Salehin, M., Kessler, H., Wessler, H., et al. (2010) A putative transporter is essential for integrating nutrient and hormone signaling with lateral root growth and nodule development in *Medicago truncatula*. *Plant J.,* 62: 100–112.

Young, N.D., Debellé, F., Oldroyd, G.E.D., Geurts, R., Cannon, S.B., Udvardi, M.K., Benedito, V.A., Mayer, K.F., Gouzy, J., Schoof, H. et al. (2011) The *Medicago* genome provides insight into the evolution of rhizobial symbioses. *Nature* 480: 520–524.

Zhukov, V., Radutoiu, S., Madsen, L.H., Rychagova, T., Ovchinnikova, E., Borisov, A., Tikhonovich, I., Stougaard, J. (2008) The Pea *Sym37* Receptor Kinase Gene Controls Infection-Thread Initiation and Nodule Development. *Mol. Plant-Microbe Interact.,* 21(12): 1600–1608.

Chapter 2

Synteny-based cloning of pea symbiotic genes using Medicago as intergenomic cloning vehicle

Evgenia Ovchinnikova,[1,2] Alexey Borisov,[2] Igor Tikhonovich,[2] Ton Bisseling,[1] and Erik Limpens[1]

[1] Wageningen University, laboratory of Molecular Biology; Droevendaalsesteeg 1, 6708 PB, Wageningen, The Netherlands;

[2] All-Russia Research Institute for Agricultural Microbiology, laboratory of Genetics of Plant-Microbe Interactions; Podbelsky chaussee 3, 196608, Pushkin 8, St. Petersburg, Russia

ABSTRACT

Garden pea (*Pisum sativum* L.) has been extensively used as a genetic system to study the Rhizobium-legume symbiosis. More than 40 pea symbiotic mutants have been characterized. However, its large genome size, low capability for genetic transformation and lack of extensive genomic tools severely hamper the positional cloning of the corresponding genes. Pea is part of the Papillionoideae legume subfamily and is closely related to the model legume *Medicago truncatula* (Medicago). It has been shown that there is extensive synteny between the pea and Medicago genomes. Therefore, Medicago offers a powerful alternative to exploit the wealth of pea genetics through comparative genomics. Here, we developed several tools to positionally clone the pea symbiotic mutants *sym31*, *sym33,* and *sym41*, which are impaired in their ability to form nitrogen-fixing symbiosomes, via a synteny-based approach using Medicago as intergenomic cloning vehicle. These tools include the development of a set of cross-species gene-based markers that link the pea and Medicago genetic maps. Furthermore, an *Agrobacterium rhizogenes* mediated root transformation protocol was developed to generate transgenic roots in pea. We provide a proof of principle that this transformation system can be used to complement pea symbiotic mutants using orthologous genes from Medicago.

INTRODUCTION

Historically, garden pea (*Pisum sativum* L.) has been the subject of numerous genetic and physiological studies because of its ease of production, autogamous and diploid nature, relatively short generation cycle and wealth of morphological variation (Knight, 1799; Mendel, 1866; McPhee 2007). Furthermore, pea is cultured worldwide as an important legume crop that is able to establish a nitrogen-fixing symbiosis with Rhizobium bacteria (rhizobia). Despite the long history of pea genetics (for review see McPhee, 2007), pea is currently unpopular as a model for genetic analysis (Ellis and Poyser, 2002). Its large genome size (~4300 Mb), low capacity for genetic transformation and lack of extensive genomics tools complicate traditional positional cloning in pea. Therefore, relatively few genes underlying the many interesting mutants have so far been identified (Ellis and Poyser, 2002).

From a genetic point of view, the nitrogen-fixing symbiosis between pea and *Rhizobium leguminosarum* bv. *viciae* is the most developed genetic system to study developmental processes in plant-microbe interactions (Borisov et al., 2004). More than 250 pea symbiotic mutants have been independently obtained in different laboratories throughout the world (Morzhina et al., 2000; Borisov et al., 2007). Intensive phenotypic and genetic allelism analysis of these mutants has allowed the identification of about 40 pea genes involved in development of the symbiosis (Tsyganov et al., 2002). However, only eight of the 40 symbiotic pea genes have been cloned in the last 20 years (Borisov et al., 2007). Therefore, two legume species *Medicago truncatula* (Medicago) and *Lotus japonicus* (Lotus) have been developed as model systems to unravel the molecular basis of the nitrogen-fixing symbiosis (Cook, 1999; Handberg and Stougaard, 1992; Jiang and Gresshoff, 1997).

These model species offer a powerful alternative to exploit the wealth of pea genetics through comparative genomics. It has become clear that the genomes of closely related plant species show a conserved gene order, i.e. synteny (Bennetzen, 2000; Schmidt, 2000). Therefore, comparative genetic mapping can facilitate gene discovery among related species (Delseny, 2004). Pea is taxonomically closely related to the model legume Medicago. Both belong to the legume subfamily of Papillionoideae and develop nodules with an indeterminate meristem (Vasse et al., 1990; Doyle et al., 1997). In contrast to pea, Medicago has a relatively small genome (~500 Mb); it is amenable for genetic transformation, and importantly, many genomics tools are available now in Medicago, including retrotransposon-tagged populations, genome-wide transcript-profiling platforms and a sequenced genome (Benedito et al., 2008; Tadege et al., 2008; Young et al., 2011).

Several recent comparative genomics studies have studied the syntenic relationship between pea and Medicago spp. and have shown a good conservation of gene order in both genomes (Choi et al., 2004; Kaló et al., 2004; Aubert et al., 2006). Because of this high level of synteny between pea and Medicago, the position of genes in the pea genome can be inferred from the location of their counterparts in the Medicago reference genome. Furthermore, comparable

phenotypes between pea and model legume mutants combined with syntenic map-positions greatly facilitate the identification of the underlying genes in the legume crop. Such strategies have been successfully used to identify the pea Nod factor signalling genes *PsSym19* (Endre et al., 2002; Stracke et al., 2002), *PsSym35* (Borisov et al., 2003), and *PsSym37* (Zhukov et al., 2008).

In addition to map-based gene identification strategies, a key component of most functional genomics approaches is an efficient transformation system (Somers et al., 2003). Although protocols for stable transformation of pea using *Agrobacterium tumefaciens* have been developed, the regeneration of transgenic peas still is not a routine (Pniewski and Kapusta, 2005). Transformed pea plants have been regenerated mainly via de novo (callus) organogenesis (Puonti-Kaertas et al., 1990; Schroeder et al., 1993; Grant et al., 1995) or directly from meristems (Davies et al., 1993; Bean et al., 1997; Nadolska-Orczyk and Orczyk, 2000). However, most of these procedures involve a long regeneration period, sometimes up to 9 months (Bean et al., 1997; Polowick et al., 2000; Grant et al., 1995) and have low (up to 4%) efficiency of transformation (Pniewski and Kapusta, 2005). As an alternative to stable transformation, *Agrobacterium rhizogenes* mediated root transformation, also called hairy root transformation has been successfully used in legumes to study root biology and symbiosis. *A. rhizogenes* induces the formation of adventitious genetically transformed roots at the site of inoculation, resulting in composite plants with a non-transformed/non-transgenic shoot (Chilton et al., 1982). The resulting transgenic roots can be nodulated and infected by arbuscular mycorrhizal fungi. Furthermore, *A. rhizogenes* transformed roots can be clonally propagated as root cultures. Rapid and efficient transformation protocols have been developed for model legumes such as Medicago (Limpens et al., 2004; Chabaud et al., 2006) and are widely used to study root endosymbioses. Pea also has been shown to be susceptible to this type of transformation (Bécard and Fortin, 1988; Schaerer and Pilet, 1991; Wen et al., 1999). However, low nodulation efficiency of pea hairy roots has likely hampered the more widespread use of this system to study the Rhizobium symbiosis in pea (Hohnjec et al., 2003; Clemow et al., 2011).

In this chapter, we describe the development of various tools to exploit the extensive Medicago genome information to clone symbiotic genes in pea. In our studies, we focused on three pea mutants *Pssym33* (Tsyganov et al., 1998), *Pssym41* (Morzhina et al., 2000; Voroshilova et al., 2008), and *Pssym31* (Borisov et al., 1992), which are impaired in their ability to form nitrogen-fixing organelle-like structures called symbiosomes (Roth and Stacey, 1989). The efficient use of a synteny-based positional cloning strategy requires a good integration of the genetic maps of pea and Medicago by using cross-species (gene-based) molecular markers (Choi et al., 2004; Aubert et al., 2006). Using the comparative mapping study by Aubert et al. (2006) as starting point, we developed a set of Medicago-pea cross-species markers that cover the seven pea linkage groups to map the mutant loci. Additional cross-species makers were developed to fine map the mutant loci in the genomic regions of interest. To support the

identification of mutated pea genes and to facilitate the genetic complementation of the mutants, we developed and compared two *A. rhizogenes* mediated root transformation protocols on three pea wild-type genotypes. In addition, we provide a proof-of-principle that this transformation system can be used to complement pea symbiotic mutants using orthologous genes from Medicago.

RESULTS AND DISCUSSION

Cross-species molecular markers for map-based cloning of pea symbiotic genes

Pea (*Pisum sativum* L.) currently has the most extensive and best-characterized set of mutants that are impaired in symbiosome development (Borisov et al., 2007). We focused on three pea mutants: *sym31* (Borisov et al., 1992), *sym33* (Tsyganov et al., 1998; Voroshilova et al., 2001), and *sym41* (Morzhina et al., 2000) those are disturbed in their ability to form nitrogen-fixing symbiosomes and aimed to clone the corresponding genes (see Chapters 3, 4, and 5). In previous studies, *PsSym31* and *PsSym33* have been localized to linkage groups III (Rosov et al., 1994; Men et al., 1999) and I (Tsyganov et al., 2006), respectively. The location of *PsSym41* was not determined. To (fine) map the mutant loci, several segregating mapping population were made by crossing the mutant lines with wild type (WT) lines that are genetically distant from the mutant genotypes (Table 1). The resulting F2 populations were analyzed for segregating mutant and WT nodule phenotypes: white (Fix^-) nodules versus pink (Fix^+) nodules (Table 1).

Table 1. Mutants and segregating populations

Mutant	Nodule phenotype	Mapping stage	Line	Genetic background	Mapping segregating population
Pssym33	Nod^+ Fix^-	Mapped to LGI (Tsyganov et al., 2006)	RisFixU SGEFix$^-$-2 SGEFix$^-$-5	Finale SGE SGE	F2 (♀WT10584 x ♂SGEFix$^-$-2) 95 plants: 73 Fix^+/23 Fix^-
Pssym41	$Nod^{+/-}$ Fix^-	Not mapped	RisFixA	Finale	F2 (♀NGB1238 x ♂RisFixA) 100 plants: 74 Fix^+/26 Fix^-
Pssym31	Nod^+ Fix^-	Mapped to LGIII (Rosov et al., 1994; Men et al., 1999)	Sprint2Fix$^-$	Sprint2	F2 (♀NGB1238 x ♂Sprint2Fix$^-$) 75 plants: 52 Fix^+/23 Fix^- F2 (♀SGE x ♂Sprint2Fix$^-$) 115 plants: 88 Fix^+/27 Fix^- F2 (♀NGB851 x ♂Sprint2Fix$^-$) 65 Fix^- plants

To map the location of the mutant loci and to link their location to syntenic regions in Medicago, cross-species functional/gene-based markers were developed. Therefore, the gene-based markers developed by Aubert et al. (2006) were initially chosen as starting point (Table 2). These markers have been integrated with previous pea genetic maps and were used to link the pea and Medicago genetic maps (Laucau et al., 1998; Lorridon et al., 2005; Aubert et al., 2006). Because the mutant and parental lines used in our study are different from the ones used by Aubert and colleagues, these PCR-based marker genes were amplified in three different genetic backgrounds (Table 1) and fragments were analyzed for polymorphisms. Next, the identified polymorphisms were converted to cleaved amplified polymorphic sequence (CAPS) markers, CAPS-derived markers or used as size molecular markers. Such PCR-based markers have been shown to be reliable and convenient for co-segregation analysis (Konieczny and Ausubel, 1993; Aubert et al., 2006; Haliassos et al., 1989; Sorscher and Huang, 1991). Thus, 35 gene-based markers were developed that cover the seven linkage groups in pea although not all genetic backgrounds (SGE, NGB1238, and Finale) are polymorphic for all marker loci (see Table 2). The corresponding Medicago genes and their location in the genome were verified by the reciprocal Basic Local Alignment Search Tool (BLAST) analyses.

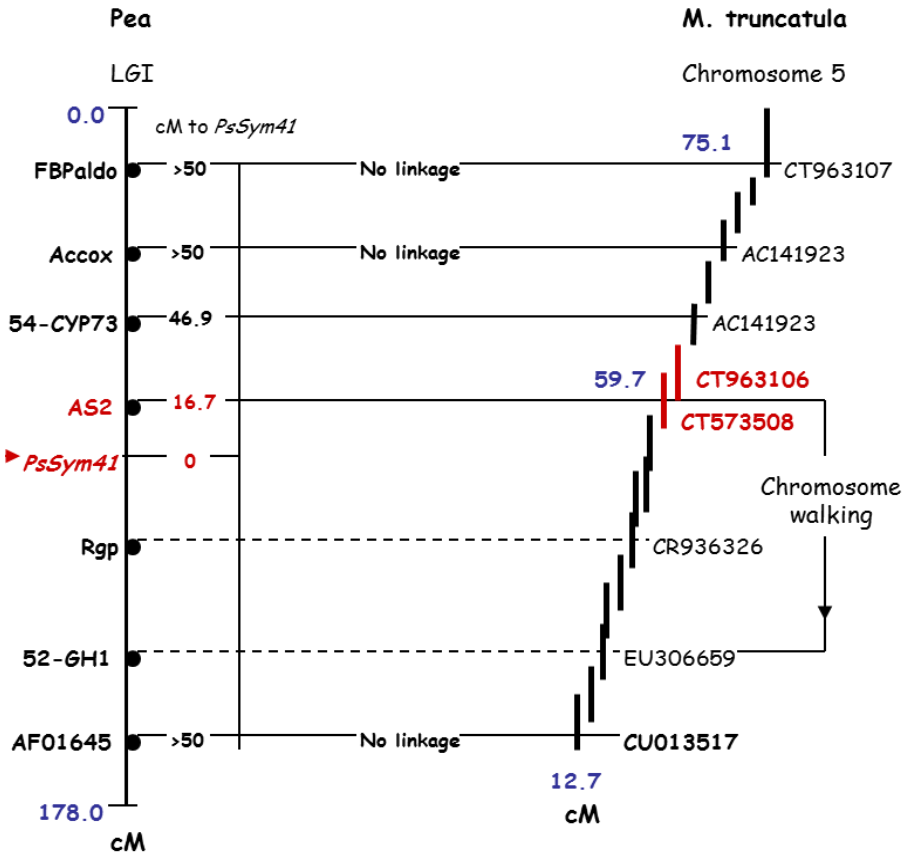

Fig.1. An approximate location of *PsSym41* in LGI of pea and corresponding chromosome 5 of *M. truncatula*. Marker AS2 showed the closest linkage with *PsSym41* is highlighted in red. Correspondence of the markers on pea LGI to BAC clones in the Medicago chromosome 5 is schematically shown by connectors; BAC clones corresponding to AS2 are also highlighted in red. Lines in dashes indicate markers that were not tested because of absence of polymorphism between Finale and NGB1238. Arrows indicate "chromosome walking" directions for fine mapping of *PsSym41* in the corresponding region of Medicago.

Table 2. General set of cross-species gene-based molecular markers developed to identify a linkage group for *PsSym41*

Linkage group, *pea*	Chromosome, *M.truncatula*	Marker name	Accession number		Marker type	Enzyme	Cleaved polymorphism (parental line)	Gene product name
			P.sativum	*M.truncatula*				
I	5	FBPaldo	X89828	CT963107.2	CAPS	SpeI	NGB1238 vs. Finale	Pisum sativum fructose-1, 6-biphosphate aldolase
	5	Accox	CD859427 CD859452	AC137995.31 CR931731.1	CAPS	RsaI	NGB1238 vs. Finale	1-aminocyclopropane-1-carboxylate oxidase
	5	54-CYP73	AF175275	AC141923.27	CAPS	NlaIII	NGB1238 vs. Finale, SGE	Pisum sativum trans-cinnamic acid hydroxylase (CYP73A9)
	5	**AS2**	X52180.1	CT963106.2 CT573508.2	CAPS	RsaI	Finale vs. NGB1238	Pisum sativum asparagine synthase 2
	5	Rgp	U31565	CR936326.2	CAPS	MboI	NGB1238, Finale vs. SGE	Pisum sativum reversibly glycosylatable polypeptide (RGP1)
	5	52-GH1	M87649	EU306659.1	CAPS	HhaI	NGB1238, Finale vs. SGE	Pisum sativum serine hydroxymethyltransferase
	5	AF01645	AF016460	CU179904.1 CU013517.1	dCAPS	TasI	NGB1238 vs. Finale	Pisum sativum 1-aminocyclopropane-1-carboxylate synthase
II	1	ThiolP	X66061	AC150207.2 XM_003589085	size	–	NGB1238 (650 bp) vs. Finale, SGE (750 bp)	Pisum sativum thiol protease
	1	PepTrans	CD860432	AC157646.35 AC202380.14	dCAPS	VspI	NGB1238 vs. Finale	Putative peptide/amino-acid transporter
	4	Gbsts1	X88789	BT052863.1 AC146329.20	CAPS	MaeII	NGB1238 vs. Finale	Granule-bound starch synthase I
	4	cOMT	CD858528	XM_003605697 AC146649.17	CAPS	HinfI	NGB1238 vs. Finale	Caffeic acid 3-O-methyltransferase
	4	Sut1	AF109922	AJ459790 AC152499.17	CAPS	AluI	NGB1238, Finale vs. SGE	Pisum sativum sucrose transport protein SUT1
	1	14-MCC	AB075695	AC139748.13	CAPS	HpaI	NGB1238 vs. Finale	Pisum sativum MCC gene for 3-methylcrotonyl CoA carboxylase
III	3	Agpl1	X96766	CU468264.8	CAPS	AvaII	NGB1238 vs. Finale	ADP-glucose pyrophosphorylase
	3	MAX4	AY557341	CR956392 XM_003603563	CAPS	MboI DraI	NGB1238 vs. Finale	Auxin-inducible polyene dioxygenase

Table 2. (Continued)

	3	Uni	AF010190	AC139708 AY928184	CAPS	TagI	NGB1238 vs. Finale	Unifoliata protein
	3	AS1	Y13321 X52179	CT030028.4	size	–	NGB1238, Finale (600 bp), vs. SGE (700 bp)	AS1 asparagine synthase
	3	Gpt	AF020814	AC122170.28 XM_003599898	CAPS	MseI	NGB1238, SGE vs. Finale	Glucose-6-phosphate/phosphate-translocator
	3	Eno12B	X56232	X68032.1 CU570869.3	CAPS	NlaIII	NGB1238 vs. Finale vs. SGE	Early nodulin 12B
	2	PepC	D64037	AC125474.16 XM_003596337	CAPS	MseI	NGB1238 vs. Finale, SGE	Phosphoenolpyruvate carboxylase (PEPC)
IV	8	Xyft	AF223643	TC66794	size	–	NGB1238, SGE (200 bp) vs. Finale (150 bp)	Xyloglucan fucosyltransferase
	-	NTH1	U44947	XM_003589087	CAPS	AvaII	NGB1238 vs. Finale	Cysteine protease homolog
	-	Soc1B	AY826729.1	BT136118	CAPS	MseI	NGB1238 vs. Finale	Pisum sativum suppressor of CONSTANS 1b
	8	Cwi2	Z83339	TC72333	CAPS	ClaI	NGB1238 vs. Finale	Cell wall invertase II
V	7	SS	AJ001071	AC169516.4	CAPS	HpaI MseI	NGB1238 vs. Finale	Second sucrose synthase
	-	Pore	Z73553	BT051255	dCAPS	HaeIII	NGB1238 vs. Finale	Pore protein
	7	TE002M14	CD860545	AC135311.13 XM_003623864	CAPS	MseI	NGB1238 vs. Finale	60S ribosomal protein L2
	5	Rbcs	X04333	XM_003600254	CAPS	DraI	NGB1238 vs. Finale	Ribulose-1,5-bisphosphate carboxylase small subunit
VI	6	Gbst2	X88790	AC166744.12	CAPS	MboI	NGB1238 vs. Finale	Granule-bound starch synthase
	6	Gly8	FG535482	AC150844	CAPS	BstUI	NGB1238 vs. Finale	Glycosyl transferase, family 8
	6	CD174	EX569166	AC174348.18	CAPS	AluI	NGB1238 vs. Finale, SGE	Protein of unknown function DUF618
VII	4	41-WD40	-	AC146651.10	CAPS	MseI	NGB1238, SGE vs. Finale	WD-40 repeat-containing protein MSI1
	4	Nlm	AJ243308	AC152446.37	CAPS	MaeI	NGB1238 vs. Finale	Nodulin26-like intrinsic protein
	4	Clpser	AJ276507	AC225505 XM_003606832	size	–	NGB1238 (200 bp) vs. Finale (150 bp)	ATP-dependent clp serine protease proteolytic subunit
	4	Pip2	AJ243307	AC229715.11 XM_003606336	CAPS	HpaII	NGB1238 vs. Finale	Putative plasma membrane intrinsic protein

The developed set of markers was used to position *PsSym41* on linkage group I in pea, which is (macro)syntenic to Medicago chromosome 5 (Fig.1). *PsSym41* showed linkage to the marker AS2 (~17 cM), which formed a starting point for chromosome walking to fine map and delineate the map position of *PsSym41* and its syntenic region in Medicago (see Fig.1).

Next, we used the well-characterized physical map (http://medicagohapmap.org/) and extensive sequence information available for Medicago to create additional cross-species markers (Young et al., 2011). Therefore, single/low copy genes were identified based on their genomic location in Medicago and primers were developed to amplify the corresponding pea genes. In case corresponding pea EST sequences were identified by reciprocal BLAST analyses, pea-specific primers were developed. In average, ~50 % of the Medicago-based primers amplified a corresponding fragment from pea genomic DNA. Using this approach, 26 additional cross-species markers were developed and used to fine map *PsSym41*, *PsSym33* and *PsSym31* (for details see Chapters 3-5). After delineating the map position of the mutant loci, their syntenic regions in Medicago were annotated to select candidate genes. Because the mutants show symbiosis/nodule-specific phenotypes, we hypothesized that the corresponding genes should be specifically expressed or transcriptionally upregulated in nodules in comparison to non-inoculated roots or other tissues. Therefore, we examined the expression profiles of the annotated genes using the Medicago Gene Expression Atlas (Benedito et al., 2008; http://mtgea.noble.org/). Further, Medicago mutants with comparable phenotypes that have been mapped to syntenic locations offered an additional criterion to identify candidate genes. Fine mapping of *PsSym33*, *PsSym41*, and *PsSym31* and identification of the corresponding genes is described in chapters 3, 4, and 5, respectively.

Hairy root transformation in pea

The next step to identify a mutant allele is to sequence the pea orthologs of the selected Medicago candidate genes. However, a pea genome has not yet been sequenced and BAC libraries with good genome coverage or extensive EST libraries are currently unavailable for pea. Therefore, obtaining the full-length sequence of a pea gene based on Medicago sequence data is not a trivial task. Furthermore, ultimate prove that an identified mutation causes the observed phenotype, especially when only one mutant allele is available, requires the genetic complementation of that mutant. To facilitate the genetic complementation of pea symbiotic mutants, we developed an *Agrobacterium rhizogenes* mediated root transformation protocol. Further, we tested whether this system could be used to complement pea symbiotic mutants using the orthologous genes from Medicago.

A number of efficient *A. rhizogenes* mediated root transformation protocols have been developed for model and crop legumes such as Medicago (Trieu and Harrison, 1996; Limpens et al., 2004), Lotus (Hansen et al., 1989; Oger et al., 1996), white clover (Larkin et al., 1996), and soybean (Olhoft and Somers, 2001; Kereszt et al., 2007). Based on these protocols, we

developed two protocols for pea and compared their efficiency in generating transgenic roots and nodules in three WT genotypes: SGE, Sprint2, and Finale.

Protocol 1

Protocol 1 was adapted from the efficient Medicago hairy root transformation protocol (Limpens et al., 2004). Because pea seedlings are relatively big and develop a large root system they cannot conveniently be grown on agar plates for a long time as used in the original Medicago protocol. Therefore, pea seedlings were first grown in perlite saturated with Färhaeus medium (Färhaeus et al., 1957) for 5-10 days to develop shoots. Next, the root system and major part of the hypocotyl was removed with a scalpel approximately 3–5 mm below the cotyledons. Plants were immediately placed in perlite saturated with SH emergence medium (Schenk and Hildebrandt, 1971) and inoculated with a culture of the low-virulent *A. rhizogenes* strain ARqual (Quandt et al., 1993). After 14-20 days, plants were transferred to perlite saturated with Färhaeus medium (lacking nitrate) and inoculated with a *Rhizobium leguminosarum* bv. *viciae* culture to induce nodulation.

Protocol 2

Protocol 2 was adapted from reported *A. rhizogenes* transformation protocols that have been used to generate pea hairy root cultures. There, pea plants were germinated and grown in darkness before transformation to increase their susceptibility to *A. rhizogenes* infection (Bécard and Fortin, 1988; Schaerer and Pilet, 1991; Wen et al., 1999). Therefore, germinated pea seedlings were first grown in darkness on agar plates containing Färhaeus medium for 7-12 days. Next, the root and major part of the hypocotyl was removed and an *A. rhizogenes* ARqual culture was injected with a syringe approximately 3–5 mm below the cotyledons. The injected plants were immediately placed in perlite saturated with Färhaeus medium (lacking nitrate, and additionally inoculated with the *A. rhizogenes* culture. After 14-20 days the plants were inoculated with *Rhizobium leguminosarum* bv. *viciae*.

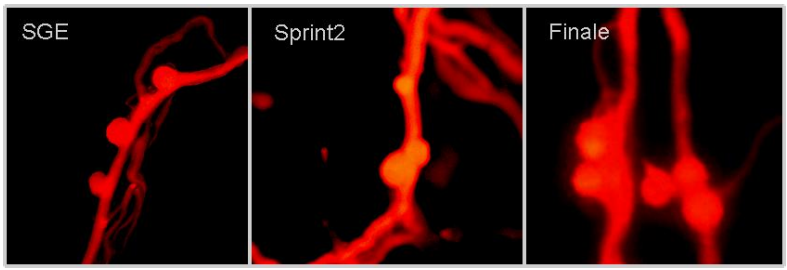

Fig.3. Photographs of pea transgenic roots and nodules expressing DsRED1. Three wild-type genotypes transformed by the empty vector pRedRoot (Limpens et al., 2004) are presented from left to right: SGE, Sprint2 at 21dpi, and Finale at 28 dpi.

Transformation efficiencies

To identify transgenic roots, we used a binary vector containing a red fluorescent reporter gene, which allows the non-destructive selection of transgenic roots and nodules based on the expression of the red fluorescent protein DsRed1 (Limpens et al., 2004). Transformed plants were analyzed 21 days (SGE, Sprint2) or 28 days (Finale) after inoculation with the *Rhizobium leguminosarum* bv. *viciae* strain CIAM1026 using a fluorescence stereo microscope (Fig.3). For both protocols, we analyzed two parameters: the average number of transgenic (red fluorescent) roots per plant and the average number of nodules per transgenic root (Table 3, Fig.4). Protocol 2 resulted in significantly ($P<0.05$) more transgenic roots per plant, ~70-80% of the transformed plants contained at least one transgenic root compared to ~20% of the plants transformed using protocol 1 (Table 3, Fig.4). Pea cultivar Finale developed ~2 times less transgenic roots per transformed plant than the genotypes SGE and Sprint2, indicating that Finale is more recalcitrant to genetic transformation by *A. rhizogenes* than SGE and Sprint2. In addition, the nodulation efficiency was higher ($P<0.05$) in plants transformed according to the protocol 2: ~3-5 nodules per transgenic root in comparison to ~1 formed on transgenic roots of plants transformed according Protocol 1 (Table 3, Fig.4). However, the plants transformed via Protocol 2 showed signs of nitrogen starvation likely due to the relative long growth period in nitrogen-free conditions before inoculation with rhizobia. Plants grown according to Protocol 1 developed normally (data not shown).

Table 3. The data of pea transformation and nodulation of transgenic roots obtained in two independent experiments testing two transformation protocols in three pea genotypes.

Genotype	Results of transformation (criteria)	Protocol 1	Protocol 2
SGE	Number of transformed plants	39.5 ±0.5	40.5 ±0.5
	Number of obtained red roots	9.5 ±0.5	29.5 ±0.5
	Average number of red roots per plant	0.225 ±0.098	0.725 ±0.13
	Average number of nodules per transgenic root	1.4 ±0.37	3.04 ±0.58
Sprint2	Number of transformed plants	40.5 ±0.5	41.5 ±0.5
	Number of obtained red roots	8.5 ±0.5	34±0.5
	Average number of red roots per plant	0.200 ±0.082	0.850 ±0.15
	Average number of nodules per transgenic root	1.0 ±0.47	2.79 ±0.59
Finale	Number of transformed plants	19.5 ±0.5	20.5 ±0.5
	Number of obtained red roots	4.5 ±0.5	8.50 ±0.5
	Average number of red roots per plant	0.200 ±0.092	0.400 ±0.13
	Average number of nodules per transgenic root	1.1 ±0.31	4.87 ±1.16

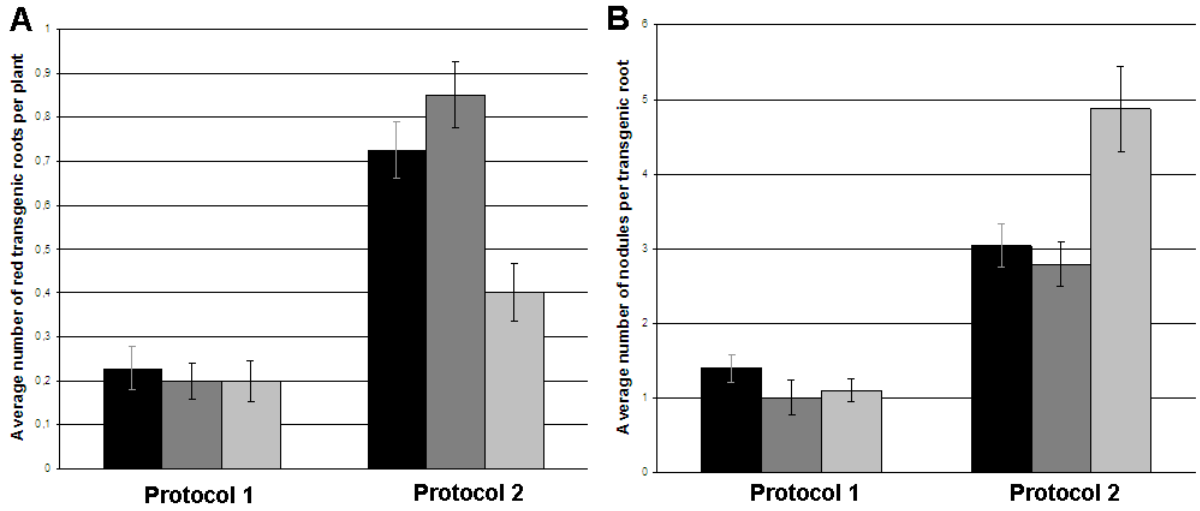

Fig.4. The efficiency of hairy root transformation and nodulation of transgenic roots in three pea genotypes. **A**, Average number of transgenic (red fluorescent) roots per plant; **B**, Average number of nodules per transgenic root. Black bar=SGE, grey bar=Sprint2, pale-grey bar=Finale. Protocol 1=the efficiency of transformation shown for the protocol adapted from the efficient Medicago hairy root transformation protocol (Limpens et al., 2004). Protocol 2=the efficiency of transformation shown for the protocol adapted from reported *A. rhizogenes* transformation protocols that have been used to generate pea hairy root cultures (Bécard and Fortin, 1988; Schaerer and Pilet, 1991; Wen et al., 1999).

Complementation of the pea *sym33* mutant

To facilitate the identification of the genes causing the mutant phenotypes, we tested whether *A. rhizogenes* mediated root transformation could be used to complement the mutant phenotypes by introducing orthologous genes from Medicago. To provide a proof of this principle, we selected the pea *sym33* mutant, which is mutated in the gene encoding the interacting protein of DMI3, IPD3 (Ovchinnikova et al., 2011, see Chapter 3). *Pssym33* is represented by three alleles: SGEFix$^-$-5, SGEFix$^-$-2, and RisFixU that are strongly impaired in their ability to form symbiosomes (Chapter 3; Ovchinnikova et al. 2011). Medicago *sym1/TE7* represents the corresponding *IPD3* mutant in Medicago. To complement the *Pssym33* mutant, a construct was made aimed to express the Medicago *IPD3* gene under the control of a constitutive Ubiquitin3 promoter from Arabidopsis; *UBQ3::GFP-IPD3* (Limpens et al., 2009). *GFP*-tagged *IPD3* was previously successfully used to complement the Medicago *sym1* mutant (Ovchinnikova et al., 2011). Introduction of *UBQ3p::GFP-IPD3* into the *sym1* mutant also fully complemented the mutant phenotype in Medicago (data not shown). Next, we introduced *UBQ3p::GFP-IPD3* into the pea *sym33* mutant allele SGEFix$^-$-5 according to *A. rhizogenes* transformation Protocol 2. SGEFix$^-$-5 plants transformed with an empty vector were used as control. Transgenic nodules (~5 nodules per root) were observed on the control (n=6 roots) and *UBQ3p::GFP-IPD3* transformed SGEFix$^-$-5 roots (n=7 roots) 21 days after inoculation with rhizobia. To examine the nodule phenotype in more detail, semi-thin nodule sections were analyzed by light microscopy. SGEFix$^-$-5 nodules transformed with the empty control vector

were identical to untransformed SGEFix⁻-5 mutant nodules: white nodules with an extensive network of broad hypertrophied infection threads, where symbiosome formation is blocked at the stage of bacterial release from the infection threads (Fig.5A, B). In contrast to the control, the *UBQ3p::GFP-IPD3* transformed SGEFix⁻-5 roots developed nodules with a clearly formed fixation zone where symbiosomes were fully developed and contained single Y-shaped bacteroids (Fig.5C, D). This shows Medicago *IPD3* can complement the pea *sym33/ipd3* mutant.

Very recently, a similar *A. rhizogenes* mediated root transformation method was developed by Clemow and co-workers and used to complement the pea *sym10* mutant using the wild-type pea *Sym10* gene, with a similar efficiency (Clemow et al., 2011). Thus, *A. rhizogenes* mediated root transformation can offer a relatively fast alternative to test the ability of multiple candidates from a syntenic region in Medicago to complement a corresponding pea symbiotic mutant, especially in case the corresponding genes from pea are difficult to isolate.

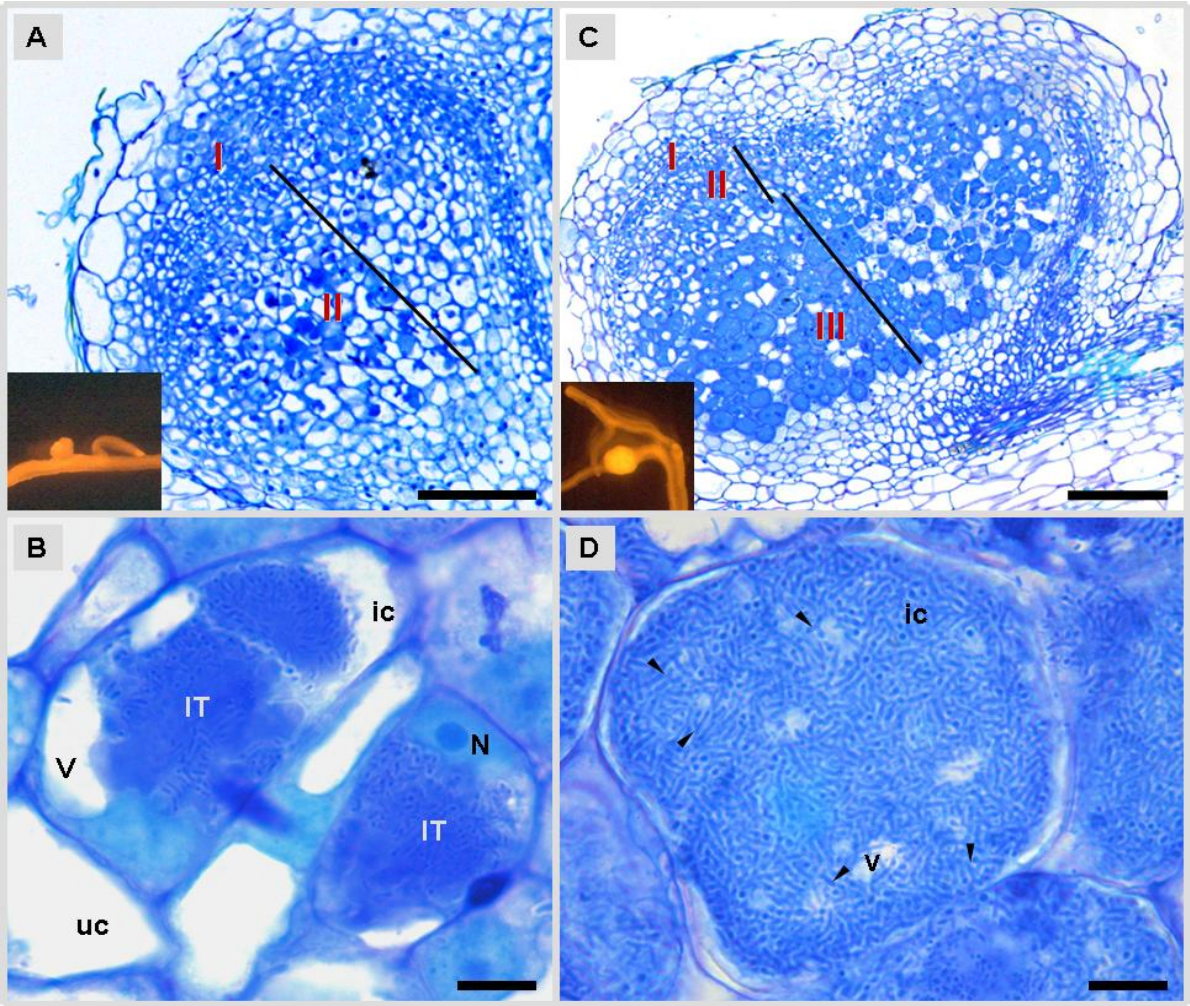

Fig.5. Nodule structural organization of SGEFix$^-$-5 (*sym33*) composite plants at 21 dpi. **A** and **B**, Control SGEFix$^-$-5 transformed by empty vector; **C** and **D**, SGEFix$^-$-5 transformed by *UBQ3p::GFP-MtIPD3*. **A** and **C**, Longitudinal section of the nodule: I – meristematic zone, II – infection zone, III – fixation zone. Note: the nodule of control SGEFix$^-$-5 does not develop zone III. Images of transgenic (red fluorescent) nodules are presented on A and C in the left lower corner. **B**, Nodule cells in zone II contain broad infection threads occupying large parts of the cells. Symbiosome formation is blocked. **D**, Nodule cells in zone III containing Y-shaped differentiated bacteroids (arrowheads). In all micrographs: ic – infected cell, uc – uninfected cell, IT – infection thread, V – vacuole, N – nucleus. Bars: A, C–100 µm; B, D–10 µm.

Conclusion

The extensive synteny between pea and Medicago offers a powerful strategy to clone pea symbiotic genes through comparative genomics. The cross-species gene-based markers developed here provide a core set to position mutant loci on the pea genetic map and to identify their syntenic regions in Medicago. This strategy allowed us to delineate the locations of the symbiosome development pea mutants: *sym33*, *sym41,* and *sym31*. The synteny-based cloning of the corresponding genes is described in the next chapters. Furthermore, the developed *A. rhizogenes* mediated root transformation protocol for pea, using the non-destructive DsRED1 fluorescent reporter, offers an alternative strategy to directly test candidate genes from syntenic regions of Medicago for their ability to complement pea symbiotic mutants.

MATERIALS AND METHODS

Plant lines, bacterial strains, and growth conditions

Homozygous mutant lines, their genetic background lines and the wild-type lines used in mapping populations are listed in Table 1.

Rhizobium leguminosarum bv. *viciae* strain CIAM1026 (Safronova and Novikova, 1996) was used for inoculation of plants in segregation analysis and nodule phenotype evaluation. Inoculation procedure was performed according to Borisov et al. (1997).

Plant seeds were sterilized with concentrated sulfuric acid for 10 min at root temperature. Ten germinated seeds were planted in plastic pots (diameter of 19 cm) with perlite and inoculated with rhizobia after 7 days. Growing plants were supplied with nitrogen free nutrient solution as described in Borisov et al. (1997).

Data collection and statistical analysis

F2 populations of the crosses and parental lines were analyzed in nitrogen free conditions to segregate mutant and WT nodule phenotypes: Fix$^-$ white nodules versus Fix$^+$ pink nodules. Plants were analyzed 28-30 days after inoculation with CIAM1026, which is coincided with early flowering. Total DNA was extracted from leaves of each analyzed plant individually using the standard cetyltrimethylammonium bromide (CTAB) method (Rogers and Bendich, 1985).

X^2 analysis ($\chi^2 > 3.84$ for independent assortment) was used to verify the significance of linkage with molecular markers (SigmaStat 2.3 for Windows, SPSS Inc., Chicago, IL, U.S.A.).

Techniques used to obtain gene-based cross-species molecular markers

PCR-based gene-sequence-polymorphism-derived technique was used to obtain cleaved amplified polymorphic sequence (CAPS), CAPS-derived and size cross-species molecular markers. Gene-based markers developed by Aubert et al. (2006) were initially chosen as starting point. PCR fragments were amplified using pea-specific primers published in Aubert et al. (2006) and sequenced in three genotypes: NGB1238, Finale and SGE. Obtained DNA sequences were analyzed for SNPs using Seqman 8.0.2(16), 412 DNASTAR®.

In case no polymorphisms were found between the three genotypes new primers were designed covering different regions of the corresponding marker genes or primers were designed for a different gene from the same corresponding BAC clone in Medicago genome. We used the well-characterized physical map (http://medicagohapmap.org/) and extensive sequence information available for Medicago to create additional cross-species markers. Single/low copy genes were identified based on their genomic location in Medicago and primers were designed to amplify the corresponding pea genes. Reciprocal BLAST analyses (http://blast.ncbi.nlm.nih.gov/Blast.cgi) were used to verify the likely orthology of the genes in Medicago and pea. In case corresponding pea EST sequences were identified, pea-specific primers were used. Characteristics of the developed gene-based cross-species markers are summarized in Table 2.

PCR assays were performed as described in Aubert et al. (2006). Genotyping conditions to identify the map position of *PsSym41* are listed in Table 3. Genotyping conditions for markers used for fine-mapping of the pea *Sym33*, *Sym41*, and *Sym31* genes are described in the Materials and Methods sections of chapters 3, 4 and 5, respectively.

Table 3. Genotyping conditions of primes for the set of markers used in rough mapping of *Pssym*41

Marker name	Sequence of primers	Annealing t, ºC	PCR fragment size, bp	Origin
FBPaldo	Fw - AAAGCATGTCTGCCTTTGTTGGA Rv - CCATGTCTTGAGTGTGCTTTGCTG	57	1200	Aubert et al., 2006
Accox	Fw - GAATCATGGCATACCTCATGACC Rv - GAGAAGGATGATCCCGCCAG	55	600	Aubert et al., 2006
54-CYP73	Fw - GTCTACGGCGAACATTGGCGTAAAATGC Rv - CAATTGCAGCAACATTGATGTTCTCAACA	50	900	This work
AS2	Fw - CTAATCACACGTTTAGGACCGG Rv - CGAAATCCAAACCGAACCTAATCC	48	370	Aubert et al., 2006
Rgp	Fw - GTATCTCCTTCAAGGATTCGGC Rv - CCCAAATGGTCACAGATAACC	54	1500	Aubert et al., 2006
52-GH1	Fw - ACCACAACTCACAAGTCACTTC Rv - TTGCTGAGAACCTGCTCTTGGTATG	55	720	This work
AF01645	Fw - TGGTGCCACTTCTGCTAATG Rv - AAACCAACCTGGTTCAGTGC	58	1100	Aubert et al., 2006
	dFw - TTCCAATACAATGCACAAGTTCAAACACTTTCCA dRv - GTTTGTTTTCAGACAGCTAATACCGGCTTTTTGC	55	600	Aubert et al., 2006
ThiolP	Fw - CCGAAGAGGATTACCCCTAcCGTGC Rv - GCTTCTCCCCAGCTACCACCCC	58	650 vs. 750	Aubert et al., 2006
PepTrans	Fw - GCCGTGATTCGGATCTGATGG Rv - CGGTCGTATAAAGGAATGACTAC	55	400	Aubert et al., 2006
	dFw - GGATCTGATGGTCCTACCGATAGCCT dRv - ATCCTGCAGGAAAATTGAAATTGCCGATTAA	55	370	Aubert et al., 2006
Gbsts1	Fw - GTCAACTGGCAACCCAATCT Rv - CACTGTAAGTCCACATTATGCC	55	490	Aubert et al., 2006
cOMT	Fw - TTAACTTTGATTTGCCTCATGTT Rv - ATGGTCGTCGCTCCAGTC	50	220	Aubert et al., 2006
Sut1	Fw - GCTGGGCCCTACAACTCTCACT Rv - TTCCCCATCCAATCAGTATCAAAC	57	1000	Aubert et al., 2006
14-MCC	Fw - TGGGAATGTTCTGCATTTGA Rv - GGGATTGACCCATTTTGATG	52	1100	This work
Agpl1	Fw - CGTCGAGAATGTATTGATCTTGG Rv - CAATCCATAATCAGATGCGCGGC	60	400	Aubert et al., 2006
MAX4	Fw - AGGTGGCAAGTGTGGAAGTG Rv - AACTTAGCCCTAGCAACCTCTTC	55	900	This work
Uni	Fw - TGCACCATCTCCCCGTCCCCAGC Rv - AGCAGCACCGTTCCTCTCCGCGT	58	1500	This work
AS1	Fw - GCATCCATCACGTCCGTGTGACG Rv - CGATGTCACTACGATAAGGGCTGC	50	600 vs. 700	Aubert et al., 2006
Gpt	Fw - GTCGGGTCGGTGGTGTCTGATAGACCTTTTTT Rv - CATTGCTGGTCCTTCCACGGCG	58	1100	Aubert et al., 2006
Eno12B	Fw - GGCTTCCCTTTTCTTGTCCTCACTA Rv - AATCAATACCAAAACAACTTCTTACTACC	50	600	Aubert et al., 2006
PepC	Fw - CCGTACCGATGAAATCAAGAGG Rv - GCATCCATCACGTCCGTGTGACG	55	1200	Aubert et al., 2006
Xyft	Fw - GTAGATCGGATCAGCATCGTGG Rv - CTCTGCAATGAGATGCAGTTGC	50	200 vs. 150	Aubert et al., 2006
NTH1	Fw - GAGTTGGGTTGAACGAGTTTTC Rv - TAGTCCCCCATGAGTTCTTCAC	60	1000	Aubert et al., 2006
Soc1B	Fw - TGCTGTTCTATCTTTTGTAATTC Rv - AGCCGGATTAATAATACTCAAACA	47	400	Aubert et al., 2006
Gwi2	Fw - CAGCCATCTTTCCATCTCAACC Rv - TTCCCTTAGCTGAATGCAAAGGGTGCATCG	55	400	Aubert et al., 2006
SS	Fw - GGGAAAGGGATTTTGCAAC Rv - CCATCAACTCACTTTTAACCGG	54	900	Aubert et al., 2006
Pore	Fw - GCCTCGTAGCAGTTTTTCAGGG Rv - CAAAGACAACGGAGACCAAGTG	55	500	Aubert et al., 2006
	dFw - ACTGTTGATGGTTTCTTGAAGATTGGAGCTGT dRv - TTTTGTTGTTGCTGGCTGCAGATACCAGAGGC	55	300	Aubert et al., 2006
TE002M14	Fw - CATGGGGATGCTCAACTGGATTC Rv - CATTTACTGTGGGAAAAAGGCTACTCT	58	1000	Aubert et al., 2006
Rbcs	Fw - TGCTTCTACGGTGCAATCG Rv - GCTCACGGTACACAAATCC	52	800	Aubert et al., 2006
Gbsts2	Fw -GCGGGCTTGGAGATGTTGCT Rv - AACGTGTGTCAGTGCGTATAT	56	800	Aubert et al., 2006
Gly8	Fw - CAGCAATGGATACTACTACGAAACGG Rv - GACAGTTTCCTAATCCAATGAACCCTG	55	570	This work
CD174	Fw - GCATTTGGGAGGAGAGAAAGGTTTTTGG Rv - GACAGCGTATTTTCAACATCTTCTACAAGCTT	55	450	This work
41-WD40	Fw - GGCTGGAATCCAAAGAATGA Rv - GCARTTCTGGTGGACCATC	50	650	This work
Nlm	Fw - GCTTTTCTCTGTTCTTCACAAGC Rv - GAGAGAAGCAGTGTCATGTGCGG	56	230	Aubert et al., 2006
Clpser	Fw - GTATTGGAGGAGGATTTTAGGG Rv - GCTTATGAGTTTGGAGGGGAGGGG	53	200 vs. 150	Aubert et al., 2006
Pip2	Fw - GCCGGTATCTCTGGTATGATACC Rv - CAGGAACATGAGAGTCCCTAGCG	55	2 bands: 600 bp and 400 bp	Aubert et al., 2006

Agrobacterium rhizogenes-mediated plant transformation

Protocol 1. Germinated pea seedlings of Sprint2, SGE, and Finale were grown in grown in perlite saturated with Färhaeus medium (Färhaeus et al., 1957) for 5-10 days to develop shoots. Next, the root system and major part of the hypocotyl was removed with a scalpel approximately 3–5 mm below the cotyledons. Plants were immediately placed in perlite saturated with SH emergence medium (Schenk and Hildebrandt, 1971) and inoculated with 2 ml (OD_{600}=0.5-0.7) culture of the low virulent *A. rhizogenes* strain ARqual (Quandt et al., 1993). After 14-20 days of growth, plants were transferred to perlite saturated with nitrate-free Färhaeus medium and inoculated with *Rhizobium leguminosarum* bv. *viciae*.

Protocol 2. Germinated pea seedlings of Sprint2, SGE and Finale were grown in darkness on agar plates containing Färhaeus medium (Färhaeus et al., 1957) for 7-12 days. Then the root system and major part of the hypocotyl was removed with a scalpel and *A. rhizogenes* culture was injected with syringe approximately 3–5 mm below the cotyledons. The injected plants were immediately placed in perlite saturated with nitrate-free Fähraeus medium and additionally inoculated with 1 ml *A. rhizogenes* culture (OD_{600}=0.5-0.7). After 14-20 days plants were inoculated with *Rhizobium leguminosarum* bv. *viciae*.

Transformed plants were analyzed 21 days (SGE, Sprint2) or 28 days (Finale) after inoculation with the *Rhizobium leguminosarum* bv. *viciae* strain CIAM1026 using a fluorescence stereo microscope.

Complementation of *Pssym33*

We used *Agrobacterium rhizogenes* mediated root transformation as described above in Protocol 2 to complement *Pssym33* (SGEFix$^-$-5 allele) using the *IPD3* gene from Medicago. A plasmid DNA containing *UBQ3p::GFP-MtIPD3* was introduced by standard electroporation into the *Agrobacterium rhizogenes* strain ARqual (Quandt et al., 1993). The Medicago *sym1* mutant was transformed according to Ovchinnikova et al. (2011).

MtIPD3 was PCR-amplified from 14-day-old nodule cDNA using the following primer combinations: MtIPD3-F CACCATGGAAGGGAGAGGATTTTCTGGT and MtIPD3-R TCAAATCTTTCCAGTTTCTGATAGA. The resulting 1,546-bp fragment was directionally cloned into pENTR-D-TOPO (Invitrogen), resulting in pENTR-MtIPD3. To construct *UBQ3::GFP-IPD3*, pENTR-MtIPD3 was recombined into UBQ3-pK7WGF2-RR (Limpens et al. 2009) using LR Clonase II (Invitrogen).

Nodule tissue fixation, staining and microscopy

Nodule tissues were fixed in 5% glutaraldehyde (v/v) in 0.1 M phosphate buffer containing 3% sucrose (w/v) (pH 7.2) under vacuum for 1-2 hours, followed by washing with the buffer and water for 15 min each. Then, ethanol dehydration series: 10%, 30%, 50%, 70%, 90%, and 100%, were carried out for 10 min each. The dehydrated nodules were embedded in Technovit 7100 (Heraeus-Kulzer, Wehrheim, Germany) according to the manufacturers protocol and sectioned on the RJ2035 microtome (Leica Microsystems, Rijswijk, The Netherlands).

Semi-thin (5 µm) nodule sections were stained with 0.05% toluidine blue solution and analyzed using a DM5500B microscope equipped with a DFC425C camera (Leica Microsystems, Wetzlar, Germany).

Transgenic roots and nodules were selected based on DsRED1 expression using a Leica MZFLIII fluorescence stereo microscope fitted with HQ470/40, HQ525/50, HQ553/30, and HQ620/60 optical filters (Leica Microsystems, Rijswijk, The Netherlands).

REFERENCES

Aubert, G., Morin J., Jacquin F.., Loridon K., Quillet M.C., Petit A., Rameau C., Lejeune-Hénaut I., Huguet T., Burstin J. (2006) Functional mapping in pea, as an aid to the candidate gene approach and for investigating the synteny with the model species *Medicago truncatula. Theor. Appl. Genet*, 112: 1024–1041.

Bean, S.J., Gooding, P.S., Mullineaux, P.M., Davies, D.R. (1997) A simple system for pea transformation. *Plant Cell Rep.,* 16: 246–252.

Bécard, G. and Fortin, J.A. (1988) Early events of vesicular-arbuscular mycorrhiza formation on Ri T-DNA transformed roots. *New Phytol.,* 108: 211–218.

Benedito, V.A., Torres-Jerez, I., Murray, J.D., Andriankaja, A., Allen, S., Kakar, K., Wandrey, M., Verdier, J., Zuber, H., Ott, T., Moreau, S., et al. (2008) A gene expression atlas of the model legume *Medicago truncatula*. *Plant J.,* 55(3): 504–513.

Benson, D.A., Karsch-Mizrachi, I., Lipman, D.J., Ostell, J., Wheeler, D.L. (2007) GenBank. *Nucleic Acids Research,* 35: D21–D25.

Bennetzen, J.L. (2000) Comparative sequence analysis of plant nuclear genomes: Microcolinearity and its many exceptions. *Plant Cell,* 12: 1021–1029.

Borisov, A.Yu., Danilova, T.N., Koroleva, T.A., Kuznetsova, E.V., Madsen, L., Mofett, M., Naumkina, T.S., Nemankin, T.A., Ovchinnikova, E.S., Pavlova et al. (2007) Regulatory genes of garden pea (*Pisum sativum* L.) controlling the development of nitrogen-fixing nodules and arbuscular mycorrhiza: a review of basic and applied aspects. *Appl. Biochemistry and Microbiology,* 43(3): 237–243.

Borisov, A.Yu., Danilova, T.N., Koroleva, T.A., Naumkina, T.S., Pavlova, Z.B., Pinaev, A.G., Shtark, O.Yu., Tsyganov, V.E., Voroshilova, V.A., Zhernakov et al. (2004) Pea (*Pisum sativum* L.) regulatory genes controlling development of nitrogen-fixing nodules and arbuscular mycorrhiza: fundamentals and application. *Biologia, Bratislava,* 59/Suppl. 13: 137–144.

Borisov, A.Y., Madsen, L.H., Tsyganov, V.E., Umehara, Y., Voroshilova, V.A., Batagov, A.O., Sandal, N., Mortensen, A., Schauser, L., Ellis, N., et al. (2003) The *Sym35* gene required for root nodule development in pea is an ortholog of *Nin* from *Lotus japonicus. Plant Physiol.,* 131(3): 1009–1017.

Borisov, A.Y., Morzhina, E.V., Kulikova, O.A., Tchetkova, S.A., Lebsky, V.K., Tikhonovich, I.A. (1992) New Symbiotic Mutants of Pea Affecting Either Nodule Initiation or Symbiosome Development, *Symbiosis*, 14: 297–313.

Callum, J.B., Dixon, R.A., Farmer, A.D., Flores, R., Inmam, J., Gonzales, R.A., Harrison, M.J., Paiva, N.L., Scott, A.D., Weller, J.W., May, G.D. (2001) The *Medicago* Genome Initiative: a model legume database. *Nucleic Acids Research,* 29(1): 114–117.

Chilton, M. D., Tepfer, D. A., Petit, A., David, C., Casse-Delbart, F., Tempé, J. (1982) *Agrobacterium rhizogenes* inserts T-DNA into the genome of the host plant root cells. *Nature,* 295: 432–434.

Choi, H., Kim, D., Uhm, T., Limpens, E., Lim, H., Mun, J., Kalo, P., Varma Penmetsa, R., Seres, A., Kulikova O., Roe, B.A., Bisseling, T., Kiss, G.B., Cook, D.R. (2004) A sequence-based genetic map of *Medicago truncatula* and comparison of marker colinearity with *M. sativa*. *Genetics* 166: 1463–1502.

Clemow, S.R., Clairmont, L., Madsen, L.H., Guinel, F.C. (2011) Reproducible hairy root transformation and spot-inoculation methods to study root symbioses of pea. *Plant Methods,* 7: 46.

Cook, D.R. (1999) Medicago truncatula: a model in the making! *Curr. Opin. Plant Biol.,* 2: 301–304

Davies, D.R., Hamilton, J., Mullineaux, P.M. (1993) Transformation of peas. *Plant Cell Rep.,* 12: 180–183.

Delseny, M. (2004) Re-evaluating the relevance of ancestral shared synteny as a tool for crop improvement. *Curr. Opin. Plant Biol.,* 7: 126–131.

Doyle, J.J., Doyle, J.L., Ballenger, J.A., Dickson, E.E., Kajita, T., Ohashi, H. (1997) A phylogeny of the chloroplast gene *RbcL* in the Leguminosae: taxonomic correlations and insights into the evolution of nodulation. *American J. of Botany,* 84: 541–554.

Ellis, T.H.N. and Poyser, S.J. (2002) An integrated and comparative view of pea genetic and cytogenetic maps. *New Phytol.,* 153: 17–25.

Endre, G., Kereszt, A., Kevei, Z., Mihacea, S., Kaló, P., Kiss, G. (2002) A receptor kinase gene regulating symbiotic nodule development. *Nature* 417: 962–966.

Fähraeus, G. (1957) The infection of clover root hairs by nodule bacteria studied by a simple glass slide technique. *J. of General Microbiology,* 16: 374 – 381.

Grant, J.E., Cooper, P.A., McAra, A.E., Frew, T.J. (1995) Transformation of pea (*Pisum sativum* L) using immature cotyledons. *Plant Cell Rep.,*15: 254–258.

Haliassos, A., Chomel, J.C., Tesson, L., Baudis, M., Kruh, J., Kaplan, J.C., Kitzis, A. (1989) Modification of enzymatically amplified DNA for the detection of point mutations. *Nucl. Acids Res.,* 17(9): 3606.

Handberg, K. and Stougaard, J. (1992) *Lotus japonicus*, an autogamous, diploid legume species for classical and molecular genetics. *Plant J.*, 2: 487–496.

Hansen, J., Jørgensen, J.E., Stougaard, J., Marcker, K.A. (1989) Hairy roots - a short cut to transgenic root nodules. *Plant Cell Rep.,* 8: 12–15.

Hohnjec, N., Perlick, A.M., Pühler, A., Küster, H. (2003) The *Medicago truncatula* sucrose synthase gene *MtSucS1* is activated both in the infected region of root nodules and in the cortex of roots colonized by arbuscular mycorrhizal fungi. *Mol. Plant-Microbe Interact.,* 16: 903–915.

Jiang, Q. and Gresshoff, P.M. (1997) Classical and molecular genetics of the model legume *Lotus japonicus*. Mol. Plant–Microbe Interact., 10: 59–68.

Kaló, P., Seres, A., Taylor, S. A., Jakab, J., Kevei, Z., Kereszt, A., Endre, G., Ellis, T. H. N., Kiss, G. B. (2004) Comparative mapping between *Medicago sativa* and *Pisum sativum. Mol Gen Genomics,* 272: 235–246.

Kereszt, A., Li, D., Indrasumunar, I., Nguyen, C.D., Nontachaiyapoom, S., Kinkema, M., Gresshoff, P.M. (2007) Agrobacterium rhizogenes-mediated transformation of soybean to study root biology. *Nature Protoc.,* 2: 948–952.

Knight T.A. (1799) Experiments on the fecundation of vegetables. *Philosophical Transactions of the Royal Society,* 89: 504–506.

Konieczny, A. and Ausubel, F.M. (1993) A procedure for mapping Arabidopsis mutations using co-dominant ecotype-specific PCR-based markers. *The Plant J.*, 4: 403–410.

Larkin, P.J., Gibson, J.M., Mathesius, U., Weinman, J.J., Gartner, E., Hall, E., Tanner, G.J., Rolfe, B.G., Djordjevic, M.A. (1996) Transgenic white clover. Studies with the auxin-responsive promoter, GH3, in root gravitropism and lateral root development. *Transgenic Res.,* 5: 325–335.

Laucou, V., Haurogné, K., Ellis, N., Rameau, C. (1998) Genetic mapping in pea. 1. RAPD-based genetic linkage map of *Pisum sativum*. *Theor. Appl. Genet.,* 97: 905–915.

Limpens, E., Ramos, J., Franken C., Raz, V., Compaan, B., Franssen, H., Bisseling, T., Geurts, R. (2004) RNA interference in Agrobacterium rhizogenes-transformed roots of Arabidopsis and Medicago truncatula. *J. Exp. Bot.,* 55: 983–992.

Limpens, E., Ivanov, S., van Esse, W., Voets, G., Fedorova, E., Bisseling, T. (2009) Medicago N2-fixing symbiosomes acquire the endocytic identity marker Rab7 but delay the acquisition of vacuolar identity. *Plant Cell,* 21: 2811–2828.

Loridon, K., McPhee, K., Morin, J., Dubreuil, P., Pilet-Nayel, M.L., Aubert, G., Rameau, C., Baranger, A., Coyne, C., Lejeune-Hènaut, I., Burstin, J. (2005) Microsatellite marker polymorphism and mapping in pea (*Pisum sativum* L.). *Theor. Appl. Genet.,* 111(6): 1022–1031.

Men, A.E., Borisov, A.Y., Rozov, S.M., Ushakov, K.V., Tsyganov, V.E., Tikhonovich, I.A., Gresshoff, P.M. (1999) Identification of DNA amplification fingerprinting (DAF) markers close to the symbiosis-ineffective *sym31* mutation of pea (*Pisum sativum* L.). *Theor Appl Genet*, 98: 929–936.

Mendel G. (1866). Versuche über Pflanzen-Hybriden. *Verhandlungen des Naturforschenden Vereins in Brünn,* 4: 3–47.

McPhee, K. E. (2007) Pea. In: Kole, C. (ed) Genome mapping and molecular breeding, vol III: Pulses, Sugar and Tuber Crops. Springer-Verlag Berlin Heidelberg (2007), 33–47.

Morzhina, E,V., Tsyganov, V.E., Borisov, A.Y., Lebsky, V.K., Tikhonovich, I.A. (2000). Four developmental stages identified by genetic dissection of pea (*Pisum sativum* L.) root nodule morphogenesis. *Plant Science*, 155: 75–83.

Nam, Y.W., Penmetsa, R.V., Endre, G., Uribe, P., Kim, D., Cook, D.R. (1999) Construction of a bacterial artificial chromosome library of *Medicago truncatula* and identification of clones containing ethylene-response genes. *Theor. Appl. Genet.,* 98: 638–646.

Nadolska-Orczyk, A. and Orczyk, W. (2000) Study of the factors influencing *Agrobacterium*- mediated transformationof pea (*Pisum sativum* L.). *Mol. Breeding,* 6: 185–194.

Neff, M., Neff, J., Chory J., Pepper, A. (1998) dCAPS, a simple technique for the genetic analysis of single nucleotide polymorphisms: experimental applications in Arabidopsis thaliana genetics. *The Plant J.*, 14(3): 387–392.

Oger, P., Petit, A., Dessaux, Y. (1996) A simple technique for direct transformation and regeneration of the diploid legume species *Lotus japonicus*. *Plant Science,* 116: 159–168.

Olhoft, P.M. and Somers, D.A. (2001) L-Cysteine increases *Agrobacterium*-mediated T-DNA delivery into soybean cotyledonary-node cells. *Plant Cell Rep.,* 20: 706–711.

Olsson, J.E., Nakao, P., Bohlool, B.B., Gresshoff, P.M. (1989) Lack of Systemic Suppression of Nodulation in Split Root Systems of Supernodulating Soybean (*Glycine max* [L.] Merr.) Mutants. *Plant Physiol.,* 90(4): 1347–1352.

Pniewski, T. and Kapusta, J. (2005) Efficiency of transformation of Polish cultivars of pea (*Pisum sativum* L.) with various regeneration capacity by using hypervirulent *Agrobacterium tumefaciens* strains. *J. Appl. Genet.,* 46(2): 139–147.

Polowick, P.L., Quandt, J., Mahon, J.D. (2000) The ability of pea transformation technology to transfer genes into peas adapted to western Canadian growing conditions. *Plant Science,* 153: 161–170.

Puonti-Kaerlas, J., Eriksson, T., Engström, P. (1990) Production of transgenic pea (*Pisum sativum* L.) plants by *Agrobacterium tumefaciens* – mediated gene transfer. *Theor. App.l Genet.,* 80: 246–252.

Quandt, H.J., Puhler, A., Broer, I. (1993) Transgenic root nodules of *Vicia hirsuta*: a fast and efficient system for the study of gene expression in indeterminate-type nodules. *Mol. Plant-Microbe Interact.,* 6: 699–706.

Rogers, S.O. and Bendich, A.J. (1985) Extraction of DNA from milligram amounts of fresh, herbarium and mummified plant tissues. *Plant Idol. Biol.,* 5: 69–76.

Roth, L.E. and Stacey, G. (1989) Bacterium release into host cells of nitrogen-fixing soybean nodules: the symbiosome membrane comes from three sources. *Eur. J. Cell Biol.,* 49:13–23.

Rozov, S.M., Borisov, A.Y., Tsyganov, V.E., Men, A.E., Tikhonovich, I.A. (1995) Mapping of pea (*Pisum sativum* L.) genes affecting symbiosis. In: Tikhonovich, I.A., Provorov, N.A., Romanov, V.I., Newton, W.E. (eds) Nitrogen fixation: fundamentals and applications*, Kluwer Academic Publishers*, Dordrecht, p. 489.

Safronova, V.I. and Novikova, N.I. (1996) Comparison of two methods for root nodule bacteria preservation: Lyophilization and liquid nitrogen freezing. *J. of Microbiolog. Meth.,* 24: 231–237.

Schaerer, S. and Pilet, P.E. (1991) Roots, explants and protoplasts from pea transformed with strains of *Agrobacterium tumefaciens* and *rhizogenes*. *Plant Science,* 78: 247–258.

Schenk, R.U. and Hildebrandt, A.C. (1971) Medium and techniques for induction and growth of monocotyledonous and dicotyledonous plant cell cultures. *Canadian Journal of Botany,* 50: 199–204.

Schmidt, R. (2000) Synteny: Recent advances and future prospects. *Curr. Opin. Plant Biol.,* 3: 97–102.

Schroeder, H.E., Schotz, A.H., Wardley-Richardson, T., Spencer, D., Higgins, T,J.V. (1993) Transformation and regeneration of two cultivars of pea (*Pisum sativum* L.). *Plant Physiol.,* 101: 751–757.

Somers, D.A., Samac, D.A., Olhoft, P.M. (2003) Recent advances in legume transformation. *Plant Physiol.,* 131: 892–899.

Sorscher, E.J. and Huang, Z. (1991) Diagnosis of genetic diseases by primer-specified restriction map modifications, with application to cystic fibrosis and retinitis pigmentosa. *Lancet* 337: 1115–118.

Stracke, S., Kistner, C., Yoshida, S., Mulder, L., Sato, S., Kaneko, T., Tabata, S., Sandal, N., Stougaard, J., Szczyglowski, K., Parniske, M. (2002) A plant receptor-like kinase required for both bacterial and fungal symbiosis. *Nature* 417: 959–962.

Tadege, M., Wen, J., He, J., Tu, H., Kwak, Y., Eschstruth, A., Cayrel, A., Endre, G., Zhao, P.X., Chabaud, M., et al. (2008) Large-scale insertional mutagenesis using the *Tnt1* retrotransposon in the model legume *Medicago truncatula*. *Plant J.,* 54(2): 335–347.

Tanksley, S.D., Ganal, M.W., Martin, G.B. (1995) Chromosome landing: a paradigm for map-based gene cloning in plants with large genomes. *Trends Genet.,* 11(2): 63–68.

Trieu, A.T. and Harrison, M.J. (1996) Rapid transformation of *Medicago truncatula*: regeneration via shoot organogenesis. *Plant Cell Rep.,* 16: 6–11.

Tsyganov, V.E., Voroshilova, V.A., Priefer, U.B., Borisov, A.Y., Tichonovich, I.A. (2002) Genetic dissection of the initiation of the infection process and nodule tissue development in the *Rhizobium*-pea (*Pisum sativum* L.) symbiosis. *Annals of Botany*, 89: 357–366.

Tsyganov, V.E., Rozov, S.M., Borisov, A.Y., Tikhonovich, I.A. (2006) Symbiotic gene *SYM33* is located on linkage group I*. Pisum Genet.,* 38: 21–22.

Tsyganov, V.E., Morzhina, E.V., Stefanov, S.Y., Borisov, A.Y., Lebsky, V.K., Tikhonovich, I.A. (1998) The pea (*Pisum sativum* L) genes *sym33* and *sym40* control infection thread formation and root nodule function*. Mol. Gen. Genet.,* 259: 491–503.

Voroshilova, V. A., Boesten, B., Tsyganov, V. E., Borisov, A. Y., Tikhonovich, I. A., Priefer, U. B. (2001) Effect of mutations in *Pisum sativum* L genes blocking different stages of nodule development on the expression of late symbiotic genes in *Rhizobium leguminosarum* bv *viciae. Mol. Plant-Microbe Interact.,* 14: 471–476.

Wen, F., Zhu, Y., Hawes, M.C. (1999) Effect of pectin methylesterase gene expression on pea root development. *Plant Cell,* 11: 1129–1140.

Young, N.D., Debellé, F., Oldroyd, G.E., Geurts, R., Cannon. S.B., Udvardi. M.K., Benedito. V.A., Mayer, K.F.X., Gouzy, J., Schoof, H., et al. (2011) The Medicago genome provides insight into the evolution of rhizobial symbioses. *Nature* 480: 520–524.

Zhukov, V., Radutoiu, S., Madsen, L.H., Rychagova, T., Ovchinnikova, E., Borisov, A., Tikhonovich, I., Stougaard, J. (2008) The pea *Sym37* receptor kinase gene controls infection-thread initiation and nodule development. *Mol. Plant-Microbe Interact.,* 21(12): 1600–1608.

Chapter 3

IPD3 controls the formation of nitrogen-fixing symbiosomes in pea and *Medicago* Spp.

Published in Molecular Plant-Microbe Interactions, Vol. 24, No. 11, 2011, pp. 1333–1344. Supplementary data available online at http://apsjournals.apsnet.org/doi/suppl/10.1094/MPMI-01-11-0013.

Evgenia Ovchinnikova,[1,2] Etienne-Pascal Journet,[3,4] Mireille Chabaud,[3,4] Viviane Cosson,[5] Pascal Ratet,[5] Gerard Duc,[6] Elena Fedorova,[1] Wei Liu,[1] Rik Op den Camp,[1] Vladimir Zhukov,[2] Igor Tikhonovich,[2] Alexey Borisov,[2] Ton Bisseling,[1,7] and Erik Limpens[1]

[1] Department of Molecular Biology, Wageningen University, Droevendaalsesteeg 1, 6708 PB, Wageningen, The Netherlands;

[2] All-Russia Research Institute for Agricultural Microbiology, Laboratory of Genetics of Plant-Microbe Interactions, Podbelsky chaussee 3, 196608, Pushkin 8, St. Petersburg, Russia;

[3] INRA, Laboratoire des Interactions Plantes-Microorganismes (LIPM), UMR441, F-31326 Castanet-Tolosan, France;

[4] CNRS, LIPM, UMR 2594, F-31326 Castanet-Tolosan, France;

[5] Institut des Sciences du Végétal, UPR2355, CNRS, Avenue de la Terrasse, 91198, Gif sur Yvette, France;

[6] Unité Mixte de Recherche en Génétique et Ecophysiologie des Légumineuses, UMR INRA 102, BP 86510, F-21065 Dijon, France;

[7] King Saud University, P.O. BOX 2454, Riyadh 11451, Kingdom of Saudi Arabia

ABSTRACT

A successful nitrogen-fixing symbiosis requires the accommodation of rhizobial bacteria as new organelle-like structures, called symbiosomes, inside the cells of their legume hosts. Two legume mutants that are most strongly impaired in their ability to form symbiosomes are *sym1/TE7* in *Medicago truncatula* (Medicago) and *sym33* in *Pisum sativum* (pea). We have cloned both *MtSYM1* and *PsSym33* and show that both encode the recently identified Interacting Protein of DMI3 (IPD3), an ortholog of *Lotus japonicus* (Lotus) CYCLOPS. IPD3 and CYCLOPS were shown to interact with DMI3/CCaMK, which encodes a calcium- and calmodulin-dependent kinase that is an essential component of the common symbiotic signalling pathway for both rhizobial and mycorrhizal symbioses. Our data reveal a novel, key role for IPD3 in symbiosome formation and development. We show that MtIPD3 participates in but is not essential for infection thread formation and that MtIPD3 also affects DMI3-induced spontaneous nodule formation upstream of cytokinin signalling. Further, MtIPD3 appears to be required for the expression of a nodule-specific remorin, which controls proper infection thread growth and is essential for symbiosome formation.

INTRODUCTION

During the Rhizobium-legume symbiosis, the Rhizobium bacteria are hosted inside the cells of a newly formed organ, the root nodule. There they participate in the formation of new transient organelle-like structures, called symbiosomes, where they find the right conditions to fix atmospheric nitrogen. In legumes such as Medicago and pea, symbiosomes consist of individual bacteria that are surrounded by a plant-derived membrane, called the peribacteroid /symbiosome membrane. What are the underlying mechanisms to accommodate the bacteria as new organelle-like structures inside the plant cells is a key question in symbiosis.

Medicago and pea form so-called indeterminate nodules that have a persistent meristem and symbiosome formation continuously occurs in a few cell layers just below this meristem. There, the bacteria, which are transported via tubular structures called infection threads, are taken up into the nodule cells to form symbiosomes (Brewin, 2004; Jones et al., 2007). Symbiosome formation begins with the formation of an unwalled infection droplet at the otherwise cell wall bound infection thread. From there, the bacteria are individually taken up into the cell via an endocytosis-like process (Verma 1996, Whitehead and Day 1997, Jones et al., 2007; Limpens et al. 2009). After release from the infection thread, the symbiosomes divide and subsequently terminally differentiate into their nitrogen-fixing form (Maunoury et al., 2010). Due to the activity of the meristem, nodules show a highly ordered zonal organization, containing symbiosomes at subsequent stages of development (Vasse 1990). The zone below the meristem where infection threads invade the cells and symbiosome formation and subsequent differentiation occur, is called the infection zone. In the adjacent fixation zone, infected nodule cells contain fully differentiated symbiosomes where nitrogen fixation takes place.

Although symbiosome formation is a crucial step to establish a successful symbiosis in most legumes, the molecular basis of this process is far from understood. Nodule organogenesis and infection thread formation both require the activation of a signalling pathway by rhizobial signal molecules called Nod factors (Oldroyd and Downie 2008). Several recent studies suggest that symbiosome formation is also controlled by this Nod factor signalling pathway. All Nod factor-signalling genes appear to be expressed in the nodule, especially in the infection zone of the nodule where symbiosome formation takes place (Bersoult et al., 2005; Limpens et al., 2005; Riely et al., 2006). Nodule specific knockdown of the LRR-containing receptor kinase *DMI2* gene blocks the release of the bacteria from the infection threads (Capoen et al., 2005; Limpens et al., 2005). Signalling by DMI2 is thought to trigger a calcium-spiking response that is decoded in the nucleus by a calcium and calmodulin-dependent kinase DMI3, which activates specific transcription factors (Levy et al., 2004; Mitra et al., 2004). Among transcription factors that are strongly upregulated during nodule formation and involved in symbiosome formation, there are the CCAAT transcription factor HAP2 and the AP2/ERF transcription factor EFD (Combier et al., 2006; Vernié et al., 2008). Knockdown of *HAP2* expression causes a block in the release of bacteria from the infection threads (Combier et al., 2006) while EFD is involved in the control of

both release and symbiosome differentiation (Vernié et al., 2008). One of the genes that is upregulated during nodule formation and essential for symbiosome formation encodes a recently identified remorin, called SYMREM. This remorin was shown to interact with DMI2 as well as with Nod factor receptors, and knockdown of this remorin blocked the release of bacteria from the infection threads in the nodule (Lefebvre et al., 2010), Both DMI2 and DMI3 are part of a common symbiotic signalling module that is also essential for the establishment of an arbuscular mycorrhizal symbiosis (Catoira et al., 2000; Capoen and Oldroyd, 2008). Recently, an interacting protein of DMI3, called IPD3 in Medicago and CYCLOPS in *Lotus japonicus*, was identified that was shown to be essential for infection thread formation as well as mycorrhizal arbuscule formation in Lotus (Messinese et al., 2007; Yano et al., 2008).

To get additional insight into the mechanism of symbiosome formation and into how Nod factor signalling might control this process, we focused on two mutants *sym1* (TE7) in Medicago and *sym33* in pea, most strongly impaired at the first step of symbiosome formation; i.e. the release of bacteria from the infection thread (Bénaben et al., 1995; Tsyganov et al., 1998; Voroshilova et al., 2009).

Mtsym1 (TE7) was reported to make two types of nodules: small nodules (primordia) (type-1) with infection threads arrested at the outer cortical cells of the root/the cortex of the nodule, and elongated nodules (type-2) filled with an extensive network of infection threads with thick cell walls (Bénaben et al., 1995). Occasionally some release of bacteria was observed in these type-2 nodules, but subsequent symbiosome differentiation did not take place, and these plant cells underwent early senescence. The lack of (proper) symbiosome formation is accompanied by a lack of endoreduplication in *Mtsym1* nodule cells, which has been postulated to be a prerequisite for symbiosome development (Maunoury et al., 2010). Similar to *Mtsym1*, pea *sym33* shows impaired invasion of the nodule primordium at early stages (Voroshilova et al., 2009). At later time points, two types of nodule structures are formed: white nodules with an extensive network of “locked” infection threads with thick cell walls that do not release bacteria and nodules containing undifferentiated symbiosomes that undergo premature senescence (Tsyganov et al., 1998, Voroshilova et al., 2001, 2009). Both mutants show signs of host defense responses such as extensive deposition of cell wall material on the infection threads and accumulation of polyphenolics. In addition to the nodulation phenotypes, *sym33 w*as also reported to show decreased root colonization by arbuscular mycorrhizal fungi although arbuscules can still be formed (Jacobi et al. 2003a, b).

Here we describe the cloning of *MtSYM1* and *PsSym33* and show that both encode the Interacting Protein of DMI3 (IPD3). Our data demonstrate that the common symbiotic signalling module in pea and Medicago has been recruited to facilitate symbiosome formation, i.e. the release of bacteria from the infection threads as well as subsequent symbiosome development. We propose a model in which IPD3 controls the activity/stability of a DMI3 complex to allow a successful symbiosis.

RESULTS

Cloning of *MtSYM1*

A map-based cloning strategy was undertaken to clone the *MtSYM1* gene. A segregating population (99 F2 plants) of a cross between *Mtsym1* (TE7) and A20 was used to map the location of *Mtsym1* to the upper arm of chromosome V, between markers 19c21a and CU469(B). Sequence analysis of the corresponding ~1Mb BAC contig (Suppl Fig. 1) identified several promising *MtSYM1* candidates as they are thought to play a role in the symbiotic signalling pathway. These include HMGR1, an interactor of DMI2 (Kevei et al. 2007), and IPD3, an interactor of DMI3 (Messinese et al., 2007). Sequence analysis of the genomic regions of these candidate genes, identified a mutation in *MtIPD3*: a deletion of G at position 1266 in the *MtIPD3* mRNA coding sequence resulting in a frame shift and premature stop leading to a truncated protein that lacks the second nuclear localization signal (NLS) and the predicted C-terminal conserved coiled-coil motif (Fig.1A, B; Table 1). To confirm that *MtSYM1* encodes MtIPD3, we complemented the mutant using the *MtIPD3* open reading frame under the control of its putative promoter (1 kb region upstream of the start codon). Two weeks after inoculation, pink nitrogen fixing nodules were formed on *IPD3p:MtIPD3* transformed *Mtsym1* roots, containing normally developed symbiosomes (Fig.2A, B). As a control, *Mtsym1* was transformed with an empty vector, which resulted in only type-1 and type-2 nodules (Fig.2C). This confirms that *MtSYM1* encodes MtIPD3. This allele was named *Mtsym1-1*.

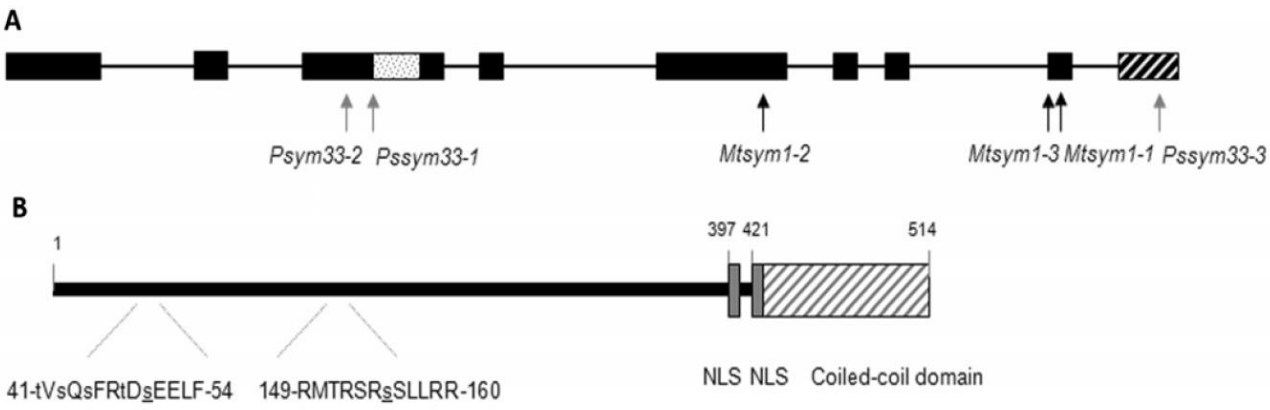

Fig.1. Interacting protein of DMI3 (*IPD3*) gene and protein structure. **A**, Schematic representation of the exon-intron structure of the *IPD3* gene. Identified mutations in the corresponding *Medicago truncatula sym1* and pea *sym33* mutants are indicated. The open box after exon 3 (black rectangles) marks intron 3, which is not spliced in *Pssym33-1*. **B**, Schematic representation of the domain structure of IPD3 protein. The conserved C-terminal coiled-coil domain, two identified phosphorylation sites (Grimsrud et al. 2010), as well as two predicted nuclear localization sites (NLS) are indicated.

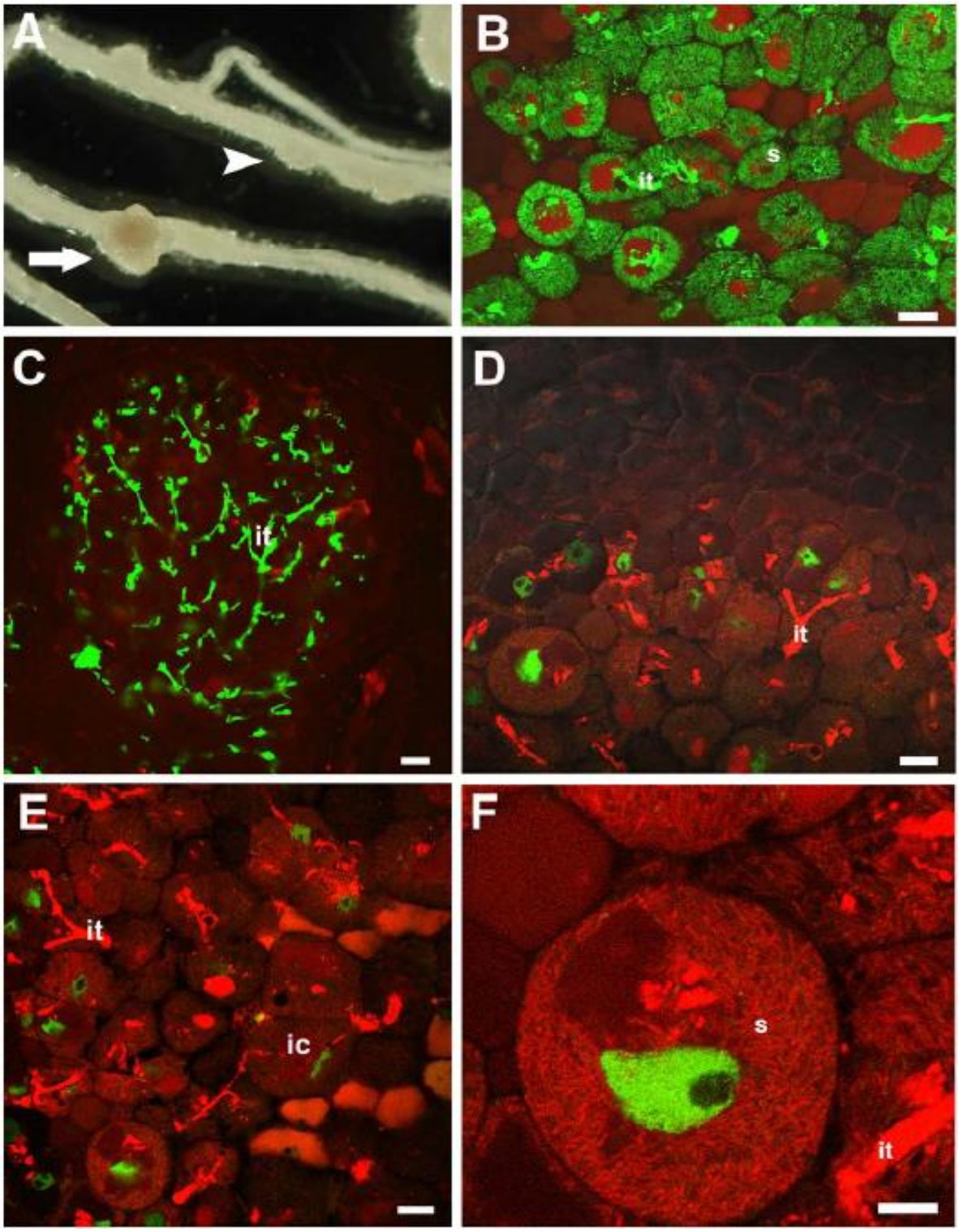

Fig.2. Complementation of *Mtsym1* with MtIPD3. **A,** Brightfield image of an *IPD3p:IPD3* transformed *Mtsym1-1* plant, showing a transgenic root (white arrow) with a pink nitrogen-fixing nodule and a nontransgenic root (arrowhead) with white ineffective nodules. **B,** Confocal image of an *IPD3p:IPD3* expressing *Mtsym1-1* nodule, showing a wild-type cytology with well developed symbiosomes (s). Rhizobia are expressing green fluorescent protein (GFP). **C,** Confocal image of a *Mtsym1-1* type 2 nodule transformed with an empty vector. Rhizobia are expressing GFP. Note the presence of infection threads in the central tissue of the nodule, but no symbiosomes. **D** and **E,** Confocal image of an *IPD3p:GFP-IPD3* expressing *Mtsym1-1* nodule showing GFP-IPD3 localization in the nucleus of cells in the **D,** infection zone and **E,** fixation zone. Rhizobia are expressing mRFP. **F,** Confocal close-up of GFP-IPD3 localizing to the nucleus of an infected cell in the nodule fixation zone. Note the full complementation of the mutant phenotype, showing well-developed symbiosomes. S = symbiosome, It = infection thread. Bars: B, D, and E = 20 µm; C = 50 µm; F = 10 µm.

Additionally, we identified a *Tnt1*/Mere-transposon tagged line (*76A-24*) that showed a phenotype comparable to *Mtsym1* and segregated as a monogenic recessive trait (data not shown). After two backcrosses (BC), BC2 lines formed both type-1 and type-2 Fix$^-$ nodules similar to *Mtsym1* (Table 1; data not shown). Crossing *76A-24* to *Mtsym1* showed that the mutants are allelic. *IPD3-Tnt1*/Mere transposon junctions in *76A-24* were determined, and it turned out that one single copy of *Mere1-1* (Rakocevic et al., 2009) is inserted after base 5 of exon 9 resulting in a premature stop (*sym1-3*, Table 1). Genotyping of 87 mutant and 3 wilde-type *76A-24* back-cross lines showed that the presence of a homozygous Mere insertion in *IPD3* is necessary for the mutant nodulation phenotype (data not shown). Previous allelism tests with Medicago Fix$^-$ mutants had shown that *Mtsym1* is allelic to the previously identified complementation group termed *Mtsym17* (Sagan et al., 1998; Morandi et al., 2005). Mutations in *MtIPD3* were confirmed in six *Mtsym17* lines by sequencing the *IPD3* genomic region (Table 1). TRV15 (*sym1-2*) contains a 4 bp deletion leading to a frame shift introducing 13 different amino acids and a premature stop, thus, deleting 180 amino acids (including both NLS sequences) at the C-terminus. The *Mtsym17* mutants TR3, TR9, TR13, TR62, and TR69 all contain the same mutation as *Mtsym1-1* (Fig.1A, Table 1). All *Mtsym1* alleles, including backcrossed lines show a very similar infection and nodulation phenotype forming two types of nodules (Table 1), although the ratio between the two nodule types varied between lines and experiments.

IPD3 is an ortholog of the recently identified CYCLOPS protein from *Lotus japonicus* (Lotus) and is highly conserved in angiosperms that are able to establish an arbuscular mycorrhizal symbiosis (Messinese et al., 2007; Chen et al., 2008; Yano et al., 2008). It contains a highly conserved C-terminal coiled coil domain and a functional nuclear localization signal. Further, two phosphorylation sites have been identified (Fig.1B) (Yano et al., 2008; Grimsrud et al., 2009).

Synteny-based cloning of *PsSym33*

The pea *Pssym33* mutants, of which three alleles (RisFixU, SGEFix$^-$-2, and SGEFix$^-$-5) have been identified, have a strikingly similar phenotype as *Mtsym1*: the formation of white nodules with an extensive network of thick-walled infection threads, but no release of bacteria (Tsyganov et al., 1998; Voroshilova et al., 2001, 2009). One of the *sym33* alleles, SGEFix$^-$-2 has been shown to occasionally make pinkish nodules, in which bacteria are released, but symbiosomes do not develop properly; such nodules are referred to as type-3 nodules in Table 1 (Tsyganov et al., 1998). SGEFix$^-$-5, like reported for RisFixU (Voroshilova et al., 2001), does not show type-3 nodules, but makes mostly type-2 nodules where the release of bacteria from the infection threads does not occur (Suppl Fig.2). *Sym33* was mapped to a region on linkage group I in pea, which is highly syntenic with the upper arm of chromosome 5 in Medicago (Tsyganov et al., 2006; Aubert et al., 2006). Additional mapping using a cross between WT10584 and SGEFix$^-$-2

(95 F2 plants) positioned *Sym33* within a 14 cM region between the markers Gst and Alat-C on pea linkage group I, corresponding to the syntenic location of *SYM1* in Medicago (Suppl. Fig.3). *PsIPD3* was converted into a genetic marker and showed complete co-segregation with the mutant phenotype, suggesting that *PsSym33* is the ortholog of *MtIPD3*. To test this, we sequenced *IPD3* from pea in the three available *sym33* mutants RisFixU, SGEFix⁻-2, and SGEFix⁻-5 (Fig.1A, Table 1). RisFixU (background Finale) showed a mutation in the 5'-splice-site (G>A) of intron 3. RT-PCR analysis confirmed that this mutation impairs the splicing of intron 3 (Suppl. Fig.4), by which a stop codon is introduced leading to a truncated protein of 390 amino acids. SGEFix⁻-5 (background SGE) shows a C319T mutation in the *PsIPD3* coding sequence, introducing an early stop at amino acid 107. SGEFix⁻-2 contains a C1357T mutation causing a premature stop eliminating the final 60 amino acids. SGEFix⁻-5 and RisFixU do not show the occasionally occurring nodules as in SGEFix⁻-2 where the release of bacteria from the infection threads occurs. This suggests that the phenotype of SGEFix⁻-2 may be somewhat leaky, which fits with C-terminal location of the mutation in the protein. Nevertheless, it indicates an important role for the highly conserved 60 amino acids in the C-terminal coiled-coil domain for the function of IPD3. The comparable phenotypes, similar map location, and mutations in *PsIPD3* strongly indicate that *Sym33* is the ortholog of *MtSYM1* and we conclude that *PsSym33* encodes PsIPD3. Together, the data from pea and Medicago reveal a novel, key function for IPD3 in symbiosome formation and development.

Table 1. *MtSYM1* and *PsSym33* mutant alleles identified in this study

Allele	Original mutant	Background [b]	Reference	Mutation		Phenotype [a]	
				cDNA	Protein [c]	ITs	Nodule
sym1-1	Mtsym1/TE7	*Mt* J5	Benaben et al., 1995	Deletion G1266	+17 aa after K421	+	1 and 2
sym1-1	TR3, TR9, TR13, TR62, TR69,	*Mt* J5	Sagan et al., 1998; Morandi et al., 2005	Deletion G1266	+17 aa after K421	+	1 and 2
sym1-2	TRV15	*Mt* J5	Sagan et al., 1998; Morandi et al., 2005	4-bp deletion from T1000	+13 aa after A333	+	1 and 2
sym1-3	T00076A-24	*Mt* Jemalong H2A	This work	Mere insertion after C1245	+1 aa after G415	+	1 and 2
sym33-1	RisFixU	*Ps* Finale	Voroshilova et al., 2001	5'-splice-site G>A mutation intron 3	+1 aa after I123	+	1 and 2
sym33-2	SGEFix⁻-5	*Ps* SGE	This work	C319T	Q107 stop	+	1 and 2
sym33-3	SGEFix⁻-2	*Ps* SGE	Tsyganov et al., 1998	C1357T	R453 stop	+	2 and 3

[a] IT = infection thread. Nodule = nodule types: 1 = small nodules with infection threads limited to the outer cortex, type 2 = elongated nodules with extensive network of infection threads, but no release of bacteria, and type 3 = elongated nodules with undifferentiated symbiosomes that under premature senescence.

[b] Genotypic background. *Mt* = *Medicago truncatula* and *Ps* = *Pisum sativum*.

[c] Abbreviation: aa = amino acids.

IPD3 localizes to the nucleus throughout the nodule infection and fixation zone

DMI3 is most strongly expressed in the infection zone of the nodule where it localizes to the nucleus (Limpens et al., 2005; Smit et al., 2005). Promoter-GUS analyses were reported to show that *IPD3* is maximally expressed in the fixation zone of the nodule (Messinese et al., 2007). Significant lower levels were observed in the distal infection zone where maximal *DMI3* expression is observed. To test whether IPD3 localizes to the nucleus in cells of the distal infection zone where symbiosome formation starts and DMI3 is present, a *IPD3p::GFP-IPD3* construct was used to complement *Mtsym1-1*. Nodules formed on these transgenic roots were pink and showed mature, elongated symbiosomes (Fig.2F). GFP-IPD3 localized to the nucleus of cells throughout the infection zone as well as in the fixation zone (Fig.2D-F). No or very low signal was observed in the nodule meristem. In contrast to the full-length *IPD3* construct, we were not able to visualize the *Mtsym1-1* encoded truncated IPD3 protein fused to GFP. This indicates that the truncated GFP-IPD3 protein is not synthesized or is rapidly degraded.

DMI3 was shown to be present throughout the infection zone, however, not in the cells of the fixation zone that contain mature nitrogen-fixing symbiosomes (Smit et al., 2005). This shows that IPD3 is present in cells that express DMI3 at the time of symbiosome formation and co-localizes with DMI3 in the nucleus. The presence of IPD3 in the fixation zone in absence of DMI3 suggests that IPD3 has an additional role during these later stages.

IPD3 controls specific genes required for symbiosome formation

The presence of IPD3 in the nucleus and the reported interaction with DMI3 (Messinese et al., 2007; Yano et al., 2008) suggest that IPD3 controls the activation of genes required for symbiosome formation. Several genes have recently been identified that show DMI3-dependent induction during nodulation and are required for proper infection thread invasion of the nodule primordium and/or the release bacteria from the infection threads in the nodule (Marsh et al. 2007). To determine whether some of these genes require a functional IPD3 to be induced in nodules we compared their expression in wild-type, type-1, and type-2 *Mtsym1-1* nodules by quantitative RT-PCR. These genes include the coiled-coil protein *RPG* gene (Arrighi et al., 2008), the U-box containing E3 ubiquitin ligase gene *LIN* (Kiss et al., 2010), *Flotillin-2* and *-4* (Haney and Long, 2010), a nodule-specific remorin *SYMREM* (Lefebvre et al., 2010), and the transcription factors *ERN* (Middleton et al., 2007), *EFD* (Vernié et al., 2008) and *HAP2* (Combier et al., 2007). Mutants of *RPG*, *LIN,* and *ERN* show impaired growth of infection threads that fail to penetrate the nodule primordium, comparable to *Mtsym1* type-1 nodules (Middleton et al., 2007; Arrighi et al., 2008; Kiss et al., 2010). Mutants of *SYMREM* and *HAP2* show the formation of nodules that are invaded by infection threads, but subsequent release of bacteria from the infection threads appears blocked, similar to *Mtsym1* type-2 nodules (Combier et al., 2007; Lefebvre et al., 2010). Similarly, *EFD* mutants show delayed release of bacteria and subsequent impaired symbiosome development (Vernié et al., 2008). *Flotillin-2* and *-4* were shown to be

required for proper infection thread growth and nodule formation although the exact nodule phenotype has not yet been described (Haney and Long, 2010). Additionally, we examined the expression of *NIN*, an early Nod factor induced gene that controls both infection and nodule organogenesis (Marsh et al., 2007).

Type-1 and type-2 nodules were excised from *Mtsym1-1* roots 12 days post-inoculation. The use of GFP-expressing rhizobia allowed the selection of type-1 and type-2 nodules based on the penetration of infection threads into the nodules. At 12 days post-inoculation, wild-type formed pink nitrogen-fixing nodules, containing fully developed symbiosomes. As shown in Fig.3, *NIN, LIN, HAP2, Flotillin-2* and *-4* show a more or less similar expression level (less than 2 fold change) in type-1 and type-2 *Mtsym1* nodules as compared to wild-type nodules. The expression level of ERN was ~3x higher in *Mtsym1* type-1 and type-2 nodules compared to wild-type nodules (Fig.3). RPG showed a ~8x higher expression in *Mtsym1* type-1 nodules, whereas type-2 nodules showed an expression level comparable to wild-type nodules (Fig. 3). On one hand, MtIPD3 does not appear to be essential for the induction of these genes. On the other hand, expression of *EFD* and *SYMREM* was significantly, respectively ~7x and >100x, reduced in *Mtsym1-1* type-1 and type-2 nodules compared to wild-type nodules (Fig.3). This indicates that MtIPD3 is required for the induction of a specific subset of genes that are required for symbiosome formation.

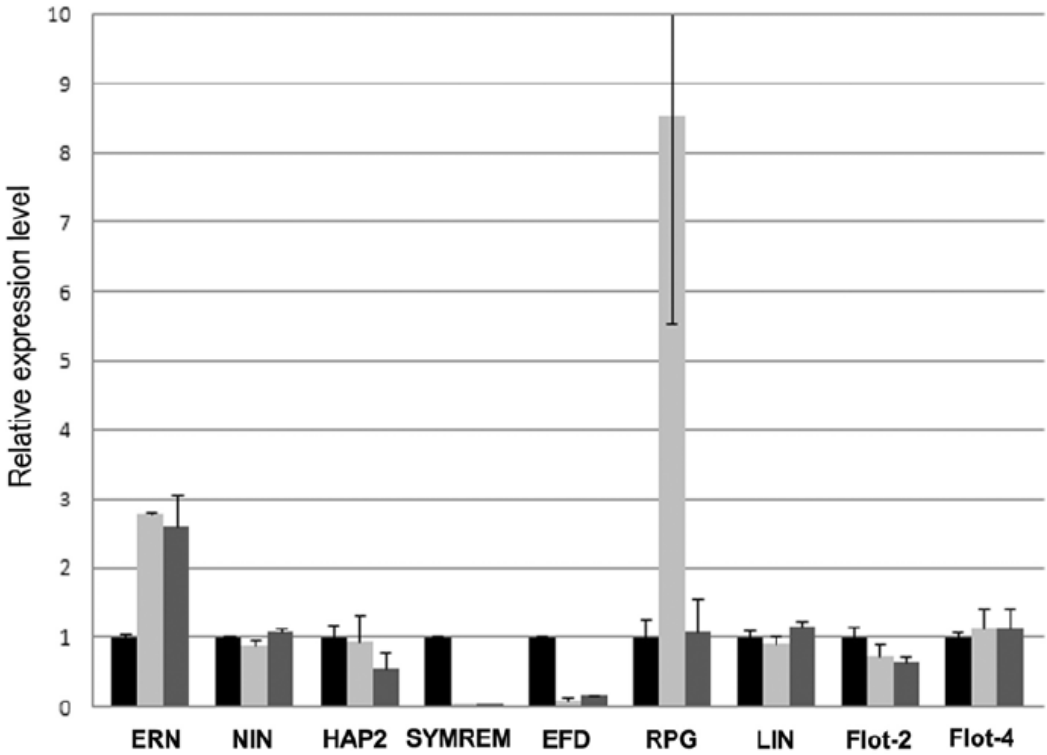

Fig.3. Quantitative reverse-transcription polymerase chain reaction (qRT-PCR) expression analyses in *Mtsym1*. qRT-PCR analysis of *ERN*, *NIN*, *HAP2*, *SYMREM, EFD*, *RPG, LIN*, and *Flotillin2-* and *-4* in wild-type control (J5) = black bars; *Mtsym1-1* type 1 = light gray bars, and *Mtsym1-1* type 2 nodules = dark gray bars 12 days post-inoculation. The expression level of the corresponding genes in the wild-type control nodules is set to one. The relative expression level corresponds to the fold change compared with the wild-type control.

IPD3 also controls infection thread growth

In Lotus, the *IPD3* ortholog *CYCLOPS* was shown to be essential for infection thread formation (Yano et al., 2010). As DMI3 is required for infection thread formation and also SYMREM controls proper infection thread growth (Godfroy et al., 2006; Lefebvre et al., 2010), we reinvestigated whether in Medicago IPD3 already affects infection thread formation in the root hairs. In wild-type control roots, most (>80%) infection threads have a tubular structure of 1-2 rhizobia wide (Fig.4A, Table 2) (Limpens et al., 2003). In contrast, many infection events in *Mtsym1-1* are blocked at the microcolony stage forming sac-like structures or infection threads grow with sac-like structures along their length and abort in the epidermis (Fig.4B, C; Table 2). This shows that IPD3 also controls infection thread growth already in the root hairs.

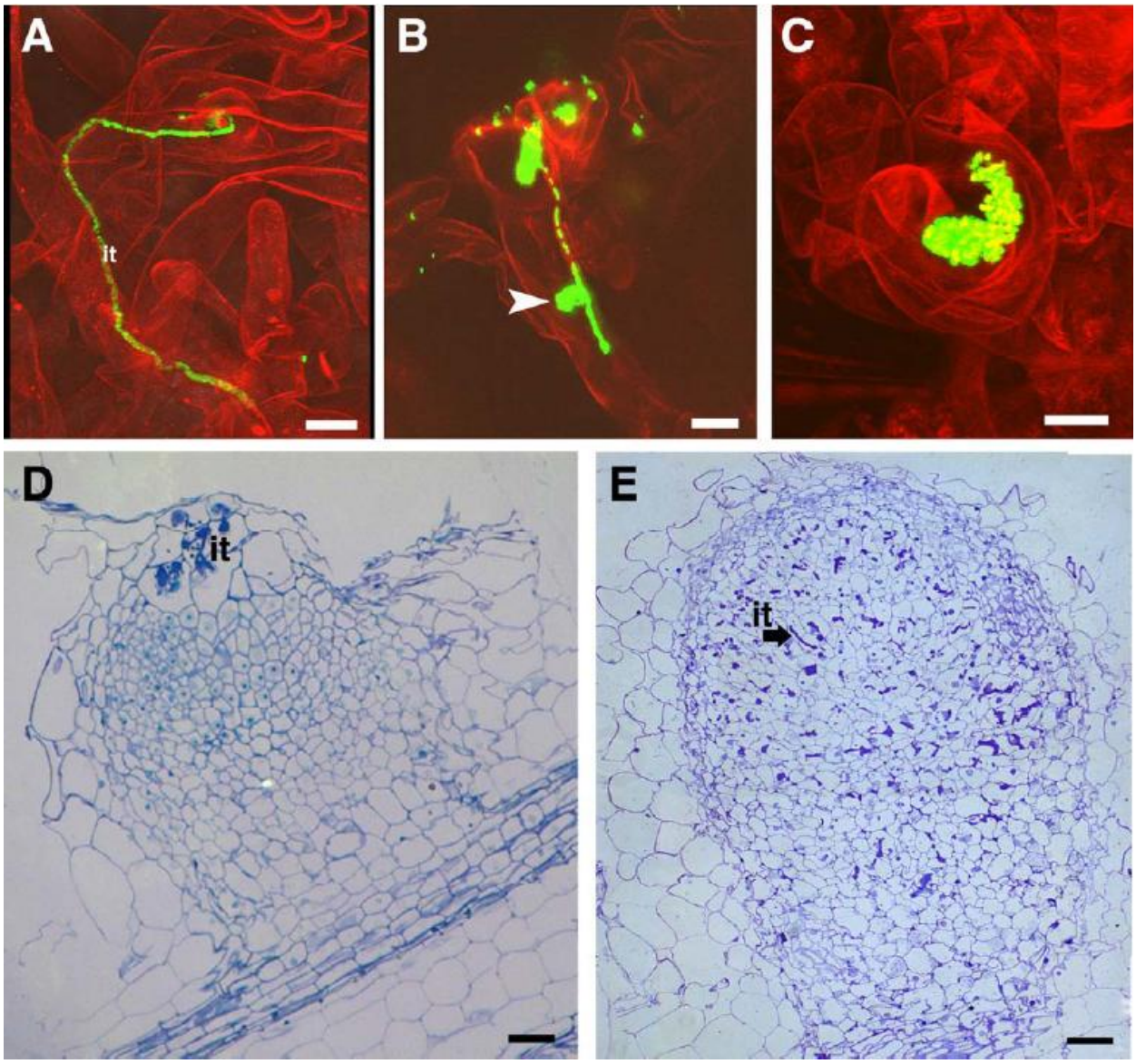

Fig.4. *Mtsym1* infection thread and nodule phenotypes. **A,** Tubular (wild-type) infection thread in a *Mtsym1-1* root hair. **B,** Infection thread with sac-like structures (arrowhead) along its length in a *Mtsym1-1* root hair. **C,** Sac-like infection arrested at the microcolony stage in a *Mtsym1-1* root hair. Bacteria in A–C are expressing green fluorescent protein. Red color of the root hairs results from autofluorescence. **D,** Semithin section through a *Mtsym1-1* type 1 nodule. **E,** Semithin section through a *Mtsym1-1* type 2 nodule. It = infection thread. Bars: A to C = 10 µm; D and E = 100 µm.

Infection thread growth is Nod factor structure dependent and likely depends on the activity of Nod factor signalling output via DMI3, which might depend on IPD3 (Ardourel et al, 1994; Limpens et al., 2003; Smit et al., 2007). Therefore, we tested whether infection and nodule formation in *Mtsym1* would be more affected by rhizobia that make aberrant Nod factors. Therefore, we inoculated plants with GFP-expressing Δ*nodL* mutant rhizobia, which make aberrant Nod factors that lack an acetate substitution at the non-reducing terminal glucosamine (Ardourel et al., 1994). In wild-type roots, Δ*nodL* rhizobia show impaired infection thread growth in root hairs; most infection threads (~80%) develop sac-like structures that are nevertheless able to reach and penetrate the primordium and form wild-type numbers of nitrogen-fixing nodules (Limpens et al., 2003). In contrast, in *Mtsym1-1* the majority of infection events by Δ*nodL* mutant rhizobia was arrested at the microcolony stage (Table 2). The infection threads that were formed all contained sac-like structures (Table 2). This resulted in the formation of only type-1 nodules whereas wild-type bacteria formed ~10-25% type-2 nodules (on average 2/root) (Fig.4D, E; Table 2). Thus, the infection thread growth defect associated to Δ*nodL* rhizobia and in *Mtsym1-1,* both appear to be exaggerated in this combination, suggesting interference between the two mutant phenotypes.

Table 2. Infection thread (IT) and nodule phenotypes of *Mtsym1-1* inoculated with different *Sinorhizobium meliloti* (*Sm*) 2011 strains [a]

		Percent nodule phenotype			Percent IT phenotype		
Bacterial strain [b]	Plant	WT	Type 1	Type 2	Sac-like infection [c]	IT with sac [d]	Tubular IT
*Sm*2011-GFP	WT (J5)	100 (9)	–	–	–	12 (3)	88 (22)
*Sm*2011-GFP	*Mtsym1*	–	75 (6)	25 (2)	56 (35)	40 (25)	4 (3)
*Sm*2011Δ*nodL*-GFP	WT (J5)	100 (4)	–	–	12 (3)	80 (20)	8 (2)
*Sm*2011Δ*nodL*-GFP	*Mtsym1*	–	100 (4)	–	81 (46)	19 (11)	–

[a] Percentage of nodule or infection thread types is given per root; numbers in parenthesis are average number of nodules or infection threads per root. WT = wild type.

[b] GFP = green fluorescent protein.

[c] Sac-like infection arrested at the microcolony stage.

[d] Infection thread with sac-like structure.

IPD3 affects DMI3-induced spontaneous nodule formation

The formation of nodules in *Mtsym1* indicates that IPD3 is not essential for nodule organogenesis. In contrast, DMI3 is also essential for nodule organogenesis and introduction of an always-active DMI3/CCaMK gene product, lacking the autoinhibitory domain or containing an autophosphorylation-mimick mutation, is sufficient to trigger the formation of spontaneous nodules in the absence of rhizobia (Gleason et al., 2006; Tirichine et al., 2006). Strikingly, when we introduced an always-active DMI3/CCaMK construct lacking the autoinhibitory domain

(*35S:DMI3**[1-311]) into *Mtsym1-1* roots no spontaneous nodules were formed (0/65 transgenic roots) whereas introduction of *35S:DMI3** in wild-type control roots resulted in the formation of ~5 spontaneous nodules/transgenic root (n=40) (Suppl. Fig.5A). To rule out secondary effects on spontaneous nodule formation, we made use of a gain-of-function mutation in the cytokinin receptor MtCRE1. A gain-of-function mutation [L266F] in the extracellular receiving domain of this receptor histidine kinase also triggers spontaneous nodule formation (Gonzalez-Rizzo et al., 2006; Murray et al., 2007; Tirichine et al., 2007; Hayashi et al., 2010). Introduction of *35S:*CRE1*[L267F] did trigger the formation of spontaneous nodules on *Mtsym1-1* roots (18 spontaneous nodules per 28 roots) with the same efficiency as on wild-type control roots (16 spontaneous nodules per 20 roots) (Suppl. Fig.5B, C). These data suggest that IPD3 affects the stability/activity of a DMI3 signalling complex upstream of cytokinin signalling.

MtIPD3 is required for efficient mycorrhizal colonization but not arbuscule formation

DMI3 is part of the common signalling cascade that is essential for both rhizobial symbiosis and arbuscular mycorrhiza (AM). In Lotus, the *IPD3* ortholog *CYCLOPS* was shown to be essential for arbuscule formation (Yano et al., 2008). However, the pea *IPD3* mutant (*Pssym33-3,* SGEFix$^-$-2) was reported to show decreased mycorrhizal colonization, but with increased arbuscule abundance (Jacobi et al., 2003a, b). Therefore, we examined the AM phenotype in Medicago *Mtsym1-1* according to Trouvelot et al. (1986), using the following parameters: the intensity of AM colonization (M%) and the arbuscule abundance (a%) at 18 and 62 dpi. *Mtsym1-1* showed decreased AM colonization at 18 dpi (M%, $P \leq 0.05$), but increased arbuscule abundance (a%, $P \leq 0.05$) at 62 dpi (Suppl. Fig.6) similar to the reported arbuscular mycorrhizal phenotype of *Pssym33-3* (Jacobi et al., 2003a, b). These data suggest that IPD3 is not essential for arbuscule formation in Medicago and pea.

DISCUSSION

Here we cloned *SYM1* from Medicago and *Sym33* from pea and show that both encode the Interacting Protein of DMI3, IPD3. From the phenotypes of the respective mutants, we reveal a novel and essential function for IPD3 in symbiosome formation and development.

One of the striking phenotypes of *Mtsym1* and *Pssym33* is the block of release of rhizobia from the infection threads into the nodule cells. A similar block was found when the essential Nod factor signalling protein *DMI2* was knocked down specifically in the nodule (Capoen et al., 2005; Limpens et al., 2005) or when a non-legume *DMI3* ortholog from rice was introduced into the Medicago *dmi3* mutant (Godfroy et al., 2006). The identification of a knockout mutation in IPD3 now clearly establishes an essential role for the common symbiotic signalling module DMI2-DMI3-IPD3 in symbiosome formation. In the orthologous *cyclops* mutant from Lotus, infection thread formation does not occur by which later roles for CYCLOPS in symbiosome formation could not be observed (Yano et al., 2008).

The presence of IPD3 in the nucleus and its interaction and likely phosphorylation by DMI3 suggest that IPD3 is required to activate specific genes to allow symbiosome formation. By analyzing the expression of a selected set of genes that are induced during nodule formation and required for nodule invasion and/or symbiosome formation, we showed that IPD3 is essential only for a subset of induced genes. Interestingly, the expression of the nodule-specific remorin, *SYMREM* was strongly reduced in *Mtsym1* nodules. Similar to *Mtsym1*, *SYMREM* mutants form nodules that are invaded by infection threads, but subsequent symbiosome formation does not occur (Lefebvre et al., 2010). Therefore, the impaired expression of *SYMREM* in *Mtsym1* can be sufficient to explain the observed *Mtsym1* phenotypes. Interestingly, this remorin protein interacts with the symbiotic receptors NFP, LYK3, and DMI2 that are essential for perception and signal transduction of rhizobial Nod factors (Lefebvre et al., 2010). IPD3-dependent induction of SYMREM may represent a feedback mechanism to regulate the function of these symbiotic receptors during rhizobial infection. However, the reported presence of SYMREM on mature symbiosomes indicates additional roles for this protein in symbiosome development (Lefebvre et al., 2010). In contrast, the expression of *ERN, RPG, LIN, HAP2, Flotillin-2,* and *-4* does not require MtIPD3 as the expression of these genes in *Mtsym1* nodules was either comparable or higher than their expression level in wild-type nodules 12 dpi (Arrighi et al., 2008; Kiss et al., 2010; Haney and Long, 2010; Middleton et al., 2007; Combier et al., 2007; Vernié et al., 2008). The transcription factor ERN and nuclear protein RPG showed respectively a ~3x and ~8x higher expression level in *Mtsym1* type-1 (and type-2 in case of *ERN*) nodules compared to wild-type, which might reflect a developmental block at early stages of nodule development.

The block in symbiosome formation in *Mtsym1* and *Pssym33* appears to correlate with the extensive deposition of cell wall material in the infection threads and accumulation of polyphenolic compounds (Bénaben et al., 1995; Tsyganov et al., 1998). This indicates that a more severe defense response is triggered that may block the progression of infection thread growth and the release of bacteria. Extensive cell wall depositions were also reported on infection threads in *DMI2* knockdown nodules in *Sesbania rostrata* where release was blocked (Capoen et al., 2005). The extensive deposition of cell wall material somewhat resembles the formation of cell wall appositions that block the invasion of plant cells by pathogenic fungi during basal defense responses (Schulze-Lefert, 2004). Therefore, IPD3 might be required to suppress/control basal defense responses to allow a successful symbiosis.

In addition to release of the bacteria from the infection threads, IPD3 is also required for subsequent symbiosome development. The pea *sym33* (SGEFix$^-$-2) mutant occasionally forms nodules where release of rhizobia from the infection threads takes place (Tsyganov et al., 1998). Similarly, although we did not observe any release of bacteria from the infection threads in *Mtsym1,* it has been reported that occasional release can occur in *Mtsym1* (Bénaben et al., 1995; Maunoury et al., 2010). In such cases, the symbiosomes remain morphologically

undifferentiated, and the nodule cells show premature senescence (Tsyganov et al., 1998). A role for IPD3 during later stages of symbiosome development fits with its observed presence in the nucleus of infected cells in the infection zone as well as in the fixation zone. The presence of IPD3 in the fixation zone where DMI3 is not present raises the possibility that, in these cells, IPD3 interacts with other components than DMI3 to control late steps of symbiosome development.

IPD3 also controls the progression of infection threads through the root outer cortex and regulates infection thread growth already in the root hairs. Although normal tubular infection threads were formed, a significant number of infection events appeared to be blocked at the microcolony stage and form sac-like structures. A more severe block of infection thread formation as reported for Lotus *cyclops* mutants (Yano et al., 2008), became apparent when Δ*nodL* rhizobial mutant that make different Nod factor structures (Ardourel et al., 1994), were used to inoculate *Mtsym1*. Almost all infection threads were arrested at the microcolony stage. This indicates an additive effect of impaired Nod factor signal input and IPD3-dependent signalling in *Mtsym1*. A less severe effect on the infection thread growth observed in *Medicago* (and pea) compared to Lotus cannot be explained through less severe mutations in IPD3. *Mtsym1-1* shows a near identical mutation to that found in the *Ljcyclops-5* allele (Yano et al., 2008); the resulting truncated peptide sequence is missing the second NLS and the coiled-coil domain, and it is likely that the protein is unstable and/or not properly targeted to the nucleus (our data). Moreover, the different alleles show similar phenotypes within each species (Medicago, pea, and Lotus), suggesting they all represent loss-of-function alleles (Table 1). In the accompanying paper, Horváth et al. identified a *Tnt1* transposon tagged insertion mutant allele of *IPD3* in the Medicago R108 genetic background. Strikingly, this mutant shows a phenotype comparable to Lotus *cyclops* which indicates that the genetic background of the plant (Jemalong versus R108) may influence the infection phenotype. Given the fact that in Medicago the ratio of type-1 and type-2 nodules is bacterial strain-dependent, it is likely that the specific combination of plant and bacteria determines the IPD3 mutant phenotype.

In addition to infection phenotypes, we found that IPD3 is also required for the induction of spontaneous nodules by an always-active truncated DMI3 construct. In Lotus *cyclops* mutants, an autophosphorylation-mimick always-active form of DMI3 was still able to trigger spontaneous nodules although the numbers were severely reduced compared to wild-type plants (Yano et al., 2008; Capoen and Oldroyd, 2008). Introduction of an always-active/more sensitive CRE1 cytokinin receptor gene was able to trigger spontaneous nodules efficiently in *Mtsym1*, indicating that activation of cytokinin signalling bypasses IPD3 requirement for nodule organogenesis. Similarly, it was recently shown in Lotus that the action of the cytokinin receptor is downstream of DMI3/CCaMK (Tirichine et al., 2007; Hayashi et al., 2010). DMI3 likely forms a multimeric signalling complex with other proteins in addition to IPD3 that trigger transcriptional responses. Loss of IPD3 could destabilize such a DMI3-dependent protein complex and thereby

affect DMI3-dependent gene expression. Different responses might require different levels of DMI3 complex activity/stability. This model implies that the truncated DMI3 protein forms a complex that is less stable/active than the wild-type form, and an additional mutation in IPD3 renders this complex unable to trigger spontaneous nodule formation. Such mechanism could also explain the additive mutant effects observed when inoculating *Mtsym1* with Δ*nodL* bacteria; the less efficient Δ*nodL* Nod factors (lacking the acetate substitution) would activate DMI3 less efficiently in *Mtsym1* background that is already reduced for the activity/stability of the DMI3 complex.

IPD3 and DMI3 are widely conserved in plants from monocots to eudicots that are able to establish arbuscular mycorrhiza indicating an ancient role in the symbiosis (Messinese et al., 2007; Yano et al., 2008). The rhizobial symbiosis is thought to have recruited part of this mycorrhizal symbiotic pathway (Catoira et al., 2000; Capoen and Oldroyd, 2008). The recent identification of a single LysM-type receptor, orthologous to a Nod factor receptor in the non-legume *Parasponia* that controls the accommodation of both rhizobia and arbuscular mycorrhizal fungi suggests a conserved ancient function for this pathway in the intracellular accommodation of symbionts (Op den Camp et al., 2010). In the pea *sym33-3* (SGEFix$^-$-2) and Medicago *sym1-1* mutants, mycorrhizal colonization is decreased, however, arbuscules can still be formed (Jacobi et al. 2003a, b; Suppl. Fig.5). In contrast, an *IPD3* knockout mutation in the Medicago R108 background blocks arbuscule formation similar to Lotus *cyclops* mutants, which indicates that the effects on the arbuscular mycorrhizal interaction are also influenced by the genetic background of the plant (Yano et al., 2008; Horváth et al. 2011). In conclusion, in pea and Medicago the DMI3-IPD3 module is essential for the accommodation of rhizobia in new organelle-like membrane compartments in analogy to the intracellular accommodation of arbuscular mycorrhizal fungi.

MATERIAL AND METHODS

Plant lines, bacterial and fungal strains, and growth conditions

The *Medicago truncatula* cv Jemalong line J5 and A17 were used as wild-type reference lines. *Mtsym1-1/TE7* (Bénaben et al., 1995) was crossed to *M. truncatula* accession A20 and selfed to generate a segregating F2 population. The *Tnt1*/Mere-transposon tagged line 76A-24 (T00076A self-descent numbered 24) was identified in a collection of *Tnt1*-tagged *M. truncatula* Jemalong lines generated at LIPM Toulouse (Iantcheva et al., 2009) screened for nodulation mutant phenotypes. Phenotypic analysis was performed after two back-crosses (BC2 lines). 76A-24 was crossed to *Mtsym1/TE7* to show allelism. *Mtsym1-1* was further crossed to TR3 (Sagan et al., 1998) to study allelism. TR3, TR9, TR13, TR62, TR69 and TRV15 were previously shown to be allelic (Sagan et al., 1998). M4 and F2 of back-cross1 seeds were used for phenotypic analysis of these alleles. For analysis of nodule phenotypes plants were grown either in perlite (as described in Limpens et al., 2004) or in aeroponic caissons (as described in Barker et al., 2006). *Sinorhizobium meliloti* strain Sm2011 was used for inoculation. Additionally,

Sm2011-*GFP* (Limpens et al., 2003), Sm2011-*mRFP* (Smit et al., 2005), and Sm2011*ΔnodL*::Tn5-*GFP* (Limpens et al., 2003) were used.

Three previously identified *Pssym33* alleles were analyzed: RisFixU (genetic background Finale) (Voroshilova et al., 2001), SGEFix-2 (Tsyganov et al., 1998) and SGEFix-5 with genetic background SGE. Finale and SGE were used as respective wild-type reference. Pea plants were inoculated with *Rhizobium leguminosarum bv. viciae* CIAM1026 in quartz sand according to Borisov et al., (1997).

Agrobacterium rhizogenes mediated root transformations were done according to Limpens et al. (2004) using strain MSU440 (Sonti et al., 1995). The *Escherichia coli* strain DH5α was used for cloning and strain DB3.1 (Invitrogen) for propagation of GATEWAY compatible vectors containing the *ccdB* gene.

Glomus intraradices Schenck and Smith isolate CIAM8 (Muromtsev et al., 1989) from the Collection of the All-Russia Institute for Agricultural Microbiology (registered in the European Bank of Glomales as isolate BEG144) was used for inoculation of Medicago plants. To inoculate plants, a living culture of *Glomus intraradices* was obtained in an inoculation system with a nurse plant (Rosewarne et al., 1997). *Allium schoenoprasum L.* was used as a nurse plant as described in Demchenko et al. (2004), except that phosphates were not included in the nutrient solution.

Arbuscular mycorrhizal phenotype analysis

Plants were collected at 18 and 62 days. Root fragments were collected individually from 6 to 10 plants per treatment combination. To visualize fungal structures in the root samples, ink staining was performed as described in Vierheilig et al. (1998). Roots were cut in fragments with a total length up to 30 cm per plant, and mounted on glass slides in glycerol. AM development in the roots was estimated according to Trouvelot et al. (1986) using a Opton 35 (Opton, Germany) light microscope for two parameters: M% – intensity of mycorrhizal colonisation in the root system, a% – arbuscule abundance in mycorrhizal root fragments. The data were compared by Student's t-test with the help of SigmaStat 2.3 for Windows, SPSS Inc.

Constructs

The inferred MtIPD3 promoter, 1048bp upstream of the IPD3 start-codon, was PCR-amplified with Phusion high fidelity Taq polymerase (New England Biolabs) from genomic DNA using primers: MtIPD3pF 5'- cacc<u>aagctT</u>AAGTGGAGTCAAAAGAAATAGTTTATATG-3' and MtIPD3pR 5'-AAA<u>GGCGCGCC</u>GAAACACTTGAATGATGCTTGAACTTATT-3'. The promoter fragment was cloned into pENTR-p4p1r using HindIII and AscI (underlined), resulting in pENTR4-1-MtIPD3p. Additionally this promoter fragment was HindIII-AscI cloned into pENTR-p4p1r-MCS-GFP (containing a multiple cloning site in front of eGFP to make N-terminal GFP fusions) to generate pENTR4-1-MtIPD3p-GFP. The MtIPD3 cds was PCR amplified from 14 day-old nodule cDNA using primers: MtIPD3-F 5'-CACCATGGAAGGGAGAGGATTTTCTGGT-3' and MtIPD-R 5'-TCAAATCTTTCCAGTTTCTGATAGA-3'. The resulting 1546 bp fragment was directionally cloned into pENTR-D-TOPO (Invitrogen), resulting in pENTR-MtIPD3. Next, a multi-site GATEWAY reaction with LR Clonase II plus (Invitrogen) was performed using pENTR4-1-MtIPD3p, pENTR-MtIPD3, pENTR-p2rp3-Stop-T35S and pKGW-RR-MGW (a modified multi-site GATEWAY compatible binary vector containing *AtUbiquitin10p:DsRED1* to select transgenic roots according to Limpens et al., 2009), to generate MtIPD3p:IPD3. A multi-site GATEWAY

reaction using pENTR-MtIPD3, pENTR4-1-MtIPD3p-GFP, pENTR-p2rp3-Stop-T35S and pKGW-RRMGW was performed to generate MtIPD3p:GFP-MtIPD3.

For the 35S:DMI3*[1-311] construct, an enhanced CaMV 35S promoter (ep35S) was first PCR-amplified from pCAMBIA1300 (www.cambia.org.au) using primers P35S_t (5'-GGGGGCGCGCCATGGTGGAGCACGACACTC-3') and P35S_b (5'-GGCCCGGGAGAGATAGATTTGTAGAGAGAGACTGGTGA-3'). It was inserted into pENTR-p2rp3-MCS-Stop-T35S using AscI and SmaI restriction enzymes. A 933-bp DMI3 cDNA fragment was PCR-amplified from A17 root cDNA using primers cMtDMI3_t (5'-GGGCCCGGGATGGGATATGGAACAAGAAAAC-3') and tMtDMI3_b (5'-GGGGTACCGGCTTTCTCACCTTTGACC-3'), and cloned into pENTR-p2rp3-ep35S-MCS-Stop-T35s using SmaI and KpnI. Finally, it was recombined into pKGW-RR-MGW in a multiple GATEWAY reaction using Clonase II plus (Invitrogen) resulting in 35S:DMI3*[1-311].

For the 35S:CRE1*[L267F] construct, MtCRE1 was PCR amplified from M. truncatula genomic DNA in two parts; using the primers 5'-CACCATGGGTCTTCTCTTGAAGATGAA-3' and 5'-TAGGCACTTACTGATACTCAAACCA-3' for part one, and 5'-CACCTTAATT-GCTGATGAAGAGTTT-3' and 5'- TCATGAATCTACTGAAGTAGGTTTTG-3' for part two. The two parts were then cloned into pENTR-D-Topo vector (Invitrogen) creating pENTR1-2_MtCRE1-part1 and pENTR1-2_MtCRE1-part2. The L267F mutation was introduced in pENTR1-2_MtCRE1-part1 using the QuikChange® XL Site-Directed Mutagenesis Kit (Stratagene) with primers 5'-GTCACTTGTGGAAAATTTAtTTGGTCAACTTG-CTGGTCATC-3' and 5'-GATGACCAGCAAGTTGACCAAaTAAATTTTCCAC-AAGTGAC-3', creating pENTR1-2_MtCRE1L267F-part1*. Next, part1* and part2 were combined by overlap PCR, using the primers 5'-ggggGCGGCCGCATGG-GTCTTCTCTTGAAGATGAA-3', 5'-tttgaccacccattagttcaacTAGGCACTTAC-TGATACTCAAACCA-3', 5'-GTAAGTGCCTAgttgaactaatgggtggtcaaa-3' and 5'-ggggGGCGCGCCTCATGAATCTACTGAAGTAGGTTTTG-3' and the product was ligated using NotI and AscI (underlined) into a pENTR-D-Topo vector creating pENTR1-2_MtCRE1L267F. The CaMV35S promoter and terminator were cloned into a pENTR4-1 and pENTR2-3 (Invitrogen) thereby creating two modified pENTR clones: pENTR4-1_p35S and pENTR2-3_T35S. All three ENTR vectors were combined into the binary destination vector pKGW-RR-MGW by a multisite gateway reaction (Invitrogen) resulting in 35S:CRE1*[L267F].

Map-based cloning

A segregating F2 population (99 plants) of a cross between Mtsym1/TE7 and A20 containing 23 homozygote mutants was used for mapping. All plants showing crossovers between markers 002C10 and 18M20 were phenotyped in the next generation (20 F3 plants per F2 plant) to determine the Mtsym1 genotype of the corresponding F2 plants. DNA was extracted using 1342/Molecular Plant-Microbe Interactions the Qiagen DNeasy plant mini kit. The following simple-sequence repeat (or cleaved amplified polymorphic sequence [CAPS]) markers were used for mapping on Medicago linkage group 5: PCR products were analyzed on a 3.5% agarose gel: **MtB60**, **MtB146**, **MtB23**, and **MtB255** (Mun et al., 2006): **18M20**, TCAGATCGACTGCAACTCCA and TGAGCACATGATCCTTTATACTTG; **8D15**, TAATTGGGGATGAAAATCTG and CCTCATGTCACTCATCATCA; **34B21**, TTCAGAAAAACCCAAACCAAG and ACATGAGAGCATCCGACCCA; **CU4695**, TGCCACCAAAGCTAACAAACTC and TGGGTTCATCATGGACCTTTTAC; **CU469(B)**, CCACAAAGCGTCCACCATAAAC and CAACCAAAGAAGAAGAACTCCAAACA; **CU914**,

GTGTCATTAATGAACTTCCAACCTT and GTCCACATCAAACACATCGTAAGA; **CU469**, GGACCTATGCAAATGACCTTCTACAA and CTTTAATGGCCGCAAATCTTACTT; 81G16 (CAPS enzyme HindIII), CCACGCGATTTTGGGACTA and CAAAAAGCCTTATGAACCTAACCT; **CU137**, GAGGAAGGAGAAGGGAAAATAATC and CAACATAATGGGAAATCAAACAAC; **CT573**, TAAATGTGACCGGGGGAGTATG and GCTCATGGATTAGGAGGTGGTCA; 1**9c21a**, AAATGGACCCTGATGATTCG and GGGGGATGGATACTAGAGGG; **002C10**, GGGAAGTTAAGCATTTCCCA and TGGTTTGTGGCATTCATTGT; **001B12**, TGATCCTTTCCAAGAAGCG and CGCTAATTGCTGGCTTCAAA.

The MtIPD3 gene was PCR amplified from genomic DNA of the different mutant lines and the corresponding WT reference lines using primers MtIPD3-F and MtIPD3-R and examined by sequence analysis. Sym33 mapping was done using a F2 population (95 plants) of a cross between WT10584 (Swiecicki and Irzykowska, 1998) and SGEFix-2(sym33) (Tsyganov et al., 1994). DNA was extracted using the standard cetyltrimethylammonium bromide method (Rogers and Bendich, 1985). The following cross-species CAPS markers were used: **Gst** (restriction-enzyme TaiI) forward (F), CAATTGAACACTCTTACTCAG and reverse (R), AGATGCAAAGCTTCCTTGCT; **IPD3** (restriction enzyme PfeI) F, TGCAAAATACTCAAGCACCA and R, TGTTTCCATGAGCTATCACAAAG; **Alat-C** F, CTGACCTTCCCTCGCCAG (restriction-enzyme FspBI), and R, CCTTGCTCGCACCATCAGT; and **Enod40** F, TGAAGGTTGTCTGGTGTCTA (WT10584-allele-specific PCR) and R, TTGAAGAAAAGAAACAGGAATTA. The *PsIPD3* gene was PCR-amplified from genomic DNA of the mutant lines and the corresponding WT reference lines using primers PsIPD3-F (5′-ATGGAAGGGAGAGGATTTTCTG-3′) and PsIPD3-R (5′-TTAAATCTTTCCAGTTTCTGATAAAAG-3′) and examined by sequence analyses.

Accession numbers

Sequence data of the genes used in this article can be found in the GenBank/EMBL data libraries or TIGR Gene Indices under the following accession numbers: MtIPD3 EF117279; PsIPD3 EF569222; MtGAPDH BT052418; MtHAP2 EF488826; MtNIN FJ719774; MtDMI3 AY496049; MtCRE1 AC141922/TC109250, MtERN EF396330, MtEFD EU251063, MtSYMREM TC116072, MtFlotillin-2 GU224279, MtFlotillin-4 GU224281, MtRPG DQ854741, MtLIN EU926661.

ACKNOWLEDGMENTS

We would like to thank Thierry Huguet for providing the *Mtsym1/TE7* mutant seeds. We wish to acknowledge David Barker (LIPM) for valuable advice on the 76A project, and José Garcia, Julie Mari and Florian Poitevin (LIPM) for expert screening and molecular work. This study was supported by: the Russian Ministry of Education and Science (Governmental contracts № 02.740.11.0276, 16.512.11.2155, П1304), President of Russia supporting the leading scientific schools (НШ-3440.2010.4), RFBR (09-04-91054, 10-04-00961, 10-04-01146), and by The Netherlands Organization for Scientific Research grants NWO-047.117.2005.006 and NWO-3184319448.

REFERENCES

Ardourel, M., Demont, N., Debellé, F., Maillet, F., de Billy, F., Promé, J. C., Dénarié, J., Truchet, G. (1994) *Rhizobium meliloti* lipooligosaccharide nodulation factors: different structural requirements for bacterial entry into target root hair cells and induction of plant symbiotic developmental responses. *Plant Cell,* 6: 1357–1374.

Arrighi, J.F., Godfroy, O., de Billy, F., Saurat, O., Jauneau, A., Gough, C. (2008) The RPG gene of Medicago truncatula controls *Rhizobium*-directed polar growth during infection. *PNAS*, 105: 9817–9822.

Aubert, G., Morin, J., Jacquin, F., Loridon, K., Quillet, M.C., Petit, A., Rameau, C., Lejeune-Hénaut, I., Huguet, T., Burstin, J. (2006) Functional mapping in pea, as an aid to the candidate gene selection and for investigating synteny with the model legume *Medicago truncatula.* Theor. Appl. Genet., 112: 1024–1041.

Barker, D.G., Pfaff, T., Moreau, D., Groves, E.D., Ruffel, S., Lepetit, M., Whitehand, S., Maillet, F., Nair, R.M., Journet, E.P. (2006) Growing *M truncatula*: choice of substrates and growth conditions In: The Medicago truncatula handbook. Mathesius U, Journet EP, Sumner LW (eds) ISBN 0-9754303-1-9 http://wwwnobleorg/MedicagoHandbook/.

Bénaben, V., Duc, G., Lefebvre, V., Huguet, T. (1995) TE7, An Inefficient Symbiotic Mutant of *Medicago truncatula* Gaertn cv. Jemalong. *Plant Physiol.,* 107: 53–62.

Bersoult, A., Camut, S., Perhald, A., Kereszt, A., Kiss, G.B., Cullimore, J.V. (2005) Expression of the *Medicago truncatula DMI2* gene suggests roles of the symbiotic nodulation receptor kinase in nodules and during early nodule development. *Mol. Plant-Microbe Interact*., 18: 869–876.

Borisov, A.Y., Rozov, S.M., Tsyganov, V.E., Morzhina, E.V., Lebsky, V.K., Tikhonovich, I. (1997) Sequential functioning of *Sym13* and *Sym31*, two genes affecting symbiosome development in root nodules of pea (*Pisum sativum* L). *Mol. Gen. Genet.*, 254: 592–598.

Brewin, N.J. (2004) Plant cell wall remodelling in the Rhizobium-legume symbiosis. *Crit. Rev. Plant Sci.*, 23: 293–316.

Capoen, W., Goormachtig, S., De Rycke, R., Schroeyers, K., Holsters, M. (2005) SrSymRK, a plant receptor essential for symbiosome formation. *PNAS,* 102: 10369-10374.

Capoen, W., and Oldroyd, G. (2008) How CYCLOPS keeps an eye on plant symbiosis. PNAS, 105: 20053–20054.

Catoira, R., Galera, C., de Billy, F., Penmetsa, R.V., Journet, E.P., Maillet, F., Rosenberg, C., Cook, D., Gough, C., Dénarié, J. (2000) Four genes of *Medicago truncatula* controlling components of a Nod factor transduction pathway. *Plant Cell,* 12: 1647–1666.

Combier, J.P., Frugier, F., de Billy, F., Boualem, A., El-Yahyaoui, F., Moreau, S., Vernié, T., Ott, T., Gamas, P., Crespi, M., Niebel, A. (2006) MtHAP2-1 is a key transcriptional regulator of symbiotic nodule development regulated by microRNA169 in *Medicago truncatula*. Genes Dev. 20: 3084–3088.

Chen, C., Ané, J.M., Zhu, H. (2008) OsIPD3, an ortholog of the *Medicago truncatula* DMI3 interacting protein IPD3, is required for mycorrhizal symbiosis in rice. *New Phytol.,* 180: 311–315.

Demchenko, K., Winzer, T., Stougaard, J., Parniske, M., Pawlowski, K. (2004) Distinct roles of *Lotus japonicus* SYMRK and SYM15 in root colonization and arbuscule formation. *New Phytol.,* 163: 381–392.

Gleason, C., Chaudhuri, S., Yang, T., Muñoz, A., Poovaiah, B.W., Oldroyd, G.E. (2006) Nodulation independent of rhizobia induced by a calcium-activated kinase lacking autoinhibition. *Nature* 441: 1149–1152.

Godfroy, O., Debellé, F., Timmers, T., Rosenberg, C. (2006) A rice calcium- and calmodulin-dependent protein kinase restores nodulation to a legume mutant. *Mol. Plant Microbe Interact.,* 19: 495–501.

Gonzalez-Rizzo, S., Crespi, M., Frugier, F. (2006) The *Medicago truncatula* CRE1 cytokinin receptor regulates lateral root development and early symbiotic interaction with *Sinorhizobium meliloti*. Plant Cell, 18: 2680–2693.

Grimsrud, P.A., den Os, D., Wenger, C.D., Swaney, D.L., Schwartz, D., Sussman, M.R., Ané, J.M., Coon, J.J. (2010) Large-scale phosphoprotein analysis in *Medicago truncatula* roots provides insight into in vivo kinase activity in legumes. *Plant Physiol*., 152: 19–28.

Haney, C.H., and Long, S.R. (2010) Plant flotillins are required for infection by nitrogen-fixing bacteria. *PNAS,* 107: 478–483.

Hayashi, T., Banba, M., Shimoda, Y., Kouchi, H., Hayashi, M., Imaizumi-Anraku, H. (2010) A dominant function of CCaMK in intracellular accommodation of bacterial and fungal endosymbionts. *Plant J.,* 63: 141–154.

Horváth, B., Yeun, L. H., Domonkos, A., Halász, G., Gobbato, E., Ayaydin, F., Míró, K., Hirsch, S., Sun, J., Tadege, M., Ratet, P., et al. (2011) *Medicago truncatula* IPD3 is a member of the common symbiotic signaling pathway required for rhizobial and mycorrhizal symbioses. *Mol. Plant-Microbe Interact.,* 24: 1345–1358.

Iantcheva, A., Chabaud, M., Cosson, V., Barascud, M., Schutz, B., Primard-Brisset, C., Durand, P., Barker, D.G., Vlahova, M., Ratet, P. (2009) Osmotic shock improves *Tnt1* transposition frequency in *Medicago truncatula* cv Jemalong during in vitro regeneration. Plant Cell Rep., 28: 1563–1572.

Jacobi, L.M., Petrova, O.S., Tsyganov, V.E., Borisov, A.Y., Tikhonovich, I.A. (2003a) Effect of mutations in the pea genes *Sym33* and *Sym40.* I. Arbuscular mycorrhiza formation and function. *Mycorrhiza* 13: 3–7.

Jacobi, L.M., Zubkova, L.A., Barmicheva, E,M., Tsyganov, V.E., Borisov, A.Y., Tikhonovich, I.A. (2003b). Effect of mutations in the pea genes *Sym33* and *Sym40*. II. Dynamics of arbuscule development and turnover. *Mycorrhiza* 13: 9–16.

Jones, K.M., Kobayashi, H., Davies, B.W., Taga, M.E., Walker, G.C. (2007) How rhizobial symbionts invade plants: the *Sinorhizobium*-Medicago model. *Nat. Rev. Microbiol.,* 5: 619–633.

Kevei, Z., Lougnon, G., Mergaert, P., Horváth, G.V., Kereszt, A., Jayaraman, D., Zaman, N., Marcel, F., Regulski, K., Kiss, G.B., et al. (2007) 3-hydroxy-3-methylglutaryl coenzyme a reductase 1 interacts with NORK and is crucial for nodulation in *Medicago truncatula*. Plant Cell, 19: 3974–3989.

Kiss, E., Oláh, B., Kaló, P., Morales, M., Heckmann, A.B., Borbola, A., Lózsa, A., Kontár, K., Middleton, P., Downie, J.A., et al. (2009) LIN, a novel type of U-box/WD40 protein, controls early infection by rhizobia in legumes. *Plant Physiol.*, 151: 1239–1249.

Lefebvre, B., Timmers, T., Mbengue, M., Moreau, S., Hervé, C., Tóth, K., Bittencourt-Silvestre, J., Klaus, D., Deslandes, L., Godiard, L., et al. (2010) A remorin protein interacts with symbiotic receptors and regulates bacterial infection. *PNAS*, 107: 2343–2348.

Lévy, J., Bres, C., Geurts, R., Chalhoub, B., Kulikova, O., Duc, G., Journet, E.P., Ané, J.M., Lauber, E., Bisseling, T., et al. (2004) A putative Ca^{2+} and calmodulin-dependent protein kinase required for bacterial and fungal symbioses. *Science* 303: 1361–1364.

Limpens, E., Franken, C., Smit, P., Willemse, J., Bisseling, T., Geurts, R. (2003) LysM domain receptor kinases regulating rhizobial Nod factor-induced infection. Science 302: 630–633.

Limpens, E., Ramos, J., Franken, C., Raz, V., Compaan, B., Franssen, H., Bisseling, T., Geurts, R. (2004) RNA interference in *Agrobacterium rhizogenes*-transformed roots of Arabidopsis and *Medicago truncatula*. J. Exp. Bot., 55: 983–992.

Limpens, E., Mirabella, R., Fedorova, E., Franken, C., Franssen, H., Bisseling, T., Geurts, R. (2005) Formation of organelle-like N2-fixing symbiosomes in legume root nodules is controlled by DMI2. *PNAS*, 102: 10375–10380.

Limpens, E., Ivanov, S., van Esse, W., Voets, G., Fedorova, E., Bisseling, T. (2009) Medicago N2-fixing symbiosomes acquire the endocytic identity marker Rab7 but delay the acquisition of vacuolar identity. *Plant Cell,* 21: 2811–2828.

Marsh, J.F., Rakocevic, A., Mitra, R.M., Brocard, L., Sun, J., Eschstruth, A., Long, S.R., Schultze, M., Ratet, P., Oldroyd, G.E. (2007) *Medicago truncatula* NIN is essential for rhizobial-independent nodule organogenesis induced by autoactive calcium/calmodulin-dependent protein kinase. *Plant Physiol.,* 144: 324–335.

Maunoury, N., Redondo-Nieto, M., Bourcy, M., Van de Velde, W., Alunni, B., Laporte, P., Durand, P., Agier, N., Marisa, L., Vaubert, D., et al. (2010) Differentiation of Symbiotic Cells and Endosymbionts in *Medicago truncatula* Nodulation Are Coupled to Two Transcriptome-Switches. *PLOS ONE*, 5(3): e9519. doi:10.1371/journal.pone.0009519.

Messinese, E., Mun, J.H., Yeun, L.H., Jayaraman, D., Rougé, P., Barre, A., Lougnon, G., Schornack, S., Bono, J.J., Cook, D.R., et al. (2007) A novel nuclear protein interacts with the symbiotic DMI3 calcium- and calmodulin-dependent protein kinase of *Medicago truncatula*. *Mol. Plant Microbe Interact.,* 20: 912–921.

Middleton, P.H., Jakab, J., Penmetsa, R.V., Starker, C.G., Doll, J., Kaló, P., Prabhu, R., Marsh, J.F., Mitra, R.M., Kereszt, A., et al. (2007) An ERF transcription factor in *Medicago truncatula* that is essential for Nod factor signal transduction. *Plant Cell,* 19: 1221–1234.

Mitra, R.M., Gleason, C.A., Edwards, A., Hadfield, J., Downie, J.A., Oldroyd, G.E., Long, S.R. (2004) A Ca^{2+}/calmodulin-dependent protein kinase required for symbiotic nodule development: Gene identification by transcript-based cloning. *PNAS*, 101: 4701–4705.

Morandi, D., Prado, E., Sagan, M., Duc, G. (2005) Characterization of new symbiotic *Medicago truncatula* (Gaertn) mutants, and phenotypic or genotypic complementary information on previously described mutants. *Mycorrhiza* 15: 283–289.

Mun, J.H., Kim, D.J., Choi, H.K., Gish, J., Debellé, F., Mudge, J., Denny, R., Endré, G., Saurat, O., Dudez, A.M., et al. (2006) Distribution of microsatellites in the genome of *Medicago truncatula*: a resource of genetic markers that integrate genetic and physical maps. *Genetics* 172: 2541–2555.

Muromtsev, G.S., Marshunova, G.A., Jacobi, L.M. (1989) USSR Inventor's Certificate no.1501509.

Murray, J.D., Karas, B.J., Sato, S., Tabata, S., Amyot, L., Szczyglowski, K. (2007) A cytokinin perception mutant colonized by *Rhizobium* in the absence of nodule organogenesis. *Science* 315: 101–104.

Oldroyd, G.E. and Downie, J.A. (2008) Coordinating nodule morphogenesis with rhizobial infection in legumes. *Annu. Rev. Plant Biol.,* 59: 519–546.

Op den Camp, R., Streng, A., De Mita, S., Cao, Q., Polone, E., Liu, W., Ammiraju, J.S.S., Kudrna, D., Wing, R., Untergasser, A., et al. (2011) LysM-Type Mycorrhizal Receptor Recruited for Rhizobium Symbiosis in Nonlegume *Parasponia.* Science, 331(6019): 909–912.

Rakocevic, A., Mondy, S., Tirichine, L., Cosson, V., Brocard, L., Iantcheva, A., Cayrel, A., Devier, B., Abu El-Heba, G.A., Ratet, P. (2009) MERE1, a low-copy-number copia-type retroelement in *Medicago truncatula* active during tissue culture. Plant Physiol., 151: 1250–1263.

Riely, B.K., Lougnon, G., Ané, J-M., Cook, D.R. (2007) The symbiotic ion channel homolog DMI1 is localized in the nuclear membrane of *Medicago truncatula* roots. *Plant J.,* 49: 208–216.

Rogers, S.O. and Bendich, A.J. (1985). Extraction of DNA from milligram amounts of fresh, herbarium, and mummified plant tissues. *Plant Mol. Biol.,* 5: 69–76.

Rosewarne G., Barker, S.L., Smith, S.E. (1997) Production of near synchronous colonization in tomato for developmental and molecular analysis of mycorrhiza. *Mycol. Res.,* 101: 966–970.

Sagan, M., de Larembergue, H., Morandi, D. (1998) Genetic analysis of symbiosis mutants in *Medicago truncatula*. In: Elmerich C, Kondorosi A, Newton WE (eds) Biological nitrogen fixation for the 21st century Kluwer, Dordrecht, pp 317–318.

Schulze-Lefert, P. (2004) Knocking on the heaven's wall: pathogenesis of and resistance to biotrophic fungi at the cell wall. *Curr. Opin. Plant Biol.,* 7: 377–383.

Smit, P., Raedts, J., Portyanko, V., Debellé, F., Gough, C., Bisseling, T., Geurts, R. (2005) NSP1 of the GRAS protein family is essential for rhizobial Nod factor-induced transcription. *Science* 308: 1789–1791.

Smit, P., Limpens, E., Geurts, R., Fedorova, E., Dolgikh, E., Gough, C., Bisseling, T. (2007) Medicago LYK3, an entry receptor in rhizobial nodulation factor signaling. *Plant Physiol.,* 145: 183–191.

Sonti, R.V., Chiurazzi, M., Wong, D., Davies, C.S., Harlow, G.R., Mount, D.W., Signer, E.R. (1995) Arabidopsis mutants deficient in T-DNA integration. *PNAS*, 92: 11786–11790.

Swiecicki, W.K. and Irzykowska, L.A. (1998) A new gene for precocious yellowing on linkage group I. *Pisum Genet.,* 30: 24.

Tirichine, L., Imaizumi-Anraku, H., Yoshida, S., Murakami, Y., Madsen, L.H., Miwa, H., Nakagawa, T., Sandal, N., Albrektsen, A.S., Kawaguchi, M., et al. (2006) Deregulation of a Ca^{2+}/calmodulin-dependent kinase leads to spontaneous nodule development. *Nature* 441: 1153–1156.

Tirichine, L., Sandal, N., Madsen, L.H., Radutoiu, S., Albrektsen, A.S., Sato, S., Asamizu, E., Tabata, S., Stougaard, J. (2007) A gain-of-function mutation in a cytokinin receptor triggers spontaneous root nodule organogenesis. *Science* 2315: 104–107.

Trouvelot, A., Kough, J.L., Gianinazzi-Pearson, V. (1986) Mesure du taux de mycorhization VA d'un système radiculaire. Recherche de méthodes d'estimation ayant une signification fonctionnelle. In: Gianinazzi-Pearson V, Gianinazzi S (eds) Physiological and genetical aspects of mycorrhizae. INRA, Paris, pp 217–221.

Tsyganov, V.E., Borisov, A.Y., Rozov, S.M., Tikhonovich, I.A. (1994) New symbiotic mutants of pea obtained after mutagenesis of line SGE. *Pisum Genet.,* 26: 36–37.

Tsyganov, V.E., Morzhina, E.V., Stefanov, S.Y., Borisov, A.Y., Lebsky, V.K., Tikhonovich, I.A. (1998) The pea (*Pisum sativum* L) genes *sym33* and *sym40* control infection thread formation and root nodule function. *Mol. Gen. Genet.,* 259: 491–503.

Tsyganov, V.E., Rozov, S.M., Borisov, A.Y., Tikhonovich, I.A. (2006) Symbiotic gene *SYM33* is located on linkage group I. *Pisum Genet.,* 38: 21–22.

Vasse, J., de Billy, F., Camut, S., Truchet, G. (1990) Correlation between ultrastructural differentiation of bacteroids and nitrogen fixation in Alfalfa nodules. *J. Bacteriol.,* 172: 4295–4306.

Verma, D.P.S. and Hong, Z. (1996) Biogenesis of the peribacteroid membrane in root nodules. *Trends Microbiol.,* 4: 364–368.

Vernié, T., Moreau, S., de Billy, F., Plet, J., Combier, J.P., Rogers, C., Oldroyd, G., Frugier, F., Niebel, A., Gamas, P. (2008) EFD Is an ERF transcription factor involved in the control of nodule number and differentiation in *Medicago truncatula*. *Plant Cell,* 20: 2696–2713.

Vierheilig, H., Coughlan, A.P., Wyss, U., Piche, Y. (1998) Ink and vinegar, a simple staining technique for arbuscular-mycorrhizal fungi. *Appl. Environ. Microbiol.,* 64: 5004–5007.

Voroshilova, V.A., Boesten, B., Tsyganov, V.E., Borisov, A.Y., Tikhonovich, I.A., Priefer, U.B. (2001) Effect of mutations in *Pisum sativum* L. genes blocking different stages of nodule development on the expression of late symbiotic genes in *Rhizobium leguminosarum* bv *viciae.* Mol. Plant Microbe Interact., 14: 471–476.

Voroshilova, V.A., Demchenko, K.N., Brewin, N.J., Borisov, A.Y., Tikhonovich I.A. (2009) Initiation of a legume nodule with an indeterminate meristem involves proliferating host cells that harbour infection threads. *New Phytol.,* 181: 913–923.

Whitehead, L.F. and Day, D.A. (1997) The peribacteroid membrane. *Physiol. Plantarum,* 100: 30–44.

Yano, K., Yoshida, S., Müller, J., Singh, S., Banba, M., Vickers, K., Markmann, K., White, C., Schuller, B., Sato, S., et al. (2008) CYCLOPS, a mediator of symbiotic intracellular accommodation. *PNAS*, 105: 20540–20545.

Chapter 4

Synteny-based cloning of pea *Sym41* identifies an essential role of the LRR-receptor kinase PsSym19 in symbiosome formation and development

Evgenia Ovchinnikova,[1,2] Oksana Shtark,[2] Elena Fedorova,[1] Sjef Moling,[1] Alexey Borisov,[2] Igor Tikhonovich,[2] Ton Bisseling,[1] and Erik Limpens[1]

[1] Wageningen University, laboratory of Molecular Biology, Droevendaalsesteeg 1, 6708 PB, Wageningen, The Netherlands;

[2] All-Russia Research Institute for Agricultural Microbiology, laboratory of Genetics of Plant-Microbe Interactions, Podbelsky chaussee 3, 196608, Pushkin 8, St. Petersburg, Russia

ABSTRACT

During the nitrogen-fixing symbiosis between legume plants and Rhizobium bacteria (rhizobia), the plant hosts the bacteria within the cells of a novel symbiotic organ, the root nodule where the bacteria differentiate and become new nitrogen-fixing organelles, called symbiosomes. Symbiosome formation forms the heart of a successful symbiosis. The pea (*Pisum sativum* L.) *sym41* mutant is strongly impaired in symbiosome formation and differentiation. Here, we cloned *PsSym41* and show that the gene encodes the common symbiotic LRR-receptor kinase PsSym19, the ortholog of *Medicago truncatula* DMI2 and *Lotus japonicus* SymRK. *PsSym41* contains a 3'-splice-site mutation in intron 9 of *PsSym19* causing a strong reduction (~90%) of wild-type *Sym19* transcript levels in the mutant, and the misspliced mRNA encodes a truncated protein that lacks the kinase domain. However, *Pssym41* retains the ability to form nodules due to the low amount of the *Sym19* wild-type transcript that is still produced. Analysis of the interaction with arbuscular mycorrhizal fungi showed that fungal infection of *sym41* roots is strongly impaired at the epidermis whereas arbuscule formation in the cortical cells does not appear to be affected. In contrast, rhizobial infection and symbiosome formation are most strongly affected in nodule meristem-derived cells. Our data suggest a higher demand for *PsSym19* levels for rhizobial infection of nodule meristem-derived cells than nodule primordium cells or epidermal cells. Furthermore, our data reveal a novel essential role for Sym19 in symbiosome differentiation.

INTRODUCTION

Legumes have the unique ability to host nitrogen-fixing bacteria, collectively called rhizobia inside their cells as nitrogen-fixing organelles (Oldroyd et al., 2011). This Rhizobium-legume symbiosis plays an important role in natural and agricultural systems as it provides fixed nitrogen to its host. The accommodation of the rhizobia requires the formation of a novel organ, the root nodule. Inside the specialized nodule cells, the bacteria are hosted within novel membrane compartments, called symbiosomes (Roth and Stacey, 1989) where they find the right conditions to fix nitrogen. Therefore, symbiosome formation is at the heart of this agriculturally important symbiosis.

Rhizobia typically invade the nodule via so-called infection threads that mostly originate in root hairs that curl around attached bacteria. Within these root hair curls, bacteria become entrapped in a closed cavity where they form a micro-colony and locally the cell wall is broken down. There, the plant plasma membrane invaginates and a tubular infection thread (IT) is formed by the deposition of new cell wall material (Brewin et al., 2004). At the same time, the division of root cortical cells is induced, which results in the formation of a nodule primordium. When infection threads reach the cells of the nodule primordium, a switch to release of rhizobia from these threads occurs and symbiosomes are formed. This release of rhizobia coincides with the establishment of a nodule meristem at the apical part of the primordium and correlates with the induction of endoreduplication cycles in infected nodule/primordium cells (Timmers et al., 1998; Voroshilova et al., 2009; Cebolla et al., 1999; Vindarell et al., 2003; Mergeart et al., 2006). Failure to reach the primordium in time (before the meristem is established) causes a block of infection threads in the outer cortex and release of bacteria does not occur. Legumes such as pea and the model *Medicago truncatula* (Medicago) form so-called indeterminate nodules. In such nodules the meristem remains active, giving rise to elongated nodules where infection and subsequent symbiosome formation continuously occur in a few cell layers just below the meristem in the so-called infection zone (Vasse et al., 1990).

Symbiosome formation starts with the formation of an unwalled infection droplet, a local region on the IT where the plasma membrane extrudes and the cell wall is degraded or not built. From there, bacteria are individually “pinched off” into the cytoplasm by which they become surrounded by a plant-derived symbiosome membrane. Next, the bacteria, now called bacteroids, divide together with the symbiosome membrane in Medicago and pea nodules, by which they remain individual compartments. Subsequently, the symbiosomes differentiate become much more elongated/bigger and in case of pea they form typical branched Y-shaped structures. The bacteroids become terminally differentiated (Mergeart et al., 2006; Van de Velde et al., 2010) and acquire the ability to fix atmospheric nitrogen that is released to the plant as ammonium in the so-called fixation zone (Vasse et al., 1990).

The establishment of a successful symbiosis requires a tight coordination between the formation of the nodule and infection by the rhizobia. These processes are controlled by a signalling pathway, of which several components have been identified by a genetic approach (Oldroyd and Downie, 2008). Upon perception of (iso)flavonoids secreted by the plant, rhizobia produce lipo-chitooligosaccharide signal molecules, called Nod factors. These Nod factors are perceived by the LysM-domain containing receptor kinases activating a signalling cascade that controls nodule and IT formation (Madsen et al., 2003; Radutoiu et al., 2003, 2007; Limpens et al., 2003; Smit et al., 2007; Zhukov et al., 2008; Arrighi et al., 2006). Nod factor (NF) perception triggers Ca^{2+} oscillations in and around the nucleus (Oldroyd and Downie, 2006; Capoen et al., 2009). Activation of this Ca^{2+} spiking response requires the plasma membrane localized leucine-rich repeat (LRR) receptor kinase PsSym19/MtDMI2/LjSYMRK (Ané et al., 2002; Postma et al., 1990; Schneider et al., 1999; Endre et al. 2002; Stracke et al. 2002), a putative cation channel PsSym8/MtDMI1/LjCastor/LjPollux located at the nuclear envelope (Ané et al., 2004; Edwards et al., 2007; Charpentier et al. 2008) as well as a nuclear pore complex (Kanamori et al., 2006; Saito et al., 2007; Groth et al., 2010). These Ca^{2+} oscillations are in turn perceived by a nuclear Ca^{2+} and calmodulin-dependent kinase PsSym9/MtDMI3/LjCCaMK (Duc and Messager, 1989; Kneen et al., 1994; Lévy et al. 2004; Catoira et al., 2000; Mitra et al., 2004; Tirichine et al., 2006). The Ca^{2+}/calmodulin kinase triggers a specific transcriptional response leading to the formation of the nodule. Interestingly, these NF signalling genes are also required to establish a symbiosis with arbuscular mycorrhizal (AM) fungi and therefore this module of the pathway is also called the common symbiotic signalling pathway (Parniske, 2008). Knockout mutations in these genes typically block infection by AM fungi and rhizobia at the epidermis and prevent nodule organogenesis.

Recent studies indicate that this signalling pathway is also essential in the nodule to control the formation of symbiosomes. All NF signalling genes are active in the nodule, especially in the (distal) infection zone where symbiosome formation takes place (Bersoult et al., 2005; Limpens et al., 2005; Riley et al., 2006). Nodule specific knockdown of the LRR-receptor kinase DMI2 caused a block of the release of rhizobia from infection threads inside the nodule (Capoen et al., 2005; Limpens et al., 2005). Complementation of the Medicago *dmi3* mutant with the *DMI3* ortholog from rice restored the ability to form nodules, but release of rhizobia from infection threads was blocked (Godfroy et al., 2006). Additional support for the involvement of the NF signalling pathway in symbiosome formation comes from the recent cloning of the *PsSym33* and *MtSym1* genes, which encode the Interacting Protein of DMI3, IPD3. Knockout mutations in the corresponding genes also cause a block in the release of bacteria from infection threads in the nodule (Horváth et al., 2011; Ovchinnikova et al., 2011, see Chapter 3).

In pea, additional plant mutants blocked at various stages of symbiosome formation and development, have been identified and are well characterized at the morphological level

(Borisov et al., 2007). To get additional insight into the molecular components that control symbiosome formation, we focused on the pea *sym41* mutant, which is strongly impaired in the symbiosome differentiation and release of bacteria from the infection threads (Morzhina et al., 2000; Voroshilova et al., 2009). The phenotype of *Pssym41* nodules was reported to be somewhat similar to *Pssym33*; however, allelism tests indicated that *Pssym41* and *Pssym33* represent different genes (Borisov et al., 2000; Morzhina et al. 2000). To identify *Sym41*, we made use of the extensive synteny between pea and the model legume Medicago and undertook a map-based cloning approach using the Medicago genome as reference. This identified a splice-site mutation in the *PsSym19* gene, an ortholog of Medicago *DMI2* (Stracke et al., 2002). A 3'-splice-site mutation in the *Pssym41* allele causes a strong reduction (~90%) of wild type (WT) *Sym19* transcript levels in the mutant, and the misspliced mRNA encodes a truncated protein lacking the kinase domain. However, *Pssym41* retains the ability to form nodules due to the low amount of the *Sym19* WT transcript that is still produced. Analysis of the interaction with AM fungi showed that fungal colonization is strongly impaired whereas arbuscule formation does not appear to be affected. Our analysis of the *sym41* nodule phenotype suggests that different threshold levels of the LRR-receptor kinase gene *PsSym19* are required for the accommodation of rhizobia in nodule primordium cells and nodule meristem-derived cells. Furthermore, it accentuates an essential role of PsSym19 in symbiosome development.

RESULTS

Synteny-based mapping of *PsSym41*

Pssym41 (RisFixA) has been identified as a recessive EMS (ethyl methanesulfonate) mutant in the pea (*Pisum sativum*) cultivar Finale (Engvild et al., 1987). Characterization of nodule development in *Pssym41* showed that the invasion of the nodule primordium by infection threads was hampered, and the release of rhizobia from infection threads was strongly impaired (Voroshilova et al., 2009). At later stages (28 days after inoculation), rhizobia were released from infection threads, however the resulting symbiosomes did not develop and showed signs of early senescence (Morzhina et al., 2000).

To identify *PsSym41*, a cross between NGB1238 and RisFixA was made and a segregating population of 100 plants (74 Fix^+/26 Fix^-) was used for the synteny-based positional cloning of *PsSym41*, using Medicago as intergenomic cloning vehicle. To map *PsSym41*, we first used a set of gene-based cross-species markers (see chapter 2) that anchor the pea and Medicago genetic maps. This initial analysis showed linkage between the *sym41* Fix^- nodule phenotype and the marker AS2 (~17 cM, Fig.1) on the pea linkage group I (LGI), which is highly syntenic with chromosome 5 of Medicago (Aubert et al., 2006). We previously (Chapter 3) mapped *PsSym33* (ortholog of Medicago IPD3) on the same linkage group. Using *PsSym33* as a cross-

species marker (mapped ~5 cM from *PsSym41*) we could delineate the location of *PsSym41* on linkage group I (Fig.1). Next, we used the well-characterized physical map and extensive sequence information available for Medicago to create additional cross-species markers in this region for fine mapping of the *Pssym41* location. This allowed us to position *PsSym41* within a 10 cM region between markers NT52 and Almo on pea linkage group I (Fig.1). This region is relatively big; it corresponds to a ~1.5 Mb region in Medicago. However, this region included the NF signalling LRR-receptor kinase gene *DMI2*, the ortholog of *PsSym19* (Ané et al., 2002; Stracke et al., 2002). Knockdown of *DMI2* expression in Medicago and *Sesbania rostrata* has been shown to cause a somewhat similar phenotype as observed for *Pssym41* nodules, namely a block in the release of bacteria from infection threads (Capoen et al., 2005; Limpens et al., 2005). Therefore, we hypothesized that *PsSym41* might represent a weak allele of *PsSym19*. *PsSym19* was converted into molecular marker and showed absolutely linked with the *Pssym41* Fix$^-$ phenotype (Fig.1).

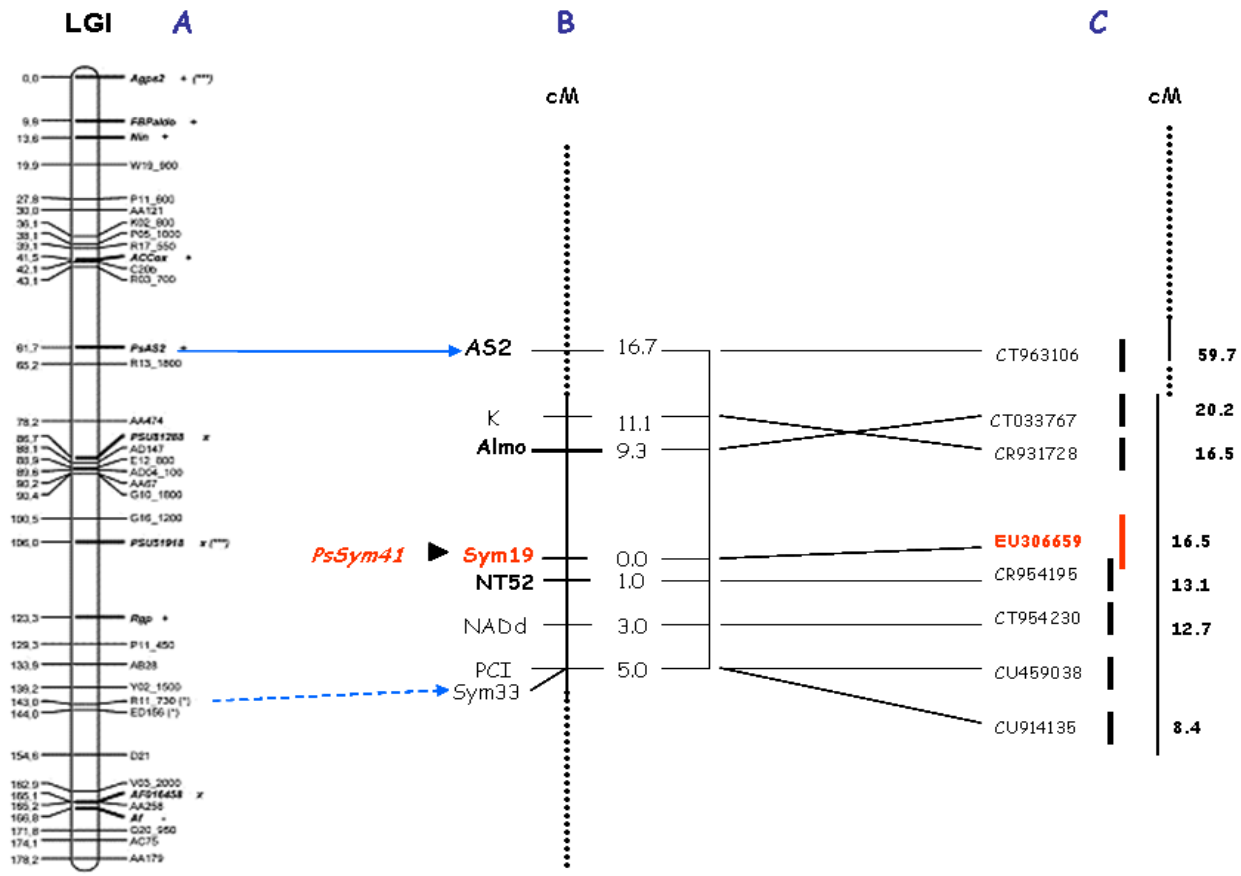

Fig.1. Synteny-based positional cloning of *PsSym41*. **A**, overview of pea linkage group I (from Aubert et al., 2006): blue arrow shows reference marker AS2; dashed arrow shows approximate location of *Sym33*. **B**, genetic map of the *PsSym41* region: dashes represent areas distant from *PsSym41*; solid line represents delineated area of the *PsSym41* region. The arrowhead shows the position of *PsSym41* (red) at the same locus as *Sym19* (red); Almo and NT52 (bold) flank *PsSym41*; **C**, the *PsSym41*corresponding region on chromosome 5 of *M. truncatula*: dashes – BAC contigs corresponding to markers distant from *PsSym41*, bold solid lines – the BAC contig corresponding to the delineated area of *PsSym41* localization. Lines between **B** and **C** connect markers with corresponding BAC clones.

To determine whether *PsSym41* encodes PsSym19 we used two complementary approaches (see below): 1) genetic complementation of the *Pssym41* mutant and 2) sequencing of the *PsSym19* gene in *Pssym41* (RisFixA).

Complementation of *Pssym41* by Medicago DMI2

First, we applied *Agrobacterium rhizogenes* mediated root transformation to complement *Pssym41* by introducing a Medicago *DMI2* gene construct. Introduction of this construct, *MtDMI2p::MtDMI2-GFP* into the *Mtdmi2* mutant TR25 fully complemented the Nod$^-$ phenotype of this mutant (Limpens et al., 2005; data not shown). Next, we introduced *MtDMI2p::MtDMI2-GFP* into the pea *sym41* mutant and WT cultivar Finale as control. Transgenic nodules (~6 nodules per root) were observed on the mutant and WT control roots 28 days after inoculation. These nodules showed a similar histological structure and organization as observed in WT nodules (Fig.2A-F). *MtDMI2* complemented the *sym41* defects in symbiosome formation and development as the symbiosomes appeared fully developed and contained single Y-shaped bacteroids (Fig.2F). This genetic complementation of the mutant strongly indicated that *PsSym41* encodes PsSym19/DMI2.

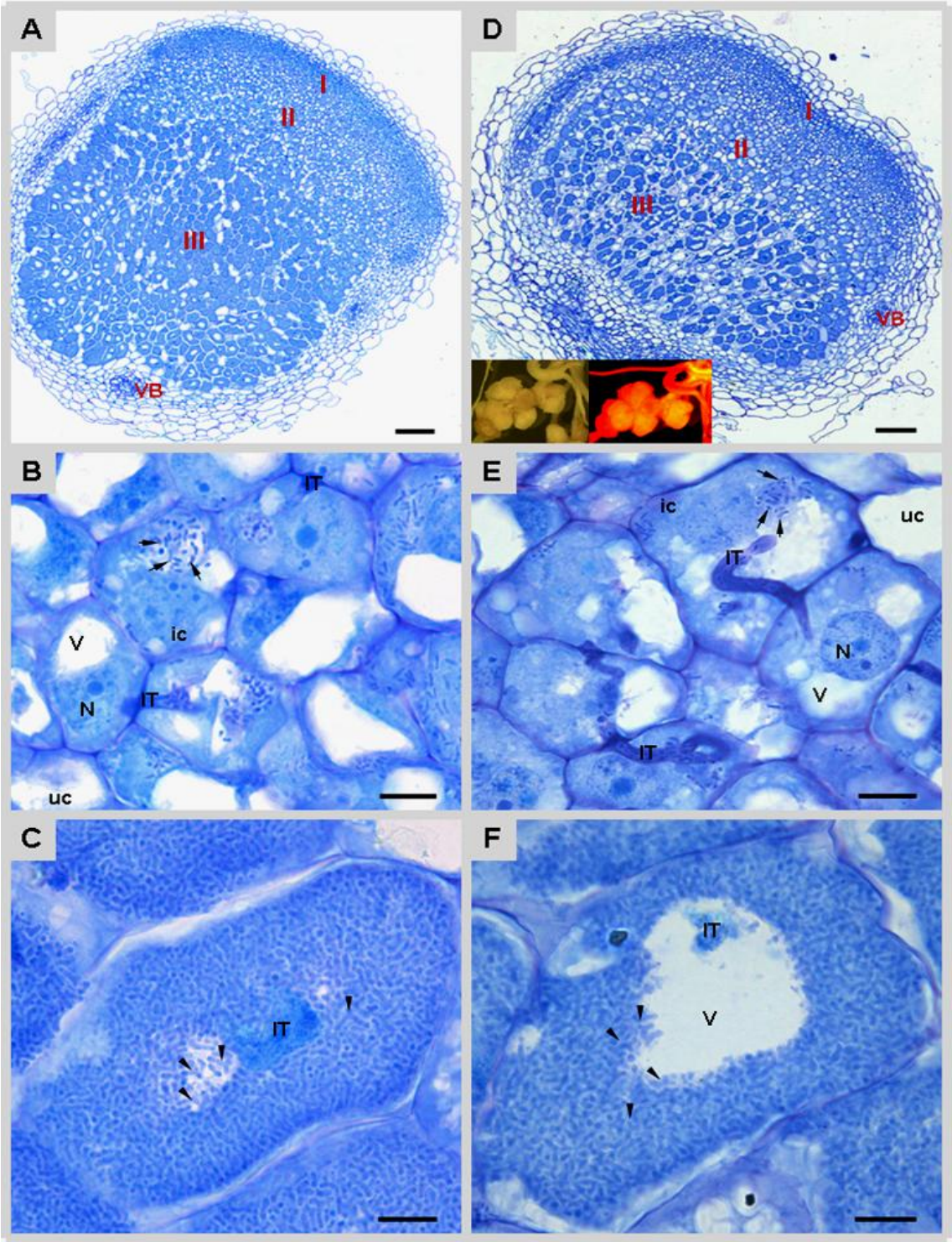

Fig.2. Structural organization of WT and *sym41* nodules transformed by *MtDMI2p::MtDMI2::GFP* at 28 dpi. **A**–**C**, Control WT nodule transformed by *MtDMI2p::MtDMI2::GFP*; **D**–**F**, *Pssym41* nodule transformed by *MtDMI2p::MtDMI2-GFP*. **A** and **D**, Longitudinal section of the nodule: I – meristematic zone, II – infection zone, III – fixation zone, VB – vascular bundle. Images of transgenic nodules are presented on D in the left lower corner. **B** (WT) and **E** (*sym41*), Nodule cells in zone II containing infection threads and released bacteria (=juvenile bacteroids). **C** (WT) and **F** (*sym41*), Nodule cells in zone III containing Y-shaped differentiated bacteroids. In all micrographs: ic – infected cell, uc – uninfected cell, IT – infection thread, V – vacuole, N – nucleus; arrows show released bacteria, arrowheads show symbiosomes containing single Y-shaped bacteroids. Bars: A, D – 100 µm; B, C, E, F – 10 µm.

Pssym41 contains a splice-site mutation in the LRR-receptor kinase PsSym19

Next, we amplified and sequenced the *PsSym19* gene from *Pssym41* genomic DNA. This identified a mutation (A>G) in the 3'splice-site of intron 9 in *PsSym19* (Fig.3A). To determine the effect of this mutation on splicing, we performed RT-PCR analyses on RNA from *Pssym41* nodules (Fig.4). Partial *Pssym41* cDNA fragments spanning intron 9 were cloned and sequenced (48 clones). This showed that the mutation caused a cryptic splice event by which a 113 bp fragment of intron 9 was included in the *PsSym19* mRNA. This introduces an early stop codon that leads to a truncated protein of 573 amino acids, by which the complete kinase domain of PsSym19 is lacking (Fig.3B, C). In addition, WT transcripts could still be detected (18 clones of 48), as well as a minor (three clones of 48) cryptic splice product with a 27 bp deletion. To quantify the relative frequency of the two major splice products (WT versus truncated protein), we performed qRT-PCR analysis on *Pssym41* nodule RNA using primer combinations that distinguish both forms (SYM19 and sym41, Fig.4B). This indicated that ~11% of WT transcript is still formed in the *sym41* nodules. Together with the genetic complementation, this confirmed that *PsSym41* represents a weak allele of *PsSym19*.

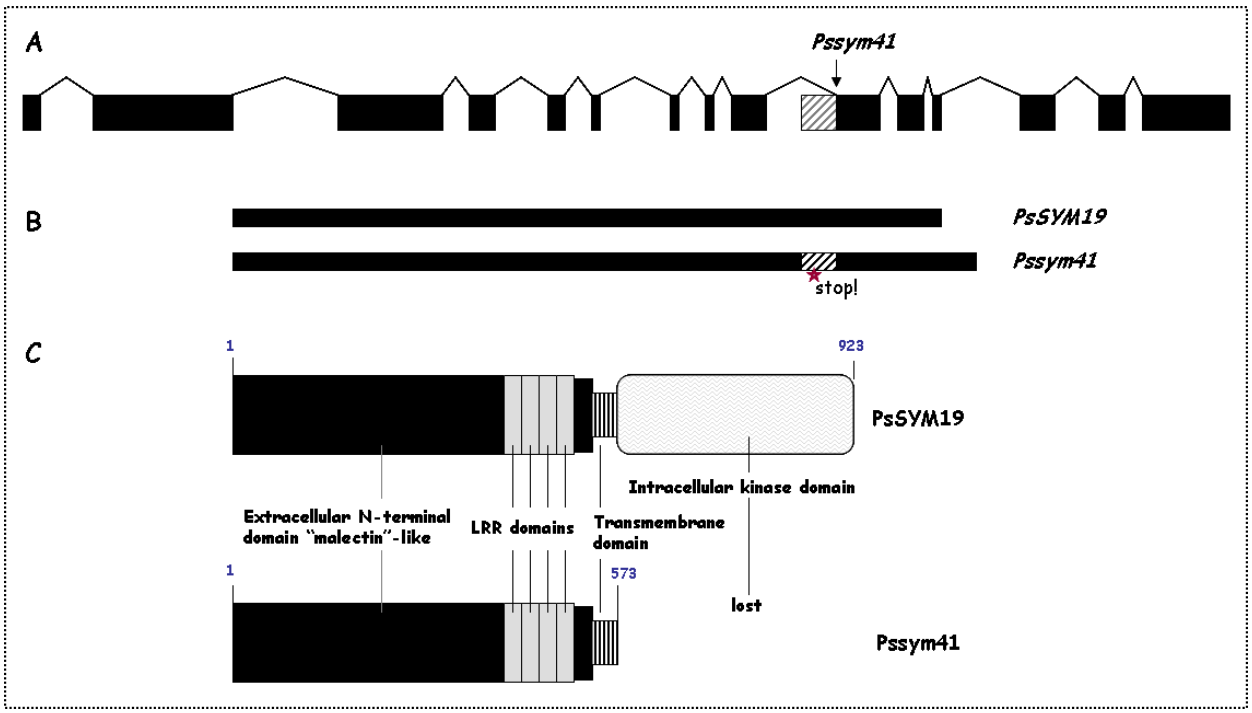

Fig.3. The *PsSym19* gene and protein structure. **A**, Schematic representation of the exon-intron structure of the *PsSym19* gene, and **B**, major transcripts of WT (*PsSYM19*) and *Pssym41*: identified mutation in *Pssym41* mutant is indicated. The diagonally arced rectangle represents a part of intron 9 that is included in the major transcript in *Pssym41*: a red star indicates stop codon that leads to a truncated protein. **C**, Schematic representation of the domain structure of WT PsSYM19 (upper figure) and truncated Sym41 (lower figure) proteins. The domains are indicated: extended N-terminal "malectin"-like, four leucine-rich repeats (LRR domains), transmembrane domain, and intracellular kinase domain (lacking in Sym41).

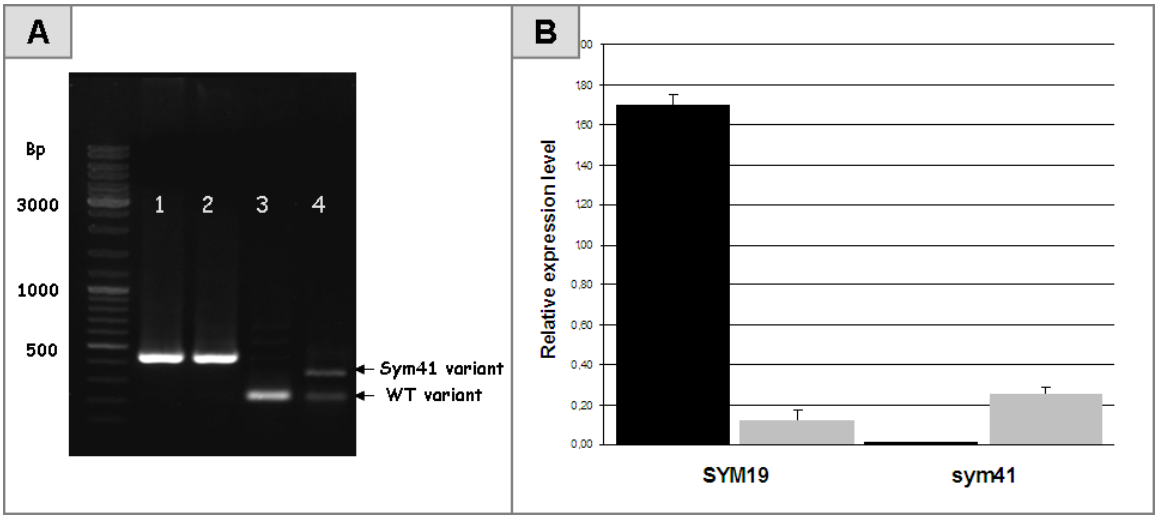

Fig.4. Impaired splicing in the *PsSym19* gene: **A**, Gel-electrophoresis photograph of RT-PCR on WT and *sym41* cDNA spanning intron 9: 1= PCR on WT genomic DNA, 2= PCR on *sym41* genomic DNA, 3=RT-PCR on WT cDNA, 4=RT-PCR on *sym41* cDNA. Arrows show two bands amplified from cDNA of the mutant: lower band (the same size with WT PCR product) and upper band (longer PCR product). **B**, Relative expression of the two major splice forms in *sym41* nodules: black bar=control WT cDNA, grey bar=*sym41* cDNA; SYM19 (on the left) – the expression level of WT splice form; sym41 (on the right) – the expression level of mutant splice form.

Pssym41 **reveals that successive stages of nodule development require different threshold levels of** ***PsSym19***

As we performed the *A. rhizogenes* mediated complementation experiment we noticed that, in contrast to the data from Voroshilova et al. (2009), all analyzed *Pssym41* Fix$^-$ nodules contained symbiosomes in the basal part of the nodule. This prompted us to analyze the phenotype of non-transformed *Pssym41* nodules in more detail and allowed us to study the effect of the reduced levels of *PsSym19* at different stages of nodule development.

A time course analysis showed an increase in nodule number with time after inoculation in both WT and mutant. However, the average number of nodules in *sym41* was significantly ($P<0.05$) lower than in the WT at each time point (Fig.5). Because PsSym19 is required for infection, we studied whether the reduction in nodule number correlates with impaired infection events at the epidermis. We examined IT numbers and their structure (Fig.6) after inoculation with the *R. leguminosarum* bv. *viciae* 248 strain expressing *lacZ* 16 days after inoculation. Most infection threads in WT roots (~98%) had a tubular structure with a small fraction (~2%) of infection threads showing sac-like structures along their length in the root hairs (Fig.6E). In contrast, *sym41* roots showed ~2.5 times less tubular infection threads than WT plants 21 days after inoculation (Fig.6E). Furthermore, *sym41* roots showed increased numbers of infection threads that were blocked at the microcolony stage (~6% IT/plant) or that aborted early after

formation and contained sac-like structures (~15% IT/plant) (Fig.6B-E). In addition, swollen root hairs that resemble a drumstick by shape (Fig.6D) were observed in *sym41* (~12/plant, Fig.6E), whereas these were not found on WT roots. Such swollen root hairs are typically observed in knock-out mutants of the common symbiotic signalling genes, including *Pssym19* (Hirsch et al., 1982; Utrup et al., 1993; Catoira et al., 2001; Endre et al., 2001; Stracke et al., 2001; Tsyganov et al., 2002). These data indicate that the reduced levels of *PsSym19* do affect IT formation in the epidermis, which could explain the reduction in nodule numbers. However, it could also well be that the induction of cortical cell divisions is more strongly affected.

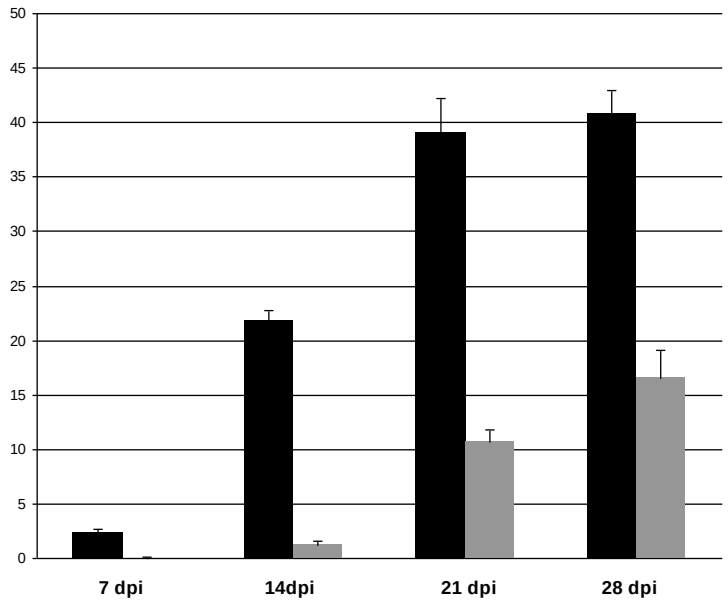

Fig.5. Average number of root nodules per plant of wt (Finale) and *sym41* (RisFixA) at 7, 14, 21, and 28 days after inoculation with *R. leguminosarum* bv. viciae 248*lacZ*: black bar=wt, grey bar=*sym41*.

Next, we examined semi-thin sections of *Pssym41* nodules by light microscopy (21 days after inoculation with rhizobia). The *Pssym41* Fix$^-$ nodules (n=20) showed an aberrant, extended infection zone that often contained broad hypertrophied infection threads occupying large parts of the infected cells (Fig.7A, D). Although some release of bacteria from the infection threads was observed, release appeared to be severely hampered in this zone of the nodule, resulting in prominent “droplet-like” structures (Fig.7E). Furthermore, the resulting juvenile bacteroids did neither frequently divide nor develop further and remained similar in size to bacteria inside the infection threads (Fig.7F). In striking contrast to the apical part, cells in the basal part (~7-16 cell layers) of the nodules were almost completely filled with symbiosomes, and no aberrant infection thread structures were observed in this part of the nodule (Fig.7D). In Medicago, it has been demonstrated that about eight basal cell layers of the nodule are directly derived from the primordium, but not from the apical meristem (Kulikova, personal communication). It is probable that this is also the case in pea root nodules. Since pea roots have more cortical cell layers than

Medicago roots, it is probable that the number of nodule cell layers formed directly from primordial cells in pea is slightly higher than in Medicago. Therefore, we expect that 7-16 cell layers at the base that are properly infected, are directly formed from the nodule primordium and are not originated from the apical meristem. Although the resulting symbiosomes appeared enlarged, they did not form the typical swollen Y-shaped structures as observed in WT nodules and contained multiple bacteroids (Fig.7C, F). The observed phenotype of the *sym41* nodules is very similar to that described by Morzhina et al. (2000), and it reveals an essential role of PsSym19 in symbiosome differentiation. The observed differences in infection phenotypes between the apical meristem-derived cells and the basal nodule primordium derived cells suggest that these cells have different requirement towards *PsSym19* levels. Meristem-derived cells seem to require higher amounts of functional *PsSym19* to allow proper infection than the nodule primordium cells.

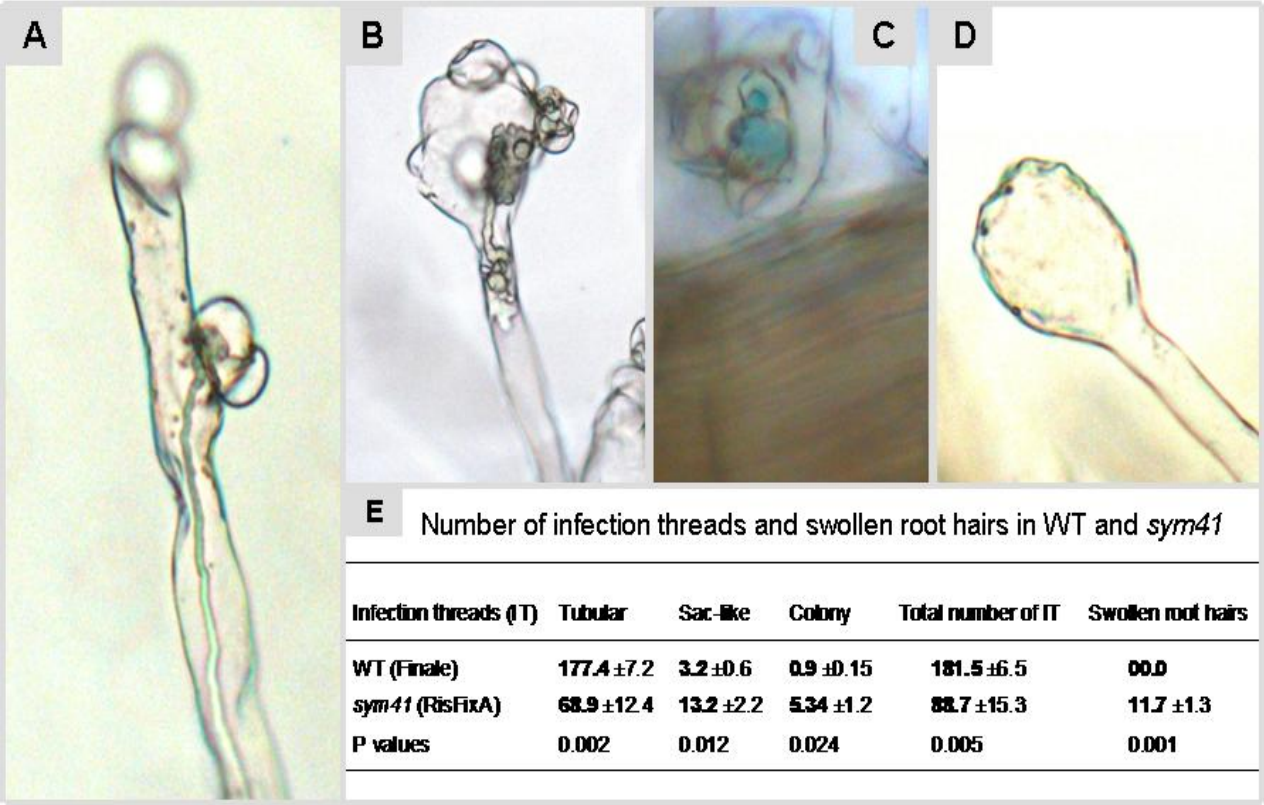

Number of infection threads and swollen root hairs in WT and *sym41*

Infection threads (IT)	Tubular	Sac-like	Colony	Total number of IT	Swollen root hairs
WT (Finale)	177.4 ±7.2	3.2 ±0.6	0.9 ±0.15	181.5 ±6.5	00.0
sym41 (RisFixA)	68.9 ±12.4	13.2 ±2.2	5.34 ±1.2	88.7 ±15.3	11.7 ±1.3
P values	0.002	0.012	0.024	0.005	0.001

Fig.6. The types and number of infection threads in WT and *sym41*: **A**, Tubular infection thread; **B**, Sac-like infection thread; **C**, Infection thread arrested micro-colony stage; **D**, Swollen root hair. **E**, Table represents data of the number of infection threads and swollen root hairs formed in the epidermis of *sym41* and WT. Infection threads and root hairs were counted per plant 21 days after inoculation.

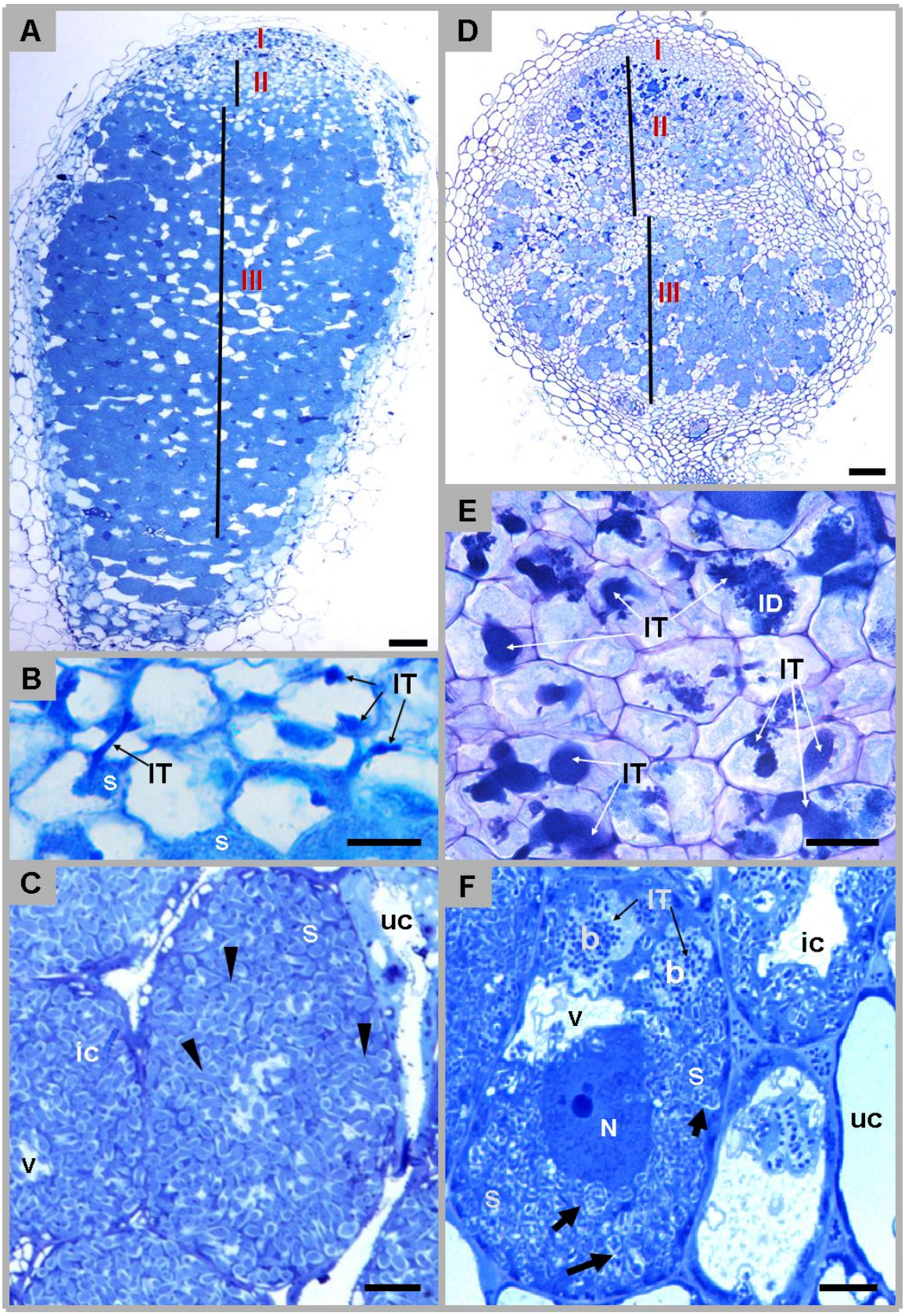

Fig.7. Nodule structural organization of WT and *sym41* at 21 dpi. **A** and **D**, Longitudinal section of the nodule: I–meristematic zone, II–infection zone, III–fixation zone; **A**–WT nodule, **D**–*sym41* nodule; note the difference in size of zones II and III between WT and the mutant. **B** (WT) and **E** (*sym41*), Nodule cells in zone II: IT–infection threads, s–(juvenile) symbiosomes. The *sym41* cells contain hypertrophied infection threads forming prominent droplet-like structures (ID). **C** (WT) and **F** (*sym41*), Nodule cells in zone III: N–nucleus, V–vacuole, ic–infected cell, uc–uninfected cell, IT–infection thread, b–bacteria, and s–symbiosomes. Bold arrows show symbiosomes containing multiple bacteroids, and arrowheads show symbiosomes containing single Y-shaped bacteroids. Bars: A, D – 100 µm; B, E – 25 µm; C, F – 10 µm.

PsSym19 controls AM fungal colonization, but not arbuscule formation

PsSym19/MtDMI2 is part of the common symbiotic signaling pathway that is also essential to establish a symbiosis with arbuscular mycorrhizal (AM) fungi. Knockout of *PsSym19* blocks the entry of the fungi into the root at the epidermis (Stracke et al., 2001; Endre et al., 2001). To test whether epidermal and cortical responses (arbuscule formation) to AM fungi require different levels of *PsSym19* we analyzed the mycorrhization phenotype in *sym41*.

The effect of *sym41* on AM formation was studied in a chive nurse plant system and analyzed by light microscopy in two independent experiments at 8, 16, 30, and 48 days of post-inoculation (dpi) with *Glomus intraradices* BEG144. To estimate mycorrhization, we used two parameters according to Trouvelot et al. (1986): M%, the intensity of AM colonization and a%, the arbuscule abundance in mycorrhizal roots (Fig.9). In WT plants, AM fungi penetrate the epidermis through appressoria/hyphopodia to form intraradical hyphae in the cortex and develop arbuscules inside cortical cells (Fig.8). Wild-type roots were already well-colonized and contained arbuscules at 8 days after inoculation (Fig.8B; 9). In contrast, the intensity of AM colonization in *sym41* roots was severely reduced ($P<0.05$) at all time points (Fig.9). In addition, many abnormally enlarged, balloon-shaped appressoria were observed on *sym41* roots, which failed to penetrate the epidermis (Fig.8C, D). The number of appressoria was significantly increased ($P<0.05$) in the mutant compared to WT roots (Fig.10). Some fungal hyphae managed to colonize the root cortex and formed arbuscules that looked the same as those in the WT (Fig.8B, D). However, due to the impaired colonization, arbuscule formation appeared reduced compared to the WT, especially at early time points (Fig.9B). This suggests that PsSym19 is not required for arbuscule formation in root cortical cells or that there is a higher demand for *PsSym19* to cross the epidermis than to invade inner cortical cells.

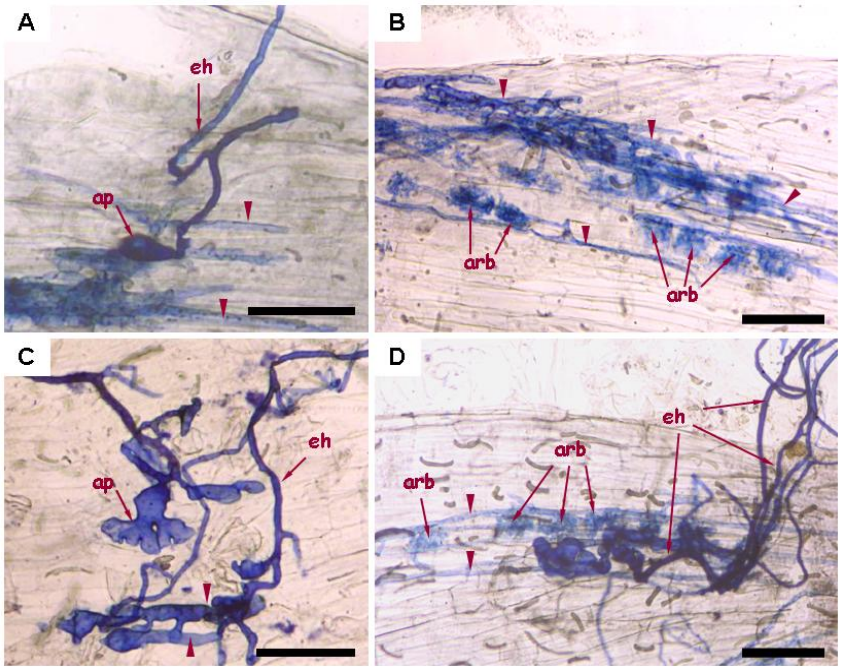

Fig.8. Mycorrhizal colonization in WT and *sym41* roots: **A**, **B**, Mycorrhizal colonization in WT; **D**, **E**, Mycorrhizal colonization in *sym41*. **A**, Appressorium, extraradical and intraradical hyphae in WT roots; **B**, Cells containing arbuscules in WT roots; **C**, Appressorium, extraradical and intraradical hyphae in *sym41* roots; **D**, Cells containing arbuscules and numerous extraradical hyphae in *sym41* roots. In all micrographs: eh – extraradical hyphae, ap – appressorium, arb – cells containing arbuscules; arrowheads shows intraradical hyphae. Bars: 50 µm

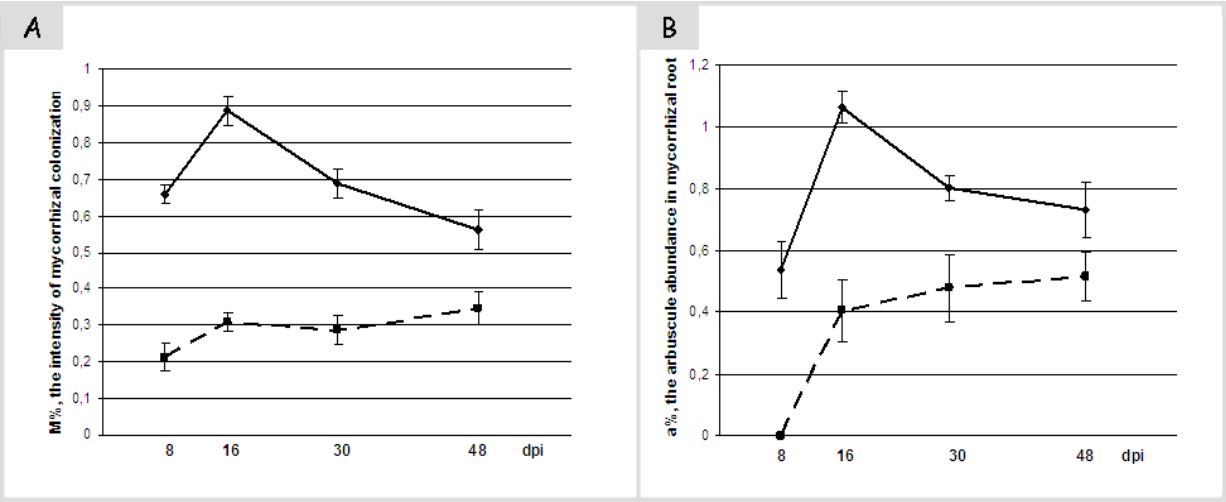

Fig.9. Dynamics of arbuscular mycorrhiza development in WT and *sym41* at 8, 16, 30, and 48 dpi. **A,** The intensity of mycorrhizal colonization in the root system (M%). Solid line=WT, dash=*sym41*. **B,** The arbuscule abundance in mycorrhizal roots, (a%). Solid line=WT, dash=*sym41*.

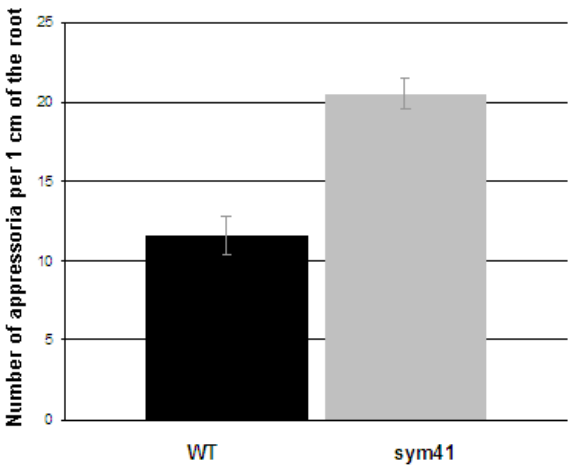

Fig.10. Average number of appressoria formed at the WT and *sym41* epidermis per 1 cm of root surface at 16 dpi.

DISCUSSION

Here, we identified the *PsSym41* gene via a synteny-based cloning approach and showed that *PsSym41* encodes a weak allele of the common symbiotic LRR-receptor kinase PsSym19; the ortholog of Medicago DMI2 and Lotus SYMRK (Endre et al., 2002; Stracke et al., 2002). The observed phenotype of the *Pssym41* nodules revealed a novel essential role of Sym19/DMI2 in symbiosome differentiation. Furthermore, the weak allele allowed us to uncover a different demand for *Sym19* in rhizobial infection of epidermal and nodule primordium cells versus nodule meristem-derived cells. In contrast, during the AM interaction epidermal responses showed a higher demand for *Sym19* than the cortical cells.

The *sym41* allele contains a 3'-splice-site mutation that affects the proper splicing of intron 9 and leads to a non-functional protein lacking the kinase domain. This splice-site mutation

reduces (~90%) but does not completely abolish the formation of WT transcripts. Therefore, *Pssym41* retains the ability to form nodules likely due to the residual amount of WT protein. A similar effect of a 3'-splice-site mutation has been observed by Smit et al. (2007) in the weak *hcl-4* mutant of the Medicago LYK3 Nod factor receptor. The delay in nodule formation shown for *Pssym41* correlates with impaired infection thread formation in the root hairs. However, as quite some wild-type looking infection threads are still formed it could also be that cortical cell divisions are more strongly impaired resulting in a reduction in nodule numbers.

Pssym41 showed reduced IT formation similar to impaired IT formation in *Pssym33/ipd3* and *hcl-4* mutants (Smit et al., 2007; Ovchinnikova et al., 2011). However, in the *hcl-4* mutant that makes ~10% of WT *LYK3* transcripts, infection thread growth is more severely impaired but the structural organization of nodules and symbiosome formation are not affected (Smit et al., 2007). This indicates that, in contrast to *Sym19/DMI2*, low levels of *LYK3* in the nodule are still sufficient to allow proper infection of the nodule meristem-derived cells (Limpens et al., 2003; Smit et al., 2007).

Symbiosome formation first starts in nodule primordium cells. Knockdown of *DMI2* in Medicago and *Sesbania rostrata* has been shown to cause a block in the release of bacteria from the infection threads, and these nodules lacked symbiosomes (Capoen et al., 2005; Limpens et al., 2005). This indicates that DMI2 is already required in the nodule primordium to control symbiosome formation. A similar block in symbiosome formation was reported for *sym41* by Voroshilova et al. (2009). However, we did not observed this block in rhizobial release in our study. Instead, we did observe symbiosomes in the basal part of the *sym41* nodules (~7-16 cell layers), which probably descend directly from the nodule primordium. Symbiosome formation was also observed in the study by Morzhina et al. (2000). The phenotypic variation could be due to different growth conditions or due to different rhizobial strains used for inoculation. Similar phenotypic variations have been reported for Medicago and pea *sym33/IPD3* mutants (Horváth et al., 2011; Ovchinnikova et al., 2011).

However, in the apical part of the nodule, which originates from the nodule meristem the release of bacteria from the infection threads was severely hampered. Large hypertrophied infection threads occupied large parts of the cells and only few symbiosomes were observed. This suggests that meristem-derived cells require a higher level of *Sym19* than the primordium cells to allow proper infection. Alternatively, we cannot rule out that *Sym19* is higher expressed in nodule primordium cells by which more WT transcripts are produced in these cells than in the nodule meristem derived cells. Further, the symbiosomes in the *sym41* nodules did not differentiate properly as the enlarged and Y-shaped symbiosomes typical for WT nodules were not observed. This shows that Sym19 also controls the differentiation of the symbiosomes/bacteroids. A similar block in symbiosome differentiation was reported by

Morzhina et al. (2000). Furthermore, the nodules showed signs of early senescence, which is likely due to the impaired bacteroid differentiation and lack of nitrogen fixation in these nodules.

Together with the reported phenotypes from the *Sym19/DMI2* knockout and knockdown nodules, we hypothesize that subsequent stages of rhizobial infection require different amounts of *Sym19*. From low to high *Sym19* levels, the following stages can distinguished: 1) infection thread formation in root hairs, 2) infection of nodule primordium cells, 3) symbiosome formation in primordium cells, 4) symbiosome formation in nodule-meristem derived, and 5) symbiosome differentiation.

Similar effects on rhizobial infection, symbiosome formation and differentiation as found for *sym41* have been described for *Pssym33* and *Mtsym1* mutants that are mutated in *IPD3* (Bénaben et al., 1995; Tsyganov et al., 1998; Horváth et al., 2011; Ovchinnikova et al., 2011; Chapter 3). Therefore, the main function of Sym19/DMI2 may be the activation of DMI3, which in turn plays an essential role in symbiosome formation via its interaction with IPD3. Reduced signalling via DMI2 may result in impaired activation of DMI3 and IPD3, possibly due to its effect on Ca^{2+} spiking (Wais et al., 2000; Walker et al., 2000; Kosuta et al., 2011). This is supported by a recent study in *Lotus japonicus* (Lotus) where an always-active mutant version of CCaMK (DMI3) in a *symrk-3* null-mutant background was sufficient to trigger fully infected nodules containing symbiosomes (Madsen et al., 2010). In contrast, introduction of this always-active CCaMK in the Lotus *cyclops* (*ipd3*) mutant was not sufficient to complement the rhizobial infection defect.

In contrast to the highest demand for Sym19 in the nodule, during the interaction with AM fungi, the strongest demand appeared to be at the epidermis. In *sym41*, we noticed that the AM fungus was severely impaired in its ability to pass the epidermis, resulting in enlarged balloon-shaped appressoria that are typical for “common symbiotic” mutants (Kistner et al., 2005, Kosuta et al., 2011). Strikingly, arbuscule formation was not affected in *Pssym41*. This suggests that Sym19 is not essential in the cortex to control arbuscule formation or that arbuscule formation requires lower *Sym19* input than that required for epidermal infection or symbiosome formation. In support of the first option, Lotus *symrk* knockout mutants occasionally form arbuscules in root sectors where the fungus manages to pass the epidermis (Wegel et al., 1998; Demchenko et al., 2004). In contrast, *ccamk* knockout mutants never form arbuscules even when the fungus manages to pass the epidermis (Demchenko et al., 2004). This suggests that additional factors independent of DMI2 can still activate CCaMK in the cortex to allow arbuscule formation. A stronger effect of reduced levels of *Sym19* at the epidermis during the AM interaction could be related to the observed oversensitivity of epidermal cells to touch in *dmi2* knockout mutants (Esseling et al., 2004). Therefore, it can be hypothesized that DMI2 may sense the physical contact with fungi and rhizobia and signal to reduce the stress (or possible defense responses) caused by this contact. Because appressoria are thought to exert pressure

to penetrate the epidermis, this might cause a stronger “stress” than during rhizobial infection. Recently, a mutant of *LjSYMRK* (*symrk-14*) was identified to uncouple epidermal from cortical symbiotic responses and showed a strikingly similar phenotype to *Pssym41* (Kosuta et al., 2011). This mutant contains a mutation in a conserved GDPC sequence in the SYMRK extracellular domain. In *Ljsymrk-14* mutants, penetration by AM fungi is mostly blocked at the epidermis where the fungus forms balloon-shaped appressoria. Occasionally, fungal hyphae manage to pass the epidermis, colonize the cortex, and form arbuscules. Similarly, rhizobial infection in the root hairs is impaired resulting in a delay in nodule formation. However, when infection threads reach the activated cortical cells, infected nodules containing symbiosomes are formed. This suggests that SYMRK/Sym19/DMI2 requires the presence of the GDPC domain to maintain its full signalling capacity. Thus, GDPC-mutated SYMRK phenocopies the reduced levels of *DMI2* in *Pssym41*, and the cortical/primordium responses require lower levels of *DMI2* than the epidermal/meristem responses. An effect on symbiosome/bacteroid formation and differentiation was not described for the Lotus *symrk-14*.

Together the recently identified plant mutants defective in common symbiotic signalling genes provide clear evidence that the components of this pathway, which are essential to trigger early symbiotic responses, are also required at later stages to promote infection, symbiosome formation as well as differentiation. How the common symbiotic signalling pathway controls the formation and development of symbiosomes will be an important question for future studies as they form the heart of the rhizobial symbiosis.

MATERIALS AND METHODS

Plant lines, bacterial and fungal strains, and growth conditions

The homozygous mutant line RisFixA (*sym41*), genetic background Finale (Engvild et al., 1987; Morzhina et al., 2000; Voroshilova et al., 2009), was used for evaluation of symbiotic mutant phenotype. Plant seeds were sterilized with concentrated sulfuric acid for 10 min at room temperature. Germinated seeds were planted in perlite in plastic pots (diameter of 19 cm) and inoculated with rhizobia after 7 days. Plants were supplied by a nitrogen free nutrient solution as described in Borisov et al. (1997).

Rhizobium leguminosarum bv. *viciae* strain 248*lacZ* (Geurts et al., 1997) was used for inoculation of plants in nodulation experiments.

Glomus intraradices N. C. Schenck & G. S. Sm., isolate CIAM8 (Muromtsev et al., 1989) from the Collection of the All-Russia Institute for Agricultural Microbiology (registered in the European Bank of *Glomales* as isolate BEG144), was used for inoculation of pea plants in AM experiments. To inoculate plants, a culture of *G. intraradices* was obtained in an inoculation system with a nurse plant (Rosewarne et al. 1997). *Allium schoenoprasum* L. was used as nurse plant, as described by Demchenko et al. (2004), except that phosphates were not included in the nutrient solution.

Nodule tissue fixation, staining, and microscopy

Nodule tissues were fixed in 5% glutaraldehyde (v/v) containing 3% sucrose (w/v) in 0.1 M phosphate buffer (pH 7.2) under vacuum for 1-2 hours, followed by subsequent washing steps with buffer and water for 15 min each. Then, ethanol dehydration series: 10%, 30%, 50%, 70%, 90%, and 100%, were carried out for 10 min each. The dehydrated nodules were embedded in Technovit 7100 (Heraeus-Kulzer, Wehrheim, Germany) according to the manufacturers protocol and sectioned on a RJ2035 microtome (Leica Microsystems, Rijswijk, The Netherlands).

Semi-thin nodule sections (5µm) were stained with 0.05% toluidine blue solution and analyzed using a DM5500B microscope equipped with a DFC425C camera (Leica Microsystems, Wetzlar, Germany).

Transgenic roots and nodules were selected based on DsRED1 expression using a Leica MZFLIII binocular fitted with HQ470/40, HQ525/50, HQ553/30, and HQ620/60 optical filters (Leica Microsystems, Rijswijk, The Netherlands).

Infection thread analysis

Roots were collected individually from six plants per biological replicate 16 days after inoculation. Root tissues were fixed and stained for LacZ activity as described in Boivin et al. (1990). Stained infection threads were observed by light microscopy and counted per plant using a binocular (Carl-Zeiss Axiovert, Oberkochen, Germany). Infection threads numbers were evaluated by t-test with the help of SigmaStat 3.5 for Windows (SPSS Inc., Chicago, U.S.A.).

AM phenotype analysis

Plants were collected 8, 16, 30, and 48 days after transplanting. Root fragments were collected individually from nine plants per time point. To visualize fungal structures in the root samples, ink staining was performed as described by Vierheilig et al. (1998). Roots were cut in fragments with a total length up to 30 cm per plant and mounted on glass slides in glycerol. AM development in the roots was estimated according to Trouvelot et al. (1986) using an Opton 35 (Opton, Germany, Oberkochen, Germany) light microscope for two parameters: intensity of mycorrhizal colonization in the root system (M%) and arbuscule abundance in mycorrhizal root fragments (a%). The data were compared by one-way ANOVA with the help of SigmaStat 3.5 for Windows (SPSS Inc., Chicago, U.S.A.).

Map-based cloning

Mapping of *PsSym41* was done using an F2 population (100 plants) of a cross between mutant line RisFixA and wild-type line NGB1238. Plants from the F2 mapping population were analyzed in nitrogen free conditions to segregate mutant and WT nodule phenotypes: Fix^- white nodules versus Fix^+ pink nodules. Total DNA was extracted from leaves of each analyzed plant individually using the standard cetyltrimethylammonium bromide (CTAB) method (Rogers and Bendich, 1985).

The cross-species CAPS molecular markers developed for map-based cloning of *Sym41* and linkage analyses are represented in Table 1.

Co-segregation of the *Sym41* fix- phenotype with CAPS molecular markers was analyzed using the following genotyping conditions: **Sym33** (PCR annealing temperature 55ºC, restriction endonuclease Hpy188I), forward primer (F) - GTTAATGTGTCTAATCAGCAAC, reverse primer (R)–

GGTATTTCGCACATTGAAAGGTAATC; **PCI** (55ºC, TasI) F–CAAAGCTTTCTATAGAGGATGTGGAGCATCTT, R–CTCGTAAGTCTCTTCGTCTTTTGTTGCCTC; **NADd** (55ºC, TagI/HinfI) F–AGCTACTGCGGTTGTCTCGACACTTGGAGGTTTTG, R–GGATCATACCCTTACTTTCTGAGCAGCCTCCTTG; **NT52** (60ºC, Eco130I) F–CACAATCCCTAATATCTCTCTCCA, R–GAAACACATACAACCCCTAAAGAAA; **Sym19** (50ºC, PstI) F–CATTACATTTATGACATTCTCCCTCAAAAACCTG, R– AGCCAAATCCTCCTTCACCTATC; K (55ºC, RsaI/AluI) F-GGCAAGTTACGTTTTCAAAGAGACGAAGAGGTTTG, R–CTCAGCAATTTCCTTGTTCAATCTCGTACAG; **Almo** (55ºC, TagI) F–GTGGATATGACCGCATTGAAGCAGATGGGAGA, R–GATTCTGGTTCCTATTTCTTACAGTTTTAAGTTGG; **AS2** (48ºC, RsaI) F–CTAATCACACGTTTAGGACCGG, R–CGAAATCCAAACCGAACCTAATCC.

X2 statistical analysis ($\chi 2 > 3.84$ for independent assortment) was used to determine the significance of linkageof the Sym41 nodule phenotype with molecular markers (SigmaStat 3.5 for Windows, SPSS Inc., Chicago, IL, USA).

Table 1. Markers developed for positional cloning of *PsSym41*

Marker name	BAC accession number	Genetic distance, cM		Name of marker gene product	χ^2
		M.truncatula	To *PsSym41*		
Sym33	CU914135	8.4 – 12.7	5.0	Interacting protein of DMI3	0.00
PCI	CU459038	8.4 – 12.7	5.0	Proteasome component region PCI	0.00
NADd	CT954230	12.7	3.0	NAD-dependent dehydratase	0.00
NT52	CR954195	13.1	1.0	Histon H3	0.00
Sym19	**EU306659**	**13.1 – 16.5**	**0.0**	**LRR receptor-like kinase (DMI2)**	0.00
K	CR931728	16.5	11.1	Transcription factor, K-box	$0.89 \cdot e^{-3}$
Almo	CT033767	20.2	9.3	Sterile alpha motif homology	0.009
AS2	CT963106	59.7	16.7	Pisum sativum asparagine synthase 2	0.005

$\chi^2 > 3.84$ contributes independent assortment for p=0.05 and q=1, where p is the probability, and q the degrees of freedom.
$\chi^2 < 3.84$ indicates linkage of the gene of interest with a particular marker.

Quantitative RT-PCR

Quantitative RT-PCR was conducted on RNA isolated from 21-day-old pea *sym41* and WT nodules of plants grown in perlite (Limpens et al. 2009). Total RNA was isolated and DNAse treated using the Plant RNeasy kit (Qiagen, Basel, Switzerland) according to the manufacturer's instructions. cDNA was synthesized from 1 µg of total RNA using the Taqman Gold RT-PCR kit (Perkin-Elmer Applied Biosystems) in a total volume of 50 µl using random hexamer primers (10 min at 25°C, 30 min at 48°C, and 5 min at 95°C) . Quantitative PCR reactions were performed in (technical) triplicate on 1 µl of cDNA

using the Quantitative PCR Core kit for SYBR Green I (Eurogentec), and real-time detection was performed on a MyiQ (Bio-Rad) (40 cycles of 95°C for 10 s and 60°C for 1 min) followed by a heat dissociation step (from 65 to 95°C). Expression data were obtained from three independent biological repetitions. Primers were used at a final concentration of 300 nM. Forward primer CTGTTGTAATTCTATTCTTTTGCCGT was used in combinations with reverse TCGTCTTTGCTTGGCAGGGAAAAAATTATAT to distinguish the WT splicing form and with reverse CTTCCATCACAGCAATTGTCTTCTACAG to distinguish the *sym41* splicing form. *Ubiquitin* was used as reference gene. *Ubiquitin* PCR fragments were amplified from primers: forward-ATGCAGATCTTTTGTGAAGAC and reverse-ACCACCACGGAAGACGGAG.

Complementation of *Pssym41*

A plasmid DNA containing *DMI2p::DMI2-GFP* (Limpens et al., 2005) was introduced by standard electroporation into the *Agrobacterium rhizogenes* strain ARqual (Quandt et al.,1993).

Germinated pea seedlings of RisFixA (*sym41*) and Finale were grown in darkness on agar plates with Färhaeus medium (Färhaeus et al., 1957) for 7-12 days. Next, the roots and the majority of hypocotyls were removed with scalpel and *A. rhizogenes* culture (OD_{600}=0.5-0.7) was injected with syringe approximately 3–5 mm below cotyledons. Plants were immediately placed in perlite and additionally inoculated with 1 ml of *A. rhizogenes* culture (OD_{600}=0.5-0.7) per plant. Transformed plants were supported by Färhaeus medium (without nitrate). After 14-20 days, plants were inoculated with *R. leguminosarum* strain 248*lacZ* as described in Borisov et al. (1997). To estimate the efficiency of genetic complementation, plants were analyzed 28 days after inoculation.

AKNOWLEDGMENTS

This study was supported by the Russian Ministry of Education and Science (Governmental contracts № 02.740.11.0276, 16.512.11.2155, П1304), President of Russia supporting the leading scientific schools (НШ-3440.2010.4), RFBR (09-04-91054, 10-04-00961, 10-04-01146), and by The Netherlands Organization for Scientific Research grants NWO-047.117.2005.006 and NWO-3184319448.

We would like to thank Dr. Olga Kulikova for valuable advises on preparation of this manuscript.

REFERENCES

Ané, J.M., Kiss, G.B., Riely, B.K., Penmetsa, R.V., Oldroyd, G.E., Ayax, C., Lévy, J., Debellé, F., Baek, J.M., Kalo, P., et al (2004) *Medicago truncatula DMI1* required for bacterial and fungal symbioses in legumes. *Science* 30: 1364–1367.

Ané, J.M., Lévy, J., Thoquet, P., Kulikova, O., de Billy, F., Penmetsa, V., Kim, D.J., Debellé, F., Rosenberg, C., Cook, D.R. et al (2002) Genetic and cytogenetic mapping of DMI1, DMI2, and DMI3 genes of Medicago truncatula involved in Nod factor transduction, nodulation, and mycorrhization. *Mol. Plant-Microbe Interact.,* 15(11): 1108–1118.

Arrighi J.F., Barre, A., Ben Amor, B., Bersoult, A., Soriano, L., Mirabella, R., Carvalho-Niebel, F., Journet, E., Ghérardi, M., Huguet, T., Geurts, R., Dénarié, J., Rougé, P., Gough, C. (2006) The *Medicago truncatula* LysM-receptor kinase gene family includes *NFP* and new nodule-expressed genes. *Plant Physiol,* 142: 265–279.

Aubert, G., Morin J., Jacquin F.., Loridon K., Quillet M.C., Petit A., Rameau C., Lejeune-Hénaut I., Huguet T., Burstin J. (2006) Functional mapping in pea, as an aid to the candidate gene approach and for investigating the synteny with the model species *Medicago truncatula. Theor. Appl. Genet*, 112: 1024–1041.

Bénaben, V., Duc, G., Lefebvre, V., Huguet, T. (1995) TE7, An Inefficient Symbiotic Mutant of *Medicago truncatula* Gaertn cv. Jemalong. *Plant Physiol*., 107: 53–62.

Bersoult, A., Camut, S., Perhald, A., Kereszt, A., Kiss, G.B., Cullimore, J.V. (2005) Expression of the *Medicago truncatula DM12* gene suggests roles of the symbiotic nodulation receptor kinase in nodules and during early nodule development. *Mol Plant Microbe Interact***,** 18: 869–876.

Boivin, C., Camut, S., Malpica, C., Truchet, G., Rosenberg, C. (1990) Rhizobium meliloti genes encoding catabolism of trigonelline are induced under symbiotic conditions. *Plant Cell,* 2: 1157–1170.

Borisov, A.Yu., Danilova, T.N., Koroleva, T.A., Kuznetsova, E.V., Madsen, L., Mofett, M., Naumkina, T.S., Nemankin, T.A., Ovchinnikova, E.S., Pavlova et al. (2007) Regulatory genes of garden pea (*Pisum sativum* L.) controlling the development of nitrogen-fixing nodules and arbuscular mycorrhiza: a review of basic and applied aspects. *Appl. Biochemistry and Microbiology,* 43(3): 237–243.

Borisov, A.Y., Barmicheva, E.M., Jakobi, L.M., Tsyganov, V.E., Voroshilova, V.A., Tikhonovich, I.A. (2000) Pea (*Pisum sativum* L.) mendelian genes controlling development of nitrogen-fixing nodules and arbuscular mycorrhiza. *Czech J. Genet. Plant Breed.,* 36: 106–110.

Borisov, A.Y., Rozov, S.M., Tsyganov, V.E., Morzhina, E.V., Lebsky, V.K., Tikhonovich, I. (1997) Sequential functioning of *Sym13* and *Sym31*, two genes affecting symbiosome development in root nodules of pea (*Pisum sativum* L). *Mol. Gen. Genet.,* 254: 592–598.

Brewin, N. J. (2004). Plant cell wall remodelling in the *Rhizobium*-legume symbiosis. *Crit. Rev. Plant Sci.,* 23: 293–316.

Capoen, W., Den Herder, H., Sun, J., Verplancke, C., De Keyser, A., De Rycke, R., Goormachtig, S., Oldroyd, G., Holster, M. (2009) Calcium spiking patterns and the role of the calcium/calmodulin-dependent kinase CCaMK in lateral root base nodulation of *Sesbania rostrata*. *Plant Cell,* 21(5): 1526– 1540.

Capoen, W., Goormachtig, S., De Rycke, R., Schroeyers, K., Holsters, M. (2005) SrSymRK, a plant receptor essential for symbiosome formation. *Proc. Natl. Acad. Sci. U.S.A.,* 102:10369-10374.

Catoira, R., Galera, C., de Billy, F., Penmetsa, R.V., Journet, E.P., Maillet, F., Rosenberg, C., Cook, D., Gough, C., Dénarié, J. (2000) Four genes of *Medicago truncatula* controlling components of a Nod factor transduction pathway. *Plant Cell*, 12: 1647–1666.

Catoira, R., Timmers, A.C., Maillet, F., Galera, C., Penmetsa, R.V., Cook, D., Dénarié, J., Gough, C. (2001) The *HCL* gene of *Medicago truncatula* controls Rhizobium-induced root hair curling. *Development* 128**:** 1507–1518.

Charpentier, M., Bredemeier, R., Wanner, G., Takeda, N., Schleiff, E., Parniske, M. (2008) *Lotus japonicus* CASTOR and POLLUX are ion channels essential for perinuclear calcium spiking in legume root endosymbiosis. *Plant Cell*, 20: 3467–3479.

Cebolla, A., Vinardell, J.M., Kiss, E., Oláh, B., Roudier, F., Kondorosi, A., Kondorosi, E. (1999) The mitotic inhibitor *ccs52* is required for endoreduplication and ploidy-dependent cell enlargement in plants. *EMBO J.,* 18: 101–109.

Demchenko, K., Winzer, T., Stougaard, J., Parniske, M., Pawlowski, K. (2004) Distinct roles of *Lotus japonicus* SYMRK and SYM15 in root colonization and arbuscule formation. *New Phytol.,* 163: 381–392.

Duc, G. and Messager, A. (1989) Mutagenesis of pea (*Pisum sativum* L.) and the isolation of mutants for nodulation and nitrogen fixation. *Plant Sci.,* 60: 207–213.

Edwards, A., Heckmann, A.B., Yousafzai, F., Duc, G., Downie, J.A. (2007) Structural implications of mutations in the pea SYM8 symbiosis gene, the DMI1 ortholog, encoding a predicted ion channel. *Mol Plant Microbe Interact.* 20:1183-1191.

Endre, G., Kereszt, A., Kevei, Z., Mihacea, S., Kaló, P., Kiss, G. (2002) A receptor kinase gene regulating symbiotic nodule development. *Nature* 417: 962–966.

Engvild, K.C. (1987) Nodulation and nitrogen fixation mutants of pea, Pisum sativum. *Theor Appl Genet.,* 74: 711–713.

Esseling, J.J., Lhuissier, F.G., Emons, A.M. (2004) A nonsymbiotic root hair tip growth phenotype in NORK-mutated legumes: implications for nodulation factor-induced signaling and formation of a multifaceted root hair pocket for bacteria. *Plant Cell,* 16: 933–944.

Fåhraeus, G. (1957) The infection of clover root hairs by nodule bacteria studied by a simple glass slide technique. *J. of General Microbiology,* 16: 374 – 381.

Geurts, R., Heidstra, R., Hadri, A.E., Downie, J.A., Franssen, H., Van Kammen, A., Bisseling, T. (1997) Sym2 of pea is involved in a nodulation factor-perception mechanism that controls the infection process in the epidermis. *Plant Physiol.,* 115: 351–359.

Godfroy, O., Debellé, F., Timmers, T., Rosenberg, C. (2006) A rice calcium- and calmodulin-dependent protein kinase restores modulation to a legume mutant. *Mol. Plant-Microbe Interact.,* 19(5): 495–501.

Gonzalez-Rizzo, S., Crespi, M., Frugier, F. (2006) The *Medicago truncatula* CRE1 cytokinin receptor regulates lateral root development and early symbiotic interaction with *Sinorhizobium meliloti. Plant Cell,* 18: 2680–2693.

Groth, M., Takeda, N., Perry, J. Uchida, H., Brachmann, A., Sato, S., Tabata, S., Kawaquchi, M., Wang, T.L., Parniske, M. (2010) NENA, a Lotus japonicus homolog of Sec13, is required for rhizodermal infection by arbuscular mycorrhiza fungi and rhizobia but dispensable for cortical endosymbiotic development. *Plant Cell*, 22: 2509–2526.

Hirsch, A.M., Long, S.R., Bang, M., Haskins, N., Ausubel, F.M. (1982) Structural studies of alfalfa roots infected with nodulation mutants of *Rhizobium meliloti*. *J Bacteriol.,* 151: 411–419.

Horváth, B., Yeun, L. H., Domonkos, A., Halász, G., Gobbato, E., Ayaydin, F., Míró, K., Hirsch, S., Sun, J., Tadege, M., Ratet, P., et al. (2011) *Medicago truncatula* IPD3 is a member of the

common symbiotic signaling pathway required for rhizobial and mycorrhizal symbioses. *Mol. Plant-Microbe Interact.,* 24: 1345–1358.

Kanamori N., **Madsen, L., Radutoiu, S., Frantescu, M., Quistgaard, E., Miwa, H., Downie, A., James, E.K., Felle, H.H., Haaning, L.L. et al.** (2006) A nucleoporin is required for induction of Ca^{2+} spiking in legume nodule development and essential for rhizobial and fungal symbiosis. *Proc. Natl. Acad. Sci. USA,* 103: 359–364.

Kevei, Z., Lougnon, G., Mergaert, P., Horváth, G. V., Kereszt, A., Jayaraman, D., Zaman, N., Marcel, F., Regulski, K., Kiss, G. B. et al. (2007) 3-Hydroxy-3-methylglutaryl coenzyme a reductase 1 interacts with NORK and is crucial for nodulation in *Medicago truncatula*. *Plant Cell,* 19: 3974–3989.

Kistner, C., Winzer, T., Pitzschke, A., Pitzschke, A., Mulder, L., Sato, S., Kaneko, T., Sandal, N., Stougaard, J., Webb, K.J. et al. (2005) Seven Lotus japonicus genes required for transcriptional reprogramming of the root during fungal and bacterial symbiosis. *Plant Cell,* 17: 2217–2229.

Kneen, B.E., Weeden, N.F., LaRue, T.A. (1994) Non-nodulating mutants of *Pisum sativum* L. cv. Sparkle. J *Hered.* 85: 129-133.

Kosuta, S., Held, M., Hossain, M.S., Morieri, G., MacGillivary, A., Johansen, C., Antolin-Liovera, M., Parniske, M., Olgroyd, G., Downie, A.J. et al. (2011) Lotus japonicus symRK-14 uncouples the cortical and epidermal symbiotic program. *The Plant J.,* 67: 929–940.

Lefebvre, B., Timmers, T., Mbengue, M., Moreau, S., Hervé, C., Tóth, K., Bittencourt-Silvestre, J., Klaus, D., Deslandes, L., Godiard, et al. (2010) A remorin protein interacts with symbiotic receptors and regulates bacterial infection. *Proc. Natl. Acad. Sci. U.S.A.,* 107: 2343–2348.

Lévy, J., Bres, C., Geurts, R., Chalhoub, B., Kulikova, O., Duc, G., Journet, E.P., Ané, J.M., Lauber, E., Bisseling, T., et al. (2004) A putative Ca^{2+} and calmodulin-dependent protein kinase required for bacterial and fungal symbioses. *Science* 303: 1361–1364.

Limpens, E., Franken, C., Smit, P., Willemse, J., Bisseling, T., Geurts, R. (2003) LysM domain receptor kinases regulating rhizobial Nod factor-induced infection. *Science* 302: 630–633.

Limpens, E., Mirabella, R., Fedorova, E., Franken, C., Franssen, H., Bisseling, T., Geurts, R. (2005) Formation of organelle-like N_2-fixing symbiosomes in legume root nodules is controlled by *DMI2. Proc Natl Acad Sci USA,* 102: 10375–10380.

Madsen, E.B., Madsen, L.H., Radutoiu, S., Olbryt, M., Rakwalska, M., Szczyglowski, K., Sato, S., Kaneko, T., Tabata, S., Sandal, N., et al. (2003) A receptor kinase gene of the LysM type is involved in legume perception of rhizobial signals. *Nature* 425: 637–640.

Madsen, L.H., Tirichine, L., Jurkiewicz, A., Sullivan, J.T., Heckmann, A.B., Bek, A.S., Ronson, C.W., James, E.K. Stougaard, J. (2010) The molecular network governing nodule organogenesis and infection in the model legume Lotus japonicus. *Nature Communications,* 1: 1–12.

Mergeart, P., Uchiumi, T., Alunni, B., Evanno, G., Cheron, A., Catrice, O., Mausset, A.E., Barloy-Hubler, F., Galibert, F., Kondorosi, A., Kondorosi, E. (2006) Eukaryotic control on bacterial cell cycle and differentiation in the Rhizobium–legume symbiosis. *PNAS*, 103(13): 5230–5235.

Mitra, R. M., Gleason, C. A., Edwards, A., Hadfield, J., Downie, J. A., Oldroyd, G. E., Long, S. R. (2004) A Ca2+/calmodulin-dependent protein kinase required for symbiotic nodule development: Gene identification by transcript-based cloning. *Proc. Natl. Acad. Sci. U.S.A.,* 101: 4701–4705.

Moreau, S., Verdenaud, M., Ott, T., Letort, S., de Billy, F., Niebel, A., Gouzy, J., de Carvalho-Niebel, F., Gamas, P. (2011) Transcription reprogramming during root nodule development in *Medicago truncatula*. *PLoS One*, 6: e16463.

Morzhina, E,V., Tsyganov, V.E., Borisov, A.Y., Lebsky, V.K., Tikhonovich, I.A. (2000) Four developmental stages identified by genetic dissection of pea (*Pisum sativum* L.) root nodule morphogenesis. *Plant Science*, 155: 75–83.

Muromtsev, G.S., Sultonov, Y.S., Kazakova, V.N. (1989) Effectiveness of the biosynthetic plant growth regulator fusicoccin on agricultural crops. *Vestnik Selkhoz. Nauki*, 1: 141–144.

Oldroyd, G. E., Murray, J. D., Poole, P. S., Downie, J. A. (2011) The rules of engagement in the legume-rhizobial symbiosis. *Annu Rev Genet.,* 45: 119–144.

Oldroyd, G.E. and Downie, J.A. (2008) Coordinating nodule morphogenesis with rhizobial infection in legumes. *Annu. Rev. Plant Biol.,* 59: 519–546.

Oldroyd, G.E.D. and Downie, J.A. (2006) Nuclear calcium changes at the core of symbiosis signalling. *Curr. Opin. Plant Biol.,* 9: 351–357.

Ovchinnikova, E., Journet, E. P., Chabaud, M., Cosson, V., Ratet, P., Duc, G., Fedorova, E., Liu, W., den Camp, R. O., Zhukov, V., Tikhonovich, I., Borisov, A., Bisseling, T., Limpens, E. (2011). IPD3 controls the formation of nitrogen-fixing symbiosomes in pea and *Medicago* Spp. *Mol Plant-Microbe Interact,* 24(11): 1333–1344.

Parniske, M. (2008) Arbuscular mycorrhiza: The mother of plant root endosymbioses. *Nat. Rev. Microbiol.,* 6: 763–775.

Postma, J.G., Jager, D., Jacobsen, E., Feenstra, W.J. (1990) Studies on a non-fixing mutant of pea (Pisum sativum L.). 1. Phenotypical description and bacteroid activity. *Plant Science,* 68: 151–161.

Quandt, H.J., Puhler, A., Broer, I. (1993) Transgenic root nodules of *Vicia hirsuta*: a fast and efficient system for the study of gene expression in indeterminate-type nodules. *Mol. Plant-Microbe Interact.,* 6: 699–706.

Radutoiu, S., Madsen, L.H., Madsen, E.B., Felle, H.H., Umehara, Y., Gronlund, M., Sato, S., Nakamura, Y., Tabata, S., Sandal. N., et al. (2003) Plant recognition of symbiotic bacteria requires two LysM receptor-like kinases. *Nature* 425: 585–592.

Radutoiu, S., Madsen, L.H., Madsen, E.B., Jurkiewicz, A., Fukai, E., Quistgaard, E.M.H., Albrektsen, A.S., James, E.K., Thirup, S., Stougaard, J. (2007) LysM domains mediate lipochitin–oligosaccharide recognition and *Nfr* genes extends the symbiotic host range. *EMBO J.,* 26: 3923–3935.

Riely, B.K., Mun, J.H., Ane, J. (2006) Unravelling the molecular basis for symbiotic signal transduction in legumes. *Mol. Plant Path.,* 7: 197–207.

Rogers, S.O. and Bendich, A.J. (1985) Extraction of DNA from milligram amounts of fresh, herbarium and mummified plant tissues. *Plant Idol. Biol.,* 5: 69–76.

Rosewarne, G.M., Barker, S.J., Smith, S.E. (1997) Production of near-synchronous fungal colonization in tomato for developmental and molecular analyses of mycorrhiza. *Mycol. Res.,* 101: 966–970.

Roth, L.E. and Stacey, G. (1989) Bacterium release into host cells of nitrogen-fixing soybean nodules: the symbiosome membrane comes from three sources. *Eur. J. Cell Biol.,* 49:13–23.

Saito, K., Yoshikawa, M., Yano, K., Miwa, H., Uchida, H., Asamizu, E., Sato, S., Tabata, S., Imaizumi-Anraku, H., Umehara, Y. et al. (2007) NUCLEOPORIN85 is required for calcium spiking, fungal and bacterial symbioses, and seed production in *Lotus japonicus. Plant Cell***,** 19: 610–624.

Smit, P., Limpens, E., Geurts, R., Fedorova, E., Dolgikh, E., Gough, C., Bisseling, T. (2007) Medicago LYK3, an entry receptor in rhizobial nodulation factor signalling. *Plant Physiol.,* 145:183–191.

Schneider, A., Walker, S.A., Poyser, S., Sagan, M., Ellis, T.H., Downie, J.A. (1999) Genetic mapping and functional analysis of a nodulation-defective mutant (*sym19*) of pea (*Pisum sativum* L.). *Mol. Gen. Genet.,* 262: 1–11.

Stracke, S., Kistner, C., Yoshida, S., Mulder, L., Sato, S., Kaneko, T., Tabata, S., Sandal, N., Stougaard, J., Szczyglowski, K., Parniske, M. (2002) A plant receptor-like kinase required for both bacterial and fungal symbiosis. *Nature* 417: 959–962.

Timmers, A.C., Auriac, M.C., de Billy, F., Truchet, G. (1998) Nod factor internalization and microtubular cytoskeleton changes occur concomitantly during nodule differentiation in alfalfa. *Development* 125: 339–349.

Timmers, A.C., Auriac, M.C., Truchet, G. (1999) Refined analysis of early symbiotic steps of the *Rhizobium*-Medicago interaction in relationship with microtubular cytoskeleton rearrangements. *Development* 126: 3617–3628.

Tirichine, L., Imaizumi-Anraku, H., Yoshida, S., Murakami, Y., Madsen, L.H., Miwa, H., Nakagawa, T., Sandal, N., Albrektsen, A. S., Kawaguchi, M. et al. (2006) Deregulation of a Ca^{2+}/calmodulin-dependent kinase leads to spontaneous nodule development. *Nature* 441: 1153–1156.

Tirichine, L., Sandal, N., Madsen, L.H., Radutoiu, S., Albrektsen, A. S., Sato, S., Asamizu, E., Tabata, S., Stougaard, J. (2007) A gain-of-function mutation in a cytokinin receptor triggers spontaneous root nodule organogenesis. *Science* 2315: 104–107.

Trouvelot, A., Kough, J. L., Gianinazzi-Pearson, V. (1986) Mesure du taux de mycorhization VA d'un système radiculaire. Recherche de méthodes d'estimation ayant une signification fonctionnelle. P. 217–221 in: Physiological and Genetical Aspects of Mycorrhizae. V. Gianinazzi-Pearson and S. Gianinazzi, eds. INRA, Paris.

Tsyganov, V.E., Voroshilova, V.A., Priefer, U.B., Borisov, A.Y., Tichonovich, I.A. (2002) Genetic dissection of the initiation of the infection process and nodule tissue development in the *Rhizobium*-pea (*Pisum sativum* L.) symbiosis. *Annals of Botany*, 89: 357–366.

Tsyganov, V.E., Morzhina, E.V., Stefanov, S.Y., Borisov, A.Y., Lebsky, V.K., Tikhonovich, I.A. (1998) The pea (*Pisum sativum* L.) genes *sym33* and *sym40* control infection thread formation and root nodule functioning. *Molecular and General Genetics*, 259: 491–503.

Utrup, L.J., Cary, A.J., Norris, J.H. (1993) Five nodulation mutants of white sweet clover *(Melilofus alba* Desr.) exhibit distinct phenotypes blocked at root hair curling, infection thread development, and nodule organogenesis. *Plant Physiol.,* 103: 925–932.

Yang, W.C., de Blank, C., Meskiene, I., Hirt, H., Bakker, J., van Kammen, A., Franssen, H., Bisseling, T. (1994) Rhizobium nod factors reactivate the cell cycle during infection and nodule

primordium formation, but the cycle is only completed in primordium formation. *Plant Cell*, 6: 1415–1426.

Van de Velde, W., Zehirov, G., Szatmari, A., Debreczeny, M., Ishihara, H., Kevei, Z., Farkas, A., Mikulass, K., Nagy, A., Tiricz, H. (2010) Plant peptides govern terminal differentiation of bacteria in symbiosis. Science 327 : 1122–1126.

Vasse, J., de Billy, F., Camut, S., Truchet, G. (1990) Correlation between ultrastructural differentiation of bacteroids and nitrogen fixation in Alfalfa nodules. *J. Bacteriol.,* 172: 4295–4306.

Verhulst, A., D'Haese, P.C., De Broe, M.E. (2004) Inhibitors of HMG-CoA reductase reduce receptor-mediated endocytosis in human kidney proximal tubular cells. *J. Am. Soc. Nephrol.,* 15: 2249–2257.

Vierheilig, H., Coughlan, A. P., Wyss, U., Piche, Y. (1998) Ink and vinegar, a simple staining technique for arbuscular-mycorrhizal fungi. *Appl. Environ. Microbiol.,* 64: 5004–5007.

Vindarell, J.M., Fedorova, E., Cebolla, A., Kevei, Z., Horvath, G., Kelemen, Z., Tarayre, S., Roudier, F., Mergaert, P., Kondorosi, A., Kondorosi, E. (2003) Endoreduplication Mediated by the Anaphase-Promoting Complex Activator CCS52A Is Required for Symbiotic Cell Differentiation in *Medicago truncatula* Nodules. *Plant Cell,* 15(9): 2093–2105.

Voroshilova, V. A., Demchenko, K. N., Brewin, N. J., Borisov, A. Y., Tikhonovich I. A. (2009) Initiation of a legume nodule with an indeterminate meristem involves proliferating host cells that harbour infection threads. *New Phytol.,* 181: 913–923.

Wegel, E., Schauser, L., Sandal, N., Stougaard, J., Parniske, M. (1998) Mycorrhiza mutants of *Lotus japonicus* define genetically independent steps during symbiotic infection*. Mol. Plant-Microbe Interact.,* 11: 933–936.

Wais, R.J., Galera, C., Oldroyd, G., Catoira, R., Penmetsa, R.V., Cook, D., Gough, C., Dénarié, J., Long, S.R. (2000) Genetic analysis of calcium spiking responses in nodulation mutants of *Medicago truncatula. Proc Natl Acad Sci USA*, 97: 13407–13412.

Walker, S.A., Viprey, V., Downie, J.A. (2000) Dissection of nodulation signalling using pea mutants defective for calcium spiking induced by Nod factors and chitin oligomers. *Proc. Natl. Acad. Sci. USA,* 97: 13413–13418.

Zhukov, V., Radutoiu, S., Madsen, L.H., Rychagova, T., Ovchinnikova, E., Borisov, A., Tikhonovich, I., Stougaard, J. (2008) The Pea *Sym37* Receptor Kinase Gene Controls Infection-Thread Initiation and Nodule Development. *Mol. Plant-Microbe Interact.,* 21(12): 1600–1608.

Chapter 5

Towards the identification of pea Sym31, a putative sucrose transporter controlling symbiosome differentiation?

Evgenia Ovchinnikova,[1,2] Alexey Borisov,[2] Jiangqi Wen,[3] Kirankumar S. Mysore,[3] Igor Tikhonovich,[2] Ton Bisseling,[1] and Erik Limpens[1]

[1] Wageningen University, laboratory of Molecular Biology, Droevendaalsesteeg 1, 6708 PB, Wageningen, The Netherlands;

[2] All-Russia Research Institute for Agricultural Microbiology, laboratory of Genetics of Plant-Microbe Interactions, Podbelsky chaussee 3, 196608, Pushkin 8, St. Petersburg, Russia;

[3] Samuel Roberts Noble Foundation, 2510 Sam Noble Parkway, Ardmore, OK 73401, USA

ABSTRACT

During symbiosome development, Rhizobium bacteria differentiate into specialized endosymbiotic forms, called bacteroids that acquire the ability to fix atmospheric nitrogen. In pea and *Medicago truncatula* (Medicago), each symbiosome typically contains a single bacteroid that terminally differentiates and loses its ability to reproduce. During this terminal differentiation, bacteroids become highly dependent on their host, especially for the provision of carbon sources. To get more insight into plant components that control bacteroid differentiation, we focused on the pea *sym31* mutant, which shows impaired differentiation of the bacteroids and has an abnormal symbiosome structure, including several bacteroids within a single symbiosome membrane. To identify the recessive *PsSym31* allele, we used a synteny-based mapping approach using the Medicago genome as reference. We fine mapped the location of *Sym31* to a ~2.5 cM region in pea, which corresponds to a ~450kb region in Medicago. In this corresponding region, one gene that is specifically upregulated in the nodule stands out as promising candidate for *Sym31*. This gene (*MtN3.1*) encodes an MtN3/SWEET-like protein that is a member of the recently identified family of sugar/sucrose transporters. We propose that *PsSym31* encodes a putative sucrose transporter, homologous to *MtN3.1* that controls symbiosome differentiation. However, the ultimate prove for the involvement of MtN3.1 in symbiosome development and the identification of its ortholog *Sym31* in pea, awaits further experimentation.

INTRODUCTION

Symbiotic nitrogen-fixing bacteria, collectively called rhizobia, engage legume plants in endosymbiosis where the bacteria are hosted as nitrogen-fixing organelles inside specialized cells of a newly formed plant organ, the root nodule (Jones et al., 2007). These nitrogen-fixing organelles, called symbiosomes, consist of one or several bacteria surrounded by a specialized plant membrane, the symbiosome membrane (Roth and Stacey, 1989; Whitehead and Day, 1997; Brewin et al., 1996). The symbiosome represents a symbiotic interface where the nitrogen fixed by rhizobia is exchanged for photosynthates from the plant. Therefore, symbiosome formation forms the heart of the nitrogen-fixing symbiosis.

During symbiosome development, the Rhizobium bacteria differentiate into specialized endosymbiotic forms, called bacteroids that acquire the ability to fix atmospheric nitrogen (Vasse et al., 1990). In pea and the model legume *Medicago truncatula* (Medicago), each symbiosome typically contains a single bacteroid that comes under full control of its host. Under this control, bacteroids terminally differentiate and lose their ability to divide and reproduce (Mergaert et al., 2006). This terminal differentiation is determined by the plant and characteristic for legumes of the so-called inverted-repeat-lacking (IRLC) clade of Papillionoideae (Wojciecowski et al., 2004; Mergeart et al., 2006). Terminal differentiation does not occur in legumes such as *Lotus japonicus* (Lotus) or soybean and it is thought to have evolved several times independently in the papilionoids (Oono et al., 2010).

Symbiosome formation starts in the nodule (primordium) cells with the formation of an unwalled infection droplet, a local region on the IT where the plasma membrane extrudes, and the cell wall is degraded or not built. From there, bacteria are individually pinched off into the cytoplasm by which they become surrounded by the plant-derived symbiosome membrane. In indeterminate nodules such as formed by pea and Medicago, a persistent meristem continuously adds cells to the tissues of the nodule. Within a few cell layers just below this meristem, called the distal infection zone, infection and rhizobial release take place after which the symbiosomes continue to divide. In the proximal part of the infection zone, symbiosomes stop dividing and start to differentiate by which they become much more elongated and swollen. In pea, bacteroids form typical Y-shaped structures. When the symbiosomes are mature, they almost completely fill the infected cells and start to fix atmospheric nitrogen. This process is supported by the low oxygen concentrations in the cells of the fixation zone and involves the induction of the rhizobial nitrogen fixation *Nif* genes (Soupène et al., 1995; Ott et al., 2005).

As the symbiosomes differentiate, the bacteria switch off most processes related to growth and division as well as their ability to assimilate ammonia into amino acids (Patriarca et al., 2002; White et al., 2007). Therefore, they become highly dependent on the host to provide key nutrients and metabolites that need to be transported across the symbiosome membrane. This especially involves the provision of carbon sources such as dicarboxylic acids (mainly malate).

These are thought to be supplied by the uninfected nodule cells where sucrose is first cleaved and processed into organic acids that are then transported to the infected cells (Craig et al., 1999; Peiter and Schubert, 2003; White et al., 2007). Furthermore, the bacteroids require the dicarboxylate carrier protein DctA to take up dicarboxylates (malate) and to fix nitrogen (Yurgel and Kahn, 2004). Rhizobial *dctA* mutants are severely impaired in bacteroid development (Yurgel and Kahn, 2004; White et al., 2007). However, the corresponding plant transporter that delivers dicarboxylates across the symbiosome membrane is still unknown. Furthermore, it has been shown in pea that bacteroids become auxotrophic for branched-chain amino acids. When the uptake of branched amino-acids is hampered, through mutation of the broad-specificity amino-acid transporters *aap* and *bra*, the bacteroids fail to fix nitrogen and to develop fully (Prell et al., 2009). In addition, bacteroids rely on their host for the transfer of essential minerals like sulfate and homocitrate by symbiosome membrane-localized transporters (Krusell et al., 2005; Hakoyama et al., 2009). Homocitrate, which cannot be synthesized by most rhizobia, is a key component of the iron molybdenum cofactor of the nitrogenase complex, the enzyme essential for biological nitrogen fixation (Hakoyama et al., 2009).

It was recently shown that terminal symbiosome/bacteroid differentiation is triggered by nodule-specific cysteine-rich (NCR) peptides that resemble defensin-like antimicrobial peptides (Van de Velde et al., 2010; Maróti et al., 2011). These NCR peptides are specific for the IRLC legumes and absent in the genomes of non-IRLC legumes such as soybean and Lotus (Alunni et al., 2007). NCR peptides contain a signal peptide sequence recognized and processed by a nodule-specific ER-resident signal peptidase complex (Wang et al., 2010; Van de Velde et al., 2010). A mutation in the signal peptidase SPC22 subunit in the Medicago mutant *defective in nitrogen fixation 1* (*dnf1)*, causes that the symbiosomes fail to differentiate and the bacteroids morphologically resemble free-living rhizobia (Mitra and Long, 2004; Wang et al., 2010). Due to mutation in the SPC22 subunit in *Mtdnf1*, signal peptidase could not remove the signal peptide sequence from the NCR peptides, and those were not targeted from ER to the symbiosomes. Furthermore, a rhizobial *bacA* mutant unable to differentiate into bacteroid form showed an increased sensitivity to the antimicrobial properties of the NCR peptides (Glazebrook et al., 1993; Manoury et al., 2010; Haag et al., 2011). Therefore, it seems that IRLC legumes use the antimicrobial NCR peptides to dominate their bacterial symbionts and the ABC-type transporter BacA appears to protect rhizobia from the negative effects of these peptides.

To get further insight into plant components that control symbiosome differentiation, we focused on the pea *sym31* mutant. *Pssym31* was identified by Borisov et al. (1992) and shown to form white root nodules that lack nitrogen fixation after inoculation with effective strains of *Rhizobium leguminosarum* bv. *viciae. Pssym31* nodules show impaired differentiation of the bacteroids accompanied by abnormal symbiosome structures, where several bacteroids are included within a single symbiosome membrane (Borisov et al., 1992, 1997; Sherrier et al.,

1997; Dahiya et al., 1998). Moreover, Romanov et al. (1995) showed that the mutant nodules contained low levels of leghemoglobin and glutamine synthase as well as reduced levels of sucrose synthase and the carbohydrate ononitol, suggesting alterations in carbon metabolism

To identify the recessive *PsSym31* allele, we undertook a synteny-based mapping approach using the Medicago genome as reference. We fine mapped the location of *Sym31* to a ~2.5 cM region in pea, which corresponds to a ~450kb region in Medicago. In this corresponding region, one gene specifically upregulated in the nodule stands out as potential candidate for *Sym31*. This gene encodes an MtN3/SWEET-like protein that is a member of the recently identified family of sugar/sucrose transporters (Chen et al., 2010, 2012). We propose that *PsSym31* encodes a putative sucrose transporter involved in the control of symbiosome differentiation.

RESULTS

Synteny-based mapping

Pssym31, also named Sprint2Fix$^-$ was identified by Borisov et al. (1992) as a recessive ethyl methanesulfonate (EMS) Fixation minus (Fix$^-$) mutant in the pea (*Pisum sativum* L.) line Sprint2. To verify the reported block of symbiosome differentiation in sym31 nodules under our growth conditions, we analyzed their ontology by light microscopy 21 days after inoculation, compared to wild-type Sprint2 nodules (Fig.1). This showed that bacteria were indeed released from the infection threads in the distal infection zone (Fig.1B, E) and the resulting symbiosomes multiplied, however the bacteroids did not differentiate as they remained similar in size to bacteria inside the infection threads (Fig.1C, F). Furthermore, in the basal part of the nodules groups of bacteroids appeared to occupy single symbiosome compartments (Fig.1F) as previously shown by electron microscopy (Borisov et al., 1997).

The *PsSym31* gene has been mapped to the upper arm of the pea chromosome III (linkage group III (LGIII)) close to the centromere (Rozov at al., 1995; Men et al., 1999; Ellis and Poyser, 2002). Later data suggested that *Sym31* located between markers MAX4 and Uni on the pea LGIII (Tsyganov, personal communication) (Fig.2). Since LGIII of pea is highly syntenic to the Medicago chromosome 3 (Aubert et al., 2006), a synteny-based cloning strategy was undertaken to clone *PsSym31* using the Medicago genome as reference (Young et al., 2011).

Genetic linkage of the *Pssym31* Fix$^-$ phenotype with generated cross-species molecular markers was analyzed using three mapping populations – crosses between Sprint2Fix$^-$ and WT lines NGB1238, SGE, and NGB851 (Table 5). Segregation analysis of the resulting F2 plants with 15 molecular cross-species markers (Table 1) allowed us to delineate the location of *PsSym31* within a ~2,5 cM region between markers UbE2 and Amyl on LGIII of pea (Fig.2). *PsSym31* showed absolute linkage with the cross-species marker SBP representing a Squamosa promoter binding protein on Medicago BAC clone CT954252 (Table 1; Fig.2B, C).

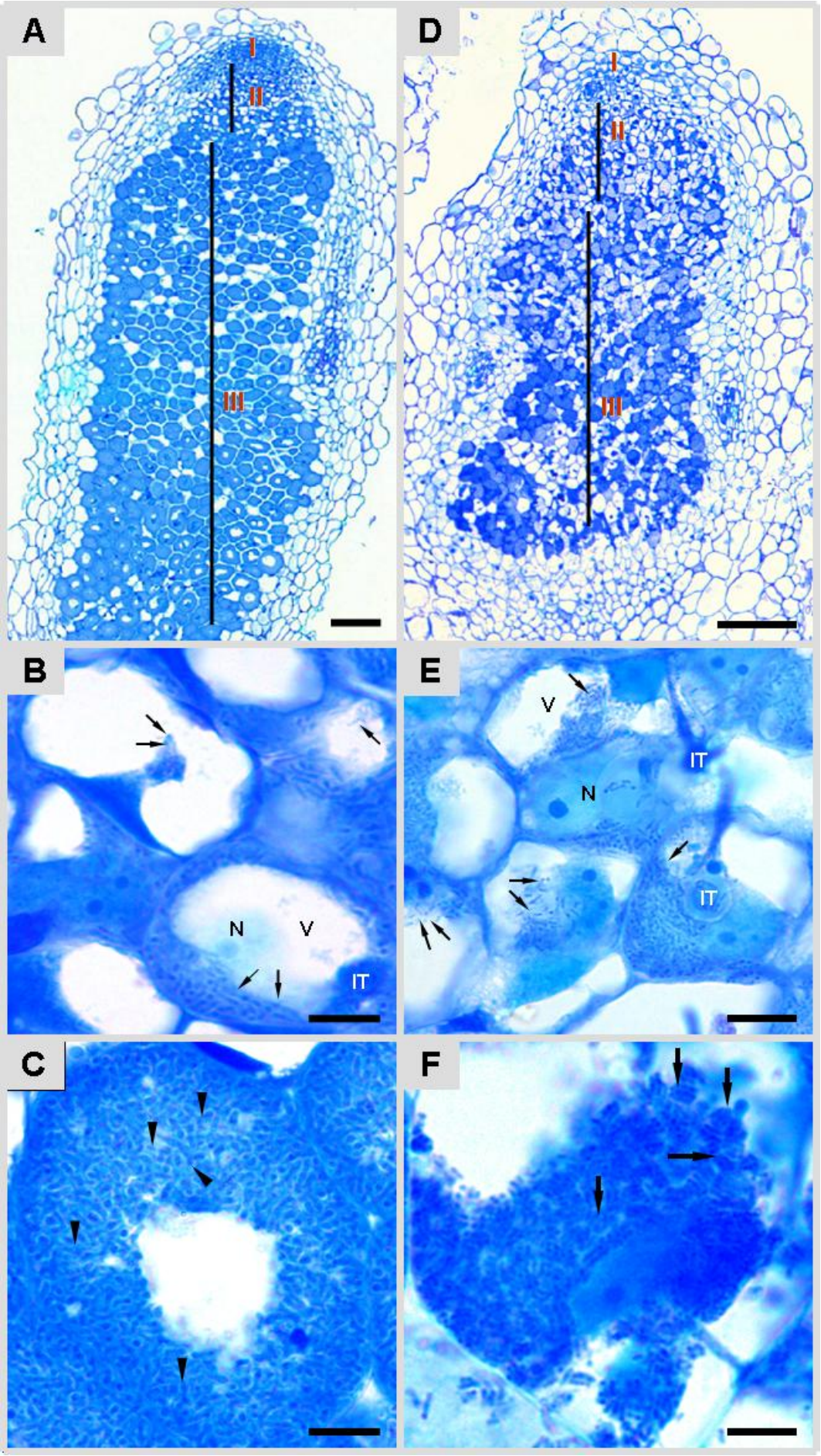
A
I
II
III
D
I
II
III
B
N
V
IT
E
V
IT
N
IT
C
F

Fig.1. Longitudinal sections of 16-day-old nodules in wild type (Sprint2) and *sym31* (Sprint2Fix-). **A–C**, wild type; **D–F**, *sym31*: I–meristematic zone, II–infection zone, III–fixation zone. **B** and **E**, Nodule cells in zone (II) where the symbiosome formation begins: N–nucleus, V–vacuole, IT –infection thread; arrows show the released bacteria (=juvenile symbiosomes). **C**, Nodule cells in zone (III) of wild type, containing differentiated symbiosomes with Y-shaped bacteroids (arrowheads). **F**, Nodule cells in zone (III) of *sym31* contain undifferentiated symbiosomes resembling bacteria in infection threads. Arrows show symbiosomes with multiple bacteroids. Bars: A, D–100 µm; B to F–10 µm. For detailed electron-microscopic analysis of the *sym31* nodule phenotype, we refer to Borisov et al. (1992), Borisov et al. (1997), and Sherrier et al. (1997).

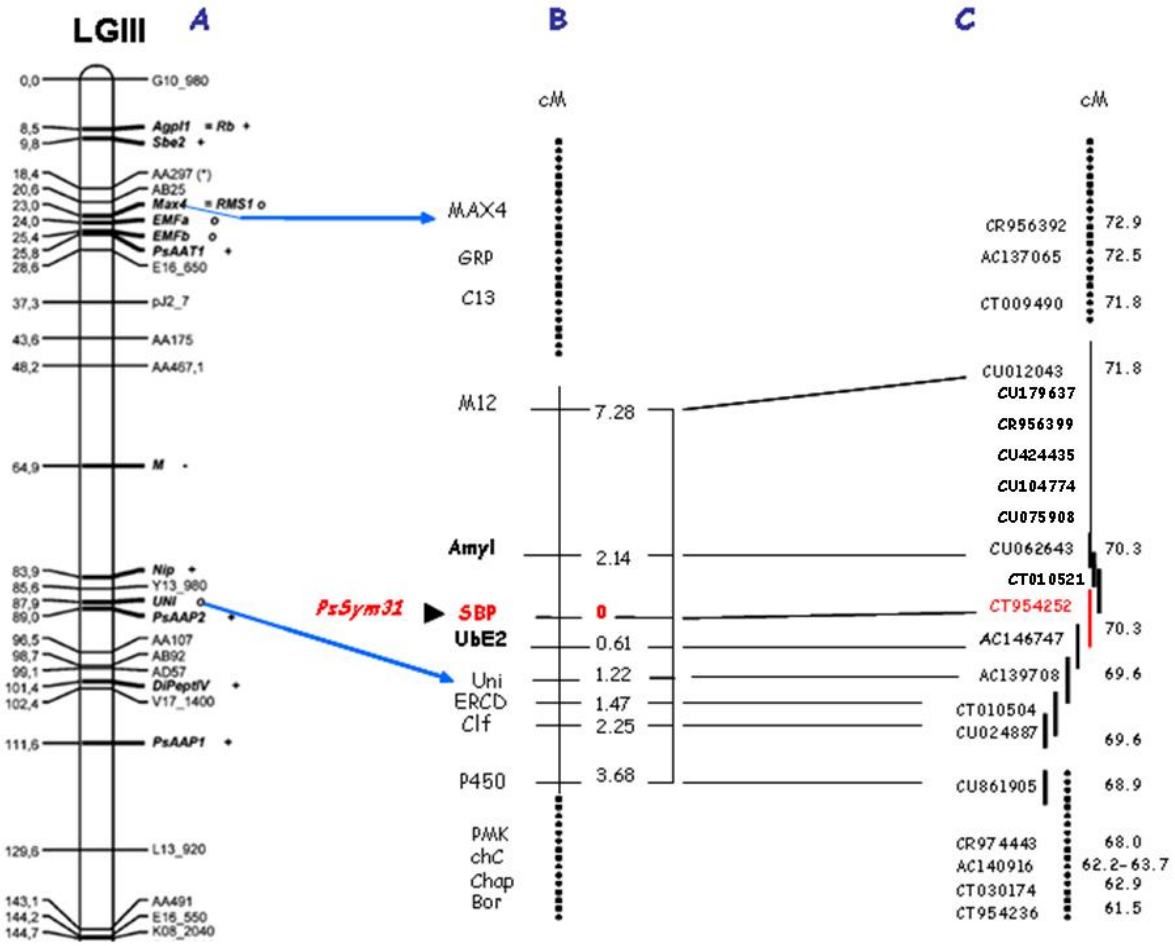

Fig.2. Synteny-based cloning of *PsSym31*. **A**–overview of the pea LGIII region containing *PsSym31* (from Aubert et al., 2006): blue arrows show reference markers MAX4 and Uni; **B**–an integrative genetic map of the *PsSym31* region: dashes represent areas of markers distant from *PsSym31* (see Table 1), solid line represents delineated area of the *PsSym31* region; the arrowhead shows the position of *PsSym31* (red) tightly linked to the marker SBP (red); Amyl and UbE2 (bold) flank *PsSym31*; C–the corresponding region of the *PsSym31* localization in chromosome III of Medicago: dashes–BAC clones corresponding to markers distant from *PsSym31*, bold solid lines–corresponding BAC clones to delineated area of the *PsSym31* localization. Lines between B and C connect markers with corresponding BAC clones in Medicago.

Table 1. Cross-species molecular markers used for *PsSym31* map-based cloning

Marker name	Mt BAC accession number	Genetic distance, cM		Name of marker gene product	χ^2
		M.truncatula	To *PsSYM31*		
MAX4	CR956392	72.9	38.46	Auxin-inducible polyene dioxygenase	0.006
GRP	AC137065	72.5	39.13	Gibberellin regulated protein	0.034
C13	CT009490	71.8	30.85	Peptidase C13, legumain	$0.73 \cdot e^{-3}$
M12	CU012043	71.8	7.28	Thioredoxin-like fold protein	0.011
Amyl	CU062643	70.3	2.14	Alpha amylase, catalytic region	0.010
SBP	**CT954252**	**70.3**	0.0	**Promoter Squamosa Binding Protein**	**0.0**
UbE2	AC146747	70.3	0.61	Ubiquitin-conjugating enzyme, E2	0.152
Uni	AC139708	69.6	1.22	Unifoliata protein	0.048
ERCD	CT010504	69.6	1.47	Extradiol ring-cleavage dioxygenase	0.140
Clf	CU024887	69.6	2.25	Cleft lip and palate ransmembrane 1	0.031
P450	CU861905	68.9	3.68	Cytochrome P450	0.026
PMK	CR974443	68.0	20.69	Phosphomevalonate kinase Erg8	0.005
chC	AC140916	62.2–63.7	23.08	SWI/SNF matrix-associated regulator of chromatin	$0.28 \cdot e^{-3}$
Chap	CT030174	62.9	30.77	GroEL-like chaperone, ATPase	0.002
Bor	CT954236	61.5	43.48	Boron transporter, putative	0.006

$\chi^2 > 3.84$ contributes independent assortment for p=0.05 and q=1, where p is as probability and q is as degrees of freedom. $\chi^2 < 3.84$ indicates linkage of the gene of interest with particular marker. Reference markers MAX4 and Uni are underlined.

PsSym31 candidate genes

The delineated syntenic region in Medicago covers a region of <450 kb. To identify putative candidate *PsSym31* genes, we annotated this sequenced region in Medicago and subsequently screened the *M. truncatula* Gene Expression Atlas (MtGEA, http://mtgea.noble.org/) (Benedito et al., 2008) for the expression profiles of corresponding putative genes. Because *Pssym31* has a symbiotic nodule-specific phenotype, we hypothesized that the corresponding gene should be specifically expressed or transcriptionally upregulated in nodules in comparison with non-inoculated roots or other tissues. An overview of the genes in this region and their expression in nodules and various plant tissues is given in Table 2.

Table 2. Genes from Medicago corresponding region of *PsSym31* localization and their expression in various plant tissues

Gene (Medicago truncatula v3.5 genome)	MtGEA identifier	Root	Nodule, 4 days	Nodule, 10 days	Nodule, 16 days	Root non-mycorrhizal	Root mycorrhizal	Leaf	Stem	Flower	Seed
>IMGA|Medtr3g098660.1 Centromere protein S	-	-	-	-	-	-	-	-	-	-	-
>IMGA|Medtr3g098680.1 ADP-ribosylation factor GTPase-activating protein	-	-	-	-	-	-	-	-	-	-	-
>IMGA|Medtr3g098690.1 Inducer of CBF expression 4	-	-	-	-	-	-	-	-	-	-	-
>IMGA|Medtr3g098700.1 Unknown Protein	-	-	-	-	-	-	-	-	-	-	-
>IMGA|Medtr3g098720.1 Unknown Protein	Mtr.45855.1.S1_at	17	15	14	15	27	22	-	-	-	-
>IMGA|Medtr3g098730.1 Hypothetical protein, contains Armadillo-like helical domain	Mtr.20861.1.S1_at	122	131	116	106	260	240	222	281	111	329
>IMGA|Medtr3g098740.1 Unknown Protein	Mtr.20860.1.S1_at	16	10	10	9	10	10	21	12	11	29
>IMGA|Medtr3g098750.1 NAD(P)H-quinone oxidoreductase chain 4	Mtr.20858.1.S1_at	259	239	208	226	236	220	158	231	136	340
>IMGA|Medtr3g098760.1 Os03g0349200 Serine/threonine protein kinase	Mtr.20857.1.S1_at	259	239	208	226	236	220	158	231	136	340
>IMGA|Medtr3g098770.1 Unknown Protein	-	-	-	-	-	-	-	-	-	-	-
>IMGA|Medtr3g098780.2 Ubiquitin-conjugating enzyme, E2	Mtr.45849.1.S1_at	1145	1009	1028	1189	1089	1483	1491	2058	1751	
>IMGA|Medtr3g098790.1 B3 domain-containing protein; transcription factor	Mtr.20853.1.S1_at	10	10	10	10	9	9	10	10	10	11
>IMGA|Medtr3g098800.1 Unknown Protein	Mtr.45841.1.S1_at	10	9	11	10	9	9	9	10	10	9
>IMGA|Medtr3g098810.1 NAC domain-containing protein 2	Mtr.20852.1.S1_at	110	39	48	61	54	50	22	29	29	22
>IMGA|Medtr3g098820.1 Mitochondrial import inner membrane translocase subunit Tim8	Mtr.45839.1.S1_at	1166	1414	731	992	1072	948	725	1262	1552	1550
>IMGA|Medtr3g098830.1 Unknown Protein	Mtr.20851.1.S1_at	15	11	12	14	10	11	15	11	14	14
>IMGA|Medtr3g098840.1 Palmitoyltransferase ZDHHC9	Mtr.20850.1.S1_at	1071	652	603	559	1124	977	202	136	314	184
>IMGA|Medtr3g098850.1 Palmitoyltransferase ZDHHC9	-	-	-	-	-	-	-	-	-	-	-
>IMGA|Medtr3g098860.1 Unknown Protein	Mtr.45838.1.S1_at	9	10	10	10	9	9	12	11	13	11
>IMGA|Medtr3g098870.1 Unknown Protein	-	-	-	-	-	-	-	-	-	-	-
>IMGA|Medtr3g098880.1 Unknown Protein	Mtr.45835.1.S1_at	9	9	9	9	9	8	8	9	9	9
>IMGA|Medtr3g098890.1 Unknown Protein	Mtr.45834.1.S1_at	14	12	14	14	11	13	15	13	16	18
>IMGA|Medtr3g098900.1 Unknown Protein	Mtr.45832.1.S1_at	21	21	22	20	18	17	24	21	22	24
>IMGA|Medtr3g098910.1 Protein RUPTURED POLLEN GRAIN 1 MtN3-like	Mtr.20846.1.S1_at	15	16	16	13	15	17	1833	681	5442	148
>IMGA|Medtr3g098920.1 Unknown Protein	-	-	-	-	-	-	-	-	-	-	-
>IMGA|Medtr3g098930.1 Protein RUPTURED POLLEN GRAIN 1 MtN3-like Sym31 candidate	Mtr.20845.1.S1_at	15	2472	272	541	13	12	17	15	17	17
>IMGA|Medtr3g098940.1 RNA pseudourine synthase 7	Mtr.20844.1.S1_at	197	232	259	233	185	205	226	200	142	429

Table 2. (Continued)

>IMGA|Medtr3g098950.1 Unknown Protein	-	-	-	-	-	-	-	-	-	-	-
>IMGA|Medtr3g098960.1 Transcription activator BRG1 ; contains Interpro domain(s) IPR020103 Pseudouridine synthase, catalytic domain	-	-	-	-	-	-	-	-	-	-	-
>IMGA|Medtr3g098970.1 Auxin-induced protein 6B; Auxin responsive SAUR protein	Mtr.34121.1.S1_at	9	8	9	8	8	8	9	9	8	9
>IMGA|Medtr3g098980.1 Hydroxycinnamoyl CoA shikimate/quinate protein	Mtr.39535.1.S1_at	244	367	73	615	278	291	81	32	656	29
>IMGA|Medtr3g098990.1 Protein DEK ; contains IPR014876 DEK, C-terminal	Mtr.7221.1.S1_at	452	801	569	538	650	648	200	567	488	483
>IMGA|Medtr3g099000.1 SWI/SNF complex subunit SMARCC2	-	-	-	-	-	-	-	-	-	-	-
>IMGA|Medtr3g099010.1 HVA22-like protein e	Mtr.40667.1.S1_at	580	232	188	194	289	288	625	221	1021	3760
>IMGA|Medtr3g099020.1 Myristoyl-acyl carrier protein thioesterase, chloroplastic	Mtr.11483.1.S1_at	178	263	329	285	209	200	179	200	226	304
>IMGA|Medtr3g099030.1 Heavy metal transport/detoxification protein	Mtr.1537.1.S1_at	44	50	26	25	25	22	175	35	205	305
>IMGA|Medtr3g099040.1 Heavy metal transport/detoxification protein	Mtr.33453.1.S1_at	11	10	12	9	11	12	56	48	478	20
>IMGA|Medtr3g099050.1 Unknown Protein	-	-	-	-	-	-	-	-	-	-	-
>IMGA|Medtr3g099060.1 Unknown Protein	-	-	-	-	-	-	-	-	-	-	-
>IMGA|Medtr3g099070.1 Unknown Protein	-	-	-	-	-	-	-	-	-	-	-
>IMGA|Medtr3g099080.1 Squamosa promoter binding protein 1	Mtr.5514.1.S1_at	25	22	21	23	23	22	28	54	104	22
>IMGA|Medtr3g099090.1 F-box/LRR-repeat protein At5g63520	Mtr.34197.1.S1_at	770	901	978	876	787	727	553	597	671	1183
>IMGA|Medtr3g099100.1 Meiotically up-regulated gene 70 protein	Mtr.42302.1.S1_at	249	229	229	192	418	385	401	282	221	185
>IMGA|Medtr3g099110.1 Unknown Protein	-	-	-	-	-	-	-	-	-	-	-
>IMGA|Medtr3g099120.1 Phospholipase C 3 -like	Mtr.2434.1.S1_s_at	52	58	49	29	203	151	52	189	105	190
>IMGA|Medtr3g099130.1 Unknown Protein	-	-	-	-	-	-	-	-	-	-	-
>IMGA|Medtr3g099140.1 Thylakoid lumenal 17.9 kDa protein, chloroplastic	Mtr.34745.1.S1_at	41	57	75	77	36	39	3130	607	430	75
>IMGA|Medtr3g099150.1 Nodulin-like protein ; contains IPR016196; Major facilitator superfamily, general substrate transporter 20100825	-	-	-	-	-	-	-	-	-	-	-
>IMGA|Medtr3g099160.1 Unknown Protein	-	-	-	-	-	-	-	-	-	-	-
>IMGA|Medtr3g099170.1 Curved DNA-binding protein ; contains Interpro domain(s) IPR003095 Heat shock protein DnaJ	-	-	-	-	-	-	-	-	-	-	-
>IMGA|Medtr3g099180.1 Nuclear transcription factor Y subunit C-1	Mtr.40976.1.S1_at	30	33	39	42	25	23	3308	1083	1073	220
>IMGA|Medtr3g099190.1 Acetolactate synthase	Mtr.6365.1.S1_at	65	112	121	113	157	126	763	335	187	70
>IMGA|Medtr3g099200.1 Molybdenum cofactor sulfurase	Mtr.43526.1.S1_at	2498	1553	1797	1594	2406	2425	34	32	73	28
>IMGA|Medtr3g099220.1 Unknown Protein	Mtr.38807.1.S1_s_	70	98	162	114	150	140	78	116	89	158
>IMGA|Medtr3g099230.1 Unknown Protein	-	-	-	-	-	-	-	-	-	-	-
>IMGA|Medtr3g099240.1 Ubiquitin-like modifier-activating enzyme 5	Mtr.12454.1.S1_at	3835	4773	3203	3598	3563	3372	1458	3335	2356	1926

Table 3. Medicago *N3* homologs and their associated expression values according to data from the *M. truncatula* Gene Expression Atlas (MtGEA)

Gene	Phytozome v.8.0 identifier	Medicago genome v.3.5 identifier	MtGEA identifier	Root	Nodule, 4 days	Nodule, 10 days	Nodule, 16 days	Root non-mycorrhizal	Root mycorrhizal	Leaf	Stem	Flower	Seed
N3.1/Sym31	Medtr3g150920.1	Medtr3g098930.1	Mtr.11146.1.S1_at	792	9380	64	723	472	442	20	22	20	25
			Mtr.20845.1.S1_at	15	2472	272	514	13	12	17	15	17	17
MtN3.2a	Medtr3g150940.2	Medtr3g098910.1	Mtr.20846.1.S1_at	15	16	16	13	15	17	1833	681	5442	148
MtN3.2b	Medtr3g150940.1	Medtr3g098910.1	Mtr.20846.1.S1_at	15	16	16	13	15	17	1833	681	5442	148
MtN3.3	Medtr2g008040.1	Medtr2g007890.1	Mtr.7205.1.S1_at	10	10	10	11	9	9	11	10	30	636
MtN3.4	Medtr5g076470.1	Medtr5g067530.1	Mtr.2934.1.S1_s_at	15	15	13	14	12	11	16	14	20	1905
MtN3.5	AC147714_1.1	AC147714_7.1	Mtr.5409.1.S1_at	25	27	18	20	22	20	34	74	45	18
MtN3.6	AC235677_9	AC235677_9.1	Mtr.43349.1.S1_at	841	1288	1439	1450	452	355	2683	814	594	518
MtN3.7	-	Medtr3g080990.1	Mtr.11905.1.S1_at	8	9	11	9	8	9	9	9	8	10
MtN3.8	-	Medtr5g067530.1	Mtr.21356.1.S1_at	13	13	12	13	11	10	13	13	15	2080
MtN3.9	-	-	Mtr.7064.1.S1_at	23	17	18	22	17	17	30	20	3073	53
MtN3.10	-	-	Mtr.42041.1.S1_at	18	30	1981	1508	14	153	29	17	16	436
MtN3.11	-	-	Mtr.7305.1.S1_at	20	19	22	28	16	21	28	93	1754	32
MtN3.12	-	-	Mtr.38292.1.S1_at	20	17	21	16	16	14	1385	123	15136	20
MtN3.13	-	-	Mtr.41025.1.S1_at	1780	3265	827	917	631	762	113	618	1317	2595
MtN3.14	-	-	Mtr.42164.1.S1_at	54	30	32	27	38	36	1797	3676	92	25
MtN3.15	Medtr7g005230.1	Medtr7g005710.1	-	-	-	-	-	-	-	-	-	-	-
MtN3.16	Medtr7g005250.1	Medtr7g005690.1	-	-	-	-	-	-	-	-	-	-	-
MtN3.17	Medtr7g005260.1	Medtr7g005650.1	-	-	-	-	-	-	-	-	-	-	-
MtN3.18	Medtr5g099910.1	Medtr5g092600.1	-	-	-	-	-	-	-	-	-	-	-
MtN3.19	Medtr3g124570.1	Medtr3g090950.1	-	-	-	-	-	-	-	-	-	-	-
MtN3.20	Medtr3g124590.1	Medtr3g090940.1	-	-	-	-	-	-	-	-	-	-	-
MtN3.21	Medtr3g109190.1	Medtr3g080990.1	-	-	-	-	-	-	-	-	-	-	-
MtN3.22	Medtr8g125450.1	Medtr4g106990.1	-	-	-	-	-	-	-	-	-	-	-

Sequences were obtained from www.phytozome.org, www.medicagohapmap.org and www.mtgea.noble.org, and were renamed MtN3.1-MtN3.22.

Regarding this criterion, one gene stood out as promising candidate for *Sym31*, namely a *MtN3*-like gene (Medtr3g098930.1), here named *MtN3.1*. This gene is specifically expressed in the nodule and most strongly in 4-day-old nodules (Mtr.20845.1.S1_at, according to MtGEA, Table 2). Because such young nodules typically have not yet formed a fixation zone, but do contain an active meristem as well as infection zone, this suggests that MtN3.1 is associated with early stages of symbiosome development (Moreau et al., 2011). This is supported by cell/tissue-specific transcriptome analyses of Medicago nodules via laser capture microdissection combined with Medicago affymetrix-microarray analyses, which show that *MtN3.1* is most specifically expressed in the infection zone of the nodule (Fig.3; Limpens et al., in preparation). This is the region where symbiosome formation begins (Fig.2A, D; Vasse et al., 1990). At the same locus in Medicago next to *MtN3.1*, a second *MtN3* homolog (MtN3.2a/b; Medtr3g098910.1) is located that does not appear to be expressed in nodules, but is highly expressed in flowers (Table 2).

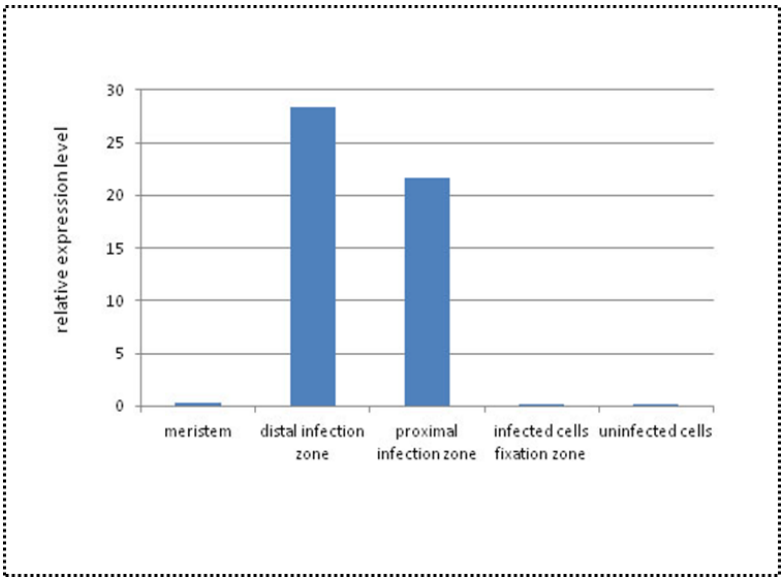

Fig.3. Relative expression pattern of *MtN3.1* based on microarray analyses of laser capture microdissected nodule tissues/cells. Note the specific expression of *MtN3.1* in the infection zone of Medicago nodules. The relative expression level represents the enrichment in a particular cell/tissue-type compared to the average of all other tissues.

MtN3.1 encodes a putative sucrose transporter

Medicago *N3.1* is part of a gene family that encode small transporter-like proteins (Pfam family: PF03083) containing seven transmembrane domains. It was recently discovered that these MtN3-like proteins, named after the founding member MtN3 (MtGEA Mtr.11146.1.S1_at; Table 3) identified as a nodule-specific EST in Medicago (Gamas et al., 1998) represent a new class of sugar transporters, called SWEET proteins in Arabidopsis that are able to import and export sugars from cells (Chen et al., 2010). Based on a phylogenetic analysis, MtN3.1 belongs to clade III of the SWEET family proteins (Fig.5) that function as low-affinity sucrose transporters (Chen et al., 2012). This suggests that *MtN3.1* also encodes a nodule-specific sucrose transporter that may play an important role in symbiosome differentiation. A list of

identified *MtN3* homologs in Medicago and their corresponding expression profiles are given in Table 3. Further phylogenetic analysis, including additional close relatives of MtN3.1 from various sequenced plant genomes, showed that MtN3.1 is not legume-specific and suggested that MtN3.1 is most closely related to AtSWEET10 (Fig.6). Analysis of close MtN3.1 homologs from soybean (Fig.6) showed that their genomic locations, which are additionally duplicated in the allotetraploid soybean genome, are indeed syntenic with the Medicago region (data not shown). However, none of these putative orthologs show a nodule-specific/enhanced expression profile according to the Soybean Genetics and Genomics Database (http://soybase.org/gb2/gbrowse/gmax1.01/), which includes soybean gene expression atlas data (Severin et al., 2010).

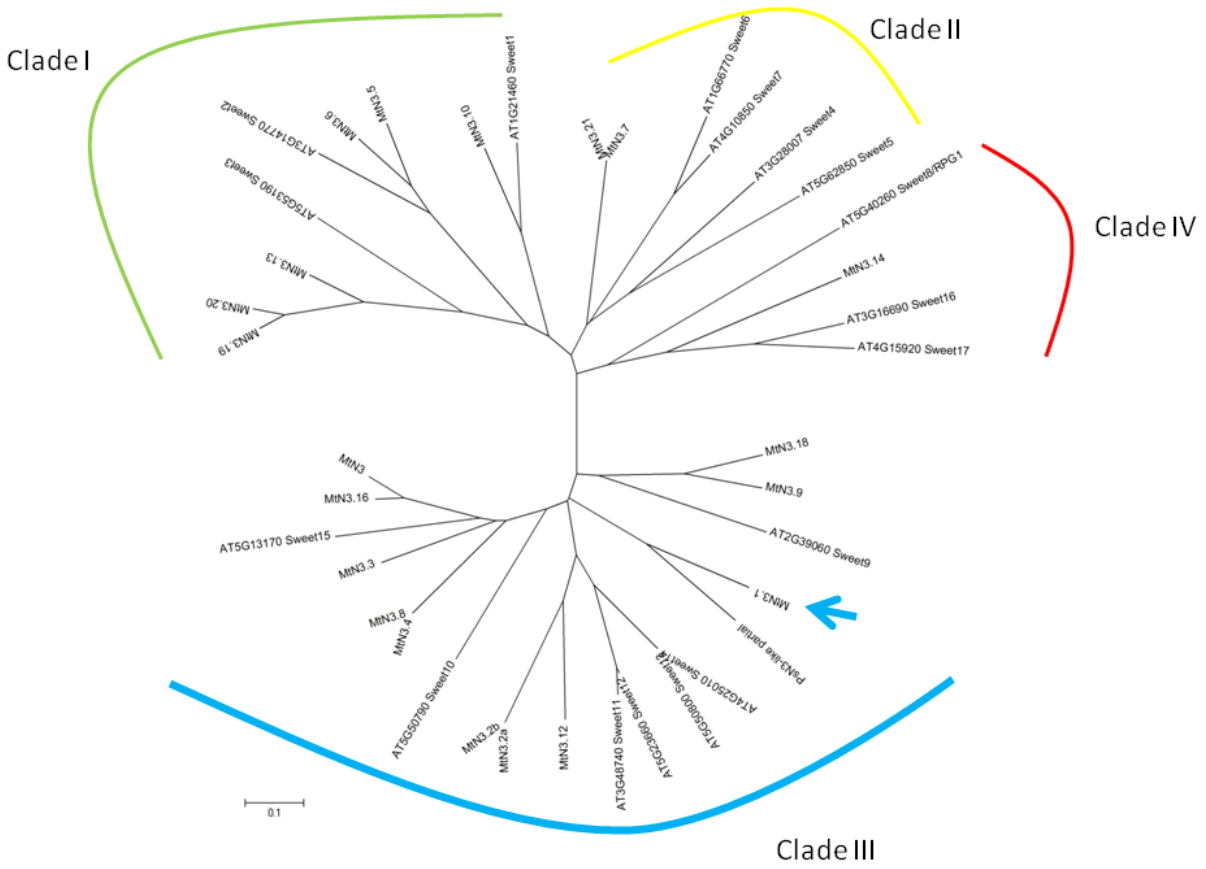

Fig.4. Phylogenetic tree of Medicago N3-like and Arabidopsis SWEET-like proteins. Corresponding Medicago identifiers are listed in Table 3. Arabidopsis SWEET proteins were retrieved from NCBI (www.ncbi.nlm.nih.gov), according to Chen et al., 2010. Protein sequences were aligned using Mega4.0 using default settings and an unrooted neighbour joining tree was generated. Note that MtN3.1 falls into clade III, which represent putative sugar/sucrose transporters.

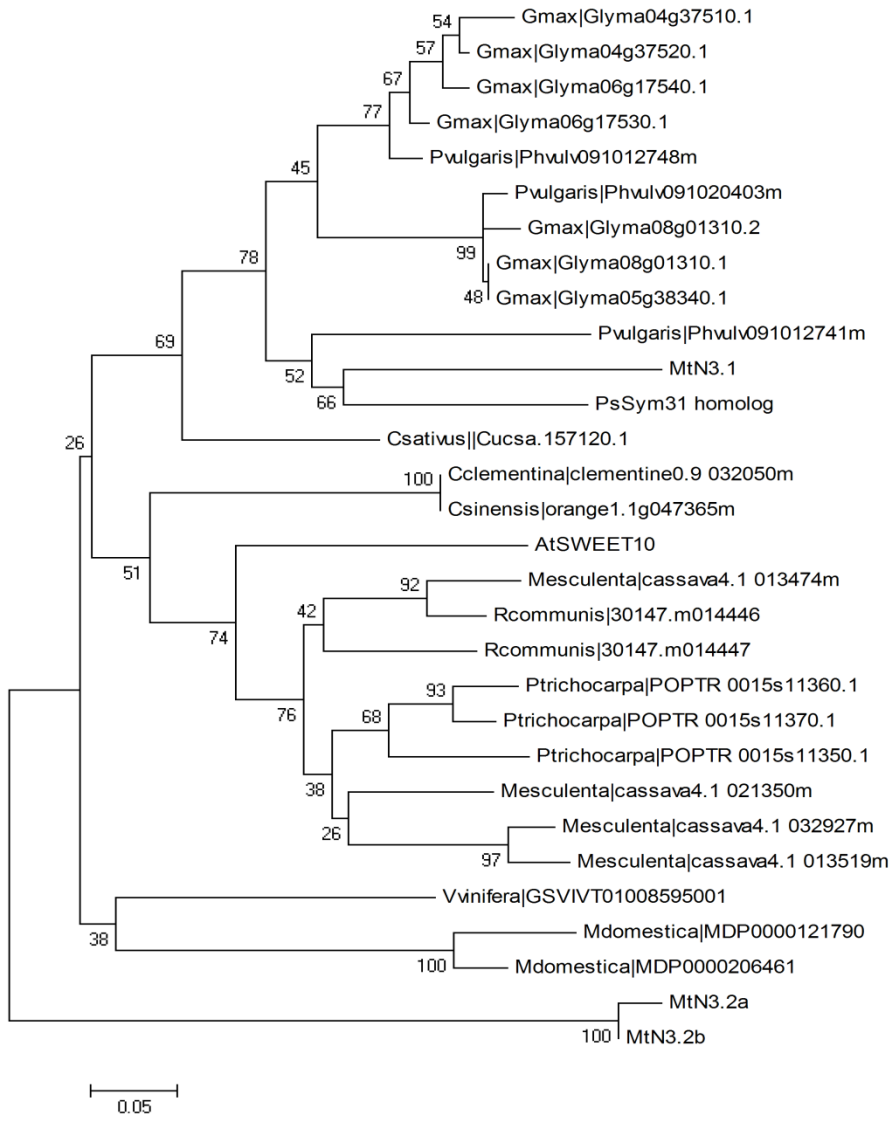

Fig.5. Phylogenetic analysis of MtN3.1 homologs. Protein sequences were obtained from Phytozome v.8.0 (www.phytozome.org). MtN3.2 was used as outgroup. Protein sequences were aligned using Mega4.0 using default settings and an mid-point rooted neighbor-joining tree was generated. The tree displays percentage of bootstrap values (1000 repetitions).

MtN3.1 functional analysis

To determine whether *PsSym31* encodes an MtN3/SWEET protein, we tried to amplify the pea ortholog of *MtN3.1* by PCR on genomic DNA (and nodule cDNA) of *sym31* (Sprint2Fix$^-$) and WT (Sprint2) using various primer combinations based on the Medicago sequence. However, we managed to amplify only a partial *MtN3.1*-like sequence from pea and were not able to obtain a full-length genomic product. As shown in Fig.5 the encoded protein fragment is indeed closely related to MtN3.1. Quantitative RT-PCR analysis showed that the identified *MtN3.1* homolog in pea is also specifically induced in nodules when compared to uninoculated roots (Fig.6). Furthermore, in the *Pssym31* nodules this gene is still expressed and even shows a ~5x higher expression level when compared to WT nodules 16 days after inoculation (Fig.6). Sequence analysis of the partial fragment covering exon 3 (partial) through exon 6 (partial), did not detect a mutation between Sprint2Fix$^-$ and the WT. As an alternative strategy, we decided to

test whether MtN3.1 plays a role in symbiosome development in Medicago. Therefore, we screened Medicago *Tnt1*-insertion populations to identify *Tnt1*-retrotransposon insertions in *MtN3.1* (Tadege et al., 2008). Screening the *Tnt1*-insertion population identified three *MtN3.1 Tnt1*-tagged lines: NF4654, NF14386, and NF12718, in the Medicago R108 genetic background, most likely representing the *MtN3.1* ortholog based on reciprocal BLAST analyses. Sequence analysis showed that NF4654 contains a *Tnt1* insertion in intron 3 of *MtN3.1*. NF14386 contains a *Tnt1* insertion in the first intron of *MtN3.1*. NF12718 contains an insertion in exon 3 of *MtN3.1*. The obtained T0 seeds were germinated, genotyped by PCR analysis and heterozygous insertion lines were identified. These lines were selected to identify homozygous insertion lines in the next generation. Based on PCR analyses, homozygous insertion lines were identified for NF4654 and NF14386, however, (due to the low number of available seeds) a homozygote insertion in NF12718 was not yet identified. Since NF12718 contains an insertion in an exon, this line would be the most promising to identify a possible mutant nodulation phenotype. Future characterization (including backcross analyses to remove additional *Tnt1* insertions) of these homozygous insertion lines will reveal whether this putative sucrose transporter is required for symbiosome development.

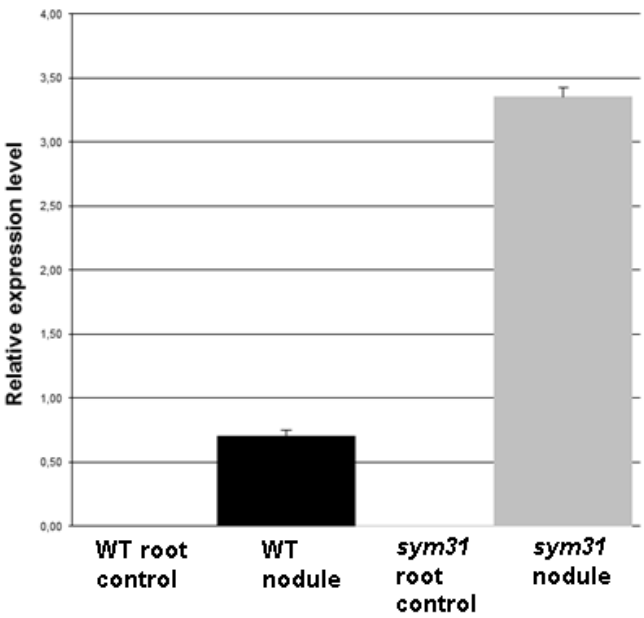

Fig.6. Relative expression of the pea *Sym31* candidate *PsN3.1* in pea wild-type and *sym31* 16 day-old nodules, compared to non-inoculated roots

DISCUSSION

The extensive synteny between Medicago and pea allowed us to delineate the *sym31* locus to a corresponding 450 kb syntenic region on Medicago chromosome 3. Based on the assumption that the gene controlling symbiosome differentiation should be (specifically) upregulated in the nodule, one candidate, *MtN3.1*, was identified. So far, the vast majority of

proteins that have been shown to be essential for symbiosome formation or development show a nodule-specific/enriched expression. These include for example the Nod factor signalling genes *IPD3* (Messinese et al., 2008; Ovchinnikova et al., 2011) and *DMI2* (Limpens et al., 2005), the symbiotic remorin *SYMREM1* (Lefebvre et al., 2010), the AP2/ERF transcription factor *EFD* (Vernie et al., 2008), the nodule-specific signal peptidase subunit *DNF1* (Wang et al., 2010), and the NCR peptide-encoding genes involved in symbiosome differentiation (Van de Velde et al., 2010).

MtN3.1 is a member of the clade III of SWEET sugar transporter proteins (Fig.5; Chen et al., 2010). Members of this clade in Arabidopsis, SWEET10-15, in addition to their ability to import and export sugars, were shown to export sucrose to the apoplast (Chen et al., 2012). Furthermore, clade III genes are identified as key targets for biotrophic pathogens. For example, the bacterial pathogen *Xanthomonas oryzae* secretes effector proteins via the type III secretion system that bind directly to SWEET promoters in rice, activating their transcription (Yang et al., 2006; Antony et al., 2010; Chen et al., 2010). Mutations in effector-binding sites of the SWEET promoters result in resistance to *X. oryzae*, suggesting that sugar supply becomes a limiting factor to the bacteria. Similarly, infection by *Pseudomonas syringae* induces the expression of various SWEET genes in Arabidopsis leaves in a type III system dependent manner (Chen et al., 2010). Furthermore, bacterial and fungal pathogens induce different sets of SWEET genes, indicating pathogen-specific roles/requirements.

In line with these data, we suggest that *PsSym31/MtN3.1* is induced in the infection zone of the nodule to transport sugars (or sucrose) across the symbiosome membrane to the developing bacteroids. The inside of a symbiosome indeed represents an apoplastic location as the symbiosome membrane has a plasma membrane identity (Catalano et al., 2004; Limpens et al., 2009). Whether MtN3.1 is indeed able to transports sugars or sucrose remains to be verified using the sugar/sucrose sensors developed by Chen et al. (2010, 2012) and by studying its subcellular localization in the nodule cells. The delivery of sugars may be required to fuel the growth of bacteroids when they shut down several metabolic pathways when they switch to differentiation (White et al., 2007). However, the fact that symbiosomes/bacteroids do multiply and fill the infected cells indicates that the bacteria are able to acquire sufficient carbon sources before switching to differentiation.

In many studies, it has been shown that sugars are not actively transported across the symbiosome membrane, but that dicarboxylates, especially malate, are the main delivered carbon source (Udvardi and Day, 1997; Day et al., 2001; White et al., 2007). However, it should be noted that all studies on sugar transport across the symbiosome membrane have been performed with differentiated symbiosomes from the fixation zone of mature nodules. The transport capacity of juvenile symbiosome membranes is unknown. Localization of MtN3.1 to the developing symbiosomes in the infection zone could give a first indication. Besides *MtN3.1*,

at least two additional *MtN3* genes (Mtr.42041.1.S1_at and Mtr.11146.1.S1_at) show nodule enhanced expression in comparison with uninoculated roots. Based on the cell/tissue-specific transcriptome analyses, transcripts of these MtN3 proteins would be predicted to be most strongly expressed in the uninfected cells, likely to export sucrose to the infected cells. The founding family member *MtN3* (Mtr.11146.1.S1_at) shows a specific expression in 4-day-old nodules (Gamas et al., 1998), however, its expression domain in mature nodules is currently unknown. Possibly, it could act redundantly with MtN3.1 in the infection zone of the nodule. Indeed, redundancy among the SWEET proteins has been shown in Arabidopsis (Chen et al., 2012).

Our phylogenetic analysis indicated that *MtN3.1* is not a legume-specific gene and it is strikingly different from *MtN3.2*, which locates next to *MtN3.1* on the Medicago BAC clone AC146747. Analysis of the *MtN3.1*-syntenic region in soybean, which also contains multiple MtN3.1 homologs, indicated that none of these soybean homologs has a nodule specific/enhanced expression pattern. Therefore, the nodule-specific expression of *MtN3.1* and its close homolog in pea may be specific for the IRLC-class of legumes, to which both Medicago and pea belong and which are characterized by the terminal differentiation of the bacteroids (Mergaert et al., 2003; Oono et al., 2010). In non-IRLC legumes such as soybean, the bacteroids do not terminally differentiate and interestingly, multiple bacteroids can be found within a single symbiosome membrane similar to what is observed in *sym31* nodules (Borisov et al., 1997). Therefore, the nodule-enhanced expression of *MtN3.1* may be an adaption to facilitate the terminal differentiation of bacteria.

Given that rhizobia acquired the ability to form a symbiotic interface from the ancient arbuscular mycorrhiza (AM) (Maillet et al., 2011; Op den Camp et al., 2011; Ivanov et al., 2012), it is tempting to speculate that AM fungi also use SWEET sugar transporters to acquire carbohydrates from the plant. In line with this idea, the induction of two SWEET genes (Mtr.42041.1.S1_at and Mtr.7305.1.S1_at.) has been shown in mycorrhized roots (Hogekamp et al., 2011).

An alternative scenario by which MtN3.1 could control symbiosome differentiation can be envisioned through its influence on carbon metabolism in the nodule cells, which may affect the glycosylation of proteins involved in symbiosome development. Low levels of ononitol (soluble carbohydrate) in *sym31* nodules compared to wild-type nodules have led to the suggestion that carbon metabolism is altered (Romanov et al., 1995, 1997). Such a scenario could explain the finding that the appearance of a lectin-like glycoprotein isoform, PsNLEC-1 in the symbiosomes was impaired in *Pssym31*. In wild-type nodules, three PsNLEC-1 isoforms were detected, two of which were associated with symbiosomes. In *sym31* nodules, only one isoform could be detected that localized to the vacuoles. Therefore, it was suggested that *sym31* was impaired in vesicle trafficking to the symbiosomes (Dahiya et al., 1998). However, it could be that the

specific isoforms that accumulate at the symbiosomes represent different glycosylated versions. Impaired glycosylation of PsNLEC-1 could explain the lack of detection of the symbiotic isoforms.

In conclusion, we propose that sugar/sucrose transport plays an important role in symbiosome/bacteroid differentiation to allow a successful nitrogen-fixing symbiosis. However, this aspect of the symbiosis requires further investigation. The ultimate prove for the involvement of *MtN3.1* in symbiosome development and the identification of its ortholog *Sym31* in pea, awaits further experimentation.

MATERIALS AND METHODS

Plant lines, bacterial strains, and growth conditions

The homozygous mutant line Sprint2Fix$^-$ (*sym31*) in the genetic background Sprint2 (Borisov et al., 1992, 1997) was used for evaluation of symbiotic mutant phenotype. In addition, pea wild-type lines NGB1238, NGB831, and SGE were used to create the segregating populations for genetic mapping.

Rhizobium leguminosarum bv. *viciae* strain CIAM1026 (Safronova and Novikova, 1996) was used to inoculate plants.

Pea seeds were surface-sterilized with concentrated sulfuric acid for 10 min at room temperature. Germinated seeds were planted in plastic pots (diameter of 19 cm) containing perlite and inoculated with rhizobia after 7 days. Plants were supplied with nitrogen free nutrient solution as described in Borisov et al. (1997).

Table 1. Mapping populations used for *PsSYM31* map-based cloning

Generation	Cross name	Number of plants
F2	♀NGB1238 x ♂Sprint2Fix$^-$	75 plants: 52 Fix$^+$/23 Fix$^-$
F2	♀SGE x ♂Sprint2Fix$^-$	115 plants: 88 Fix$^+$/27 Fix$^-$
F2	♀NGB851 x ♂Sprint2Fix$^-$	65 Fix$^-$ plants

Data collection and statistical analysis

F2 populations of the crosses (Table 1) and parental lines were analyzed in nitrogen free conditions to segregate mutant and WT nodule phenotypes: Fix$^-$ white nodules versus Fix$^+$ pink nodules. Plants were analyzed at 28-30 days after inoculation by CIAM1026. Total DNA was extracted from leaves of each analyzed plant individually using the standard cetyltrimethylammonium bromide (CTAB) method (Rogers and Bendich, 1985).

X^2 analysis ($\chi^2 > 3.84$ for independent assortment) was used to determine the significance of linkage between the *sym31* Fix- phenotype and molecular markers (see Table 2) using SigmaStat 2.3 for Windows (SPSS Inc., Chicago, IL, USA).

Synteny-based mapping

The CAPS molecular markers used in the co-segregation analysis are listed in Table 2. The following genotyping conditions were used: **MAX4** (PCR annealing temperature 55ºC, restriction endonuclease Hpy188I), forward primer (F)–AGGTGGCAAGTGTGGAAGTG, reverse primer (R)–AACTTAGCCCTAGCAACCTCTTC; **GRP** (55ºC; HinfI, NlaIII) (F)–TATATCTACTGCGTCAAGCTCAATGG, (R)–CCCAACCAATTACATTTACCTAGTTTATTC; **C13** (52ºC; NlaIII, HpaII) (F)– CAGAAACTTTGCACCAACAATATGAATTG; (R)–GTTTTATGCTGTCATCTATATGCAATCTG; **M12** (57ºC; size) (F)–GTACATAGAACAGGGTTTTGCAAAGTTG, (R)–TCCCCAAACATTCAAGGATAGTACTCC; **AmyI** (55ºC, TagI) (F)– ATACTAGTATAAGAGCTTTGCGGTCGAGG, (R)–CTAAAGTGATCACCCTTCCTTGCATCTAACT; **SBP** (58ºC, HaeIII) (F)–GACAAACAAGATCTTTTTCTCGGCTCTACTGCGG, (R)–GAAATAGTTGAGGTGCATCATTGCCTTGTGA; **UbE2** (58ºC; BstUI, AvaII, TagI) (F)–GGCACTTACTCTGAAGACTGCACTACTTTC, (R)–GAGCTTCAGGAAATCCCATCTCAACCAGTT; **Uni** (60ºC; TagI, MaeII) (F)–TGCACCATCTCCCCGTCCCCAGC, (R)–AGCAGCACCGTTCCTCTCCGCGT; **ERCD** (55ºC, HinfI) (F)–AATCACCAAGACCATCACAGAATAAG, (R)–GTCAAAGAAATATGGCCCATCTCT; **ClF** (55ºC, TasI) (F)–TGCCTTCGTCATTAAAATGCCAACTCT, (R)–CTGCCTTGTAGTAGTCAGATACCC; **P450** (55ºC; RsaI, NlaIII) (F)–CTTAGCACTTCTTGAATCACCATAGTCACC, (R)–GGAGTAACTGAAATTTCGGACGAAGAAGG; **PMK** (55ºC, AciI) (F)–ATGGCAAAAGTCTGACCCT, (R)–GAACACCTGCAGCCTCACCCA; **chC** (55ºC, HaeIII) (F)–GCAGAAATTGAAACATTGTTGATGAAGG, (R)–CTATAGAACATCAAATGCTACTTATTTCC; **Chap** (55ºC, AluI) (F)–ATGGAGTTGTTGTGTTGGCTGGAT, (R)–ATTGCTTCATCATCAAAACCCCATTGG; **Bor** (55ºC, AvaII) (F)–ACTGGTCTCGTCGGAGCACC, (R)–GATGTCTTAATGATGTGCAATCGACC.

Nodule tissue fixation, staining, and microscopy

Nodule tissues were fixed in 5% glutaraldehyde (v/v) with 3% sucrose (w/v) in 0.1 M phosphate buffer (pH 7.2) under vacuum for 1-2 hours, followed by washing phosphate buffer and water for 15 min each. Then, dehydrated using an ethanol series: 10%, 30%, 50%, 70%, 90%, and 100%, 10 min each. The dehydrated nodules were embedded in Technovit 7100 (Heraeus-Kulzer, Wehrheim, Germany) according to the manufacturers protocol and sectioned on a RJ2035 microtome (Leica Microsystems, Rijswijk, The Netherlands).

Semi-thin nodule sections (5 µm) were stained with 0.05% toluidine blue solution and analyzed using a DM5500B microscope equipped with a DFC425C camera (Leica Microsystems, Wetzlar, Germany).

Database searches and phylogenetic analysis

Phylogenetic analyses were conducted using MEGA version 4.0.2 (Tamura, Dudley, Nei, and Kumar 2007). A multiple protein alignment was made using default parameters: gap opening, 10.00; gap extension, 0.20; residue-specific penalties, on; hydrophilic penalties, on; gap separation distance, 4; end gap separation, off; negative matrix, off; delay divergent sequences, 30%; protein weight matrix, Gonnet Series. From this alignment a midpoint-rooted neighbor-joining tree with bootstraps values (1000

replicates) or an unrooted circle diagram was drawn. Sequences were obtained from Phytozome v.8.0 (www.phytozome.org), MtGEA (www.mtgea.noble.org) and NCBI (www.ncbi.nlm.nih.gov).

Expression values were obtained from the Medicago Gene Expression Atlas (www.mtgea.noble.org).

A detailed description and report on the cell-/tissue-specific transcriptome data from Medicago nodules via laser capture microdissection using Medicago Affymetrix Arrays is *in preparation* (Limpens et al., unpublished). Briefly, 3-week old Medicago nodules were fixed in farmer's fixative and embedded in Paraffin. 8 µm sections were deparaffinized using xylene, air-dried and used for laser capture microdissection using an Arcturus PixCell II LCM (Arcturus). For each tissue/cell-type 3 biological replicates each consisting of ~50 cells pooled from 8 consecutive sections were collected and used for RNA isolation using the Qiagen RNeasy micro kit (Qiagen) in the presence of 50 ng poly-I as carrier. The isolated RNA was amplified using the two-round TargetAmp™ aRNA Amplification Process (Epicentre Biotechnologies) as specified by the manufacturer. Quantity and quality of total RNA as well as T7-amplified aRNA was checked via capillary electrophoresis in RNA pico and nano chips, respectively, using an Agilent 2100 bioanalyzer (Agilent). Affymetrix GeneChip Medicago genome array hybridizations were performed according to Hogekamp et al. (2011). Data analysis was performed according to Liu et al. (2011).

Tnt1-retrotransposon insertion screening in *MtN3.1*

The MtN3.1 *Tnt1*-insertion lines, NF4654, NF14386 and NF12718, were isolated by PCR-screening of a *Tnt1*-insertional population of *M. truncatula* genotype R108 (Tadege et al., 2008). The screen was carried out using primers N3-F: AGGAGACACAGTGTATGCA and Tnt1-F: TCCTTGTTGGATTGGTAGCCAACTTTGTTG with ExTaq DNA Polymerase (TaKaRa) in DNA pools of 500, 100, 10 to reach single plants. PCR-amplified fragment were sequenced to identify the exact insertion site of the 5.3-kb *Tnt1* retrotransposon. The resulting T0/T1 seeds were germinated, heterozygote insertion lines selected and selfed. The following primers were used to genotype the insertion lines: MtN3-F3 GTGGGTAGGCCCGCAAACAT; MtN3-TntR ACAAGTGTAAAGAAAGGACCGAAGA; NF12718-F ATCTCTTGTATGACCTTCCTCGCT; NF14386-RACTGTTGCTCTTGTTGGGTAATG.

Quantitative RT-PCR

Quantitative RT-PCR was conducted on RNA isolated from roots and 16-day-old pea *sym31* and WT nodules of plants grown in perlite (Limpens et al. 2009). Total RNA was isolated and DNAse treated using the Plant RNeasy kit (Qiagen, Basel, Switzerland) according to the manufacturer's instructions. cDNA was synthesized from 1 µg of total RNA using the Taqman Gold RT-PCR kit (Perkin-Elmer Applied Biosystems) in a total volume of 50 µl using random hexamer primers (10 min at 25°C, 30 min at 48°C, and 5 min at 95°C). Quantitative PCR reactions were performed in (technical) triplicate on 1 µl of cDNA on three independent biological repetitions using the Quantitative PCR Core kit for SYBR Green I (Eurogentec), and real-time detection was performed on a MyiQ (Bio-Rad) (40 cycles of 95°C for 10 s and 60°C for 1 min) followed by a heat dissociation step (from 65 to 95°C). Primers were used at a final concentration of 300 nM. *Ubiquitin* was used as reference gene, primers: forward-

ATGCAGATCTTTTGTGAAGAC and reverse-ACCACCACGGAAGACGGAG. The qPCR primers used for *PsN3.1* were forward-TGGACTTGTGGTGGAATCAA and reverse-ACAAGCATTGCTCCAAATCC.

REFERENCES

Alunni, B., Kevei, Z., Redondo-Nieto, M., Kondorosi, A., Mergaert, P., Kondorosi, E. (2007) Genomic organization and evolutionary insights on *GRP* and *NCR* genes, two large nodule-specific gene families in *Medicago truncatula*. *Mol. Plant-Microbe Interact.*, 9: 1138–1148.

Antony, G., Zhou, J., Huang, S., Li, T., Liu, B., White, F., Yang, B. (2010) Rise *xa13* Recessive Resistance to Bacterial Blight Is Defeated by Induction of the Disease Susceptibility Gene *Os-11N3*. *Plant Cell*, 22(11): 3864–3876.

Aubert, G., Morin J., Jacquin F.., Loridon K., Quillet M.C., Petit A., Rameau C., Lejeune-Hénaut I., Huguet T., Burstin J. (2006) Functional mapping in pea, as an aid to the candidate gene approach and for investigating the synteny with the model species *Medicago truncatula. Theor. Appl. Genet*, 112: 1024–1041.

Benedito, V.A., Torres-Jerez, I., Murray, J.D., Andriankaja, A., Allen, S., Kakar, K., Wandrey, M., Verdier, J., Zuber, H., Ott, T., Moreau, S., et al. (2008) A gene expression atlas of the model legume *Medicago truncatula*. *Plant J.,* 55(3): 504–513.

Borisov, A.Y., Morzhina, E.V,, Kulikova, O.A., Tchetkova, S.A., Lebsky, V.K., Tikhonovich, I.A. (1992) New symbiotic mutants of pea *(Pisum sativum* L.) affecting either nodule initiation or symbiosome development. *Symbiosis* 14: 297–313.

Borisov, A.Y., Rozov, S.M., Tsyganov, V.E., Morzhina, E.V., Lebsky, V.K., Tikhonovich, I. (1997) Sequential functioning of *Sym13* and *Sym31*, two genes affecting symbiosome development in root nodules of pea (*Pisum sativum* L). *Mol. Gen. Genet.,* 254: 592–598.

Brewin, N.J. (1996) Plant membrane structure and function in the Rhizobium-legume symbiosis. In: Smallwood, M., Knox, J.P., Bowles, D.J. (eds) Membranes: specialized functions in plants. *Bios Scientific Publishers*, Oxford, pp. 507–524.

Chen, L.Q., Hou, B.H., Lalonde, S., Takanada, H., Hartung, M.L., Qu, X.Q., Guo, W.J., Kim, J.G., Underwood, W., Chaudhuri, B., et al. (2010) Sugar transporters for intercellular exchange and nutrition of pathogens. *Nature* 468: 527–534.

Chen, L.Q., Qu, X.Q., Hou, B.H., Sosso, D., Osorio, S., Fernie, A.R., Frommer, W.B. (2012) Sucrose Efflux Mediated by SWEET Proteins as a Key Step for Phloem Transport. *Science* 335(6065): 207–211.

Craig, J., Barratt, P., Tatge, H., Dejardin, A., Handley, L., Gardner, C.D., Barber. L., Wang, T., Hedley, C., Martin, C., et al. (1999) Mutations at the *rug4* locus alter the carbon and nitrogen metabolism of pea plants through an effect on sucrose synthase. *Plant J.,* 17: 353–362.

Dahiya, P., Sherrier, D.J., Kardailsky, I.V., Borisov, A.Y., Brewin, N.J. (1998) Symbiotic Gene Sym31 Controls the Presenceof a Lectinlike Glycoprotein in the Symbiosome Compartment of Nitrogen-Fixing Pea Nodules. *Mol. Plant-Microbe Interact.,* 11(9): 915–923.

Ellis, T.H.N. and Poyser, S.J. (2002) An integrated and comparative view of pea genetic and cytogenetic maps. *New Phytol.,* 153: 17–25.

Gamas, P., de Billy, F., Truchet, G. (1998) Symbiosis-specific expression of two Medicago truncatula nodulin genes, *MtN1* and *MtN13*, encoding products homologous to plant defense proteins. *Mol. Plant-Microbe Interact.,* 11**:** 393–403.

Glazebrook, J., Ichige, A., Walker, G.C. (1993) A *Rhizobium meliloti* homolog of the *Escherichia coli* peptide-antibiotic transport protein SbmA is essential for bacteroid development. *Genes Dev.,* 7: 1485–1497.

Haag, A.F., Baloban, M., Sani, M., Kerscher, B., Pierre, O., Farkas, A., Longhi, R., Boncompagni, E., Hérouart, D., Dall'Angelo, S., et al. (2011) Bacterial resistance to legume antimicrobial peptides is essential for symbiosis. *PLoS Biol.* 9:e1001169. Published online.

Haliassos, A., Chomel, J.C., Tesson, L., Baudis, M., Kruh, J., Kaplan, J.C., Kitzis, A. (1989) Modification of enzymatically amplified DNA for the detection of point mutations. *Nucl. Acids Res.,* 17(9): 3606.

Hakoyama, T., Niimi, K., Watanabe, H., Tabata, R., Matsubara, J., Sato, S., Nakamura, Y., Tabata, S., Jichun, L., Matsumoto, T., et al. (2009) Host plant genome overcomes the lack of a bacterial gene for symbiotic nitrogen fixation. *Nature* 462: 514–517.

Hogekamp, C., Arndt, D., Pereira, P.A., Becker, J.D., Hohnjec, N., Küster, H. (2011) Laser microdissection unravels cell-type-specific transcription in arbuscular mycorrhizal roots, including CAAT-box transcription factor gene expression correlating with fungal contact and spread. *Plant Physiol.,* 157(4): 2023–2043.

Ivanov, S., Fedorova, E., Limpens, E., De Mita, S., Genre, A., Bonfante, P., Bisseling, T. (2012) *Rhizobium*–legume symbiosis shares an exocytotic pathway required for arbuscule formation. *PNAS*, 10.1073/pnas.1200407109. Published online.

Jones, K.M., Kobayashi, H., Davies, B.W., Taga, M.E., Walker, G.C. (2007) How rhizobial symbionts invade plants: The *Sinorhizobium*-Medicago model. *Nat. Rev. Microbiol.,* 5: 619–633.

Konieczny, A. and Ausubel, F.M. (1993) A procedure for mapping Arabidopsis mutations using co-dominant ecotype-specific PCR-based markers. *The Plant J.*, 4: 403–410.

Krusell, L., Krause, K., Ott, T., Desbrosses, G., Krämer, U., Sato, S., Nakamura, Y., Tabata, S., James, E.K., Sandal et al. (2005) The sulfate transporter SST1 is crucial for symbiotic nitrogen fixation in *Lotus japonicus* root nodules. *Plant Cell*, 17: 1625–1636.

Lefebvre, B., Timmers, T., Mbengue, M., Moreau, S., Hervé, C., Tóth, K., Bittencourt-Silvestre, J., Klaus, D., Deslandes, L., Godiard, et al. (2010) A remorin protein interacts with symbiotic receptors and regulates bacterial infection. *Proc. Natl. Acad. Sci. U.S.A.,* 107: 2343–2348.

Maillet, F., Poinsot, V., Andre, O., Puech-Pages, V., Haouy, A., Gueunier, M,, Cromer, L., Giraudet, D., Formey, D., Niebel, A., et al. (2011) Fungal lipo-chitooligosaccharide symbiotic signals in arbuscular mycorrhiza. *Nature* 469:58–63.

Maunoury, N., Redondo-Nieto, M., Bourcy, M., Van de Velde, W., Alunni, B., Laporte, P., Durand, P., Agier, N., Marisa, L., Vaubert, D., et al. (2010) Differentiation of symbiotic cells and endosymbionts in Medicago truncatula nodulation are coupled to two transcriptome-switches. *PLoS One,* 5(3): pp. e9519. Published online.

Moreau, S., Verdenaud, M., Ott, T., Letort, S., de Billy, F., Niebel, A., Gouzy, J., de Carvalho-Niebel, F., Gamas, P. (2011) Transcription reprogramming during root nodule development in *Medicago truncatula*. *PLoS One*, 6: e16463.

Maróti, G., Kereszt, A., Kondorosi, E., Mergaert, P. (2011) Natural roles of antimicrobial peptides in microbes, plants and animals. *Res. Microbiol.,* 162: 363–374.

Men, A.E., Borisov, A.Y., Rozov, S.M., Ushakov, K.V., Tsyganov, V.E., Tikhonovich, I.A., Gresshoff, P.M. (1999) Identification of DNA amplification fingerprinting (DAF) markers close to the symbiosis-ineffective *sym31* mutation of pea (*Pisum sativum* L.). *Theor. Appl. Genet.*, 98: 929–936.

Mergeart, P., Uchiumi, T., Alunni, B., Evanno, G., Cheron, A., Catrice, O., Mausset, A.E., Barloy-Hubler, F., Galibert, F., Kondorosi, A., Kondorosi, E. (2006) Eukaryotic control on bacterial cell cycle and differentiation in the Rhizobium–legume symbiosis. *PNAS*, 103(13): 5230–5235.

Mitra, R.M. and Long, S.R. (2004) Plant and bacterial symbiotic mutants define three transcriptionally distinct stages in the development of the *Medicago truncatula*/*Sinorhizobium meliloti* symbiosis. *Plant Physiol.,* 134: 595–604.

Oldroyd, G. E., Murray, J. D., Poole, P. S., Downie, J. A. (2011) The rules of engagement in the legume-rhizobial symbiosis. *Annul. Rev. Genet.,* 45: 119–144.

Oono, R., Schmitt, I., Sprent, J.I., Denison, R.F. (2010) Multiple evolutionary origins of legume traits leading to extreme rhizobial differentiation. *New Phytol.,* 187: 508–520.

Op den Camp, R., Streng, A., De Mita, S., Cao, Q., Polone, E., Liu, W., Ammiraju, J.S.S., Kudrna, D., Wing, R., Untergasser, A., et al. (2011) LysM-Type Mycorrhizal Receptor Recruited for Rhizobium Symbiosis in Nonlegume *Parasponia. Science*, 331(6019): 909–912.

Ott, T., van Dongen, J. T., Gunther, C., Krusell, L., Desbrosses, G., Vigeolas, H., Bock, V., Czechowski, T., Geigenberger, P. & Udvardi, M. K. (2005) Symbiotic leghemoglobins are crucial for nitrogen fixation in legume root nodules but not for general plant growth and development. *Curr. Biol.*, 15(6): 531–535.

Patriarca, E.J., Tate, R., Iaccarino, M. (2002) Key role of bacterial NH_4^+ metabolism in *Rhizobium*-plant symbiosis. *Microbiol. Mo.l Biol. Rev.,* 66: 203–222.

Peiter, E. and Schubert, S. (2003) Sugar uptake and proton release by protoplasts from the infected zone of *Vicia faba* L. nodules: evidence against apoplastic sugar supply of infected cells. *J. Exp. Bot.,* 54: 1691–1700.

Prell, J., White, J. P., Bourdes, A., Bunnewell, S., Bongaerts, R. J., Poole, P. (2009) Legumes regulate *Rhizobium* bacteroid development and persistence by the supply of branched-chain amino acids. Proc. Natl. Acad. Sci. U.S.A., 106: 12477–12482.

Romanov, V.I., Gordon, A.J., Minchin, F.R., Witty, J.F., Skøt, L., James, C.L., Borisov, A.Y., Tikhonovich, I.A. (1995) Anatomy, physiology and biochemistry of root nodules of Sprint-2Fix$^-$, a symbiotically defective mutant of pea (*Pisum sativum* L.). *J. Exp. Bot.,* 46: 1809–1816.

Rozov, S.M., Borisov, A.Y., Tsyganov, V.E., Men, A.E., Tikhonovich, I.A. (1995) Mapping of pea (*Pisum sativum* L.) genes affecting symbiosis. In: Tikhonovich, I.A., Provorov, N.A., Romanov, V.I., Newton, W.E. (eds) Nitrogen fixation: fundamentals and applications*, Kluwer Academic Publishers*, Dordrecht, p. 489.

Roth, L.E. and Stacey, G. (1989) Bacterium release into host cells of nitrogen-fixing soybean nodules: the symbiosome membrane comes from three sources. *Eur. J. Cell Biol.,* 49:13–23.

Severin A.J., Woody, J.L., Bolon, Y., Joseph, B., Diers, B.W., Farmer, A.D., Muehlbauer, G.J., et al. (2010) RNA-Seq Atlas of *Glycine max*: A guide to the soybean transcriptome. *BMC Plant Biology,* 10: 160.

Sherrier, D.J., Borisov, A.Y., Tikhonovich, I.A., Brewin, N.J. (1997) Immunocytological evidence for abnormal symbiosome development in nodules of the pea mutant line Sprint2Fix⁻ (*sym31*). *Protoplasma* 199: 57–68.

Soupène, E., Foussard, M., Boistard, P., Truchet, G., Batut, J. (1995) Oxygen as a key developmental regulator of *Rhizobium meliloti* N2-fixation gene expression within the alfalfa root nodule. *Proc. Natl. Acad. Sci. U.S.A.,* 92: 3759–3763.

Tadege, M., Wen, J., He, J., Tu, H., Kwak, Y., Eschstruth, A., Cayrel, A., Endre, G., Zhao, P.X., Chabaud, M., et al. (2008) Large-scale insertional mutagenesis using the Tnt1 retrotransposon in the model legume *Medicago truncatula*. *Plant J.,* 54(2): 335–347.

Udvardi, M.K. and Day, D.A. (1997) Metabolite transport across symbiotic membranes of legume nodules. *Annul. Rev. Plant Physiol. Plant Mol. Biol.,* 48: 493–523.

Van de Velde, W., Zehirov, G., Szatmari, A., Debreczeny, M., Ishihara, H., Kevei, Z., Farkas, A., Mikulass, K., Nagy, A., Tiricz, et al. (2010) Plant peptides govern terminal differentiation of bacteria in symbiosis. *Science* 327: 1122–1126.

Vasse, J., de Billy, F., Camut, S., Truchet, G. (1990) Correlation between ultrastructural differentiation of bacteroids and nitrogen fixation in Alfalfa nodules. *J. Bacteriol.,* 172: 4295–4306.

Wang, D., Griffitts, J., Starker, C., Fedorova, E., Limpens, E., Ivanov, S., Bisseling, T., Long S.R. (2010) A nodule-specific protein secretory pathway required for nitrogen-fixing symbiosis. *Science* 327: 1126 – 1129.

White, J., Prell, J., James, E. K., Poole, P. (2007) Nutrient sharing between symbionts. *Plant Physiol.*, 144: 604–614.

Whitehead, L. F. and Day, D. A. (1997) The peribacteroid membrane. Physiol. Plant.,100: 30–44.

Wojciechowski, M. F., Lavin, M., Sanderson, M. J. (2004) A phylogeny of legumes (*Leguminosae*) based on analysis of the plastid *matK* gene resolves many well-supported sublcades within the family. *Am. J. Bot.,* 91:1846–1862.

Young, N.D., Debellé, F., Oldroyd, G.E., Geurts, R., Cannon. S.B., Udvardi. M.K., Benedito. V.A., Mayer, K.F.X., Gouzy, J., Schoof, H., et al. (2011) The *Medicago* genome provides insight into the evolution of rhizobial symbioses. *Nature* 480: 520-524.

Yang, B., Sugio, A., White. F.F. (2006) *Os8N3* is a host disease-susceptibility gene for bacterial blight of rice. *Proc. Natl. Acad. Sci. U.S.A.,* 103: 10503–10508.

Yurgel, S.N. and Kahn, M.L. (2004) Dicarboxylate transport by rhizobia. *FEMS Microbiol. Rev.,* 28: 489–501.

Chapter 6

Summarizing discussion

The nitrogen-fixing symbiosis between legumes and rhizobia plays an important role in natural and agricultural systems as it provides the most important source of biologically fixed nitrogen. At the heart of this symbiosis, the rhizobia are accommodated as nitrogen-fixing organelles, called symbiosomes. Symbiosome formation is a crucial step to establish an efficient nitrogen-fixing symbiosis, and it involves the formation of new membrane compartments inside root nodule cells where the bacteria differentiate into specialized nitrogen-fixing forms, called bacteroids (Jones et al., 2007). Therefore, understanding how these novel organelles are made is a matter of vital importance to fully exploit the potential of this symbiosis in agriculture. The major goal of the research described in this thesis was to identify plant components that control this key step in the symbiosis. At the start of the research, the most extensive and morphologically best-characterized set of plant mutants disturbed in symbiosome formation and development, was available in pea (Borisov et al., 2007). However, positional cloning in pea is severely hampered by its large genome size (~5000 Mb), difficulties in genetic transformation, and lack of extensive genomics tools. Therefore, we adopted a synteny-based cloning strategy using *Medicago truncatula* (Medicago) as intergenomic cloning vehicle. In the last decade, Medicago has been developed as a model legume, and many genomics tools are now available, including a sequenced genome (Young et al., 2011). Furthermore, pea and Medicago are taxonomically closely related, and their genomes have been shown to be highly syntenic (Choi et al., 2004; Aubert et al., 2006). This extensive synteny offered an efficient strategy to clone pea genes using the Medicago genome as reference. In this thesis, we focused on three mutants that are most strongly impaired in their ability to form symbiosomes; *sym33* and *sym41* in pea and *sym1* in Medicago, as well as pea *sym31* where symbiosomes fail to differentiate. Here, we summarize our results on the identification of the underlying genes and discuss our current insight into symbiosome formation and development.

Medicago as intergenomic cloning vehicle

To facilitate the identification of pea symbiotic genes we first developed a set of tools to exploit the wealth of genomic information available in Medicago (Chapter 2). Therefore, we developed a set of gene-based cross-species PCR markers, which link the Medicago and pea genetic maps, and which are suitable for the various genotypes used in our studies. The identification of single/low copy genes in the Medicago genome and amplification of corresponding pea sequences using primers based on the Medicago sequences, proved to be an efficient strategy to develop gene-based cross-species markers (Aubert et al., 2006). Thus, ~50% of the primers developed based on conserved sequences in the Medicago genes allowed the amplification of corresponding gene fragments in pea. Targeting intron-spanning regions

gave the highest probability to identify polymorphisms in the genetically distant genotypes used in the segregation analyses. This strategy allowed us to delineate the location of all three pea mutants and to identify the corresponding syntenic regions in Medicago. The similar block in symbiosome formation, i.e. no release of the rhizobia from the infection threads, and syntenic locations of the mutant loci *Pssym33* and *Mtsym1*, suggested that both were mutated in an orthologous gene. Previous studies had shown that similar phenotypes in combination with syntenic map positions in legume model species offer a powerful strategy to identify the corresponding pea genes. For example, such strategies were successfully used to identify the pea Nod factor signalling genes *PsSym19* (Endre et al., 2002; Stracke et al., 2002), *PsSym35* (Borisov et al., 2003), and *PsSym37* (Zhukov et al., 2008). However, in the case that a model legume mutant with a comparable phenotype and corresponding map-position is not available, identification/testing of candidate genes for a particular pea mutant is less straightforward because a pea genome and extensive EST sequence are currently not available. To facilitate the identification of genes underlying a mutant phenotype, we developed an *Agrobacterium rhizogenes* mediated root transformation system for pea (Chapter 2) and provided a proof-of-principle that orthologous genes from Medicago can be used to complement symbiotic pea mutants (Chapter 2 and Chapter 4). This offers a powerful alternative strategy to test candidate genes by introducing genes from Medicago directly into pea. Further, this hairy root transformation system, which allows the selection of transgenic roots based on the expression of a red fluorescent reporter, can be used to silence candidate pea genes via RNA interference as used in Medicago (Limpens et al., 2004). Because most mutants disturbed in symbiosome formation and development have symbiosis-specific defects, an additional criterion to select candidate genes can be to identify genes that are specifically or preferentially expressed in nodules. Although gene order (and content) is not always completely conserved due to inversions, duplication, insertions, and deletions, even for (or within) closely related species, this strategy was successful in the identification of the pea *Sym33* and *Sym41* genes (Chapter 3 and 4). This shows that the comparative genomics strategy greatly facilitates the identification of symbiotic pea genes. However, this cloning strategy remains quite time-consuming and labour-intensive. In light of the recent rapid developments in next-generation sequencing technology, it is expected that in the near future a sequenced pea genome and/or full transcriptome (based on RNA sequencing) will become available. Such an invaluable resource would significantly speed up the exploitation of the wealth of genetic resources that have been generated in pea (Borisov et al., 2007).

Nod factor signalling controls symbiosome formation and development

Via synteny-based positional cloning, we identified the pea *Sym33* (Chapter 3) and *Sym41* (Chapter 4) genes as well as Medicago *Sym1* (Chapter 3) and showed that these genes encode key components of the Nod factor (NF) signalling pathway (Fig. 1; Oldroyd et al., 2011). This

highlights an important role for the NF signalling, not only at early stages of the interaction but also at later stages related to symbiosome formation and development. This fits with the observation that all NF signalling genes are expressed in the infection zone of the nodule where symbiosome formation occurs (Bersoult et al., 2005; Limpens et al., 2005). Furthermore, the characterization of the mutant phenotypes suggested that subsequent stages of rhizobial infection require different threshold levels of NF signalling.

IPD3

In Chapter 3, we identified pea *Sym33* and Medicago *Sym1* and showed that both genes encode the recently identified interacting protein of DMI3, IPD3, an ortholog of CYCLOPS in *Lotus japonicus* (Lotus) (Messinese et al., 2007; Yano et al., 2008; Horváth et al., 2011; Ovchinnikova et al., 2011). Knockout mutations in the corresponding pea and Medicago genes cause a block in the release of bacteria from cell wall bound infection threads (Horváth et al., 2011; Ovchinnikova et al., 2011; Chapter 3). In *Mtsym1*, infection thread formation is hampered in the epidermis, and infection threads often abort in the outer cortex of developing nodule primordia. However, some infection threads do manage to invade the developing nodules. IPD3 was shown to interact with DMI3/CCaMK (Messinese et al., 2007; Yano et al., 2008) and to co-localize with DMI3 in the nucleus of cells of the nodule infection zone where symbiosome formation occurs (Smit et al., 2007; Ovchinnikova et al., 2011; Chapter 3). Previously it was shown that introduction of a non-legume *DMI3* ortholog from rice into the Medicago *dmi3* mutant resulted in a similar block of release of bacteria from the infection threads as observed in the *ipd3* mutants (Godfroy et al., 2006). This suggests that IPD3 controls the activity or stability of a DMI3 signalling complex. This is further supported by the observation that introduction of an always-active truncated DMI3 construct into the Medicago *sym1* mutant was not able to trigger spontaneous nodule formation whereas it does so in wild-type plants (Gleason et al., 2006; Tirichine et al., 2006; Ovchinnikova et al., 2011). We postulate that the always active truncated DMI3 protein (35S:DMI3*[1-311]) is less stable than wild-type DMI3 and in an *ipd3* background is insufficiently active to trigger spontaneous nodule formation.

Although we did not observe symbiosome formation in the *ipd3* mutants, previous studies on pea *sym33* (Tsyganov et al., 1998) and Medicago *sym1* (Bénaben et al., 1995) reported that occasional release of bacteria did occur. In such cases, the symbiosomes/bacteroids remained morphologically undifferentiated, and the nodules showed premature senescence. The different phenotypes suggest that the severity of the *ipd3* nodule phenotypes is sensitive to environmental factors (growth conditions) or rhizobial strains. Furthermore, work by Horváth et al. (2011) indicated that the genetic background of the plant also influences the *ipd3* mutant phenotype (Horváth et al., 2011).

Sym19/DMI2

A similar variation in symbiosome formation ability has been observed in the pea *sym41* mutant, showing either impaired invasion of the nodule primordium accompanied by a block in the release of the bacteria (Voroshilova et al., 2009) or the formation of nodules where symbiosomes do form, but fail to differentiate (Morzhina et al., 2000; Chapter 4). In Chapter 4, we cloned the pea *Sym41* gene and showed that it represents a weak allele of the Nod factor signalling LRR-receptor kinase gene *Sym19*, the ortholog of Medicago *DMI2* and Lotus *SymRK* (Stracke et al., 2002; Endre et al., 2002). A 3'-splice-site mutation in the *Pssym41* allele causes a strong reduction (~90%) of wild-type *Sym19* transcript levels in the mutant and the appearance of a truncated protein lacking the kinase domain. However, *Pssym41* retains the ability to form nodules due to the residual amount of *Sym19* wild-type transcripts that are still produced.

The similar phenotypic variation as observed in *ipd3/dmi3* mutants suggests that the main function of Sym19/DMI2 is to activate DMI3, which in turn plays an essential role in infection thread growth and symbiosome formation via its interaction with IPD3. Reduced signalling via DMI2 may result in impaired activation of DMI3 and IPD3, possibly due to its effect on calcium spiking (Wais et al., 2000; Walker et al., 2000; Kosuta et al., 2011). This is also supported by a recent study in Lotus where an always-active mutant version of CCaMK (DMI3) in a *symrk-3* null-mutant background was sufficient to trigger fully infected nodules containing symbiosomes (Madsen et al., 2010).

We further noticed that there was a striking difference between infection events in the apical and basal parts of the *sym41* nodules. In the basal part of the nodule, which consists of the cells that are first infected in the nodule primordium (Timmers et al., 1998; Kulikova et al. personal communication), release from the infection threads occurred normally, however the resulting symbiosomes failed to differentiate properly. In contrast, in cells of the apical part of the nodule that derive from the nodule meristem, rhizobial release was severely hampered, and only few symbiosomes were formed. Previous studies have shown that knockdown of DMI2 specifically in the nodule and nodule primordia caused a complete block in the release of the bacteria from the cell wall bound infection threads (Capoen et al., 2005; Limpens et al., 2005). The absence of symbiosomes in these nodules implies that the release of bacteria is already blocked in the first incipient cells of the nodule primordium. These data, as well as the upregulation of several NF signalling components in the infection zone of the nodule (including DMI2 and IPD3), suggest that subsequent stages of rhizobial infection require increasing levels of NF signalling, and that nodule-meristem derived cells show the highest threshold level to allow the switch from infection thread growth to symbiosome formation and subsequent differentiation.

Cross-talk between NF signalling genes

We further showed that MtIPD3 is required for the expression of a nodule-specific remorin *SYMREM1* (Chapter 3), which has been reported to control proper infection thread growth and symbiosome formation (Lefebvre et al., 2010). SYMREM1 has been shown to interact with the LRR receptor kinase DMI2 as well as with the NF receptors NFP and LYK3 in Medicago (Lefebvre et al., 2010). Based on the structural homology of SYMREM1 to caveolins involved in non-clathrin mediated endocytosis, a role for SYMREM1 in endocytosis of the signalling receptors was proposed, thereby controlling the signalling activity of these receptors (Lefebvre et al., 2010). Interestingly, a knockout mutant of *MtSYMREM1* also causes a block in the release bacteria from infection threads inside the nodule (Lefebvre et al., 2010). Therefore, the IPD3 dependent induction of SYMREM1 during nodule formation may offer a feedback regulation on the activity the NF signaling receptors. SYMREM1 as a lipid raft localized protein could also provide a scaffold for the formation of signalling complexes at the plasma membrane. A similar scaffolding function can be envisioned for the recently identified lipid-raft localized flotillins that control rhizobial infection in the epidermis and co-localize with LYK3 in distinct domains upon inoculation with rhizobia (Stuermer, 2009; Haney et al., 2011). However, the reported presence of SYMREM1 on mature symbiosomes suggests that SYMREM1 has additional roles in symbiosome development (Lefebvre et al. 2010).

Understanding how the NF signalling pathway controls symbiosome formation downstream of DMI3/IPD3 will be a major task for the future. It is now becoming clear that this molecular mechanism is derived from the mechanism used by ancient arbuscular mycorrhizal fungi to form arbuscules.

Rhizobium co-opted the mechanism for intracellular accommodation from the ancient arbuscular mycorrhiza

In addition to their essential role in the Rhizobium-legume interaction, the NF signalling components DMI2, DMI3, and IPD3 are also essential to allow a symbiotic association with arbuscular mycorrhizal (AM) fungi, and therefore this pathway has been called the common symbiotic (SYM) signalling pathway (Parniske, 2008). During the AM symbiosis, fungal hyphae invade the root, and a symbiotic interface compartment is formed inside root cortex cells where highly branched hyphae are contained in a specialized host membrane (periarbuscular membrane), and together are called arbuscules (Parniske, 2008). Knockout mutations in the common SYM genes typically block infection by arbuscular mycorrhizal fungi at the epidermis (Parniske, 2008). The AM endosymbiosis dates back ~450 million years and occurs in >80% of current land plants. Therefore, rhizobia are thought to have co-opted the common SYM pathway from the ancient arbuscular mycorrhiza. This is supported by the recent finding that AM fungi produce lipo-chitooligosaccharide signal molecules that are strikingly similar to the rhizobial Nod factors (Maillet et al., 2011). Furthermore, a recent study in the only non-legume able to

establish a rhizobial symbiosis, *Parasponia*, showed that a single NFP ortholog controls both arbuscule formation and fixation thread formation (Op den Camp et al., 2011). Such fixation threads are highly branched intracellular thread-like structures that form the symbiotic interface compartment where the rhizobia fix nitrogen. Similar fixation threads are observed in more basal legume species and are thought to represent a more primitive stage from which symbiosomes evolved (Naisbitt et al., 1992; Sprent, 2007). Therefore, it is probable that during evolution rhizobia acquired the ability to produce Nod factors (Sullivan and Ronson, 1998), and this allowed them to use the ancient AM machinery to establish an intracellular symbiotic interface. This would imply that NF perception (e.g. NF receptors) in the nodule controls symbiosome formation. Such a role is supported by the observation that the rhizobial *nod* genes are active in the bacteria inside infection threads in the nodule where the NF receptor genes *NFP* and *LYK3* are also expressed (Sharma and Signer, 1990; Schlaman et al., 1991; Limpens et al., 2005), and that, upon rhizobial release, the *nod* genes are switched off (Marie et al., 1994). However, a direct involvement of NF perception in symbiosome formation remains to be demonstrated. Furthermore, the expression domains of *DMI1*, *DMI2*, *DMI3*, and *IPD3* in the nodule appear to be wider than the expression domain of the NF receptor genes (Limpens et al., 2005; Smit et al., 2007; Moreau et al., 2011). This suggests that the common SYM pathway may be activated in the nodule via alternative ways in cells that contain/form symbiosomes.

In contrast to our finding that the symbiosome formation has a higher demand on Sym19/DMI2 and IPD3 than infection thread formation in the root epidermis, arbuscule formation in the root cortex cells did not appear to be affected in the corresponding mutants of pea and Medicago. Instead, AM fungi were most strongly hampered in their ability to pass the epidermis, resulting in enlarged balloon-shaped appressoria (Chapter 4) typical for “common SYM” mutants (Kistner et al., 2005, Kosuta et al., 2011). As a result, root colonization was markedly reduced in *ipd3/sym33* and *sym41* mutants. Similarly, Lotus *symrk* knockout mutants are still able to form arbuscules in root sectors where the fungus manages to pass the epidermis (Wegel et al., 1998; Demchenko et al., 2004). In contrast, *dmi3*/ccamk knockout mutants never form arbuscules even when the fungus manages to pass the epidermis (Demchenko et al., 2004). This suggests that Sym19/DMI2/SYMRK is not required in the root cortex to allow arbuscule formation. It implies that additional factors lead to the activation of DMI3/CCaMK in the cortex. A similar uncoupling of epidermal and cortical responses was observed in the Lotus *symrk-14* mutant, which contains a mutation in a conserved GDPC sequence in the SymRK extracellular domain (Kosuta et al., 2011).

In contrast to IPD3 in pea and Medicago, CYCLOPS in Lotus is essential for arbuscule formation (Yano et al., 2008), and a knockout of rice *IPD3* completely blocked the interaction already at the epidermis (Chen et al., 2008). This further indicates that additional genetic factors control DMI3/CCaMK activity. Furthermore, DMI3/CCaMK regulation appears to differ between Rhizobium symbiosis and arbuscular mycorrhiza (Shimoda et al., 2012).

A nodule-specific exocytotic pathway controls symbiosome formation

Recently it has become clear that fusion of distinct exocytotic vesicles with the plasma membrane plays a key role in the formation of symbiosomes as well as arbuscules. Despite their different morphology, symbiosomes and arbuscules share a plasma membrane identity (Catalano et al., 2004; Limpens et al., 2009; Pumplin and Harrison, 2009). Furthermore, they both are characterized by the lack of a structured cell wall. Ivanov and co-workers (2012) showed that two specific exocytotic vesicle-associated membrane proteins (v-SNAREs/VAMPs) are required for the formation of symbiotic membrane interface in both Rhizobium–legume symbiosis and arbuscular mycorrhiza. Silencing of these Medicago *VAMP72* genes blocked symbiosome as well as arbuscule formation whereas it did not affect root colonization by the microbes (Ivanov et al., 2012). Interestingly, orthologs of these "symbiotic *v-SNAREs*" are lacking in the genome of Arabidopsis, which cannot establish a symbiosis with either rhizobia or AM fungi, correlating with a symbiosis-specific role. Identification of these VAMP72s as common symbiotic regulators in exocytotic vesicle trafficking suggests that the ancient exocytotic pathway forming the periarbuscular membrane compartment, also has been co-opted in the Rhizobium–legume symbiosis (Ivanov et al., 2012). Thus, the Rhizobium symbiosis and arbuscular mycorrhiza use not only the same signalling pathway but also the same cellular process, namely a specific exocytotic pathway, to form intracellular symbiotic compartments (Fig.1).

Because the formation of unwalled infection droplets (i.e. the beginning of a symbiotic interface) was blocked in the *VAMP72* knockdown nodules, it can be hypothesized that the VAMP72 marked vesicles deliver cargo to degrade (or prevent the build-up) of a cell wall at these sites and to allow the uptake of bacteria. Induction of such cargo may be controlled by the common DMI3/IPD3 module activated via upstream DMI2 and DMI1 signalling (Fig.1). Alternatively or additionally, the common SYM pathway (Fig.1) could control the targeting of specific vesicles to the infection threads by affecting the cytoskeleton (Timmers et al., 1998; Popp and Ott, 2011). It has been previously suggested that the cytoskeleton rearrangements and targeted vesicle transport play a role in this process as release of bacteria from the infection threads seemed to involve a change in the kind of vesicles and their cargo fusing with the tips of the infection thread (Brewin, 1996). Such induced exocytotic pathway could be also involved in infection thread formation/growth. Recently a nodule-specific secreted pectin methyl esterase (LjNPL) involved in cell wall remodeling was found to control the infection thread formation (Xie et al., 2012). Knockout mutations of this gene in Lotus blocked the formation of infection threads after the bacteria formed a microcolony in curled root hairs, a similar phenotype as observed in Lotus cyclops/ipd3 mutants (Yano et al., 2008). Interestingly, the orthologous *NPL* gene in Medicago is most strongly expressed specifically in the distal infection zone where infection threads invade the nodule cells, and symbiosomes are formed (Limpens unpublished).

Therefore, this pectin methyl esterase may be one of the putative cargos of the VAMP72 vesicles that contribute to the formation of an unwalled infection droplet.

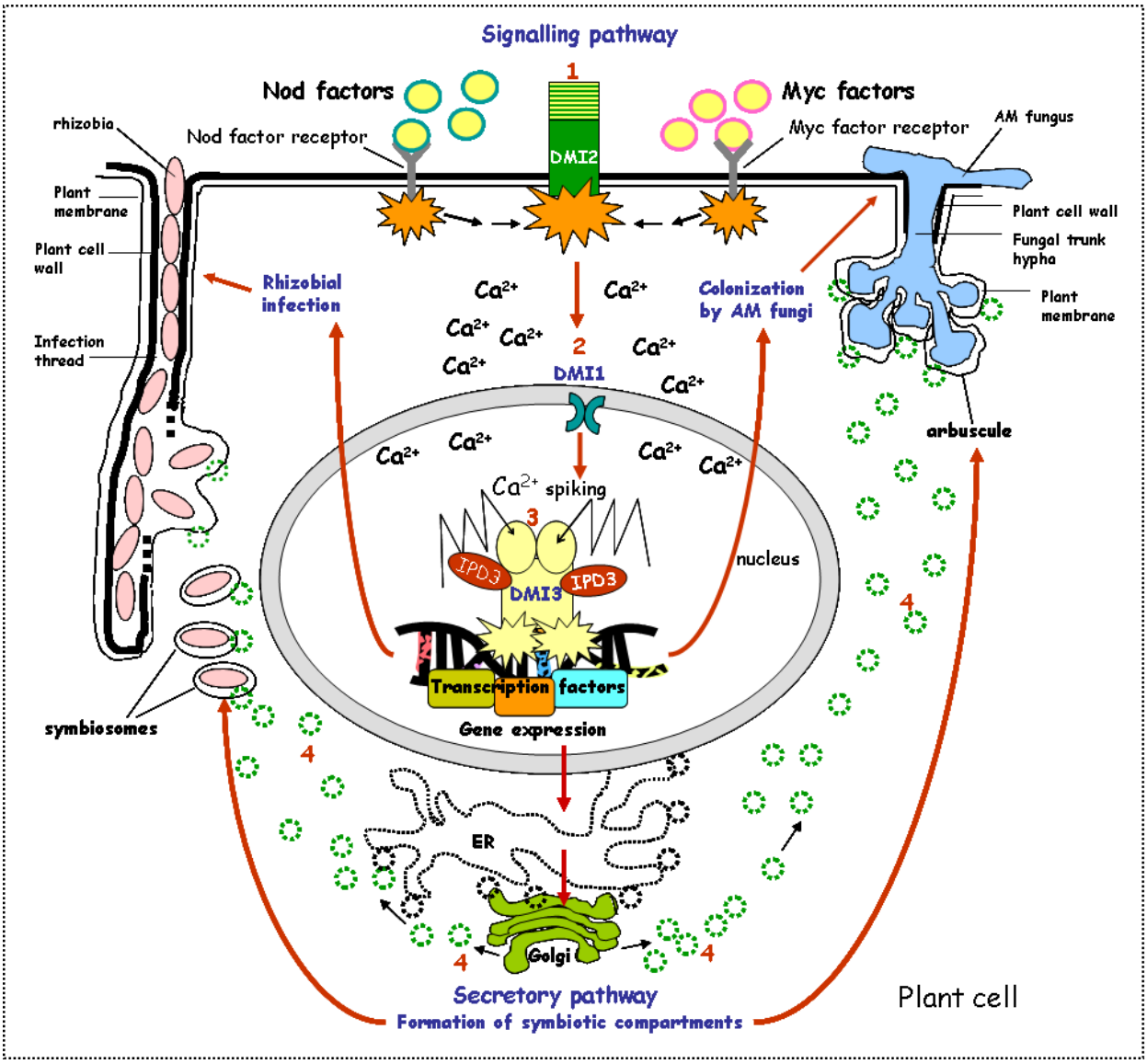

Fig.1. Shared symbiotic pathways for arbuscular mycorrhiza (AM) and rhizobial symbiosis. Both symbioses are controlled by the common SYM pathway (signalling pathway, **1-3**). Similar lipo-chitooligosaccharide signal molecules (Nod and Myc factors) are perceived by LysM domain containing receptor kinases MtNFP/LYK3/LYK4 (PsSym10/Sym37/Sym2 and LjNFR5/NFR1; Nod factor receptors). These receptors trigger ion fluxes leading to a depolarization of the plasma membrane and calcium oscillations (Ca^{2+} spiking) in and around the nucleus via the plasma membrane-localized common SYM receptor kinase MtDMI2 (PsSym19/LjSYMRK) (**1**) and a putative cation channel MtDMI1 (PsSym8/LjCastor/Pollux) (**2**) located at the nuclear envelope. The calcium signature is decoded by a nuclear Ca^{2+}/calmoduling-dependent kinase MtDMI3 (PsSym9/LjCCaMK) (**3**) that forms a protein complex with MtIPD3 (PsSym33/LjCYCLOPS). This complex triggers transcriptional changes leading to specific symbiotic responses such as colonization of the plant by the microsymbionts and formation of symbiotic compartments (arbuscules and symbiosomes). Furthermore, a symbiotic exocytotic pathway (secretory pathway, 4) is involved in arbuscule and symbiosome formation and development. Recently identified exocytotic v-SNARE proteins control the fusion of specific vesicles and their associated cargo to the infection threads and invading hyphae (4). The common SYM pathway may control the symbiosis-specific induction of cargos that enter this exocytotic pathway to allow the formation of a symbiotic interface in both symbioses.

Insight into symbiosome differentiation

During symbiosome development, the rhizobia differentiate into bacteroids that acquire the ability to fix atmospheric nitrogen (Vasse et al., 1990). Evolutionally advanced legumes of the inverted-repeat-lacking (IRLC) clade of Papilionoidea, such as pea and Medicago, develop extreme dominance over their microbial symbionts as they push the rhizobia to terminal differentiation (Mergaet et al., 2006; Oono et al., 2010). During the terminal differentiation, bacteria lose their ability to divide and reproduce, they modify their metabolism, endoreduplicate their DNA, and enlarge (Bisseling et al. 1977, Vasse et al., 1990; Van de Velde et al., 2010). The infected plant cells also undergo endoreduplication, which correlates with symbiosome formation (Truchet et al., 1980, 1991; Mergeart et al., 2006) and could be under the control of the common SYM pathway. Terminal differentiation does not occur in non-IRLC legumes such as Lotus or soybean, and it is thought to have evolved several times independently (Oono et al., 2010). Terminal differentiation has been shown to be triggered by small cysteine-rich peptides (NCRs) that are specific for IRLC legumes and resemble defensin-like antimicrobial peptides (Van de Velde et al., 2010; Maróti et al., 2011). These peptides are processed by a nodule-specific signal peptidase complex (Wang et al., 2010). Failure to remove the signal peptide from these NCRs results in the accumulation of these peptides in the ER instead of accumulating at the symbiosomes, and in a block in symbiosome differentiation (Van de Velde et al., 2010; Wang et al., 2010). This further indicates the involvement of a nodule-specific exocytotic pathway in symbiosome differentiation (Fig. 1). Thus, pea and Medicago use the NCR peptides to “domesticate” their microbial symbionts which turn into ”true” nitrogen-fixing plant organelles (Patriarca et al., 2002; White et al., 2007; Oldroyd et al., 2011).

To get additional insight into plant components that control symbiosome differentiation, we focused on the pea *sym3*1 mutant. In *Pssym31* nodules, the bacteroids fail to differentiate, and this is accompanied by the formation of abnormal symbiosome structures where several bacteroids are included within a single symbiosome membrane (Borisov et al., 1992, 1997; Sherrier et al., 1997; Dahiya et al., 1998). In Chapter 5, we delineated the location of *Sym31* to a ~2.5 cM region on linkage group III, which corresponds to a ~450 kb syntenic region on Medicago chromosome 3. Within this region, one gene that is specifically expressed in the nodule stands out as promising candidate for *Sym31*. This gene, *MtN3.1*, encodes an MtN3-like protein that is a member of the recently identified family of SWEET sugar/sucrose transporters (Chen et al., 2010; 2012). Members of this family in Arabidopsis and rice have been identified as key targets for biotrophic pathogens to obtain carbon from the host plant (Yang et al., 2006; Antony et al., 2010; Chen et al., 2010). It is generally believed that dicarboxylates, especially malate, are the main carbon source for the symbiosomes, but not sugars (Udvardi and Day, 1997; Day et al., 2001; White et al., 2007). However, the transport capacity of symbiosome membranes has been determined only for mature symbiosomes from the fixation zone, and not for developing juvenile symbiosomes. We hypothesize that *Sym31* encodes an MtN3-like

sugar/sucrose transporter that localizes to the symbiosome membrane and controls symbiosome differentiation. The delivery of sugars may be required to fuel the growth of the bacteroids when they switch metabolism to differentiate (White et al., 2007). Because terminal symbiosome differentiation is specific for IRLC-clade legumes the nodule-specific expression of MtN3.1 may reflect an evolutionary adaptation to facilitate this terminal differentiation, as close MtN3.1 homologs in the non-IRLC soybean are not specifically expressed in the nodules. Alternatively, an altered carbon metabolism in the *sym31* nodule cells (Romanov et al., 1995) could affect the glycosylation of proteins involved in symbiosome development. This could explain the observed absence of several glycosylated isoforms of a lectin-like protein in *sym31* nodules (Dahiya et al., 1998). It could also explain the aberrant symbiosome structures by affecting the strict coupling of bacteroid division with division of the symbiosome membrane as observed in wild-type nodules, resulting in the symbiosomes containing multiple bacteroids in *sym31*. It could also reflect the inability of the symbiosomes to prevent their fusion, which occurs upon nodule senescence, although the symbiosomes in *sym31* nodules do not appear to turn prematurely into lytic compartments (Limpens et al., 2009; Borisov et al., 1992, 1997; Sherrier et al., 1997; Dahiya et al., 1998). Although intriguing, ultimate prove for a role of MtN3.1 in symbiosome differentiation awaits further experimentation. Furthermore, the *A. rhizogenes* pea root transformation method developed in Chapter 2 may facilitate the determination whether *PsSym31* indeed encodes an *MtN3.1* orthologous gene.

REFERENCES

Antony, G., Zhou, J., Huang, S., Li, T., Liu, B., White, F., Yang, B. (2010) Rise *xa13* Recessive Resistance to Bacterial Blight Is Defeated by Induction of the Disease Susceptibility Gene *Os-11N3*. *Plant Cell*, 22(11): 3864–3876.

Aubert, G., Morin J., Jacquin F.., Loridon K., Quillet M.C., Petit A., Rameau C., Lejeune-Hénaut I., Huguet T., Burstin J. (2006) Functional mapping in pea, as an aid to the candidate gene approach and for investigating the synteny with the model species *Medicago truncatula. Theor. Appl. Genet*, 112: 1024–1041.

Bénaben, V., Duc, G., Lefebvre, V., Huguet, T. (1995) TE7, An Inefficient Symbiotic Mutant of *Medicago truncatula* Gaertn cv. Jemalong. *Plant Physiol*., 107: 53–62.

Bersoult, A., Camut, S., Perhald, A., Kereszt, A., Kiss, G.B., Cullimore, J.V. (2005) Expression of the *Medicago truncatula DM12* gene suggests roles of the symbiotic nodulation receptor kinase in nodules and during early nodule development. *Mol Plant Microbe Interact***,** 18: 869–876.

Bisseling, T., Bos, R.C. van den, Kammen A. van, Ploeg, M. van der, Duijn, P. van, Houwers, A. (1977) Cytofluorometrical determination of the DNA contents of bacteroids and corresponding broth-cultured *Rhizobium* bacteria. *J. Gen. Microbiol.,* 101: 79–84.

Borisov, A.Yu., Danilova, T.N., Koroleva, T.A., Kuznetsova, E.V., Madsen, L., Mofett, M., Naumkina, T.S., Nemankin, T.A., Ovchinnikova, E.S., Pavlova et al. (2007) Regulatory genes of garden pea

(*Pisum sativum* L.) controlling the development of nitrogen-fixing nodules and arbuscular mycorrhiza: a review of basic and applied aspects. *Appl. Biochemistry and Microbiology,* 43(3): 237–243.

Borisov, A.Y., Madsen, L.H., Tsyganov, V.E., Umehara, Y., Voroshilova, V.A., Batagov, A.O., Sandal, N., Mortensen, A., Schauser, L., Ellis, N., et al. (2003) The *Sym35* gene required for root nodule development in pea is an ortholog of *Nin* from *Lotus japonicus. Plant Physiol.,* 131(3): 1009–1017.

Borisov, A.Y., Morzhina, E.V,, Kulikova, O.A., Tchetkova, S.A., Lebsky, V.K., Tikhonovich, I.A. (1992) New symbiotic mutants of pea *(Pisum sativum* L.) affecting either nodule initiation or symbiosome development. *Symbiosis* 14: 297–313.

Borisov, A.Y., Rozov, S.M., Tsyganov, V.E., Morzhina, E.V., Lebsky, V.K., Tikhonovich, I. (1997) Sequential functioning of *Sym13* and *Sym31*, two genes affecting symbiosome development in root nodules of pea (*Pisum sativum* L). *Mol. Gen. Genet.,* 254: 592–598.

Brewin, N.J. (1996) Plant membrane structure and function in the Rhizobium-legume symbiosis. In: Smallwood, M., Knox, J.P., Bowles, D.J. (eds) Membranes: specialized functions in plants. *Bios Scientific Publishers*, Oxford, pp. 507–524.

Capoen, W., Goormachtig, S., De Rycke, R., Schroeyers, K., Holsters, M. (2005) SrSymRK, a plant receptor essential for symbiosome formation. *Proc. Natl. Acad. Sci. U.S.A.,* 102:10369-10374.

Catalano, C. M., Lane, W. S., Sherrier, D. J. (2004) Biochemical characterization of symbiosome membrane proteins from *Medicago truncatula* root nodules. *Electrophoresis* 25: 519–531.

Chen, C., Ané, J.M., Zhu, H. (2008) OsIPD3, an ortholog of the *Medicago truncatula* DMI3 interacting protein IPD3, is required for mycorrhizal symbiosis in rice. *New Phytol.,* 180: 311–315.

Chen, L.Q., Hou, B.H., Lalonde, S., Takanada, H., Hartung, M.L., Qu, X.Q., Guo, W.J., Kim, J.G., Underwood, W., Chaudhuri, B., et al. (2010) Sugar transporters for intercellular exchange and nutrition of pathogens. *Nature* 468: 527–534.

Chen, L.Q., Qu, X.Q., Hou, B.H., Sosso, D., Osorio, S., Fernie, A.R., Frommer, W.B. (2012) Sucrose Efflux Mediated by SWEET Proteins as a Key Step for Phloem Transport. *Science* 335(6065): 207–211.

Choi, H., Kim, D., Uhm, T., Limpens, E., Lim, H., Mun, J., Kalo, P., Varma Penmetsa, R., Seres, A., Kulikova O., Roe, B.A., Bisseling, T., Kiss, G.B., Cook, D.R. (2004) A sequence-based genetic map of *Medicago truncatula* and comparison of marker colinearity with *M. sativa*. *Genetics* 166: 1463–1502.

Dahiya, P., Sherrier, D.J., Kardailsky, I.V., Borisov, A.Y., Brewin, N.J. (1998) Symbiotic Gene Sym31 Controls the Presenceof a Lectinlike Glycoprotein in the Symbiosome Compartment of Nitrogen-Fixing Pea Nodules. *Mol. Plant-Microbe Interact.,* 11(9): 915–923.

Day, D.A., Poole, P.S., Tyerman, S.D., Rosendahl, L. (2001) Ammonia and amino acid transport across symbiotic membranes in nitrogen-fixing legume nodules. *Cell Mol. Life Sci.,* 58: 61–71.

Demchenko, K., Winzer, T., Stougaard, J., Parniske, M., Pawlowski, K. (2004) Distinct roles of *Lotus japonicus* SYMRK and SYM15 in root colonization and arbuscule formation. *New Phytol.,* 163: 381–392.

Endre, G., Kereszt, A., Kevei, Z., Mihacea, S., Kaló, P., Kiss, G. (2002) A receptor kinase gene regulating symbiotic nodule development. *Nature* 417: 962–966.

Gleason, C., Chaudhuri, S., Yang, T.B., Munoz, A., Poovaiah, B.W., Oldroyd, G.E.D. (2006) Nodulation independent of rhizobia induced by a calcium-activated kinase lacking autoinhibition. *Nature* 441: 1149–1152.

Godfroy, O., Debellé, F., Timmers, T., Rosenberg, C. (2006) A rice calcium- and calmodulin-dependent protein kinase restores modulation to a legume mutant. *Mol. Plant-Microbe Interact.,* 19(5): 495–501.

Haney, C.H., Riely, B.K., Tricoli, D.M., Cook, D.R., David, W., Ehrhardt, D.W., Long, S.R. (2011) Symbiotic rhizobia bacteria trigger a change in localization and dynamics of the *Medicago truncatula* receptor kinase LYK3. *Plant Cell*, 23: 2774–2787.

Horváth, B., Yeun, L. H., Domonkos, A., Halász, G., Gobbato, E., Ayaydin, F., Míró, K., Hirsch, S., Sun, J., Tadege, M., Ratet, P., et al. (2011) *Medicago truncatula* IPD3 is a member of the common symbiotic signaling pathway required for rhizobial and mycorrhizal symbioses. *Mol. Plant-Microbe Interact.,* 24: 1345–1358.

Ivanov, S., Fedorova, E., Limpens, E., De Mita, S., Genre, A., Bonfante, P., Bisseling, T. (2012) *Rhizobium*–legume symbiosis shares an exocytotic pathway required for arbuscule formation. *PNAS*, 10.1073/pnas.1200407109. Published online.

Jones, K.M., Kobayashi, H., Davies, B.W., Taga, M.E., Walker, G.C. (2007) How rhizobial symbionts invade plants: The *Sinorhizobium*-Medicago model. *Nat. Rev. Microbiol.,* 5: 619–633.

Kistner, C., Winzer, T., Pitzschke, A., Pitzschke, A., Mulder, L., Sato, S., Kaneko, T., Sandal, N., Stougaard, J., Webb, K.J. et al. (2005) Seven Lotus japonicus genes required for transcriptional reprogramming of the root during fungal and bacterial symbiosis. *Plant Cell,* 17: 2217–2229.

Kosuta, S., Held, M., Hossain, M.S., Morieri, G., MacGillivary, A., Johansen, C., Antolin-Liovera, M., Parniske, M., Olgroyd, G., Downie, A.J. et al. (2011) Lotus japonicus symRK-14 uncouples the cortical and epidermal symbiotic program. *The Plant J.,* 67: 929–940.

Lefebvre, B., Timmers, T., Mbengue, M., Moreau, S., Hervé, C., Tóth, K., Bittencourt-Silvestre, J., Klaus, D., Deslandes, L., Godiard, et al. (2010) A remorin protein interacts with symbiotic receptors and regulates bacterial infection. *Proc. Natl. Acad. Sci. U.S.A.,* 107: 2343–2348.

Limpens, E., Ramos, J., Franken C., Raz, V., Compaan, B., Franssen, H., Bisseling, T., Geurts, R. (2004) RNA interference in Agrobacterium rhizogenes-transformed roots of Arabidopsis and Medicago truncatula. *J. Exp. Bot.,* 55: 983–992.

Limpens, E., Mirabella, R., Fedorova, E., Franken, C., Franssen, H., Bisseling, T., Geurts, R. (2005) Formation of organelle-like N_2-fixing symbiosomes in legume root nodules is controlled by *DMI2. Proc Natl Acad Sci USA,* 102: 10375–10380.

Limpens, E., Ivanov, S., van Esse, W., Voets, G., Fedorova, E., Bisseling, T. (2009) Medicago N_2-fixing symbiosomes acquire the endocytic identity marker Rab7 but delay the acquisition of vacuolar identity. *Plant Cell,* 21: 2811–2828.

Madsen, L.H., Tirichine, L., Jurkiewicz, A., Sullivan, J.T., Heckmann, A.B., Bek, A.S., Ronson, C.W., James, E.K. Stougaard, J. (2010) The molecular network governing nodule organogenesis and infection in the model legume Lotus japonicus. *Nature Communications,* 1: 1–12.

Maillet, F., Poinsot, V., Andre, O., Puech-Pages, V., Haouy, A., Gueunier, M., Cromer, L., Giraudet, D. Formey, D., Niebel, A. et al. (2011) Fungal lipochitooligosaccharide symbiotic signals in arbuscular mycorrhiza. *Nature* 469: 58–63.

Marie, C., Plaskitt, K.A., Downie, J.A. (1994) Abnormal bacteroid development in nodules induced by glucosamine synthase mutant of *Rhizobium leguminosarum*. *Mol. Plant-Microbe Interact.,* 7: 482–487.

Maróti, G., Kereszt, A., Kondorosi, E., Mergaert, P. (2011) Natural roles of antimicrobial peptides in microbes, plants and animals. *Res. Microbiol.,* 162: 363–374.

Mergeart, P., Uchiumi, T., Alunni, B., Evanno, G., Cheron, A., Catrice, O., Mausset, A.E., Barloy-Hubler, F., Galibert, F., Kondorosi, A., Kondorosi, E. (2006) Eukaryotic control on bacterial cell cycle and differentiation in the Rhizobium–legume symbiosis. *PNAS*, 103(13): 5230–5235.

Messinese, E., Mun, J. H., Yeun, L. H., Jayaraman, D., Rougé, P., Barre, A., Lougnon, G., Schornack, S., Bono, J. J., Cook, D. R., Ané, J. M. (2007) A novel nuclear protein interacts with the symbiotic DMI3 calcium- and calmodulin-dependent protein kinase of *Medicago truncatula*. *Mol. Plant-Microbe Interact.,* 20: 912–921.

Morzhina, E,V., Tsyganov, V.E., Borisov, A.Y., Lebsky, V.K., Tikhonovich, I.A. (2000) Four developmental stages identified by genetic dissection of pea (*Pisum sativum* L.) root nodule morphogenesis. *Plant Science*, 155: 75–83.

Naisbitt, T., James, E.K., Sprent, J.I. (1992) The evolutionary significance of the legume genus *Chamaecrista*, as determined by nodule structure. *New Phytol.,* 122: 487–492.

Oldroyd, G. E., Murray, J. D., Poole, P. S., Downie, J. A. (2011) The rules of engagement in the legume-rhizobial symbiosis. *Annul. Rev. Genet.,* 45: 119–144.

Oono, R., Schmitt, I., Sprent, J.I., Denison, R.F. (2010) Multiple evolutionary origins of legume traits leading to extreme rhizobial differentiation. *New Phytol.,* 187: 508–520.

Op den Camp, R., Streng, A., De Mita, S., Cao, Q., Polone, E., Liu, W., Ammiraju, J.S.S., Kudrna, D., Wing, R., Untergasser, A., et al. (2011) LysM-Type Mycorrhizal Receptor Recruited for Rhizobium Symbiosis in Nonlegume *Parasponia. Science*, 331(6019): 909–912.

Ovchinnikova, E., Journet, E. P., Chabaud, M., Cosson, V., Ratet, P., Duc, G., Fedorova, E., Liu, W., den Camp, R. O., Zhukov, V., Tikhonovich, I., Borisov, A., Bisseling, T., Limpens, E. (2011). IPD3 controls the formation of nitrogen-fixing symbiosomes in pea and *Medicago* Spp. *Mol Plant-Microbe Interact,* 24(11): 1333–1344.

Parniske, M. (2008) Arbuscular mycorrhiza: The mother of plant root endosymbioses. *Nat. Rev. Microbiol.,* 6: 763–775.

Patriarca, E.J., Tate, R., Iaccarino, M. (2002) Key role of bacterial metabolism in *Rhizobium*-plant symbiosis. *Microbiol. Mol. Biol. Rev.,* 66: 203–222.

Popp, C. and Ott, T. (2011) Regulation of signal transduction and bacterial infection during root nodule symbiosis. *Cur. Opin. Plant Biol.,* 14: 458–467.

Pumplin, N. and Harrison, M.J. (2009) Live-cell imaging reveals periarbuscular membrane domains and organelle location in *Medicago truncatula* roots during arbuscular mycorrhizal symbiosis. *Plant Physiol.,* 151: 809–819.

Romanov, V.I., Gordon, A.J., Minchin, F.R., Witty, J.F., Skøt, L., James, C.L., Borisov, A.Y., Tikhonovich, I.A. (1995) Anatomy, physiology and biochemistry of root nodules of Sprint-2Fix$^-$, a symbiotically defective mutant of pea (*Pisum sativum* L.). *J. Exp. Bot.,* 46: 1809–1816.

Schlaman, H.R.M., Horváth, B., Vijgenboom, E., Okker, R.J.H., Lugtenberg, B.J.J. (1991) Suppression of nodulation gene expression in bacteroids *of Rhizobium leguminosarum* biovar *viciae.* Journal of Bacteriol., 173: 4277–4287.

Sharma A. and Signer E.R. (1990) Temporal and spatial regulation of the symbiotic genes of *Rhizobium meliloti in planta* revealed by transposon Tn5-gusA. *Genes Dev.,* 4: 344–356.

Sherrier, D.J., Borisov, A.Y., Tikhonovich, I.A., Brewin, N.J. (1997) Immunocytological evidence for abnormal symbiosome development in nodules of the pea mutant line Sprint2Fix^{-} (*sym31*). *Protoplasma* 199: 57–68.

Shimoda, Y., Han, L., Yamazaki, T., Suzuki, R., Hayashi, M., Imaizumi-Anraku, H. (2012) Rhizobial and fungal symbioses show different requirements for calmodulin binding to calcium calmodulin-dependent protein kinase in *Lotus japonicus*. Plant Cell, 24(1):304–21.

Smit, P., Limpens, E., Geurts, R., Fedorova, E., Dolgikh, E., Gough, C., Bisseling, T. (2007) Medicago LYK3, an entry receptor in rhizobial nodulation factor signalling. *Plant Physiol.,* 145: 183–191.

Sprent, J.I. (2007) Evolving ideas of legume evolution and diversity: a taxonomic perspective on the occurrence of nodulation*. New Phytol.,* 174: 11–25.

Stracke, S., Kistner, C., Yoshida, S., Mulder, L., Sato, S., Kaneko, T., Tabata, S., Sandal, N., Stougaard, J., Szczyglowski, K., Parniske, M. (2002) A plant receptor-like kinase required for both bacterial and fungal symbiosis. *Nature* 417: 959–962.

Stuermer, C.A.O. (2009) The reggie/flotilin connection to growth. *Trends Cell Biol*., 20: 6–13

Sullivan, J. T. and Ronson, C. W. (1998) Evolution of rhizobia by acquisition of a 500-kb symbiosis island that integrates into a phe-tRNA gene. *PNAS,* 95: 5145–5149.

Timmers, A.C., Auriac, M.C., de Billy, F., Truchet, G. (1998) Nod factor internalization and microtubular cytoskeleton changes occur concomitantly during nodule differentiation in alfalfa. *Development* 125: 339–349.

Tirichine, L., Imaizumi-Anraku, H., Yoshida, S., Murakami, Y., Madsen, L.H., Miwa, H., Nakagawa, T., Sandal, N., Albrektsen, A. S., Kawaguchi, M. et al. (2006) Deregulation of a Ca^{2+}/calmodulin-dependent kinase leads to spontaneous nodule development. *Nature* 441: 1153–1156.

Truchet, G., Roche, P., Lerouge, P., Vasse, J., Camut, S., de Billy, F., Prome, J., Denarie, J. (1991) Sulphated lipo-oligosaccharide signals of *Rhizobium meliloti* elicit root nodule organogenesis in alfalfa. *Nature* 351: 670–673.

Truchet, G., Miche,. M., Dénarié, J. (1980) Sequential analysis of the organogenesis of lucerne (*Medicago sativa*) root nodules using symbiotically-defective mutants of *Rhizobium meliloti*. Differentiation 16: 163–172.

Tsyganov, V.E., Morzhina, E.V., Stefanov, S.Y., Borisov, A.Y., Lebsky, V.K., Tikhonovich, I.A. (1998) The pea (*Pisum sativum* L) genes *sym33* and *sym40* control infection thread formation and root nodule function*. Mol. Gen. Genet.,* 259: 491–503.

Udvardi, M.K. and Day, D.A. (1997) Metabolite transport across symbiotic membranes of legume nodules. *Annu. Rev. Plant Physiol. Plant Mol. Biol*., 48: 493–523.

Van de Velde, W., Zehirov, G., Szatmari, A., Debreczeny, M., Ishihara, H., Kevei, Z., Farkas, A., Mikulass, K., Nagy, A., Tiricz, et al. (2010) Plant peptides govern terminal differentiation of bacteria in symbiosis. *Science* 327: 1122–1126.

Vasse, J., de Billy, F., Camut, S., Truchet, G. (1990) Correlation between ultrastructural differentiation of bacteroids and nitrogen fixation in Alfalfa nodules. *J. Bacteriol.,* 172: 4295–4306.

Voroshilova, V. A., Demchenko, K. N., Brewin, N. J., Borisov, A. Y., Tikhonovich I. A. (2009) Initiation of a legume nodule with an indeterminate meristem involves proliferating host cells that harbour infection threads. *New Phytol.,* 181: 913–923.

Wais, R.J., Galera, C., Oldroyd, G., Catoira, R., Penmetsa, R.V., Cook, D., Gough, C., Dénarié, J., Long, S.R. (2000) Genetic analysis of calcium spiking responses in nodulation mutants of *Medicago truncatula. PNAS*, 97: 13407–13412.

Wang, D., Griffitts, J., Starker, C., Fedorova, E., Limpens, E., Ivanov, S., Bisseling, T., Long S.R. (2010) A nodule-specific protein secretory pathway required for nitrogen-fixing symbiosis. *Science* 327: 1126 – 1129.

Walker, S.A., Viprey, V., Downie, J.A. (2000) Dissection of nodulation signalling using pea mutants defective for calcium spiking induced by Nod factors and chitin oligomers. *Proc. Natl. Acad. Sci. USA,* 97: 13413–13418.

Wegel, E., Schauser, L., Sandal, N., Stougaard, J., Parniske, M. (1998) Mycorrhiza mutants of *Lotus japonicus* define genetically independent steps during symbiotic infection*. Mol. Plant-Microbe Interact.,* 11: 933–936.

White, J., Prell, J., James, E.K., Poole, P. (2007) Nutrient Sharing between Symbionts. *Plant Physiol.,* 144: 604–614.

Xie, F., Murray, J.D., Kim, J., Heckmann, A.B., Edwards, A., Oldroyd, G.E.D, Downie, A. (2012) Legume pectate lyase required for root infection by rhizobia*. PNAS*, 109: 633–638.

Yang, B., Sugio, A., White. F.F. (2006) *Os8N3* is a host disease-susceptibility gene for bacterial blight of rice. *Proc. Natl. Acad. Sci. U.S.A.,* 103: 10503–10508.

Yano, K., Yoshida, S., Müller, J., Singh, S., Banba, M., Vickers, K., Markmann, K., White, C., Schuller, B., Sato, S., et al. (2008) CYCLOPS, a mediator of symbiotic intracellular accommodation. *PNAS,* 105: 20540–20545.

Young, N.D., Debellé, F., Oldroyd, G.E.D., Geurts, R., Cannon, S.B., Udvardi, M.K., Benedito, V.A., Mayer, K.F., Gouzy, J., Schoof, H. et al. (2011) The *Medicago* genome provides insight into the evolution of rhizobial symbioses. *Nature* 480: 520–524.

Zhukov, V., Radutoiu, S., Madsen, L.H., Rychagova, T., Ovchinnikova, E., Borisov, A., Tikhonovich, I., Stougaard, J. (2008) The Pea *Sym37* Receptor Kinase Gene Controls Infection-Thread Initiation and Nodule Development. *Mol. Plant-Microbe Interact.,* 21(12): 1600–1608.

Nederlandse samenvatting

Tijdens een endosymbiose leeft een organisme, vaak een microbe, binnenin de cellen van een ander organisme, de gastheer. Dit soort interacties wordt gekarakteriseerd door de vorming van nieuwe gespecialiseerde membraancompartimenten door de gastheer waarin de microben gehuisvest worden. Deze intieme samenlevingsverbanden vormen een fundament van het leven zoals we dat kennen en spelen een belangrijke rol in de evolutie. Bijvoorbeeld, cruciale organellen zoals mitochondriën en chloroplasten zijn waarschijnlijk ontstaan vanuit een endosymbiose tussen bacteriën en voorlopers van eukaryote cellen. Een belangrijke hedendaagse endosymbiose is de interactie tussen vlinderbloemige planten, zoals erwt, soja, boon en klaver, en stikstofbindende Rhizobium bacteriën. Tijdens deze endosymbiose worden de Rhizobium bacteriën binnenin de cellen van een nieuw gevormd orgaan, de zogenaamde wortelknol, gehuisvest als nieuwe stikstofbindende organellen die we symbiosomen noemen. Daar vinden de bacteriën de juiste omstandigheden om atmosferische stikstof om te zetten in ammonia. Deze gebonden vorm van stikstof wordt afgegeven aan de plant in ruil voor koolhydraten. Hierdoor zijn vlinderbloemigen in staat om te groeien in stikstofarme bodems zonder dat ze extra bemest hoeven te worden. De vorming van symbiosomen vormt dus het hart van deze interactie en vormt als het ware de symbiontische marktplaats waar nutriënten efficiënt uitgewisseld kunnen worden. De heilige graal in het onderzoek naar deze landbouwkundig belangrijke symbiose is de mogelijkheid om deze eigenschap over te zetten naar niet-vlinderbloemige gewassen. Het begrijpen van hoe de stikstofvormende organellen gemaakt worden is hierbij van cruciaal belang en vormde een hoofddoel van het onderzoek beschreven in dit proefschrift.

In de meeste vlinderbloemigen vindt symbiosoomvorming plaats nadat de bacteriën via buisvormige celwand-gebonden structuren, de infectiedraden, getransporteerd worden naar de cellen van het knolprimordium. Dit knolprimordium ontstaat doordat cellen in de cortex van de wortel herprogrammeren en tot delen worden aangezet. Beide processen, infectie en knolprimoridumvorming, worden in gang gezet door de perceptie en signaaltransductie van bacteriele signaalmoleculen genaamd Nod factoren. Eenmaal aangekomen in de cellen van het knolprimordium, vindt er een overgang plaats van infectiedraad groei naar het vrijkomen van de bacteriën uit de infectiedraden. Hierbij vormt zich een lokaal gebiedje op de infectiedraad waar de celwand wordt afgebroken (of niet opgebouwd) en stulpt de plasma membraan uit. Van hieruit worden de bacteriën een voor een afgesnoerd in de cel, waardoor ze omgeven worden door een membraan van de plant, de symbiosoommembraan. Vervolgens vermenigvuldigen de symbiosomen zich, waarna ze differentiëren tot hun stikstofbindende vorm en vullen ze bijna volledig de geïnfecteerde cellen. In vlinderbloemigen zoals de erwt wordt er een knolmeristeem gevormd dat actief blijft waardoor symbiosoomvorming en ontwikkeling continue plaatsvinden in cellen die afkomstig zijn van dit meristeem.

In dit onderzoek hebben we een genetische benadering gebruikt om componenten in de plant te vinden die essentieel zijn voor de vorming van de symbiosomen. Bij de start van dit onderzoek was de meest uitvoerige en als beste gekarakteriseerde verzameling van plantenmutanten verstoord in symbiosoomvorming beschikbaar in de erwt (*Pisum sativum*). Echter, het positioneel kloneren van genen in de erwt wordt sterk gehinderd door het feit dat erwt een groot genoom heeft, moeilijk te transformeren is en door het gebrek aan “genomics tools”. Daarom is gekozen voor een op synteny gebaseerde positionele klonering in de evolutionair nauw verwante vlinderbloemige model plant *Medicago truncatula* (Medicago). Synteny houdt in dat overeenkomstige genen in dichtverwante organismen vaak op overeenkomstige locaties (en in eenzelfde volgorde) in de genomen te vinden zijn. Voorgaand onderzoek heeft aangetoond dat de genomen van Medicago en erwt inderdaad een grote mate van synteny hebben. Het voordeel van Medicago is dat er veel genomics tools beschikbaar zijn. Zo is de genoomsequentie (de basepaarvolgorde) van Medicago bekend en zijn er uitvoerige transcriptoom data beschikbaar. In dit onderzoek hebben we ons gericht op drie mutanten in de erwt, genaamd *Pssym33*, *Pssym41* en *Pssym31*, en een mutant in Medicago, *Mtsym1*, die allen sterk verstoord zijn in de vorming (en ontwikkeling) van symbiosomen. In Hoofdstuk 1 wordt een algemene introductie op symbiosoomvorming gegeven en worden recente inzichten in dit proces samengevat, op basis van genetische studies in de erwt en de model vlinderbloemigen Medicago en *Lotus japonicus*.

Om de genoominformatie van Medicago te kunnen exploiteren zijn er in Hoofdstuk 2 eerst een aantal tools ontwikkeld die het kloneren van deze genen in de erwt via “comparative genomics” mogelijk maken. Hiervoor zijn er moleculaire markers ontwikkeld op basis van geconserveerde genen in beide genomen die de genetische kaarten van Medicago en erwt koppelen. Deze markers zijn vervolgens gebruikt om de locatie van de corresponderende genen in de erwt genetisch af te bakenen en om de orthologe gebieden in Medicago te identificeren. Vervolgens kan de uitvoerige genoominformatie van Medicago gebruikt worden om kandidaat genen uit een ortholoog gebied te selecteren. Echter, het vervolgens isoleren en achterhalen van de basenpaarvolgorde van orthologe genen in de erwt is geen sinecure, omdat een genoomsequentie van de erwt momenteel ontbreekt. Daarom is er een methode opgezet om genetisch gemodificeerde (transgene) wortels te generen door middel van *Agrobacterium rhizogenes* gebaseerde transformatie van de erwt. Deze relatief snelle methode kan gebruikt worden om de functie van genen in de symbiose te bestuderen. We laten zien dat deze methode gebruikt kan worden om genen van Medicago te introduceren in de wortels van de erwt en dat zo orthologe genen van Medicago direct gebruikt/getest kunnen worden om erwten mutanten te complementeren.

In Hoofdstuk 3 wordt de positionele klonering en identificatie van het *Sym33* gen uit de erwt en *Sym1* van Medicago beschreven. Mutanten in deze genen zijn het sterkst verstoord in het vrijlaten van de bacteriën uit de infectiedraden. Als gevolg worden er geen symbiosomen

gevormd. Beide genen (*PsSym33* en *MtSym1*) blijken te coderen voor een geconserveerd eiwit dat interacteert met DMI3, genaamd IPD3 (voor “Interacting Protein of DMI3”). DMI3 is een calcium- en calmoduline-afhankelijke kinase en is een centrale component van de zogenaamde Nod factor signaleringscascade, die essentieel is om een wortelknolorgaan te maken en voor het bacteriële infectieproces. IPD3 en DMI3 lokaliseren beide in de kern van cellen in de knol waar symbiosomen gevormd worden. Naast een essentiële rol in symbiosoomvorming is IPD3 nodig voor de efficiente groei van infectiedraden in de wortelharen. Deze infectiedraden transporteren de bacteriën richting de zich ontwikkelende knol. Ook speelt IPD3 een rol bij het induceren van corticale celdelingen, waarschijnlijk door de stabiliteit of activiteit van een DMI3 complex te beinvloeden. Verder laten we zien dat IPD3 essentieel is voor de symbiose-specifieke expressie van een recent geïdentificeerd remorin eiwit, genaamd SYMREM1. Uitschakeling van SYMREM1 leidt ook tot een blokkade in het vrijkomen van de bacteriën uit de infectiedraden in de knol (symbiosoomvorming), vergelijkbaar met het uitschakelen van IPD3.

Behalve voor de Rhizobium-symbiose is DMI3 ook essentieel voor de symbiose tussen planten en arbusculaire mycorrhiza (AM) schimmels. Dit is een eeuwenoude endosymbiose die in bijna alle landplanten voorkomt. Tijdens deze endosymbiose dringen de AM schimmeldraden de wortel binnen en worden ze in de binnenste cortex cellen gehuisvest als sterk vertakte structuren, genaamd arbuscules, die omringd worden door een gespecialiseerd membraan van de plant. Hier levert de schimmel essentiele mineralen, vooral fosfaat, aan de gastheer plant in ruil voor koolhydraten. In erwt en Medicago blijkt IPD3 niet nodig te zijn voor het maken van arbuscules, maar speelt het wel een belangrijke rol in de epidermis bij het binnendringen van de schimmel.

In Hoofdstuk 4 wordt de synteny-gebaseerde positionele klonering van *Sym41* uit de erwt beschreven. *Pssym41* knollen zijn sterk verstoord in symbiosoomvorming en in de differentiatie van de symbiosomen. *Sym41* codeert voor de receptor kinase Sym19, de ortholoog van DMI2 in Medicago. Sym19/DMI2 is, net als DMI3, een essentieel onderdeel van de signaleringscascade die nodig is voor zowel de Rhizobium symbiose als de AM symbiose. *PsSym41* bevat een mutatie in een 3’ splice-site in intron 9 van het *Sym19* gen. Dit veroorzaakt een sterke (~90%) reductie in de vorming van normaal (wild-type) boodschapper RNA en het verkeerd gesplice’de boodschapper RNA codeert voor een verkort receptor eiwit waar het kinase domein ontbreekt. *sym41* kan nog steeds knollen vormen door de kleine hoeveelheid wild-type transcript dat gevormd wordt. In het basale gedeelte van deze knollen, in de cellen die afstammen van de knolprimodiumcellen, worden symbiosomen gevormd maar deze differentiëren niet goed. Echter, in de cellen die afstammen van het knolmeristeem blijkt symbiosoomvorming sterk verstoord. Samen met data uit eerdere studies suggereert dit dat opeenvolgende stappen in het rhizobium infectieproces meer input van de Sym19/DMI2-DMI3-IPD3 module vereisen. Een analyse van de AM interactie in *sym41* laat zien dat arbuscule-

vorming niet verstoord is, maar dat vooral het binnendringen door de epidermis van de wortel geblokkeerd is.

In Hoofdstuk 5 is gefocust op de erwtenmutant *sym31*. In *sym31* worden symbiosomen gevormd maar de bacteriën in deze symbiosomen (de bacteroiden) zijn niet instaat om te differentiëren en er worden abnormale symbiosoomstructuren gevormd waarbij meerdere bacteroiden in één symbiosoommembraan voorkomen. Via de synteny-gebaseerde aanpak hebben we de locatie van *Sym31* kunnen afbakenen tot een ~2,5 cM gebied op chromosoom 3. Dit correspondeert met een <450 kb gebied op chromosoom 3 van Medicago, welke het *Sym31*-orthologe gebied representeert. In dit gebied sprint er één gen uit als kansrijke kandidaat voor *Sym31,* doordat het specifiek tot expressie komt in de infectiezone van de knol waar symbiosoomdifferentiatie plaatsvindt. Dit gen codeert voor MtN3/SWEET-achtig eiwit en is een lid van de recentelijk geïdentificeerde familie van suiker/sucrose transporters. We hypothetiseren dat *Sym31* codeert voor zo'n suiker transporter. Onze vorderingen om aan te tonen of dit gen werkelijk een rol speelt bij symbiosoomdifferentiatie worden besproken, maar het ultieme bewijs voor een rol van dit eiwit in symbioomdifferentiatie zal nog geleverd moeten worden.

In Hoofdstuk 6 worden de belangrijkste resultaten van het onderzoek samengevat en worden de verkregen inzichten in symbiosoomvorming en de relatie tot arbuscule-vorming tijdens de AM symbiose bediscussieerd.

Curriculum Vitae

Evgenia Ovchinnikova was born on 15 September 1984 in Legnitsa, Poland. She attended the Faculty of Biology of Hertsen State Pedagogical University of Russia (St.Petersburg, Russia) in 2001 and graduated in 2006 with diploma in biology. After graduation, Evgenia started her scientific career in All-Russia Research Institute for Agricultural Microbiology (St.Petersburg, Russia) as a trainee, studying pea (*Pisum sativum* L.) genetic system controlling development and function of nitrogen-fixing nodules and arbuscular mycorrhiza. In 2007, she has been involved in doctoral collaboration program (Centre of Excellence) between Russia (St.Petersburg) and The Netherlands (Wageningen), which was resulted in this thesis. In July 2012, Evgenia has started working as a postdoctoral research associate in The University of Adelaide (Adelaide, Australia), studying the nutrient transport in plants.

Education Statement of the Graduate School Experimental Plant Sciences

The Graduate School EXPERIMENTAL PLANT SCIENCES

Issued to: Evgenia Ovchinnikova
Date: 19 September 2012
Group: Laboratory of Molecular Biology, Wageningen University & Research Centre

1) Start-up phase		date
►	**First presentation of your project**	
	Genetics of symbiosome formation	Apr 11, 2008
►	**Writing or rewriting a project proposal**	
►	**Writing a review or book chapter**	
►	**MSc courses**	
►	**Laboratory use of isotopes**	
	Course 'Radiation Hygiene', level 5B	Jan 11-15, 2010
	Subtotal Start-up Phase	*3.0 credits**

2) Scientific Exposure		date
►	**EPS PhD Student Days**	
	EPS PhD student day, Leiden University	Feb 26, 2009
	2nd Joint Retreat for Ph.D. students in Plant Sciences, Cologne, Germany	Apr 15-17, 2010
	EPS PhD student day, Wageningen University	May 20, 2011
►	**EPS Theme Symposia**	
	EPS theme 1 "Developmental Biology of Plants", Leiden University	Jan 30, 2009
	EPS theme 1 "Developmental Biology of Plants", Wageningen University	Jan 28, 2010
	EPS theme 1 "Developmental Biology of Plants", Leiden University	Jan 20, 2011
►	**NWO Lunteren days and other National Platforms**	
	ALW meeting "Experimental Plant Sciences', Lunteren	Apr 07-08, 2008
	ALW meeting "Experimental Plant Sciences', Lunteren	Apr 06-07, 2009
	ALW meeting "Experimental Plant Sciences', Lunteren	Apr 19-20, 2010
	ALW meeting "Experimental Plant Sciences', Lunteren	Apr 04-05, 2011
►	**Seminars (series), workshops and symposia**	
	Seminar Koen Visscher	Dec 21, 2007
	Seminar Michael Lampson	Jan 31, 2008
	Flying seminar Richard Viersta	Apr 14, 2008
	Seminar Jean-Philipp Combier	Apr 15, 2008
	Seminar Florian Frugier	Mar 24, 2010
	Seminar Matteo Brilli	Apr 29, 2010
	Plant Science Seminar	Oct 12, 2010
	Flying seminar Peter Cook	Oct 27, 2010
	Seminar Jan Henderson	Dec 13, 2010
►	**Seminar plus**	
►	**International symposia and congresses**	
	8th European Nitrogen-fixation Conference (Ghent, Belgium)	2008
	9th European Nitrogen-fixation Conference (Geneva, Switzerland)	Sep 06-10, 2010
►	**Presentations**	
	Poster: Towards synteny-based cloning of four pea (Pisum sativum L.) symbiotic genes Sym31, Sym32, Sym41 and Sym42 controlling symbiose formation	Aug 28-Sep 03, 2008
	Oral: Intracellular accomodation of Rhizoium bacteria is controlled by the common symbiotic signalling pathway	Jan 20, 2010
	Poster: Genetic analysis of symbiosome formation in Pisum sativum L. and Medicago truncatula Gaerth	Apr 15-17, 2010
	mycorrhizal fungi	Sep 06-10, 2010
	Poster: IPD3 controls the formation of nitrogen-fixing symbiosome in pea and Medicago	Oct 18-22, 2010
►	**IAB interview**	Dec 04, 2009
►	**Excursions**	
	Subtotal Scientific Exposure	*14.4 credits**

3) In-Depth Studies		date
►	**EPS courses or other PhD courses**	
	Bioinformatics: a User's Approach (practical course), Wageningen	Mar 15-19, 2010
	Targeted Genome Editing Using Zinc Finger Nucleases, EMBL, Germany	Jun 21-24, 2010
	The Legume-Rhizobium Symbiosis: From Molecules to farmers' fields, Wageningen	Oct 18-22, 2010
	Basic statistics, Wageningen	Jun 22-23,27-29,
►	**Journal club**	
	Literature discussion MOLBI	2008-2010
►	**Individual research training**	
	Subtotal In-Depth Studies	*7.2 credits**

4) Personal development		date
►	**Skill training courses**	
	English I (Speaking, Writing, Listening, Reading)	2008
	5,28-5) 20 days	Feb-May, 2009
	Scientific Writing (13-1,3-2,10-2,24-2,3-3) 5 days	2010
	Techniques for Writing and Presenting Scientific Papers	Dec 14-17, 2010
	Lecture course "Phylosophy of science", St.Petersburg, Russia (12-7,19-7,21-7,26-7,28-7)	Jul 12-28, 2011
►	**Organisation of PhD students day, course or conference**	
►	Membership of Board, Committee or PhD council	
►	**Organisation of PhD students day, course or conference**	
►	**Membership of Board, Committee or PhD council**	
	Subtotal Personal Development	*6.8 credits**
	TOTAL NUMBER OF CREDIT POINTS*	**31.4**

Herewith the Graduate School declares that the PhD candidate has complied with the educational requirements set by the Educational Committee of EPS which comprises of a minimum total of 30 ECTS credits

** A credit represents a normative study load of 28 hours of study.*